

**PhD Thesis**  
**Doctorate in Energy, Chemical and  
Environmental Engineering**

**Achieving energy-efficient  
districts: contributions through  
large-scale characterization and  
demand side management**



**Author: Laura Romero Rodríguez**

**Supervisors: Servando Álvarez Domínguez**

**José Sánchez Ramos**



Energy Engineering Department  
Higher Technical School of Engineering  
University of Seville



2018



PhD Thesis  
Doctorate in Energy, Chemical and  
Environmental Engineering

Achieving energy-efficient districts:  
contributions through large-scale  
characterization and demand side  
management

Author:

Laura Romero Rodríguez

Supervisors:

Servando Álvarez Domínguez

José Sánchez Ramos

Energy Engineering Department  
Higher Technical School of Engineering  
University of Seville

Seville, 2018



*A mi familia, amigos,  
Servando y José*



# Acknowledgments

---

I embarked on the journey of doing a PhD on the 1st of December 2014, the day of my 26th birthday. Since then, there have been many challenging moments, which would have been very difficult for me to deal with had it not been for the support I received from those closer to me. I am so grateful for being surrounded by such good people in my life, and would like to dedicate some words to them.

## *To my parents.*

First of all, to my mother Amor and my father Juan Luis, for supporting me always in all my decisions, for being there for me no matter what and for having the patience of spending so many weekends and holidays at home because I had to work. Thank you for having made so many sacrifices, for helping me so much during my studies and for making me what I am today.

## *To my family.*

To those who left us while I was doing this research, my uncle Jeronimo and my aunt Amalia. To my aunt Pilar, for always putting everyone above herself and taking care of all her nieces and nephews so well. To my cousin Nieves, who is for me the best role model I could have asked for. And of course to the rest of my family: cousins, nephews, aunts and uncles. Thank you all.

## *To my friends.*

To Antonio, Carlos, Rocio, Rocio and Rocio, without whom the years I have spent since I came to Sevilla wouldn't have been so full of happy memories, and who have supported me so much during all this time. To my friends from my hometown: Belen, Max, Elena, Karma and Nerea. Thank you for being there for so many years, especially Nerea. I thank life for having met you so many years ago, and I thank you for walking by my side, spending with me such a wonderful time and making me the proud godmother of your daughter. The best is yet to come. To Sergio, Monty, Alberto and Javi, thank you for our trips, for so many happy memories, for our Monday/Wednesday nights chatting and for being responsible of most messages in my mobile phone, which made me feel you a bit closer. I will forever be grateful for having decided to fly to Krakow that 20th September 2011, which allowed me to meet you. To my friends from Stuttgart, especially Pilar, Dani and Patri: thank you for helping me so much during my time there and receiving me with open arms from the very beginning. To Curro, who has become one of my best friends at the speed of light: I thank the universe for putting us together in that English classroom five years ago. And last but not least, thank you again to Cespi: I can't even begin to thank you for being there always for me. You have been my greatest support. Don't ever stop being the way you are with those around you, that's what makes you so special.

*To my coworkers.*

I would like to thank the Professors of my research group, José Luis Molina, José Manuel Salmerón and Francisco Sánchez, for allowing me to work by their side and learn from their great experience, both academically and personally. Thank you so much for everything. I would also like to thank Ursula Eicker, who was my supervisor during my two research stays in Stuttgart and welcomed me there with open arms. Last of all, thank you to the rest of my colleagues in the office in Sevilla, with whom I have shared so many projects, had countless interesting conversations, shared many questionable meals and made the endless working hours much more bearable.

*To my supervisors.*

Thank you to José Sánchez, with whom I have shared so much. Thank you for our many conversations, our joint efforts in projects, in presentations, in fixing Excel tools with black cells, for your quick replies and struggles even during the weekends, for our jokes between serious emails and for your patience when I was so intense. Thank you for thinking the same way I do about so many things and above all for having guided me during these past years. I have learnt so much from you.

Last of all, I would like to express my greatest appreciation to my supervisor Servando Álvarez for having allowed me to work the past four years by his side. For his guidance, help and encouragement. For teaching me so much. For his ability to find a wrong value among hundreds of results with just a glance at a huge table. Of course he was always right, and after I spent hours looking at my programming code, I would find the mistake that I had made. Thank you for believing in research the way you do, for having your door always opened (literally), and for dedicating so much of your time to young students and improving the lectures year after year. I remember when nine years ago I attended for the first time a class at this University. It was 08:30 in the morning, first day of the third year of the engineering degree, the subject was Heat Transfer, but it was my first class in Seville because until then I had studied in another city. I didn't have any friends here yet, didn't know how I could get the lecture notes, or even where the library was or how the schedules and the room numbers worked. After that class finished, I went to talk to the professor, who was Servando, and even though he was always so incredibly busy, he still took some time to explain me such banalities and help me to adapt. That day it was me, but during these past years I have seen him helping students in many different ways, in countless times. And here we are today, having had the pleasure of teaching and working by his side. Thank you so much for everything.

*Laura.*

*Sevilla, 2018.*



# Abstract

---

Buildings are increasingly expected to be more efficient and sustainable since they are essential to energy policies and climate change mitigation efforts. For this reason, it is very important to develop new energy models, with special attention to the residential sector. The present Thesis aims to justify the selection of the district scale as the optimal one to improve the energy performance of the built environment. In this way, renewable energy integration may be increased and innovative approaches such as demand side management may be carried out through the accurate characterization of districts.

Several applications are shown to evaluate the solar potentials and the energy demands for entire regions by using 3D city models. The advantages offered by demand side management approaches in buildings and districts are investigated, presenting two applications that benefit from dynamic pricing strategies or the participation in reserve markets. The drawbacks of most current approaches on a large scale are highlighted, and a new tool capable of performing dynamic simulations of whole districts in a user-friendly and accurate way is presented.

In addition, a methodology for a proper characterization of districts through monitoring is developed, validated, and used for two applications. The first one characterizes a district consisting of buildings with a limited use of air-conditioning, and the second one evaluates the benefits that could be obtained from the exploitation of the synergies between the buildings of a district. As a last contribution of this Thesis, a new comprehensive methodology for the characterization and optimization of any existing district is proposed.



# Resumen

---

Se espera que los edificios sean cada vez más eficientes y sostenibles, puesto que son esenciales para las políticas energéticas y los esfuerzos hacia la mitigación del cambio climático. Por esta razón, es muy importante desarrollar nuevos modelos energéticos, con especial atención al sector residencial. La presente Tesis parte de que la escala de distrito es la óptima para mejorar el comportamiento de la edificación. Además, permite aumentar la integración de energías renovables y llevar a cabo planteamientos innovadores como la gestión de la demanda a través de una precisa caracterización de los distritos.

Se muestran varias aplicaciones para la evaluación de los potenciales solares y las demandas energéticas de regiones enteras, usando modelos 3D de ciudades. Las ventajas ofrecidas por los procedimientos de gestión de la demanda en edificios y distritos también son investigadas, presentando dos aplicaciones que se benefician de estrategias de tarificación dinámica o de la participación en los mercados de reserva. Las desventajas de la mayoría de procedimientos actuales a gran escala también son destacadas, y se presenta una nueva herramienta capaz de llevar a cabo simulaciones dinámicas de distritos completos de forma simple y precisa.

Además, se desarrolla una metodología para la caracterización apropiada de distritos a través de monitorización, validada y empleada en dos aplicaciones. La primera trata la caracterización un distrito compuesto por edificios con un uso limitado de la climatización, y la segunda la evaluación de los beneficios que podrían obtenerse de la explotación de las sinergias entre los edificios de un distrito. Como última contribución de la Tesis, se propone una nueva metodología completa para la caracterización y optimización de cualquier distrito existente.



# Contents

<b>Acknowledgments</b> .....	<b>v</b>
<b>Abstract</b> .....	<b>vii</b>
<b>Resumen</b> .....	<b>ix</b>
<b>Contents</b> .....	<b>xi</b>
<b>Index of figures</b> .....	<b>xv</b>
<b>Index of tables</b> .....	<b>xxi</b>
<b>Abbreviations</b> .....	<b>xxiii</b>
<b>1. INTRODUCTION</b> .....	<b>1</b>
1.1. <i>Energy and buildings: international commitments and gradual strengthening of requirements</i> .....	1
1.2. <i>Background</i> .....	3
1.2.1. The role of cities.....	3
1.2.2. Sustainable urban development .....	3
1.2.3. Smart cities.....	4
1.2.4. Information and communication technologies.....	6
1.2.5. Energy storage .....	7
1.2.6. Demand side Management and Demand Response .....	8
1.3. <i>From NZEB to NZED</i> .....	8
1.3.1. Nearly Zero Energy Buildings (NZEB).....	8
1.3.2. Nearly Zero Energy Districts (NZED).....	9
1.4. <i>Smart cities within the H2020 programme</i> .....	10
1.5. <i>Reasons for choosing the district scale</i> .....	10
1.6. <i>Road-map for an optimal design, sizing and operation of NZED</i> .....	12
1.6.1. Preliminary analysis of the district .....	12
1.6.2. Conceptual design and optimization of the technologies to be implemented at the district scale	12
1.6.3. Design development and final sizing of the optimal solution .....	12
1.6.4. Optimal management of the district and the grid .....	13
1.7. <i>Aim of the Thesis</i> .....	13
<b>2. WIDENING THE SCOPE OF ENERGY ANALYSES IN THE BUILT ENVIRONMENT</b> .....	<b>15</b>
2.1. <i>Introduction</i> .....	15
2.1.1. Redefining the NZE concept: from individual buildings to districts .....	15
2.1.2. Use of GIS for analysing energy performances at large scales.....	16
2.1.3. Approaches for evaluating the thermal performance of buildings at urban level .....	17
2.1.4. Domain reduction.....	18
2.1.5. Evaluating solar potentials at urban level.....	18
2.1.6. Aim of this chapter .....	20
2.2. <i>Evaluating solar potentials at urban level by using 3D city models</i> .....	20
2.2.1. Introduction .....	20
2.2.2. Methodology.....	21
2.2.3. Results and discussion.....	22
2.2.4. Conclusions .....	25
2.3. <i>Improving the accuracy of solar potential assessments at urban level</i> .....	25
2.3.1. Introduction .....	25
2.3.2. Brief description of the case studies .....	26

2.3.3.	Solar radiation calculation approaches for urban energy analysis.....	27
2.3.4.	Identifying the best tiling strategies for middle and high-density urban areas.....	27
2.3.5.	Solar potential “Identity Cards” .....	29
2.3.6.	Conclusions.....	32
2.4.	<i>Urban energy demand evaluation through 3D city models.....</i>	32
2.4.1.	Introduction.....	32
2.4.2.	Obtained results of heating demands .....	33
2.4.3.	Conclusions of this study .....	34
2.5.	<i>New tool for modelling and estimating the energy performance of districts .....</i>	35
2.5.1.	HULCGIS .....	35
2.5.2.	Creation of HULC models.....	37
2.5.3.	HULCGIS validation.....	38
2.5.4.	Tool for the estimation of demand reduction measures in districts.....	38
2.6.	<i>Review of clustering techniques for decision making in districts.....</i>	39
2.6.1.	General concepts of clustering approaches.....	39
2.6.2.	Studies based on clustering techniques .....	40
2.7.	<i>Brief summary.....</i>	41
<b>3.</b>	<b>SMART END-USE: DEMAND SIDE MANAGEMENT APPROACHES .....</b>	<b>43</b>
3.1.	<i>Introduction.....</i>	43
3.1.1.	The concept of DSM.....	43
3.1.2.	Review of the existing literature on DSM.....	45
3.1.3.	Aim of this chapter .....	48
3.2.	<i>Contributions of heat pumps to Demand Response: a case study of a plus-energy dwelling.....</i>	49
3.2.1.	Introduction.....	49
3.2.2.	Case study: Modelling and Simulation .....	49
3.2.3.	Analysis of results.....	52
3.2.4.	Conclusions.....	56
3.3.	<i>Heuristic optimization of clusters of heat pumps: a simulation and case study of residential frequency reserve.....</i>	56
3.3.1.	Introduction.....	56
3.3.2.	Market integration: frequency restoration reserve .....	57
3.3.3.	Case study: Modelling and Simulation .....	58
3.3.4.	Results: DR potential of a cluster of dwellings.....	61
3.3.5.	Conclusions and outlook.....	66
3.4.	<i>Summary of findings of this Chapter .....</i>	66
<b>4.</b>	<b>BASELINE MODELS FOR CHARACTERIZATION, FORECASTING AND DECISION-MAKING IN DISTRICTS .....</b>	<b>69</b>
4.1.	<i>Fundamentals of baseline models .....</i>	70
4.2.	<i>Mathematical basis of the developed QT model.....</i>	71
4.2.1.	Initial hypotheses .....	71
4.2.2.	Development of the baseline models.....	72
4.3.	<i>Validation of the model.....</i>	76
4.3.1.	Theoretical validation .....	76
4.3.2.	Experimental validation.....	79
4.4.	<i>Integration of the QT model and DSM techniques.....</i>	81
4.4.1.	Conclusions.....	83

<b>5. CHARACTERIZATION OF DISTRICTS: APPLICATION FOR BUILDINGS WITH LIMITED USE OF AIR-CONDITIONING .....</b>	<b>85</b>
5.1. <i>Characterization of a district without monitored air-conditioning consumptions .....</i>	85
5.1.1. Description of the case study .....	85
5.1.2. Monitoring of the district .....	86
5.1.3. Identification of air-conditioning consumptions .....	88
5.1.4. Estimation of the matching climate .....	88
5.1.5. Primary baseline .....	88
5.1.6. Secondary baseline .....	90
5.2. <i>Applications based on the characterization of districts .....</i>	92
5.2.1. Calculation of comfort indices .....	92
5.2.2. Energy needs .....	93
5.3. <i>Novel approach for benefitting from PV potentials .....</i>	94
5.3.1. Aim of the study .....	94
5.3.2. Justifying the need for intervention in the district .....	94
5.3.3. Electricity consumption of the district .....	97
5.3.4. Building typologies .....	98
5.3.5. Methodological description .....	100
5.3.6. PV potential simulation .....	102
5.3.7. Thermal behaviour of the dwellings .....	102
5.3.8. Description of the proposed strategies .....	103
5.3.9. Analysis of results .....	105
5.3.10. Conclusions .....	110
<b>6. APPLICATION FOR A SMART MANAGEMENT OF MICROGRIDS .....</b>	<b>111</b>
6.1. <i>Introduction .....</i>	111
6.1.1. Literature review .....	112
6.1.2. Aim of the study .....	116
6.2. <i>Description of the case study .....</i>	116
6.2.1. Characteristics of the district .....	116
6.2.2. Monitoring and modelling of the district .....	118
6.3. <i>Calculation methodology .....</i>	121
6.3.1. Scenarios .....	121
6.3.2. Preconditioning alternatives .....	122
6.3.3. Proposed rule-based control strategy .....	124
6.3.4. Simulation framework .....	126
6.3.5. Self-consumption and self-sufficiency ratios .....	127
6.4. <i>Results and discussion .....</i>	127
6.4.1. Comparison of management alternatives .....	127
6.4.2. Comparison of precooling strategies .....	129
6.4.3. Sensitivity analysis: feed-in tariff .....	131
6.5. <i>Conclusions and future work .....</i>	132
<b>7. CONCLUSIONS AND FUTURE DEVELOPMENTS .....</b>	<b>133</b>
7.1. <i>Conclusions and summary of key findings .....</i>	133
7.1.1. Achieving accurate energy analyses on a district scale .....	133
7.1.2. Exploring demand side management opportunities .....	134
7.1.3. Development of energy baselines .....	135
7.1.4. Characterization of districts: application of the methodology .....	135
7.1.5. Exploiting the synergies between buildings through DSM approaches .....	136
7.2. <i>A new methodology towards achieving comprehensive energy analyses at large scales .....</i>	137
7.3. <i>Future work .....</i>	139

**ACKNOWLEDGMENTS OF FUNDING.....141**  
**ANNEX A. MATCHING CLIMATE .....143**  
**ANNEX B. PROCEDURE FOR THE DISAGGREGATION OF HOUSEHOLD ELECTRICITY CONSUMPTIONS ..155**  
**ANNEX C. GENERAL CONCEPTS OF DEMAND SIDE MANAGEMENT .....163**  
**ANNEX D. IMPROVEMENT MEASURES CONSIDERED IN THIS THESIS.....175**  
**ANNEX E. JOURNAL PUBLICATIONS.....185**  
**REFERENCES.....195**



# Index of figures

---

Figure 1: Final energy consumption by sector, EU-28, 2016. Source: Eurostat .....	2
Figure 2: Final energy consumption in the residential sector by type of end-use, EU-28, 2016. Source: Eurostat.....	2
Figure 3: Shares of energy demand coverage in Spain, 2017. Source: Red Eléctrica Española. ....	2
Figure 4: Urban scales proposed in the present Thesis. ....	4
Figure 5: Devised evolution of the electricity grids. Source: IEEE. ....	5
Figure 6: Smart Grid concept [7].....	5
Figure 7: General architecture of Smart Grid communications [9].....	7
Figure 8: Pillars of a NZED considered in the present work.....	9
Figure 9: Five LODs of CityGML 2.0 [31]. ....	16
Figure 10: 3D city models may be applied in a multitude of application domains for environmental simulations and decision support [32]. ....	16
Figure 11: Flowchart of the available roof area calculation process. ....	21
Figure 12: Percentage of the electricity demand covered in each municipality by PV for the technical potential strategy.....	23
Figure 13: Percentage of the electricity demand covered in each municipality by PV for the economic potential strategy.....	23
Figure 14: Percentage of the electricity demand covered by PV in the whole region for the two scenarios: technical and economic potential. ....	24
Figure 15: Representation of the case study Ludwigsburg with an East view (up) and Manhattan with a North-West view (down). ....	26
Figure 16: Example of tiling (tile size = 500m; overlap = 150m) for a studied area. ....	27
Figure 17: Computational time versus tile size for the considered strategies in Ludwigsburg (left) and Manhattan (right). The labels show also the number of tiles in each case. ....	27
Figure 18: Urban Shading Ratios on roofs as a function of the used tiling strategy. Annual USR in Ludwigsburg (left) and annual USR in Manhattan (right).....	28
Figure 19: Urban Shading Ratios on facades as a function of the used tiling strategy. Annual USR in Ludwigsburg (left) and annual USR in Manhattan (right).....	29
Figure 20: Cumulative solar radiation distribution in Ludwigsburg.....	30
Figure 21: Cumulative solar radiation distribution in Manhattan.....	30
Figure 22: Monthly Urban Shading Ratio on roofs and facades in Manhattan .....	31
Figure 23: Monthly Urban Shading Ratio on roofs and facades in Ludwigsburg. ....	31
Figure 24: Comparison of simulated and measured aggregated heating consumption of residential buildings with gas heating.....	34
Figure 25: Specific heating demand for different building types in the municipality Hemmingen as a consequence of the refurbishment scenarios. ....	34

Figure 26: Screen capture of the HULCGIS plugin within QGIS. ....	36
Figure 27: Example of HULC building model created by HULCGIS. ....	37
Figure 28: Comparison between the building models. ....	38
Figure 29: Comparison of the results between the detailed model and the HULCGIS model. ....	38
Figure 30: User interface of the tool for the estimation of demand reduction measures in districts. ....	39
Figure 31: Example of visualization of results for some buildings in La Graciosa Island (Las Palmas, Spain). ....	39
Figure 32: Demand Side Management within the Smart Grid environment [7]. ....	44
Figure 33: SketchUp model of the building. ....	50
Figure 34: Simplified representation of the TRNSYS model. ....	50
Figure 35: Example of different modes of operation depending on the strategy (ST). ....	52
Figure 36: Comparison of heat pump monthly cost for heating electricity. ....	52
Figure 37: Comparison of the daily temperature of different strategies. Case $20 \pm 0 \text{ }^\circ\text{C}$ . ....	53
Figure 38: Comparison of the amount of excess degree-hours. Positive values show $>20^\circ\text{C}$ and negative values $<20^\circ\text{C}$ . ....	53
Figure 39: Percentage of HP use during peak hours [%]. ....	54
Figure 40: Example of the duration of the activation calls vs. energy price bid. Own analysis of data for calendar year 2015. Data published by Transmission System Operators (TSOs) and publicly available at <a href="http://www.regelleistung.net">www.regelleistung.net</a> . ....	57
Figure 41: Overview of the cluster manager framework. ....	59
Figure 42: Comparison of the number of activation calls for the three scenarios depending on the duration. Real FRR data from February 2015. ....	60
Figure 43: Flowchart of the simulations. ....	61
Figure 44: Example of activation call decisions and indoor temperatures. ....	62
Figure 45: Percentage of accepted activations. ....	62
Figure 46: Total excess degree hours ( $> 20 \text{ }^\circ\text{C}$ ). ....	63
Figure 47: Cost savings [%] of the proposed strategies (negative values mean higher costs than their base case). ....	64
Figure 48: Power provided for price scenario FRR (0). ....	65
Figure 49: Cluster cost savings depending on different price scenarios. Positive values mean the achievement of cost savings compared to the case with no FRR participation. ....	66
Figure 50: Baseline concept [140]. ....	70
Figure 51: Example of direct and diffuse solar irradiance for the South orientation during several days. ....	74
Figure 52: Example of gross solar gains on a building. ....	75
Figure 53: Thermal load on the space due to solar gains. ....	75
Figure 54: Location of the dwelling under study. ....	76
Figure 55: HULC model of the dwelling (left) and real image (right). ....	77

Figure 56: Illustration of the evolution of the indoor and outdoor temperatures. ....	77
Figure 57: Effect of the internal and solar gains on the indoor temperature. ....	77
Figure 58: Comparison between simulated and estimated temperature and consumption measurements. ....	78
Figure 59: Evolution of the full free-floating temperature and the indoor temperature. ....	78
Figure 60: Installation of the temperature sensor (left) and smart plug on the air-conditioning system (right). ....	79
Figure 61: Measurements obtained from the monitoring campaign.....	80
Figure 62: Comparison between the measured and estimated indoor temperatures. ....	80
Figure 63: QT diagram of the dwelling during 3 weeks in August 2017. ....	80
Figure 64: District under study. ....	86
Figure 65: Location of some of the monitored dwellings and the developed models. ....	86
Figure 66: Plan of the dwelling and location of the temperature sensors. ....	87
Figure 67: Comparison between the daily average indoor temperature measurements of the different spaces. ....	87
Figure 68: Example of temperature and consumption measurements in the dwelling under study. ....	87
Figure 69: Example of days with and without air-conditioning. ....	88
Figure 70: Chosen weather station in La Puebla de Cazalla, Seville, Spain.....	88
Figure 71: Comparison of horizontal radiation and solar gains. The black arrow points to the North. ...	89
Figure 72: Monthly ESSA of the living room per m <sup>2</sup> of conditioned area. Real climate. ....	89
Figure 73: Comparison between the estimated and the real daily average indoor temperatures in two of the bedrooms.....	89
Figure 74: Comparison between the temperatures estimated by the primary baseline and the real measurements in February (left), April (center) and July (right). ....	90
Figure 75: Fit between the measured temperatures and the estimated ones at hourly time-steps. Living room (left) and bedroom (right).....	90
Figure 76: Example of a comparison between measured indoor temperatures, full free-floating temperatures and their associated consumptions. ....	90
Figure 77: Comparison between the indoor temperature/consumption estimations and measurements and full free-floating temperatures. ....	91
Figure 78: Comparison between the measured air conditioning consumption and the one estimated. ..	91
Figure 79: Comparison of total excess degree-hours in winter of the considered spaces. ....	93
Figure 80: Comparison of heating demands obtained by the application of the energy baselines for the real and the standard climate. ....	93
Figure 81: Hourly temperatures of the living rooms in the monitored households (left) and average daily temperatures (right).....	95
Figure 82: Hourly temperatures of the bedrooms in the monitored households (left) and average daily temperatures (right).....	96
Figure 83: Percentage of time outside the comfort zone of all the households.....	96

Figure 84: Comparison of temperatures in the conditioned household D6 (up) and the non-conditioned household D7 (down).....	97
Figure 85: Average monthly energy consumption per household in the district.....	98
Figure 86: Electricity consumption of the district for every hour of the year. ....	98
Figure 87: Control diagram of the proposed strategies. ....	101
Figure 88: Example of layout of the district in Helioscope: south orientation in the flat roofs. ....	102
Figure 89: Validation of the simulated and measured indoor temperature of dwelling 4 for the whole year. ....	103
Figure 90: Obtained results in all the analyzed strategies. In each column, green cells represent the best options while red cells represent the worst ones. The marked alternatives are those chosen for the thermal comfort study. ....	105
Figure 91: Example of simulated indoor temperatures and consumptions in the dwelling 130 for some of the analyzed strategies (case maximization of exported PV production). ....	106
Figure 92: Example of thermal energy storage before and after the heat pump operation in the dwelling 130. ....	107
Figure 93: Comparison of total excess degree hours of the households for each strategy (case maximization of exported PV production).....	108
Figure 94: Hourly and daily free floating temperature of the living room in dwelling 147 vs. temperatures achieved with strategy T=20/25.....	109
Figure 95: Location of La Graciosa Island.....	117
Figure 96: Location of the case study district within the island of La Graciosa (left) and IDs of its buildings (right).....	117
Figure 97: Interconnections between the buildings of the district. ....	117
Figure 98: Example of PV modules installed in the island. ....	118
Figure 99: Annual electricity consumption of every building in the district. ....	118
Figure 100: Depiction of the PV modules installed in the district. ....	119
Figure 101: Monthly PV production of the district. ....	119
Figure 102: Electricity surplus of the two dwellings under study, calculated through the difference between PV production and electricity consumption. Positive values mean an electricity surplus, while negative values mean the need to import electricity.....	120
Figure 103: Variation of the electricity prices of the considered two-period tariff. 1 <sup>st</sup> of July 2016.....	120
Figure 104: HULC detailed models of dwelling 1 (left), dwelling 2 (center) and the school (right). ....	121
Figure 105: Effect of a precooling strategy on the indoor temperature and cooling consumption. ....	124
Figure 106: Proposed rule-based control strategy for each time-step. ....	125
Figure 107: Illustration of the simulation framework. ....	126
Figure 108: Comparison of annual costs for different management scenarios. ....	128
Figure 109: Comparison of monthly imports, exports and costs for the self-consumption and district scenarios. ....	128
Figure 110: Comparison of the self-consumption and self-sufficiency ratios in different management alternatives.....	129

Figure 111: Example of selection of the best strategy that minimizes daily costs (positive values) or maximizes the benefits (negative values). .....	129
Figure 112: Percentage of days during summer that each precooling strategy considered was chosen for different scenarios. ....	130
Figure 113: Sensitivity analysis of feed-in tariff rates for scenarios 1 and 5. ....	131
Figure 114: Example of dendrogram of hierarchical clustering on energy demand data as shown in [184]. ....	138
Figure 115: Depiction of the transition from the HULCGIS model of a representative building to a more detailed, multi-zone model. ....	138
Figure 116: Location of the closest weather stations in the case of Almanjayar. ....	144
Figure 117: Procedure to obtain the modified weather file. ....	145
Figure 118: Direct solar radiation: angles between the sun and the receiving surface. ....	148
Figure 119: Direct radiation on a horizontal and inclined surface. ....	148
Figure 120: Monthly radiation for different orientations in a specific location. ....	149
Figure 121: Influence of the solar and internal gains on the average daily temperature of a building. ...	150
Figure 122: Evolution of the monthly ESSA. ....	151
Figure 123: Hourly proportion of the solar gains during the second week of January. ....	151
Figure 124: Hourly proportion of the solar gains during the first week of July. ....	152
Figure 125: Comparison of hourly values of the solar gains for every day in January. ....	152
Figure 126: Monthly averages of the hourly solar gains. ....	152
Figure 127: Validation of the hourly direct radiation. ....	153
Figure 128: Comparison of the measured and estimated direct radiation. Months of January and July. ....	153
Figure 129: Comparison of the measured and estimated global radiation. Month of April. ....	154
Figure 130: Monthly comparison between the estimated and measured direct, diffuse and global radiations. ....	154
Figure 131: Example of data obtained from the Smart Meter of a dwelling in Seville, Spain. ....	155
Figure 132: Consumption pattern of one use of a washing machine (left) and dishwasher (right). ....	156
Figure 133: Consumption patterns of different TVs (left) and laptops (right). ....	156
Figure 134: Consumption patterns of a Smartphone and a Tablet. ....	156
Figure 135: Disaggregated monthly energy consumption. ....	156
Figure 136: Example of average daily indoor temperature and total daily electricity consumption of a household in Seville, Spain. ....	157
Figure 137: Example of average daily indoor temperature and total daily electricity consumption of a household in Granada, Spain. ....	158
Figure 138: Example of average daily consumption profile. ....	159
Figure 139: Comparison between measurements and the estimation made by the tool. ....	160
Figure 140: Comparison between the estimated and the real average daily consumptions of the dwellings	

in the district.....	160
Figure 141: Measured hourly consumption of different dwellings on the 3 <sup>rd</sup> of April 2017 and estimated profile for April.....	161
Figure 142: Hourly consumption of several dwellings during a whole week and comparison with the estimated profile for April.....	161
Figure 143: Comparison between the real measurements and the electricity consumption pattern of Monday.....	161
Figure 144: General architecture of DSM frameworks [186]. .....	163
Figure 145: Basic load shaping techniques [87]. .....	164
Figure 146: Example of hourly electricity demand and prices.....	166
Figure 147: Example of a Smart Home and its sensors [193].....	167
Figure 148: Smart meters implementation. Source: Endesa. ....	168
Figure 149: From left to right: temperature and humidity sensor, motion sensor, door/window sensor. ....	169
Figure 150: Example of Area Network boundaries. Source: Fusion Energy Consortium. ....	170
Figure 151: Common impact factors leading from occupant behavior to energy consumption [200]. ...	171
Figure 152: Average household electricity savings by feedback type [202].....	172
Figure 153: Integration of storage and Demand Side Management. Source: Energy Storage Association, 2012. ....	173
Figure 154: Design parameters for solar-control systems [208]. .....	176
Figure 155: Example of control of automatic shading devices [218].....	178
Figure 156: Night cooling technique. Source: Illinois Institute of Technology.....	178
Figure 157: Model of the dwelling and surrounding buildings. ....	179
Figure 158: Measured temperature of the household, July 2017.....	180
Figure 159: Results of cooling demand reduction for the analyzed solar control strategies.....	180
Figure 160: Results of excess degree-hours reduction for the analyzed solar control strategies.....	181
Figure 161: Example of baseline in summer with and without night ventilation. Free-floating mode...181	181
Figure 162: Example of the evolution of the indoor temperature and consumption with and without night ventilation. 6 <sup>th</sup> to 10 <sup>th</sup> of July. Standard climate and user. ....	182
Figure 163: Results of cooling demand reduction for the analyzed solar control strategies.....	182
Figure 164: Results of excess degree-hours reduction for the analyzed solar control strategies.....	182

# Index of tables

---

Table 1: Summary of reduction coefficients. ....	21
Table 2: CO <sub>2</sub> emissions of the region for each approach of the study. ....	24
Table 3: Economic results for each proposed strategy and scenario. ....	25
Table 4: Example of attribute table in HULCGIS. ....	36
Table 5: Analyzed strategies using day-ahead electricity market prices. ....	51
Table 6: Selection of the optimal strategies. ....	55
Table 7: Strategies and FRR price scenarios considered. ....	60
Table 8: Characteristics of the different models used in previous publications. Source: [141]. ....	70
Table 9: Possibilities offered by the proposed baselines for DSM purposes. ....	82
Table 10: Comfort indices in some spaces of dwellings of the district for neutralized users, considering the real climate. ....	92
Table 11: Characteristics of the monitored dwellings. ....	95
Table 12: Characteristics of all the dwelling typologies in the district. ....	100
Table 13: Overview of the average obtained results in the district. ....	107
Table 14: Results of the analyzed options. ....	109
Table 15: Considered scenarios. ....	122
Table 16: Operating schedules of the air-conditioning systems for the dwellings and the school of the district. ....	123
Table 17: Precooling strategies considered. ....	124
Table 18: Results of different management alternatives for the district. ....	127
Table 19: Results of the considered precooling scenarios. ....	130
Table 20: Example of data in the reference weather files. ....	143
Table 21: Example of the selection of the two most similar days. 15 <sup>th</sup> of March. ....	147
Table 22: Monthly values of the solar gains, radiation in the south orientation and obtained ESSA. ....	151
Table 23: Daily profiles, monthly variation and yearly output provided by several projects on consumption patterns in residential buildings. ....	159
Table 24: Total costs and annual savings of the strategies that were evaluated. ....	183





# Abbreviations

---

ACH	Air Changes per Hour
CHP	Combined Heat and Power
DER	Distributed Energy Resources
DHW	Domestic Hot Water
DR	Demand Response
DSM	Demand Side Management
EPBD	Energy Performance of Buildings Directive
ESC	Energy Sharing Coordinator
ESSA	Equivalent South Solar Area
FAR	Floor Area Ratio
FCR	Frequency Containment Reserve
FRR	Frequency Restoration Reserve
GIS	Geographic Information Systems
HAN	Home Area Network
HP	Heat Pump
HULC	Unified LIDER-CALENER software tool
HVAC	Heating, Ventilation and Air Conditioning
ICT	Information and Communication Technologies
IEA	International Energy Agency
LCC	Life Cycle Cost
LiDAR	Light Detection And Ranging
LOD	Level Of Detail
MPC	Model Predictive Control
NREL	National Renewable Energy Lab
NZEB	Nearly Zero Energy Buildings
NZED	Nearly Zero Energy District
P2P	Peer-to-Peer
PV	Photovoltaics
RES	Renewable Energy Sources
SOC	State Of Charge
TABS	Thermally Activated Building Systems
TCL	Thermostatically Controlled Loads
TES	Thermal Energy Storage
TOU	Time-of-Use
TSO	Transmission System Operator
USR	Urban Shading Ratio



# 1. INTRODUCTION

---

## 1.1. Energy and buildings: international commitments and gradual strengthening of requirements

Buildings are fundamental to energy policies and climate change mitigation efforts. Nowadays, buildings are increasingly expected to be more efficient and sustainable, driven mainly by new legislation. In the case of Europe, the European Commission is looking at cost-efficient ways to make the European economy more climate-friendly and less energy-consuming [1]. At the end of the year 2014, the European Council agreed on a new 2030 Framework built on the 2020 climate and energy package, including EU-wide targets and policy objectives for the period between 2020 and 2030 [2]. Looking beyond the short-term, those targets would help meeting the more ambitious 2050 Roadmap, designed to achieve even greater emission reductions for a more competitive low carbon economy in the long term.

The targets of the Europe 2020 strategy for climate change and energy, discussed by many studies, are [3]:

- 20% cut in greenhouse gas emissions (from 1990 levels).
- 20% of EU energy from renewables.
- 20% improvement in energy efficiency.

On the other hand, the 2030 framework for climate and energy sets three key targets for the year 2030 [2]:

- At least 40% cuts in greenhouse gas emissions (from 1990 levels).
- At least 27% share for renewable energy.
- At least 27% improvement in energy efficiency.

Also, the low-carbon economy 2050 Roadmap [1] suggests that:

- By 2050, the EU should cut greenhouse gas emissions to 80% below 1990 levels.
- Milestones to achieve this are 40% emissions cuts by 2030 and 60% by 2040.
- The low-carbon transition is feasible & affordable.
- All sectors need to contribute.

The conclusion of the 2050 roadmap is that the transition to a low-carbon society is feasible and affordable, but requires innovation and investments. As the roadmap indicates, all sectors should contribute to a more competitive low-carbon economy in the future. Figure 1 shows the final energy consumption by sector in the EU. As it can be seen, households represent a quarter of the total final energy consumption. Therefore, it is very important to develop new energy models directed at the improvement of the performance of the built environment, with emphasis on the residential sector.

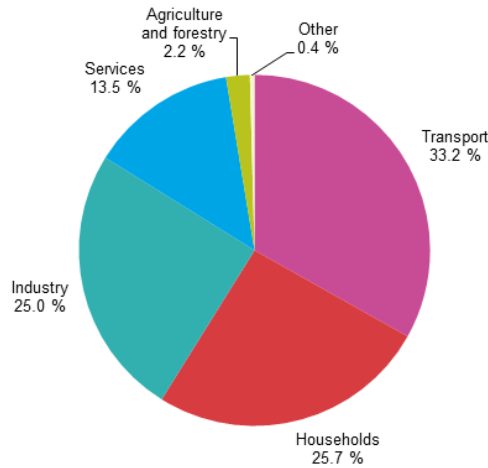


Figure 1: Final energy consumption by sector, EU-28, 2016. Source: Eurostat.

Focusing on the residential sector, if we look at the types of end-uses responsible for the final energy consumption, we can see in Figure 2 that space conditioning represents a very significant proportion. It should be noted that the figure shows the average for the EU, where heating demands are the most meaningful. However, there are countries such as Spain where the cooling demands are also significant.

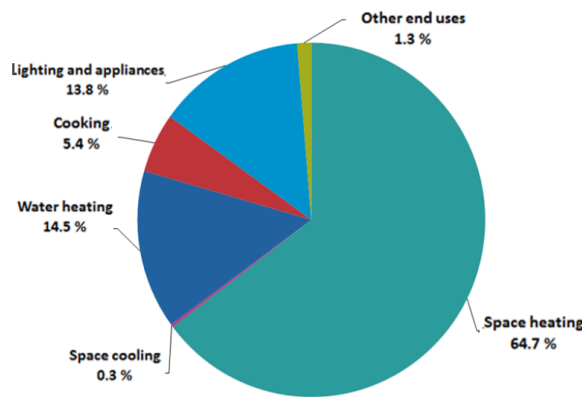


Figure 2: Final energy consumption in the residential sector by type of end-use, EU-28, 2016. Source: Eurostat.

With regards to renewable energy production, which is another of the requirements of the legislation that should be met, EU member countries have increased their share of renewables during the past years to meet their targets. In Spain, renewable energies represent nowadays a significant portion of the energy demand coverage, as can be seen in Figure 3.

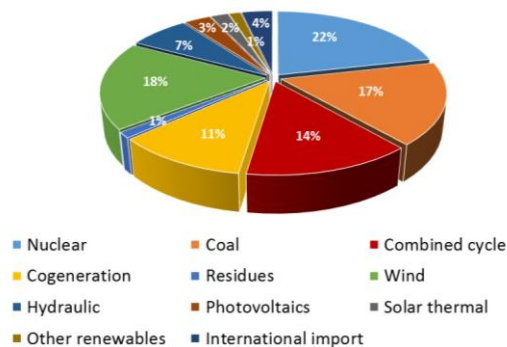


Figure 3: Shares of energy demand coverage in Spain, 2017. Source: Red Eléctrica Española.

## 1.2. Background

### 1.2.1. The role of cities

Most of the world's population lives currently in urban areas. Cities concentrate a large proportion of economic development, technological change and resource consumption, intensifying climate change and energy security issues. For those reasons, there is a growing need for collective action and innovation in the urban environment. Such a collective action would ensure a higher involvement of the citizens, and also of the demand side, which would lower the pressure on the generation infrastructure. Promoting the match between energy production and energy consumption at small scales such as districts could bring many benefits, both economic and environmental. In addition, the high densities of population and high consumption of resources that characterize cities present a great potential for the implementation of innovative energy models.

### 1.2.2. Sustainable urban development

Sustainable development has been traditionally defined as "development that meets the needs of the present without compromising the ability of future generations to meet their own needs". However, a new agenda is needed to ensure that urban areas will become resource-efficient: not only by being sustainable, but also by improving the current conditions and enabling policy frameworks that lay the foundations for positive social and environmental change. Smart Grids play a crucial role in this regard. The ongoing progress that we are facing towards unsustainability can only be mitigated by changing our way of thinking, modifying the normative, promoting education and developing new energy models. The following lines have been inspired by recent research sources and the interesting charter included in [4].

The increase of urban population is approximately exponential, and probably around the middle of this century more than 70% of people will live in cities. The unsustainability and deterioration of the quality of life in most cities of the world calls for a thorough regeneration of the energy systems at all scales. The proposed solutions should pay attention to new urban developments, but more importantly, they should look into solutions for the systems that already exist, which are the cause of the ongoing deterioration.

The profound impact that we are exerting on the earth's ecosystems obliges us to change our way of behaving. Cities are extremely complex urban ecosystems due to their mixed uses and functions, and the only way to approach this complexity is to develop models that simplify the reality and allow us to concentrate the efforts and apply multidisciplinary perspectives. The principles for urban development given in [4] lay out the general guidelines that should be followed in cities. They summarize the keys for urban regeneration, and allow obtaining a systemic equilibrium that guarantees the challenges that we are facing. These proposed requirements for the regeneration of existing urban developments include:

- To maximize the efficiency of the collected energy, Smart Grids will be implemented through the use of Information and Communication Technologies (ICT), which will be decentralized in high density urban areas that consume most of the on-site generated energy.
- To create a decentralized, efficient, clean and renewable energy system is the main issue. This decentralization reduces the vulnerability of the system and increases energy efficiency. Therefore, self-sufficiency is preferred over dependency.
- To encourage the maximization of energy self-sufficiency in buildings by taking advantage of the PV solar potential.
- The use of intelligent systems to enhance efficiency and reduce the consumption of resources will be promoted.

From the point of view of the present Thesis, several scales have to be distinguished in the urban environment in order to analyze alternatives that contribute to a sustainable urban development when focusing in buildings. The reason is that each scale approaches this mitigation from a different angle. Of course, the behavior of a single building is important, both for its occupants and the whole energy system. However, the present work will emphasize the even greater importance of considering larger scales, which allow for a more widespread use of energy-efficient systems and integration of renewable energies, taking advantage of the potential synergies between different buildings. The proposed scales are depicted in Figure 4. Each scale entails different assumptions, levels of detail and potential approaches.



Figure 4: Urban scales proposed in the present Thesis.

### 1.2.3. Smart cities

The term “Smart City” has been widely used in recent years, but there is no clear definition yet. In [5], several qualitative definitions of the “smart city” concept are considered. Even though every city has different characteristics, a set of core technical energy measures towards a sustainable supply and use of energy can be identified. and there are three main characteristics that seem to be common [6]: friendliness towards the environment, use of ICT as a tool for smart management and ultimate goal of sustainable development.

#### 1.2.3.1. Electricity generation from renewable sources in the urban environment

Traditionally, renewable energies have been implemented away from cities, in facilities such as wind farms, hydropower plants or solar field installations. However, they could (and should) also be integrated in the urban environment. The deployment of PV modules on the rooftops of buildings for instance is an interesting way to generate local electricity, substituting partially or even totally the electricity taken from the grid. Nevertheless, the microclimatic or morphologic conditions of cities should be carefully considered, since for instance wind might have poor characteristics for the implementation of micro-turbines or the solar access might be hampered by mutual shading between buildings in high-density cities. Therefore, a proper assessment of the suitability of renewable energy implementations in cities is paramount for their deployment, considering also the economics involved.

#### 1.2.3.2. Development of smart grids

The increase of electricity generated in the urban environment thanks to the implementation of renewable energies or micro-CHP technologies, together with requirements related to energy security, requires the adaptation of the current power grids for an optimal management: smart grids. Several deployment programs and demonstration projects of smart grids are already available, and others are currently under way.

In general terms, a smart grid is an evolution of the existing electricity grid with additional intelligent monitoring, control and communication systems, maximizing the efficiency of the grid, empowering consumers and providing flexibility by relying on information coming from all participants. The European Smartgrids Technology Platform, substituted since July 2016 by the European Technology and Innovation Platform Smart Networks for Energy Transition, defined Smart grids as “electricity networks that can

intelligently integrate the behavior and actions of all users connected to it - generators, consumers and those that do both – in order to efficiently deliver sustainable, economic and secure electricity supplies”.

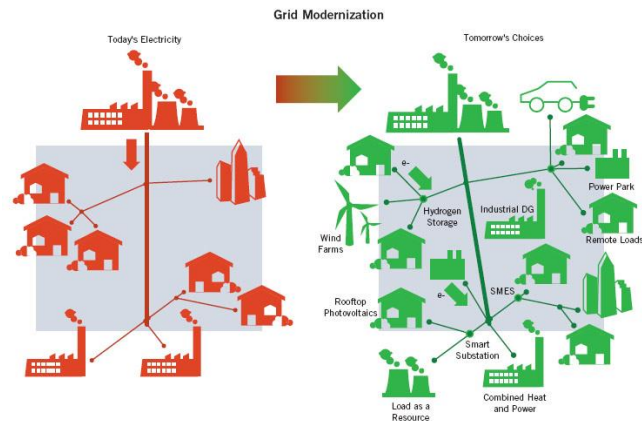


Figure 5: Devised evolution of the electricity grids. Source: IEEE.

One of the main capabilities of a smart grid is that it encourages local renewable electricity production, which is becoming increasingly important. However, a smart grid not only encourages local Renewable Energy Sources (RES) electricity production, but also offers energy storage, Demand Response (DR) opportunities and grid balancing. The main benefits associated with smart grids include:

- An increased integration of RES.
- Reduction of the environmental impacts.
- Simpler connections between technologies and generators of all sizes.
- Allowing customers to play an important role regarding the operation of the system.
- Consumers are more informed about the different alternatives of energy supply.
- More efficient transmission of electricity.
- Quicker restorations of the grid after perturbances.
- Reduced peaks and improved security and quality of supply.

The smart grid concept and all the potentially involved participants, from generators to smart appliances, are depicted in Figure 6.

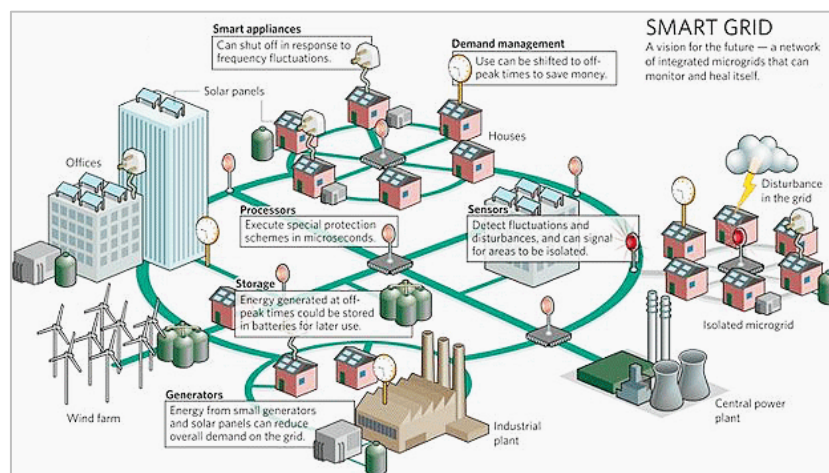


Figure 6: Smart Grid concept [7].

On the other hand, in [8] the following capabilities are considered essential for the implementation of smart grids:

- To enable the massive deployment and efficient use of distributed energy resources, including renewable energy sources and energy storage systems;
- To enhance the efficiency, resilience and sustainability of an electric grid by incorporating real-time distributed intelligence enabling automated protection, optimization and control functions;
- To allow the interaction of consumers with energy management systems to enable demand-response and load shaping functionalities;
- To enable real-time, scalable situational awareness of grid status and operations through the deployment of advanced metering and monitoring systems;
- To support the electrification of transportation systems by facilitating the deployment of plug-in electric vehicles and their use as mobile energy resources.

Despite all its advantages, there are still some barriers which need to be overcome for a large-scale implementation of smart grids, the most important of which are regulatory uncertainty, complexity of the technology and lack of experience, since the operation under real conditions is still under study. In addition, there are many different designs of distributed systems, which makes it difficult to have standardized products.

There is an important issue that should be borne in mind: the evolution of the Smart Grid concept to that of “Smart Energy Networks” or “Smart Energy Systems”, which do not only integrate the electricity grid but also every source of energy that is available, with different management methods. The purpose is to combine the knowledge of both worlds (thermal and electrical), frequently distinguished, and see the energy system as a whole. In particular, cogeneration systems in Smart Energy Networks may be a promising solution to supply energy in an effective way. The existing infrastructure should therefore be modified so as to satisfy this new broader concept beyond the limitations of a merely electrical vision. Due to its more widespread use, this Thesis will still refer to smart grids from now on, but bearing in mind that thermal energy will be also considered.

Smart grids are a key factor in future urban developments, composed of the following main elements: energy generation, renewable energy systems, transmission, distribution and grid operation, communication systems, energy storage and energy demands. So as to provide with a general overview, some of these elements will be briefly discussed in the following subsections.

#### **1.2.4. Information and communication technologies**

The measures that were previously suggested for their implementation in the built environment could be managed in an effective way by using Information and Communication Technologies. Although ICT are not a measure in itself, they could be a useful tool. In addition, ICT could help raising the awareness on climate change problems and informing private citizens and businesses about their contributions to GHG emissions, making them more active on reducing their energy needs and helping to integrate different sectors to reduce the energy demands [6].

The cornerstone of Smart Grids is to employ ICTs to gather and act on information of both generators and consumers in an automated way, interacting via a communication infrastructure. The communication infrastructure needed in smart grids consists of a set of different communication technologies, networks and protocols that support the connectivity amongst devices or grid sub-systems and enable the distribution of information within the power system, requiring scalability, timeliness and security [8]. This infrastructure may make smart grids more reliable, efficient, economical and sustainable for the electricity distribution and production.



There are different fields of communications within Smart Grids: smart metering, sensors, actuators, building automation, substation automation, power line networking, Home Area Network standards, application-level energy management systems, inter-control and interoperability center communications, cyber security, electric vehicles, and control systems [9] among them. Nowadays, many technologies exist to allow communications within the smart grid framework, including: cellular network, wireless communications, ZigBee, Ethernet or power line communications, each of which has a specific usage in a network. However, communication infrastructures require more than just a media and a standard to communicate: they also require protocols to transmit the data reliably. There are many different protocols for smart grid communication, some of which achieve the same tasks through different means since many different utilities, engineering and telecom governing bodies produce their own standards [10]. In the case of home or neighborhood-level communications, the best methods would be wireless. Among the different possibilities, one of the planned communication standards to be used for the home is Zigbee, which has the advantage of being low power and providing reasonable ranges for the communication between different devices in the home [9].

Figure 7 illustrates a general architecture for smart grid communication infrastructures. The electricity is distributed between the generators and the end-users with the use of bi-directional information, increasing system reliability. Smart metering provides real-time energy consumption, and the networks' operation centers can retrieve the power usage data to optimize the electricity generation and distribution.

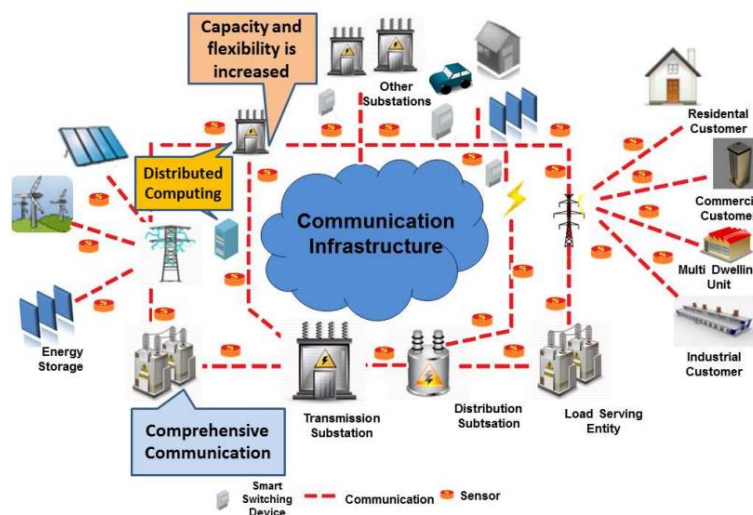


Figure 7: General architecture of Smart Grid communications [9].

### 1.2.5. Energy storage

One of the major challenges associated with distributed generation, smart grids and renewable energies in particular, is that they fluctuate with weather conditions, so storage needs to be used for mitigating their variability. Energy storage devices will be one of the keys of success for smart grids, and they will be needed to store excess electricity during hours, days, or even weeks.

The opportunities for storage are growing as a result of the increasing use of RES, the maturity of the technology, commercial availability, awareness of their benefits, and increasing support from regulators. Depending on the technology, some of them will supply energy during short periods, while others could last longer. Energy storage technologies fall into five different categories: mechanical, electrochemical, chemical, electrical, and thermal. Among those, electrical and mainly thermal storage (water tanks or structural thermal energy storage in buildings) will be considered in the present Thesis.

According to [11], structural thermal energy storage intends to activate the thermal mass so as to increase its use on top of its passive behavior to store energy, allowing an interesting potential in a smart grid context where moving loads contributes to increasing flexibility for the grid through demand response approaches. The previous study also claims that since this approach is exploiting the mass of a material that has been built for another purpose, it does not require additional investment in storage devices.

Previous studies on this subject have mainly focused on discussing the requirements to use the thermal mass for flexibility purposes, their benefits and limitations in terms of energy consumption savings during grid peaks [11]. In addition, the existing literature has shown that preheating or precooling strategies may achieve great benefits given the right conditions [12–17]. These preheating and precooling strategies are further discussed in Annex D.

### **1.2.6. Demand side Management and Demand Response**

The last link in the energy chain is, obviously, its use. In contrast to the past, when energy suppliers used costly backup reserves, consumers will be very important in future energy concepts. Energy is consumed in four main sectors: industrial, transportation, commercial and residential. Among those, buildings are responsible for the most significant portion globally – more than transportation or industry. Consumers in smart grids will be able to purchase electricity depending on different signals, adapting their behavior in accordance with their own needs, the state of the grid and the market prices. Building users will also play a vital role in establishing realistic consumption forecasts, since they are familiar with the processes in the buildings.

Equipped with automations, buildings may turn into “smart buildings” and be used to balance the generation and demand of energy thanks to two increasingly important approaches: Demand Side Management (DSM) and, similarly, Demand Response. The distinction between them is addressed in Annex C. The balance can be achieved through very different perspectives, such as shifting the time of use of appliances or using the thermal storage capacity of the buildings themselves. From the point of view of the author of this Thesis, considering these relatively novel approaches together with other traditional energy-efficiency improvement strategies will be a decisive step in order to attain the objectives set in recent standards.

## **1.3. From NZEB to NZED**

### **1.3.1. Nearly Zero Energy Buildings (NZEB)**

The concept of NZEBs has become very important during the past years, particularly after the release of the European Energy Performance of Buildings Directive (EPBD) Recast, which required all new buildings (and existing buildings undergoing major renovations) to be NZEB by 31st December 2020 (31st December 2018 for public buildings). According to the EPBD, the definition of a NZEB is “a building that has a very high energy performance and the nearly zero or very low amount of energy required should be covered to a very significant extent by energy from renewable sources, including energy from renewable sources produced on-site or nearby”. Even though the EPBD does not stipulate a specific procedure to implement NZEBs due to the great variety of buildings and climates that may be found in the built environment across Europe, it provides some clues for their implementation, such as the use of renewable sources or the use of district heating and cooling.

### 1.3.2. Nearly Zero Energy Districts (NZED)

According to [18], net zero energy communities are the next frontier in energy efficiency and sustainability, paving the way for the development of future smart cities and playing a key role in fulfilling the EU's ambitious targets. The previous study also claims that these communities should be places of advanced social progress, environmental regeneration and engines of economic growth. In addition, [19] states that opportunities for future growth will be created by innovating the built environment to zero, minimizing the energy consumption, eradicating energy poverty and mitigating the urban heat island and climate change.

The term NZED originates from NZEB, which is more popular. The idea of Nearly Zero Energy Districts is similar to that of NZEBs, but applied to clusters of buildings. Therefore, NZEDs, designed to maximize energy efficiency and the use of renewable energies at a district scale, are able to provide cost savings, bring environmental and economic benefits and achieve nearly zero energy by sharing infrastructure and resources. A Nearly Zero Energy District is an example of sustainable development, based on a holistic integrated approach. It is not just a fancy name used to describe a building with solar panels, but a new lifestyle that changes many details of a community, increases the energy awareness of its occupants and paves the way for the development of the future smart cities. In general, it is agreed that if a community is wasting energy or relying on fossil fuels, turning one of its buildings into a NZEB is almost meaningless. If an entire community is net-zero, that's more valuable, even if its individual buildings are not [20]. Therefore, the concept of NZED is becoming increasingly more important.

Instead of focusing on individual buildings, better results in energy savings may be achieved with integrated systems at a district level. However, even though the focus is not on individual buildings, the approaches should not rely on having highly efficient energy systems but poorly efficient buildings: they should consider a compromise solution. NZEDs will not be achieved without driving down the energy demand of the individual buildings, but not every building will be necessarily net-zero. NZEDs also support the energy efficiency in both new and existing buildings. If the district is new, this means that many design decisions have to be evaluated, including locations, orientations, and so on. If the district already exists, those parameters cannot be changed.

Even though there are some real examples of NZEBs that show that they are feasible, there are only a few cases that demonstrate the NZE concept at district level. An overview of existing models and approaches for sustainable development in districts is shown in [21], claiming that their review indicates limited literature in district experiences, lack of informative support for district evaluation and limitations of tools for individual buildings neglecting phenomena on urban agglomerations. The state of the art review given in [22] also revealed that several challenges exist in the initial stages of energy performance assessments of districts.

In Figure 8, a representation of the pillars of a NZED as considered in the present Thesis is shown.

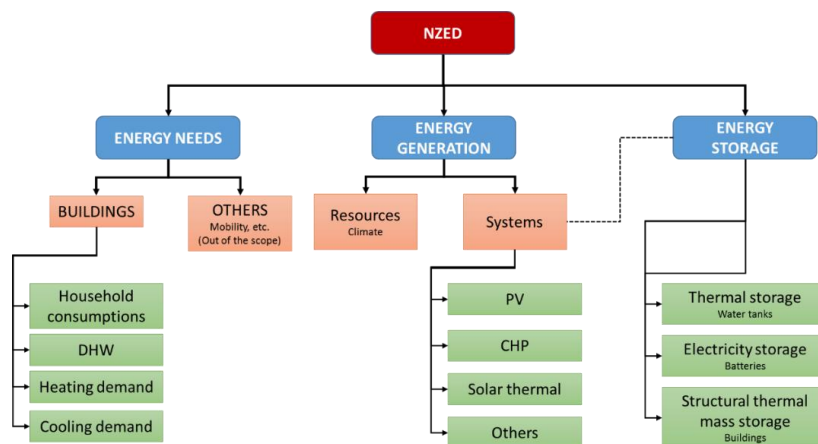


Figure 8: Pillars of a NZED considered in the present work.

First, the energy needs of the district have to be considered. This includes energy consumptions of buildings such as household electricity consumptions, Domestic Hot Water (DHW) and air-conditioning (heating and cooling), but also other district consumptions such as transport that are out of the scope of the present work. Also, energy production has to be taken into account, with an emphasis on renewable energies in the present work. Last of all, energy storage plays a very important role, since it allows a more efficient integration of renewable energies.

## 1.4. Smart cities within the H2020 programme

The Horizon 2020 programme is one of the major pillars of research and innovation initiatives in Europe. Among the calls for proposals available during the past years, we can find the topic “Smart Cities and Communities”. Here we may identify specific challenges such as “to demonstrate solutions at district scale integrating smart homes and buildings, smart grids, energy storage, electric vehicles and smart charging infrastructures as well as latest generation ICT platforms, accompanied by energy efficiency measures and the use of very high shares of renewables at the level of districts”. More specifically, the European Commission considers essential that the proposals in this case should:

- Integrate smart buildings to form a smart district with increased synergies and eventually increased efficiency and decreased costs.
- Consider the importance of a smart management of the different energy systems at district level and going far beyond classical electricity grids management only (e.g. smart solutions for storage including the intelligent use of the thermal mass of buildings that exploit synergies between these urban grids in order to increase efficiency and reduce energy costs).
- Incorporate renewable energy sources maximizing the use of local resources (including waste heat, electricity and/or heat storage) and high shares of self-consumption.

Within the scope of the most recent call in this respect [23], we may also find that integrated innovative solutions for positive energy districts will be developed and tested, considering the interaction and integration between buildings. Among the expected impacts of the proposals, we may find the contribution to meeting EU climate mitigation goals, increasing the share of renewable energies, leading the way towards wide scale roll out of positive energy districts, improved energy efficiency and district level optimized self-consumption. All these topics will be addressed in the present Thesis.

## 1.5. Reasons for choosing the district scale

As seen in the previous section, current efforts are directed at demonstrating solutions at the district scale. In order to achieve NZE in the built environment, several issues have to be considered. According to the International Energy Agency, the appropriate planning level to achieve a successful urban energy and climate change policy is at the neighborhood or district level. Besides, [24] claims that recent studies expose the need to explore energy efficiency solutions for buildings at the neighborhood scale (block to city district), since it is a scale large enough to identify patterns of energy consumption and supply beyond the boundaries of the single building, but small enough to address concrete solutions. Contrary to single demonstration buildings, the aim of neighborhood scale energy plans must be to find an economically optimized solution for the whole neighborhood rather than the latest technical solution for a few showcase buildings, otherwise a comprehensive implementation would not be achievable [25].

On a district scale, the NZED status is obviously easier to achieve in new communities. Renovating an existing neighborhood is more intricate, since some opportunities to increase the energy efficiency are no longer available (building orientation, thermal envelope,...). Until now, achieving NZE in an existing building meant to maximize its energy efficiency and use on-site energy. However, achieving NZE on a large scale needs looking beyond individual buildings for several causes that justify extending the scope of action. Therefore, there are various reasons why the district scale should be chosen instead of considering individual buildings:

- 1) Depending on the characteristics of each individual building, some might be able to achieve NZE but some may not. Widening the scale solves this issue, allowing the compensation between prosumers (consumers that also produce energy). In addition, NZED are a better approach for buildings that have more than a few stories. One of the reasons for this is that a NZEB is easier to achieve in low-rise buildings or low-density sites due to better solar access and more space available for the installation of PV modules, which is the most frequent way to generate their own energy.
- 2) NZED are able to use approaches that are not available for individual buildings, such as energy recovery, energy sharing or district heating/cooling systems. District energy systems require less fuel to operate than individual systems, using underground pipes with hot or chilled water delivered to the buildings of a district. They are able to exploit the load diversities in ways that are impractical for individual buildings. Also, the capacity of a district heating/cooling system may be smaller than the sum of the capacities of the individual buildings.
- 3) Using larger scales and perimeters allows to use not only the energy produced by the buildings themselves, but also in power generation systems located in their surroundings. This could correspond to the consideration of “nearby” produced energy of the new EPBD in ISO 52000-1. In particular, public spaces, streets or parking areas could be used.
- 4) Considering energy systems that contain many buildings offers also the possibility of sharing the energy between them and taking advantage of load diversities. For example, residential buildings are mainly used during the last hours of the day and during the night, while commercial or office buildings operate during the day. This would eventually allow one single energy system to supply both types instead of using two of them, with the consequent higher installed capacity, costs and energy use. In addition, there is also a possibility of sharing energy, for example using cooling waste heat for DHW use in dwellings [20].
- 5) Self-sufficiency could also be enhanced on larger scales. For example, the results in [26] indicate a shift in the economically optimal level of electrical self-sufficiency with scale, which in single-family houses means from around 30% at the individual building level to almost 100% in districts of 1000 single-family households.
- 6) The costs of a NZEB are usually high and paid by the users, while NZED could be funded by investors, energy services providers or even governments who seek sustainability. Approaching zero energy at a district scale creates opportunities for new business models, financing and utility incentive programs [27].
- 7) Many energy systems are more efficient and reliable in large sizes, such as Combined Heat and power (CHP), large boilers, chillers or other innovative technologies. The operation and maintenance is also easier. They are also able to achieve more cost-efficient solutions, since benefits can be obtained from economies of scale. For instance, the study in [28] is aimed at comparing the long-term system cost of three heat supply options: “individual”, “on-site” and “large heat network”. Their results showed that the large heat network option had the lowest system cost, whereas in most cases the individual option had the highest system cost.
- 8) Finally, many demand side management opportunities arise from the consideration of larger scales by taking advantage of the synergies between buildings, with approaches such as dynamic pricing or the participation in reserve markets with clusters of buildings. The aggregation of the loads at

district level and their control enables the creation of new revenue streams related to ancillary services, for example peak demand reduction, load shifting or frequency regulation [27]. This will be discussed in detail in Chapter 3, including two applications.

- 9) Considering the district scale allows to utilize public spaces as a means to increase energy efficiency by implementing techniques that allow to improve the microclimate around the buildings, reducing their energy needs.
- 10) The number of degrees of freedom is increased, so there are more possibilities to reach the final objective of achieving energy-efficient districts.

## **1.6. Road-map for an optimal design, sizing and operation of NZED**

In this section, a summary of the stages that should be followed for achieving NZED will be presented. From the point of view of the author of this Thesis, these are the key issues that are currently encountered when performing large scale analyses for a proper optimization of districts.

### **1.6.1. Preliminary analysis of the district**

*Aim:* To gather information about the district and all the resources at hand.

*Requirements:* Location, climate, building use, geometry and construction, energy requirements and their variation.

*Problem:* Too many buildings, uncertainties related to the requirements.

### **1.6.2. Conceptual design and optimization of the technologies to be implemented at the district scale**

*Aim:* To develop a procedure for the evaluation of different alternatives based on cost-benefit analyses, including solutions that affect energy demand reduction, the improvement of the HVAC installations or the implementation of new systems.

*Requirements:* Estimation of the energy demands in the initial situation of the district at least on an hourly basis and during a whole year, using a reference weather file. Tools for modelling and simulating energy production installations to satisfy the energy demands.

*Problem:* Too many buildings. Uncertainties regarding the electricity, heating and cooling demands. In the optimization of renewable systems (solar for instance), there is an additional problem due to the complexity of mutual shading on a large scale.

### **1.6.3. Design development and final sizing of the optimal solution**

*Aim:* Final dimensioning of the elements that compose the optimal alternative chosen during the previous stage, and selection of the optimal control strategy.

*Requirements:* Accurate determination of the energy demands of the buildings through monitoring and the laws governing the variation of the energy demands with climate and buildings' use.

*Problem:* Inability to measure every building of the district in detail. Difficulty to link the measured demands with the use of the building, especially in residential buildings. Knowledge gaps for the energy characterization of buildings in the previously mentioned conditions.

#### 1.6.4. Optimal management of the district and the grid

*Aim:* Guarantee the selection of the optimal operating strategy by using an objective function and taking into account energy production and different storage possibilities (such as thermal mass storage).

*Requirements:* Climate forecasting. Energy demand forecasting in simultaneous time scales (15 minutes, 1 hour, 1 day), to contemplate energy production and energy storage elements. Ability to anticipate the effect of preheating, precooling, solar control or night ventilation strategies on the energy demands.

*Problems:* Existing forecasting algorithms that adapt to the decision-making process are not sufficiently fast, especially if an optimal management includes simultaneous evaluations of the energy demands (including thermal mass storage) and the distributed generation installations.

### 1.7. Aim of the Thesis

The present Thesis is based on the belief that the consideration of the district scale is necessary to undertake enhancing energy efficiency in the built environment, as well as to address the commitments and obligations of the existing regulatory requirements. The main purpose is to contribute to the elimination (or at least reduction) of the problems linked to the development of NZED, which were mentioned in the previous section. The work in this Thesis has an instrumental aspect, focused on the problems derived from widening the scope of energy analyses to a district scale instead of considering individual buildings. In addition, there is a conceptual aspect that puts emphasis on the characterization, forecasting and manipulation of the energy demands of buildings. This is done with the purpose of finding solutions to the barriers that constraint the implementation of smart management systems (demand side management and grid management) on a district scale.

The present chapter of this Thesis has established that the former approach to enhance energy efficiency in the built environment, which traditionally focused on the individual level performance of buildings, was not optimal. This was justified by the fact that looking beyond the individual level offers many advantages, such as the exploitation of the synergies between different buildings.

Chapter 2 will address the drawbacks of most current approaches for urban energy analyses at large scales, which frequently make many simplifications. Several applications supported by 3D models will be shown to perform evaluations of the solar potentials or the energy demands for entire regions. Then, to overcome the drawbacks of simplified energy performance simulations, a new open-source tool will be developed. This tool will be capable of performing dynamic simulations of whole districts in a user-friendly, accurate way.

Once the advantages offered by large-scale energy analyses have been highlighted, Chapter 3 will explore different demand side management approaches in buildings and districts, presenting two applications. The first application will focus on the performance of a single dwelling, located in a plus-energy district in Germany. In this case, the impacts of different dynamic pricing strategies that manage the activation of a heat pump in response to price changes will be evaluated. As a continuation, the second application will increase the scale and evaluate the benefits of allowing direct control of all the heat pumps in a district to provide flexibility and obtain benefits from the participation in secondary reserve markets.

From the point of view of the author of this Thesis, the best way to evaluate a real district is to carry out a monitoring campaign to reflect the reality of the operation of the buildings with sufficient accuracy. Therefore, Chapter 4 of this Thesis will focus on defining a methodology for a proper characterization of districts through monitoring. A novel proposal for obtaining energy baselines in residential buildings will be developed and validated, both theoretically and experimentally, suggesting several possibilities for combining the proposed models with DSM techniques.

In Chapter 5, the methodology developed in Chapter 4 will be applied to characterize a district consisting of buildings with a limited use of air-conditioning, where temperature and total electricity consumption measurements are available. An innovative study will also be proposed, introducing the possibility of using surplus electricity to power the heat pumps of a social housing district and improve the thermal comfort conditions of the occupants.

Finally, Chapter 6 will combine several of the findings of the previous chapters to evaluate the benefits that could be obtained from the exploitation of the synergies between buildings. This will be done by implementing demand side management approaches on a district scale.

As a last contribution of this Thesis, Chapter 7 will summarize the results that were obtained. In addition, a new comprehensive methodology for the characterization of any existing district will be proposed, mentioning the necessary tools and procedures so that urban energy analyses can be carried out on a large scale, in an accurate way.



## 2. WIDENING THE SCOPE OF ENERGY ANALYSES IN THE BUILT ENVIRONMENT

---

In recent years, the research community is beginning to realize how important it is to focus on the building-group-level performance instead of considering individual buildings in order to support the Net Zero Energy concept. As highlighted in Chapter 1, the main reason is that individual actions are usually performed in an uncoordinated way, leading to much less benefits compared to the assessment of groups of buildings or districts as a whole, considering the interactions and synergies between them. Successfully predicting and modeling the energy performance of urban buildings has the potential to inform the decision-making of a wide variety of urban sustainability stakeholders including architects, engineers and policy-makers [29]. However, the knowledge gap between what works and the widespread adoption of practical implementations is a major preoccupation for them, since there seems to be no infallible solution for a successful implementation of new innovations on a large scale. Thus, developing strong and reliable evidence on the overall behavior of such innovations is a compulsory task.

Still, when a district needs to be characterized accurately, the energy performance of all of its buildings is not easy to estimate. A monitoring campaign should be planned to evaluate the real performance and use of the buildings, but the budgetary or technical constraints might only allow to monitor a few of them, and it is very intricate to select the most representative ones. As a valuable addition to current knowledge, the present chapter of the Thesis aims to provide the means so that evaluating approaches that require dynamic interactions (such as accurate energy demand estimations, solar potential evaluations or innovative demand side management opportunities) can be possible not only for individual buildings, but also on a district level.

### 2.1. Introduction

#### 2.1.1. Redefining the NZE concept: from individual buildings to districts

During the last decades, the concept of energy efficiency has received widespread attention thanks to the realization that energy generation requires fossil fuel resources that are finite, as well as the fact that climate change is related to carbon emissions. This has encouraged a tremendous amount of studies with different approaches related to the implementation of technologies capable of both producing energy in a more efficient way and diminishing its environmental impact. Researchers should also bear in mind the evolution in recent years from the concept of distributed generation and Smart Grids, to that of Smart Energy Networks. Several studies point out that the existing infrastructure and the electricity generation process will have to evolve in order to satisfy the new concept of Smart Energy Networks beyond the constraints of distributed generation. In addition, due to their high contribution to energy consumption, buildings should be particularly targeted in climate protection actions.

As mentioned in the introductory chapter, in order to achieve NZE in the built environment several issues have to be considered. By creating solutions that start at the city scale but address both districts and buildings, the potential for the uptake of synergistic and scalable solutions could be significant [30]. However, most approaches on a large scale do not have a detailed representation of the buildings in the area and make many simplifications. For this reason, further research is necessary to optimize urban energy systems on a district scale.

## 2.1.2. Use of GIS for analysing energy performances at large scales

To help in the process of analyzing the energy performance of districts, Geographic Information Systems (GIS) are a powerful tool. A GIS is a system able to store and manage geographic information of real objects. This allows to analyze spatial information of many different elements in a certain area such as a district or a city, as well as include additional information of such elements (in the case of a building, year of construction for example). As mentioned in the introductory chapter, standards such as CityGML may be used for the modelling of the 3D building data. 3D city models have shown huge potentials in the field of city planning, and the number of cities represented is increasing exponentially, at the same time that the investment costs and time required to build these models is decreasing thanks to new data collection technologies such as Light Detection and Ranging (LiDAR). Drones have also become a very efficient and low-cost solution.

Another important characteristic of 3D models is that they may have different Levels of Detail (LOD). According to [31], the CityGML 2.0 standard defines five LODs: LOD0 is a representation of footprints and optionally roof edge polygons marking the transition from 2D to 3D GIS, LOD1 is a coarse prismatic model usually obtained by extruding an LOD0 model, LOD2 is a model with a simplified roof shape, LOD3 is a detailed model with windows and doors, and LOD4 completes an LOD3 by including indoor features.



Figure 9: Five LODs of CityGML 2.0 [31].

GIS systems and 3D models may be used for many applications (see Figure 10). Estimating the solar potential on a large scale is one of their most prominent ones. Without 3D models, evaluating the solar potential for whole districts in an efficient way would be almost impossible. In addition, 3D models simplify greatly the process of obtaining the real geometry of the buildings in a district. The difficulty to produce detailed building models on a large scale is the reason why accurate simulation tools are usually only applied to individual buildings. Therefore, the availability of 3D models of districts facilitates the process of evaluating energy demands or solar potentials on a large scale.

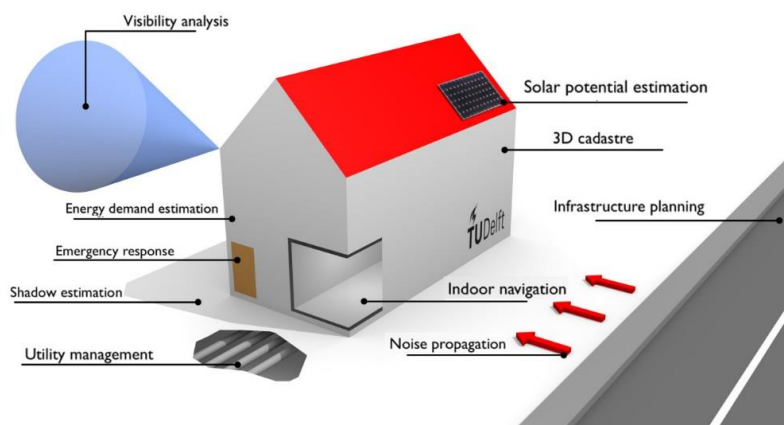


Figure 10: 3D city models may be applied in a multitude of application domains for environmental simulations and decision support [32].

### 2.1.3. Approaches for evaluating the thermal performance of buildings at urban level

A lot of information needs to be collected to estimate accurately the energy demand in a single building: year of construction, materials, area, shape, orientation, number of floors, height, glazing area and so on. For this reason, most energy evaluation tools currently available are only able to effectively analyze individual buildings. Therefore, there is a strong need to develop tools to precisely and easily perform a forecast of energy demands from single buildings to a district level [33].

According to [24], there are two different approaches to characterize energy services in buildings: top-down and bottom-up. Top-down approaches relate energy consumption to other macroeconomic variables and treat the built environment as a black box without describing demand characteristics. Conversely, bottom-up approaches analyze single buildings and address physical properties. Many bottom-up models have been developed, the most relevant of which are based on statistical, analytical (building physics) or hybrid methods of calculation. Statistical methods that are commonly used for the mentioned tasks are simple and robust, and based on historical data such as building typology and occupancy. They require relatively small amounts of information, but their limited characterization of energy services combined with coarse spatial and temporal resolutions of analysis makes difficult their use for the study of concrete energy efficiency measures in neighborhoods. On the other hand, analytical methods are based on physical approaches describing the dynamic exchanges of energy and matter among buildings, users, and the surrounding environment. However, their implementation in entire urban areas is usually constrained to data requirements and overall high modeling complexity [24].

There are many reduced-order methods which simplify the process of modelling urban energy use. Among them, we can find electrical circuit analogy based on resistor-capacitor networks, energy demand calculations based on quasi-static monthly energy balance, degree-day estimations based on heat transfer coefficient, steady-state methods based on energy balance equations, thermal shoebox models based on insolation analysis or clustering and reduced complexity models based on simplified state space methods [29]. However, such reduced-order methods often require large oversimplifications and require making strong assumptions (e.g., the heating set point is constant). Therefore, although these models provide a useful overview of the spatial distribution of energy demand, they cannot realistically represent the temporal dynamics of load patterns and their dependency on transient phenomena [34].

According to [35], building simulation tools currently available that evaluate energy consumptions are numerous, but the main lack of most of them is the ability of consider the environment around the building under study. Moreover, a key challenge in enhancing the energy efficiency of buildings in dense urban areas is the lack of accurate energy performance prediction models that consider the urban context, since building's energy use is significantly affected by other buildings (e.g., shading impacts heating and natural lighting) and microclimate factors (e.g., changes in wind patterns impact heat transfer and cooling loads) [29]. The urban context's implications for the solar gains through mutual shading are frequently ignored, and the effect of surrounding buildings in the reduction of heat emitting envelope area is only sporadically considered [34]. Also, according to [24] most current approaches on a large scale fail to address parameters such as solar radiation, self-shading phenomena, building thermal envelope, HVAC system performances or building real geometry, which highly influence both the intensity and the temporal response of energy services and represent important variables for a detailed characterization of energy consumption and the analysis of energy efficiency strategies in buildings.

Some tools have been developed to evaluate microclimatic effects in the built environment. For example, ENVI-met, a 3D microclimate model, has been integrated into EnergyPlus in order to quantify the interactive effects of computational fluid dynamics and thermodynamics on building energy consumption, and Urban Modeling Interface (UMI) is focused on modeling conditions such as shading and urban heat island effects in addition to energy use within the context of urban planning [29]. However, it is worth noting that even though UMI is able to simulate many buildings, the process of creating an urban 3D model including all the studied buildings, attaching the required information for thermal simulation purposes to every building,

and running a stock energy simulation is labor intensive and time consuming, which limits its usability [36]. Also, the 3D numerical tool SOLENE-Microclimate takes into account the unsteady building thermal behaviors, using the SOLENE thermo-radiative model which could be coupled with the outside airflow computed by a CFD tool.

For all the mentioned reasons, performing accurate dynamic simulations of the thermal performance of the buildings in a district on an hourly basis is essential when approaches such as demand side management strategies want to be assessed in a whole district. However, as previously mentioned, obtaining all the necessary information and carrying out simulations on such a scale is not an easy task. This issue will be examined in depth in following sections of this chapter.

#### **2.1.4. Domain reduction**

If a whole district needs to be accurately assessed, the first option could be to create a model for every single building. However, if it is desired to evaluate the buildings through precise dynamic simulations, this could be an almost impossible task when dealing with districts composed of many buildings, even if 3D models are available. The second option could be to choose and analyze in detail just a few buildings of the district, obtaining their heating and cooling demands and extrapolating the results to the whole district. However, this could lead to outcomes that are not representative of the district's behavior, since apparently similar buildings could in fact behave in very different ways.

Various methods for scaling such single building simulations have been developed, which include: using a single aggregated building to represent all individual buildings in a district, multiplying energy use of a single building by the number of buildings per archetype, scaling up results of an individual building model by a floor area weighting function, or adding up the energy use of individual buildings to represent the larger scale energy use [29]. Building performance simulation tools provide the means for an accurate evaluation of the energy demands, but in order to employ them, a systematic approach toward stock representation and domain reduction is required [34]. In this respect, clustering of the building sector has been widely used in the literature to perform a first step in finding representative buildings (centroids) and develop archetypes [36]. Choosing the representative buildings of a district also allows another possibility: if a NZED wants to be achieved, it is possible to focus only on the optimal candidates, instead of making economic efforts in buildings that might not easily achieve the NZE concept. The number of selected samples or developed archetypes depends on the diversity of energetic behavior in the investigated urban area, the computational and informational requirements of the underlying performance assessment method, as well as the available resources [34]. These clustering techniques to reduce the study domain will be further discussed in Section 2.6.

#### **2.1.5. Evaluating solar potentials at urban level**

An accurate assessment and understanding of the solar potential of cities is also paramount in the context of the urban energy transition. In the conceptual phase of new urban environments, it enables urban planners to design sustainable urban layouts and forms with optimized passive (influencing the heating and cooling demand) or active (integration of photovoltaic or solar thermal systems) solar energy strategies and better quality of life (daylighting). In existing neighborhoods, a solar potential analysis is a pre-requisite to identify the roofs suitable for solar technologies and reach the renewable energy objectives essential in the framework of energy policies and regulations [37]. Global estimates of suitable roofs for solar integration are about 60% of the entire roof area in Europe [38]. The calculated solar potentials are often integrated in a solar atlas (also called solar cadastre), which presents solar-related information for every roof of an entire city [39], region or state [40].

Electricity production by PV is growing world-wide and grid-parity is a reality in many places, even in low irradiance countries such as Sweden [41]. Solar radiation is a clean and abundant source of energy and PV is expected to contribute even more significantly in the future, since rooftops provide large areas suitable for solar energy exploitation. However, unlike the non-urban environment with little constraints to energy production, buildings have limitations on the available area, and many factors have to be considered such as construction restrictions or obstructions due to the surroundings.

The better the knowledge about the PV potential and investment cost of a region, the easier it is to help policy-making processes, prevent future disparities between supply and demand, and communicate the advantages of building integrated systems to the general public [42]. Therefore, the first step for this approach is an analysis to determine the solar potential of regions, which might be a challenging task due to the complexity of the urban environment.

Although a lot of research has been developed to measure the PV potential of buildings and plenty of studies have focused on the improvement of solar assessment by developing software and algorithms, 3D city models have not been made available in public domain on a full-scale yet. In order to estimate the PV potential, different approaches are applied, from simple estimations to airborne LiDAR technologies [43]. Depending on the scale and the level of detail required, some methodologies will be more appropriate than others.

#### **2.1.5.1. Methods for estimating solar potentials**

The first step for solar potential evaluations involves the use of models for estimating solar radiation. Since solar radiation measurements on tilted surfaces are rarely available, they must be assessed based on local global horizontal solar irradiance and the city geometry [44]. The total solar radiation on a tilted surface is the sum of three basic components: direct (also called beam), reflected and diffuse radiations. Different methods and models allow to estimate each of these components and to calculate inter-reflections between objects. A review of these models can be seen in the publication [45] by the author of the present Thesis.

As regards to the methods for estimating the solar potential, the literature review which has been carried out shows that there are many different methodologies which aim to determine the PV potential of a region, but as yet few methods for assessing urban scale impacts of solar energy system applications have been developed [46]. One of the most important aspects which should be borne in mind is the scale, since the same techniques cannot be applied at all levels (local, regional or continental). The study performed in [47] does a very complete methodology review and intercomparison. According to it, the main difference among the different procedures is the method used to determine the roof area: based on the ratio roof surface per capita, establishing a correlation between the population density and the roof area, or computing the total roof area of the target region. In [48] the solar potential in urban residential buildings is investigated at different levels of site densities, comparing the solar potential under different urban forms whose total available roof area was calculated with sample urban settings and weather data as the inputs. Other possible options are based on building typology through on-site data collection and visual inspection of a certain area [43] or statistical calculation models which compute the total roof area through aerial object-specific image recognition [49].

On the other hand, the three most important roof-area estimation methods according to [50] are the following: constant-value methods, manual selection methods and GIS-based methods. Our focus in this Thesis will be on GIS-based methods, since they can play a very important part in supporting decision making by tackling the urgently required energy transition [51]. For very precise calculations the most appropriate option is 3D modeling and building simulation [43].

### 2.1.6. Aim of this chapter

As justified in the previous sections, the evaluation of energy performances on a large scale, for instance the energy consumption of buildings or the solar potentials, can be very time-consuming when carried out with single building simulation approaches, mainly due to the process of gathering all the necessary data. This issue will be addressed in the present chapter. In order to show the possibilities offered by 3D models at district level, Section 2.2 proposes a study on the evaluation of solar potentials, estimating the economic and technical potential offered by the installation of rooftop PV systems in some 160000 buildings located in several municipalities of Germany. As a follow up to that work, Section 2.3 introduces innovative city tiling strategies for much more accurate estimations of urban shading and solar availability on a large scale, since in this case it will be possible to consider the influence of mutual shading between buildings instead of using reduction coefficients.

On the other hand, Section 2.4 develops a study on urban energy demand evaluation through 3D city models, using a steady-state method to calculate the demand of thousands of buildings at municipality level. To overcome the drawbacks of simplified thermal performance simulations that do not allow to evaluate approaches such as demand side management, a new open-source tool which overcomes this issue has been developed in Section 2.5, which allows the dynamic simulation of whole districts. Finally, clustering techniques will also be introduced in Section 2.6, which allow to reduce the study domain and choose the representative buildings of a district.

## 2.2. Evaluating solar potentials at urban level by using 3D city models

### 2.2.1. Introduction

The assessment of energy improvement measures at large scales such as districts is of paramount importance for the increase of renewable energy integration within energy markets. Nowadays, photovoltaics is considered as the most cost-effective option among the different renewable energy alternatives. For this reason, its technology has been chosen here to show the potential of using 3D models for promoting renewable energy integration in large areas. The scope of this section of the Thesis is to determine the solar photovoltaic potential at an urban and regional scale by using CityGML 3D city models, introducing an innovative tool: the Java-based SimStadt platform [52], which contains simulation models from the INTEgrated Simulation Environment Language (INSEL) [53], both developed at the Stuttgart University of Applied Sciences.

With the view of showing its full capabilities when dealing with PV potential analyses for whole regions, SimStadt has been used to estimate the PV potential of the Ludwigsburg County in south-west Germany, in which every individual building was simulated (157724 buildings in total). Both technical and economic potential (considering roof area and insolation thresholds) are investigated, as well as two different PV efficiency scenarios. The main purpose of this study is to determine what fraction of the electricity demand could be covered in both each municipality and the whole region, deciding the best strategy so as to reach that aim, the profitability of the investments and determining the optimal locations. An economic analysis and emission assessment has also been included, as well as some insights into the uncertainty of PV potential estimations.

The contents of this section have been extracted from the paper *“Assessment of the photovoltaic potential at urban level based on 3D city models”* [54], by *L. Romero Rodríguez et al* and published in the journal *“Solar Energy”*. For more detailed information about the urban modeling platform, methodology followed and obtained results, the reader is referred to that publication.

## 2.2.2. Methodology

The first step to estimate the solar potential of the municipalities under study is to figure out how much space is available for the installation of PV modules. Once the 3D models of the region are available, it is possible to know the total built area and the geometry of the buildings that shape it by using SimStadt. However, many circumstances may lead to the reduction of the initial roof area. An extensive literature review showed the great variety of different reduction coefficients used for calculating the available roof area of a region. After gathering all the information from related publications, it was decided to use for this study the approach shown in the flowchart in Figure 11, which illustrates the way to calculate the utilization factor. It should be noted that no previous study has used all of these factors at the same time, but only partially. Also, unlike previous publications in which these coefficients are applied to the aggregated results of a whole region, our study considers their application for each building individually, which increases the accuracy of the procedure. Once the available roof area is known, the PV potential can be calculated taking into account modules efficiencies, losses for temperature and irradiance, or the inverters efficiencies among others.

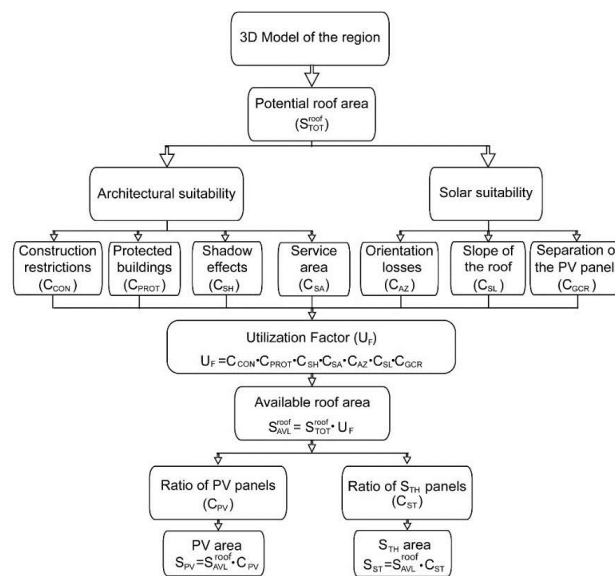


Figure 11: Flowchart of the available roof area calculation process.

The summary of all the selected reduction factors in this study is presented in Table 1. Some of them were selected by carrying out an extensive literature review. For further explanations about why these values were chosen, the reader is referred to the publication.

Reduction factor	Value	Reduction factor	Value
$C_{CON}$	Flat roofs: 0.8 ; Tilted roofs: 0.9	$C_{PV}$	1
$C_{PROT}$	1	$C_{ST}$	0
$C_{SH}$	Flat roofs: 0.7 ; Tilted roofs: 0.8	$\eta_{ef}$	Scenario A: 0.16 ; Scenario B: 0.11
$C_{SA}$	Flat roofs: 0.97 ; Tilted roofs: 1	$\eta_{TH}$	0.9
$C_{AZ}$	1 (considered in SimStadt)	$\eta_{AZ}$	$Az=0: 1 ; Az \neq 0: 0.95$
$C_{SL}$	1 (considered in SimStadt)	$\eta_{SYS}$	0.84
$C_{GCR}$	Flat roofs: 0.46 ; Tilted roofs: 1		

Table 1: Summary of reduction coefficients.

The methodology was then applied to the German County district Ludwigsburg. This county is located in the south-west of Germany, covers a ground area of approximately 700 km<sup>2</sup> and has a population of 354551 inhabitants. There is a total of 39 municipalities, of which 34 participated in a climate protection concept and could be analyzed. In total, 157724 buildings were considered. Based on the 3D models, the photovoltaic potential was calculated and compared with the electricity demand for each municipality. The calculation of the electricity demand is based on the available concession bills of each municipality, with data of 2013 or 2012 depending on the case.

### **2.2.2.1. Technical and economic potential**

The technical potential is defined as the implementation of PV panels on all available roof surfaces. This means that the whole available roof area after applying the reduction coefficients in the previous section is used. On the other hand, the economic potential is the result of considering only buildings with solar yields on their roof above a threshold value, which indicates a minimum amount of radiation that is required for the installation to be economically worth considering [38], or could be a percentage of the maximum PV yield in the region [55]. In addition, a minimum roof area will be considered, so that buildings whose roof areas are below that minimum will not be taken into account. These two thresholds reduce the number of PV installations as a function of the economic profitability of their implementation. As justified in the publication, the present study will consider for the economic potential an annual insolation threshold of 1000 kWh/(m<sup>2</sup> · year) and a minimum roof area of 40 m<sup>2</sup> for each building.

## **2.2.3. Results and discussion**

### **2.2.3.1. Technical and economic PV potential**

After gathering all the 3D CityGML models of the municipalities which constitute the County of Ludwigsburg, each of them was simulated within the SimStadt platform. Once the software calculated the area and solar radiation for each roof surface of the buildings by using the weather and radiation processors, the reduction coefficients proposed in Table 1 were applied, depending on the characteristics of each individual building. Then, the aggregated values of PV potential nominal power [kW<sub>p</sub>] and PV potential yield [MWh/year] were calculated. This was done for the technical and economic potential, as well as for the two PV efficiency devised scenarios.

As can be seen in Figure 12, the technical PV potential (installing PV modules on as much surface as is available) differs in each of the 34 municipalities. Scenario A (wafer-based modules with a higher efficiency) is always better than Scenario B (thin-film modules), due to the fact that the PV yield depends linearly on the efficiency of the modules. While Scenario A suggests that many municipalities could achieve more than a 100% coverage of the electricity demand, which means an electricity surplus in the region, only two of them would achieve it when Scenario B is considered.



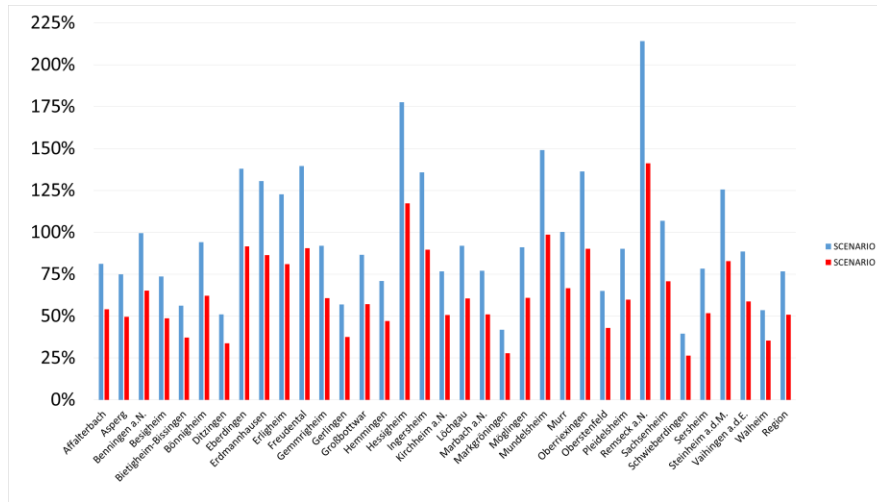


Figure 12: Percentage of the electricity demand covered in each municipality by PV for the technical potential strategy.

On the other hand, Figure 13 shows the results for the economic potential in each municipality, discarding every building with a roof area lower than 40 m<sup>2</sup> or an insolation lower than 1000 kWh/(m<sup>2</sup>·year). As it is apparent, the results are much lower than those of the technical potential in every municipality. In this case only a few municipalities could achieve more than a 100% electricity demand coverage.

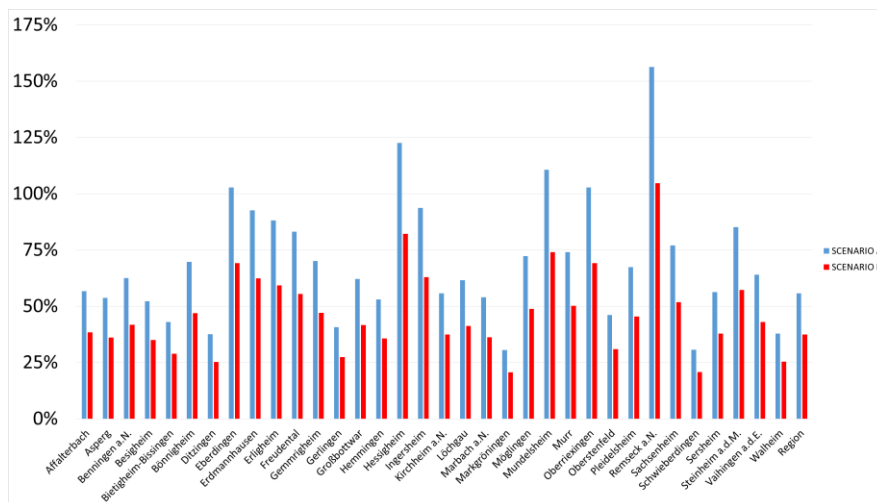


Figure 13: Percentage of the electricity demand covered in each municipality by PV for the economic potential strategy.

Regarding the aggregated values for the whole county, the results can be seen in Figure 14. If PV modules could be installed on all the available surface (technical potential), using wafer-based silicon modules (scenario A) could cover 77 % of the electricity demand of the region. On the other hand, if thin-film modules were used (scenario B with less efficiency), then only 51% could be achieved. It should be noted that the efficiency of the PV modules improves every year, so these percentages would increase accordingly. Conversely, taking the economic potential into account would result in lower payback periods, but the met electricity demand would be lower than that of the technical potential. Wafer-based silicon modules would cover 56% of the electricity demand, while thin-film based modules would cover only 37 %. The summary of the obtained results for the region is shown in Figure 14.

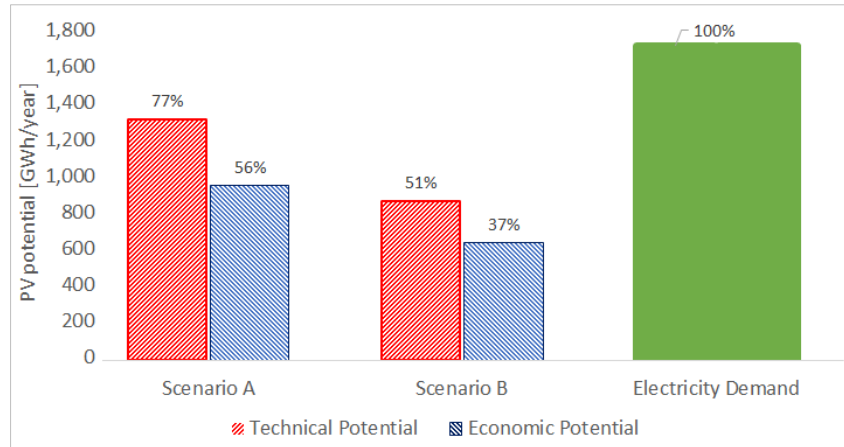


Figure 14: Percentage of the electricity demand covered by PV in the whole region for the two scenarios: technical and economic potential.

### 2.2.3.2. Emission savings

Quantifying the potential CO<sub>2</sub> emission savings thanks to the implementation of PV modules is another important outcome that may be inferred from this study. In this way, we are able to evaluate for each strategy and scenario the amount of CO<sub>2</sub> emissions avoided and the percentage of reduction compared to the initial situation, in which all the electricity is obtained from the grid. Table 2 presents the results for the technical and economic potential of the two considered scenarios. The results show the huge potential contributions of rooftop PV to the reduction of CO<sub>2</sub> emissions (and therefore other pollutants).

SCENARIO	Strategy	CO <sub>2</sub> emissions avoided [tCO <sub>2</sub> /year]	CO <sub>2</sub> emissions produced [tCO <sub>2</sub> /year]	CO <sub>2</sub> savings achieved [%]
SCENARIO A	Technical potential	639141	279674	70%
	Economic potential	464262	454552	51%
SCENARIO B	Technical potential	422907	495907	46%
	Economic potential	312288	606527	34%

Table 2: CO<sub>2</sub> emissions of the region for each approach of the study.

### 2.2.3.3. Economic feasibility

Another purpose of the present study was to develop an economic analysis of the implementation of PV modules in the region regarding the proposed strategies, so as to assess their feasibility. After extracting the required variables from SimStadt and applying certain chosen economic indicators, the results were obtained for each proposed strategy and scenario (see Table 3). Several findings can be deduced from the presented results. As can be seen, the economic potential of both scenarios would translate into much lower necessary investment costs for the implementation of the PV modules compared to the technical potential strategies. Nevertheless, it would also mean less PV yield, annual electricity savings and emissions reduction.

SCENARIO	Strategy	Energy yield [GWh/year]	Nominal power [MW <sub>P</sub> ]	Total Investment Costs [M€]	Total Annual Savings [M€/year]
		$E_{PV}$	$P_{PV}$	$C_t$	$A_s$
SCENARIO A	Technical potential	1318	1642	2101	116
	Economic potential	957	1107	1416	89
SCENARIO B	Technical potential	872	1087	1391	77
	Economic potential	644	744	953	60

Table 3: Economic results for each proposed strategy and scenario.

## 2.2.4. Conclusions

This section proposed to use 3D urban data models based on the CityGML standard to analyze the photovoltaic potential on an urban or even regional scale. The simulation methodology is based on a building by building roof surface analysis and irradiance simulation and carefully revises reduction factors for the energy yield determination, applying them for each building separately. Realistic strategies and scenarios for PV implementation were developed for a case study in Germany. Economic calculations were also performed so as to analyze the feasibility of the required investments. The proposed methodological approach should contribute valuably in helping policy-making processes and communicating the advantages of distributed generation and PV systems in buildings to regulators, researchers and the general public.

According to the results obtained, it is possible to achieve high rates of electricity demand covered by PV in many municipalities (even more than 100% for low density municipalities, which means an electricity surplus). Within the entire region with 34 municipalities investigated, PV systems could generate 77 % of the electricity consumption by using all available roof space, producing a total of 1318 GWh/year through the installation of 1642 MW<sub>P</sub>, thus reducing the CO<sub>2</sub> emissions noticeably. Conversely, 56% of the electricity demand could be produced if only roofs with enough insolation and a minimum surface area for an economically feasible PV installation are used. To realize the economically viable PV installations and reduce the electricity related CO<sub>2</sub> emissions by 51%, the estimated investment per capita is around 4000 Euros or a total of 1416 million Euros in the County. In conclusion, if properly designed these PV systems could significantly decrease primary energy consumption and emissions, reaffirming their usefulness and the important role they can play in the near future.

## 2.3. Improving the accuracy of solar potential assessments at urban level

### 2.3.1. Introduction

Assessing accurately the solar potential of all building surfaces in cities, including shading and multiple reflections between buildings, is essential for urban energy modelling. Although Section 2.2 introduced a complete study on solar potentials at urban level, the mutual shading between buildings was estimated through reduction coefficients found in the literature, since evaluating the interactions between such a huge amount of buildings was not possible due to the fact that the number of surface interactions and radiation exchanges increase exponentially with the scale of the district. Therefore, innovative computational

strategies are needed, some of which will be introduced in the present work. They should hold the best compromise between result accuracy and computational efficiency, i.e., computational time and memory requirements.

Hence, the present section addresses the issue of calculating more accurately and efficiently the solar potential of regions, using 3D city models. Studies such as the one presented here are essential for energy planning, with the aim of helping to guide the process of developing future policies and being able to make informed decisions at large scales. In this work, different approaches that may be used for the computation of urban solar irradiance in large areas are presented. Two concrete urban case studies of different densities (Manhattan in New York and Ludwigsburg in Germany) have been used to compare and evaluate the results derived from three different methods: the Perez Sky model, the Simplified Radiosity Algorithm and a new scene tiling method implemented in the urban simulation platform SimStadt, used for feasible estimations on a large scale. The main objective is to find out the most suitable computational methods, showing the best compromise between accurate shading calculation and reasonable computational complexity and requirements for large scale potential analyses. In addition, the solar potential for various solar energy thresholds as well as the monthly variation of the Urban Shading Ratios have been quantified for both case studies, distinguishing between roofs and facades of different orientations.

The information of this section has been extracted from the paper *“Setting intelligent city tiling strategies for urban shading simulations”* [45], by *L. Romero Rodríguez et al* and published in the journal *“Solar Energy”*. For more detailed information about the methodology followed and the obtained results, the reader is referred to that publication.

### 2.3.2. Brief description of the case studies

Two case studies of different densities have been selected in this work in order to analyze the impact of urban morphology on different Urban Shading Ratios: a medium density area typical of German “middle cities” (Ludwigsburg) and a part of Manhattan that represents high-density urban areas. Putting aside the differences of ground areas which do not play a role in our urban shading study, these two case studies have very different urban morphologies. Manhattan’s Floor Area Ratio (FAR) is ten times bigger than Ludwigsburg’s FAR, while the building average height is three times higher. Manhattan’s buildings are also more compact. The site coverage is higher in the case of Manhattan, with less solar penetration in particular at low solar elevation angles. Finally, the facade density of Manhattan is twice as big as in Ludwigsburg.

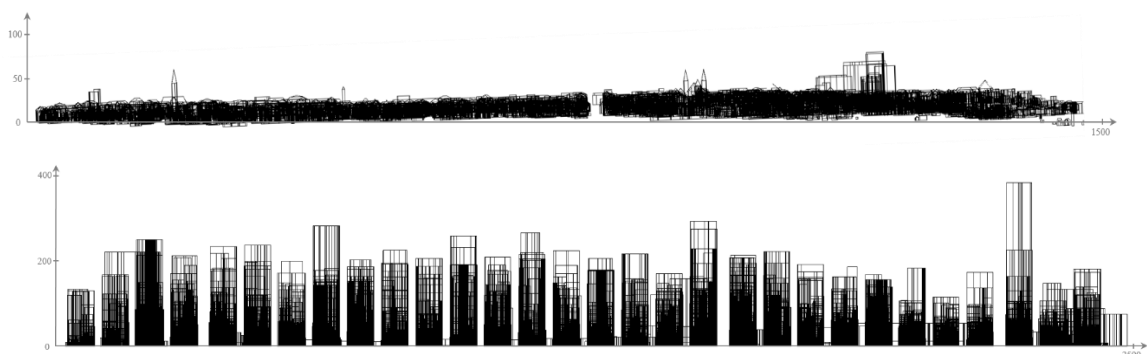


Figure 15: Representation of the case study Ludwigsburg with an East view (up) and Manhattan with a North-West view (down).

### 2.3.3. Solar radiation calculation approaches for urban energy analysis

This study is based on different radiation models and approaches implemented in SimStadt and compatible with urban scale applications: the Perez sky model, the Simplified Radiosity Algorithm (based on Perez sky model), and the newly introduced adaptation of the latter by using automatic tiling strategies. These models are explained in detail in the referred publication. The new automatic tiling algorithm was implemented in the SimStadt platform to overcome the memory and computing time limitations of the SRA algorithm for large districts or cities. This batch computing method divides the studied area in a number of square tiles and runs the Radiosity algorithm separately on each of them. The user may define the length of each square tile size, as well as the overlap length (see Figure 16). Besides reducing the required computational memory and time, this process is highly parallelizable, which may reduce even more the computational time by using a cloud computing approach.

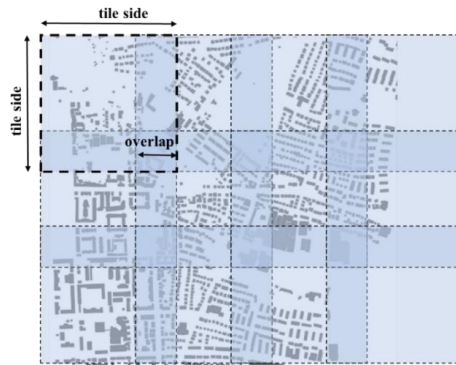


Figure 16: Example of tiling (tile size = 500m; overlap = 150m) for a studied area.

### 2.3.4. Identifying the best tiling strategies for middle and high-density urban areas

In this section, 23 tiling strategies which combine different tile sizes (50 to 500 meters) and overlaps (0 to 200 meters) were tested for both case studies. These tiling strategies generate different numbers of tiles and considered radiation exchanges between the building surfaces, which potentially corresponds to the square of the computed building surfaces number summed in all the tiles. This has a significant impact on the computational time and memory capacity requirement. In Figure 17, the computational times of the simulations related to the different tiling strategies and case studies that were carried out have been plotted in function of the tile size and overlap. It becomes apparent that the behavior of the computational time is more regular for Manhattan than for Ludwigsburg, since the buildings are more homogeneously distributed.

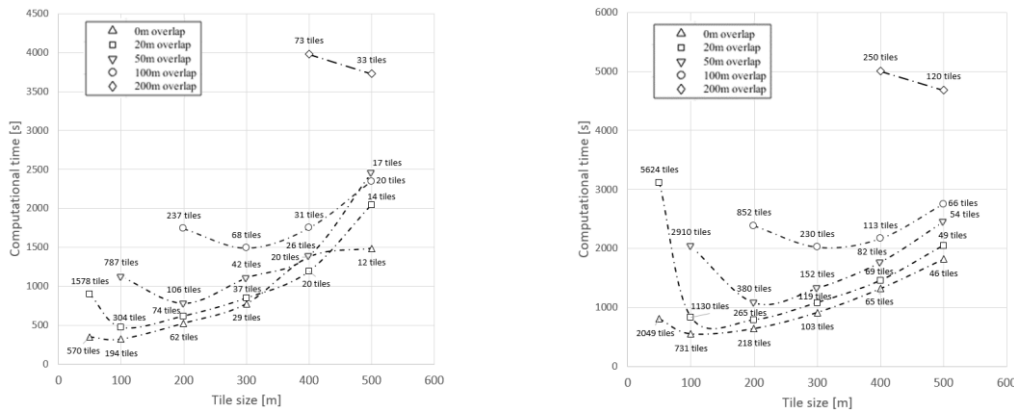


Figure 17: Computational time versus tile size for the considered strategies in Ludwigsburg (left) and Manhattan (right). The labels show also the number of tiles in each case.

### 2.3.4.1. Tiling strategy comparison for roof irradiance calculation

The Urban Shading Ratio (USR) is calculated as the quotient of the yearly solar radiations on all building surfaces computed using the studied tiling strategy, over the radiations computed with the reference tiling strategy (size=0, overlap=0), which corresponds to a Perez sky model without SRA (i.e. unobstructed scenario with the maximum solar potential). The 3D surfaces of Figure 18 represent the average USR of all building roofs weighted by their area as a function of the two tiling strategy parameters (size and overlap). The higher these parameters are, the more complete the consideration of the solar surface inter-obstructions and reflections is and therefore the more accurate the calculation. On the other side, smaller tile sizes fail to consider numerous surface interactions, and are therefore less accurate to evaluate urban shading impact. As it can be seen, higher tile sizes have higher Urban Shading Ratios. This means that when the number of considered buildings increases, the impact of obstructions is generally higher than the impact of reflections. A second clear outcome of Figure 18 is the relative difference of USR between both case studies: the high-density urban area of Manhattan has an USR two times higher than the middle-density area of Ludwigsburg. For the most accurate tested tiling strategy {tile size=500m, overlap=200m}, the annual USR reaches 12.8% and 25.7% for the case studies of Ludwigsburg and Manhattan respectively. As can be seen in the referred publication, focusing on the winter period this USR goes up to 17.4%, respectively 32.4%. Conversely, the worst tiling strategies {tile size = 50 m, no overlap} present USR for both case studies between 5 and 10%.

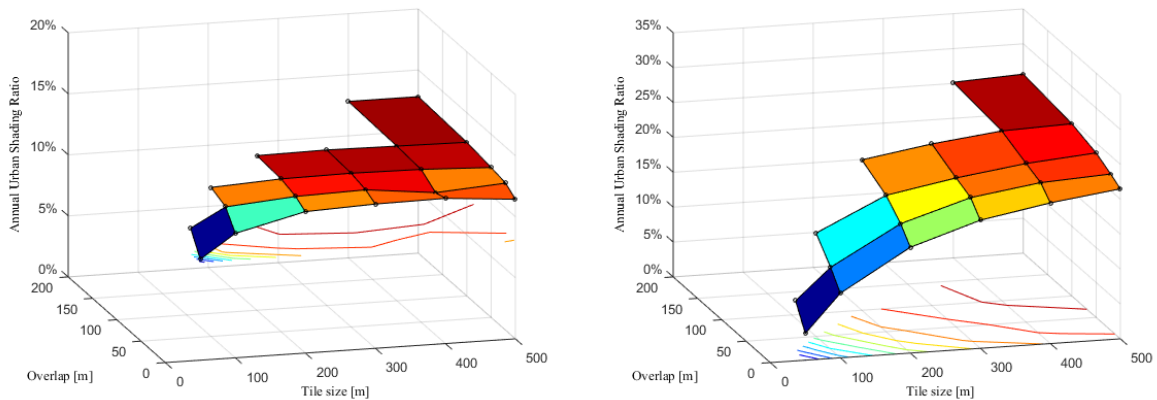


Figure 18: Urban Shading Ratios on roofs as a function of the used tiling strategy. Annual USR in Ludwigsburg (left) and annual USR in Manhattan (right).

### 2.3.4.2. Tiling strategy comparison for facade irradiance

In this section, only the solar radiations on the building facade surfaces are considered, as it is generally the case for building heating or cooling demand simulations, daylighting analyses or studies of building integrated photovoltaics, which may have a relevant role in urban environments [56]. The USR presented in Figure 19 is the average of the USR on all facades, weighted by their area. As illustrated by Figure 18 and Figure 19, the USR of facades are much higher (factor 2 to 3) than for roofs. This result is due to the bigger surrounding occlusions and therefore lower sky view factor of the facades.

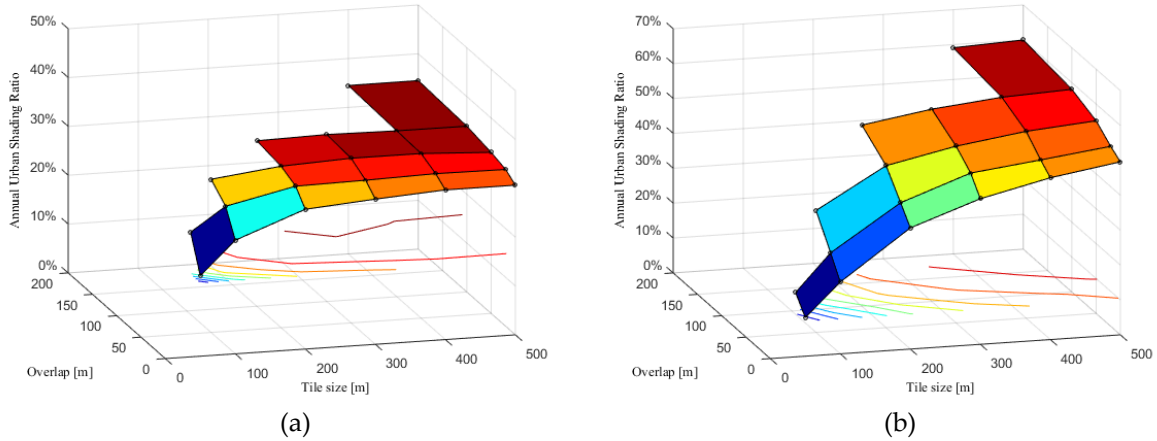


Figure 19: Urban Shading Ratios on facades as a function of the used tiling strategy. Annual USR in Ludwigsburg (left) and annual USR in Manhattan (right).

As an outcome of this study for both roofs and facades, the tiling strategy {size=300m, overlap=100m} can be considered as an accurate solar radiation calculation method for the case study Ludwigsburg, with a relative uncertainty below 1%. It represents a good compromise between accuracy and computational performance. For the case study Manhattan, any tiling strategy below {size=500m, overlap=200m} reduces the USR significantly (by 5% or more), and therefore would be considered as inaccurate in comparison. Consequently, the solar radiations on roofs and facades should be calculated at least with these “best tiling strategies”, which are used in the next section.

### 2.3.5. Solar potential “Identity Cards”

In order to assess the solar potential of a district, it is often useful to quantify the total building surface area that exceeds different solar energy thresholds. Facades of different orientations, flat roofs, and pitched roofs will be distinguished from now on for both case studies. As previously mentioned, only flat roofs are considered in Manhattan whereas an important part (60%) of the buildings of Ludwigsburg are represented with pitched roofs. The cumulative solar radiation distribution represented in Figure 20 and Figure 21 show an example of solar potential “identity cards” of the case studies.

In the case study Ludwigsburg, the total building external surface area is two square kilometers. Two thirds of it are facade surfaces, 20% are pitched roofs and the remaining 13% are flat roofs. Half of this surface area does not receive more than 600 kWh/(m<sup>2</sup>.yr), mainly due to shading and unfavorable orientation of the facades. Regarding the surfaces receiving more than 800 kWh/(m<sup>2</sup>.yr) solar radiation: only 15% of them are facades (representing 7% of all facades), 50% are pitched roofs and 34% are flat roofs. This trend is emphasized if one considers the surface areas receiving a minimum of 1000 kWh/(m<sup>2</sup>.yr), the typical threshold of photovoltaic installation profitability: 57% are pitched roofs, 43% are flat roofs, and no facades are present. The solar radiation received by flat roofs is limited by the global horizontal radiation (approximately 1150 kWh/(m<sup>2</sup>.yr) in Ludwigsburg). However, mounting solar systems on flat roofs with a favorable tilt and orientation (35° South) enable to collect up to 1350 kWh/(m<sup>2</sup>.yr).

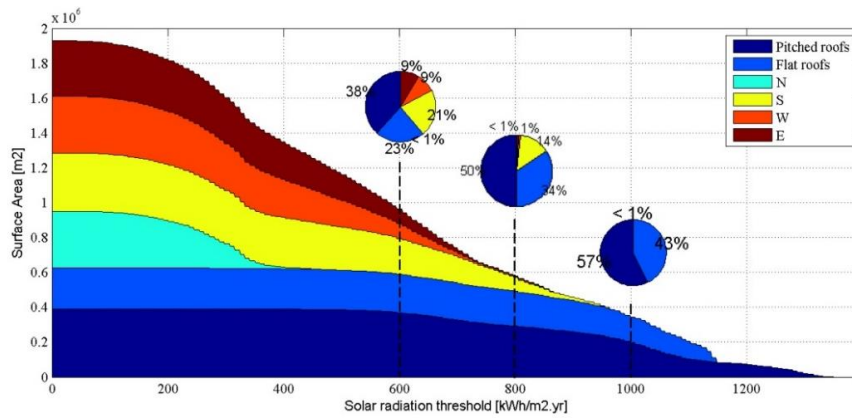


Figure 20: Cumulative solar radiation distribution in Ludwigsburg.

The Manhattan case study includes a total of almost 25 km<sup>2</sup> building surface area, of which 85% are facades. However, the latter represents only 39% and 20% of the surface area receiving more than 600, respectively 800 kWh/(m<sup>2</sup>.yr), and none of them receive more than 1000 kWh/(m<sup>2</sup>.yr). In comparison, 54% of all roof area receives more than 1000 kWh/(m<sup>2</sup>.yr) in Manhattan. While comparing both cumulative solar radiation distributions, the curve of Ludwigsburg is almost linear between the radiation thresholds 200 and 1200 kWh/m<sup>2</sup>.yr, whereas the curve of Manhattan is much more convex.

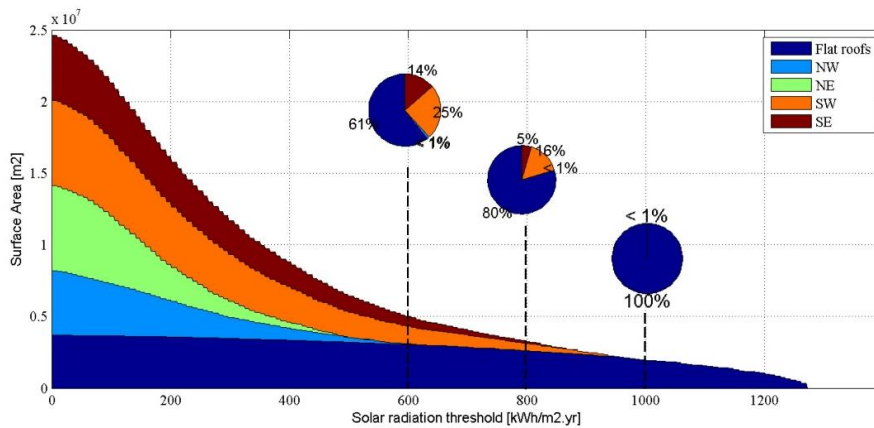


Figure 21: Cumulative solar radiation distribution in Manhattan.

In conclusion, although facades represent most of building surface areas (two thirds in Ludwigsburg and 85% in Manhattan), roofs have a greater potential for an economic exploitation of available solar energy than facades do. However, the use of facades should not be disregarded for photovoltaic generation due to the large areas concerned. The solar radiation on flat roofs may be optimally used by mounting tilted solar panels with a favorable orientation (between 25 and 35° south in latitudes like in Manhattan and Ludwigsburg).

### 2.3.5.1. Solar irradiance per facade orientation

The solar potential of a facade with consideration of the urban shading depends obviously on the surface orientation and the period of the year. In this section, the solar irradiances received on different facade orientations are investigated in more detail for both case studies. A “no-shading” reference case, which corresponds to the unobstructed scenario with the maximum solar potential, is compared with the “best tiling strategies” found out in Section 2.3.4. Facades are regrouped by orientations, with a ± 22.5° azimuth tolerance.



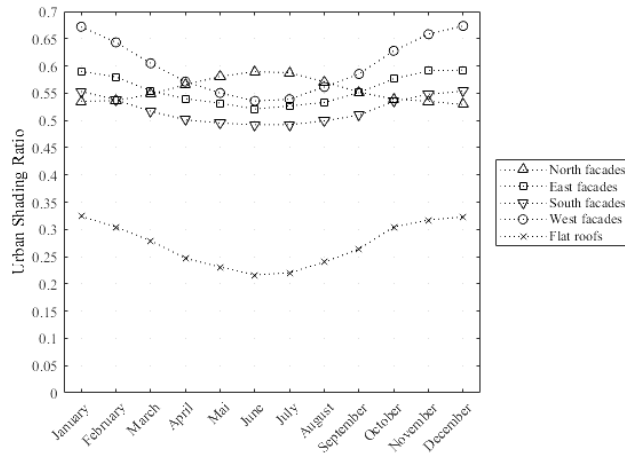


Figure 22: Monthly Urban Shading Ratio on roofs and facades in Manhattan

In Figure 30 we can observe that the USR yearly variation of the North facades with higher values in summer than in winter is the opposite to that of the other facades. The sun trajectories in front of the different facade orientations explain part of this outcome: contrary to other facade orientations, north facades receive direct radiations only in summer and middle seasons. However, in a dense urban area like Manhattan this direct beam is often shaded by surrounding buildings, since the morning and evening sun position is relatively low. This tends to increase the USR in the summer season.

The general trends are similar in the case study of Ludwigsburg, although the USR are significantly lower than in Manhattan (see Figure 23), as already seen in the previous section. The USR yearly variation has a wider amplitude from 0.25 to 0.51 as compared to Manhattan. The street layouts, regular in the case of Manhattan and without real pattern in the case of Ludwigsburg, explain this difference. For the South facades, the solar irradiance maxima are less pronounced and closer to each other than for Manhattan, due to the difference of latitude between these two locations.

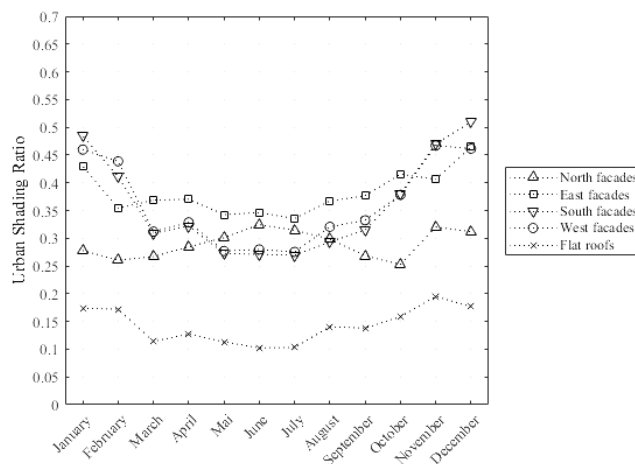


Figure 23: Monthly Urban Shading Ratio on roofs and facades in Ludwigsburg.

### 2.3.6. Conclusions

In this study, different methods of solar radiation computation in urban areas have been compared. Two representative urban case studies of different densities, New York (USA) and Ludwigsburg (Germany), have been used for the evaluation, employing 3D city models based on the CityGML format for a full and realistic urban environment analysis. Since the number of surface interactions and radiation exchanges increase exponentially with the scale of districts, innovative computational strategies for solar irradiance modeling that consider shading and inter-reflections have been introduced, partitioning the two case studies in square tiles of different sizes and overlaps to evaluate the computing performance.

The main contribution of this study is the accurate quantification at urban scale of the considerable impact of urban shading and multiple reflections on the solar radiation incoming on the building surfaces. They reduce annual solar irradiance by up to 60% for facades and 25% for roofs in high-density urban areas such as Manhattan. In medium density areas such as Ludwigsburg, tiles of 300 meters width and 100 meters overlap are sufficient to calculate with 1% uncertainty the solar radiation including shading and inter-reflections. In high-density districts like Manhattan, tiles of 500 meters width and 200 meters overlap are a minimum requirement in this case to compute solar irradiance with an acceptable accuracy.

This work has also justified quantitatively that the traditional method applied in building performance simulations, which considers only the direct-neighbor buildings, is far from enough to calculate reliably the solar radiation reaching a given building. Therefore, assessing this phenomenon accurately is of paramount importance for any reliable energy analysis in an urban context, including solar potential analyses, daylighting analyses as well as heating and cooling load calculations.

## 2.4. Urban energy demand evaluation through 3D city models

### 2.4.1. Introduction

The two previous sections have dealt with the estimation of solar potentials at urban level, which is one of the most frequently used applications of GIS. Another possibility offered by 3D models is the joint evaluation of the thermal performance of all the buildings of a district, which is paramount for enhancing energy efficiency at such scales. The present section will tackle this challenge by including a summary of the outcomes from the paper *“New 3D model based urban energy simulation for climate protection concepts”* [57] to this respect. This paper is co-authored by the author of this Thesis and was published in the journal *“Energy and Buildings”*. All the information in this section has been extracted from that publication.

First of all, let me recall that climate protection concepts for cities and regions are designed to establish CO<sub>2</sub> emission baselines and develop measures for climate change mitigation. Up to now, such concepts were based on aggregated consumption and emission data and only qualitative estimations of the effect of measures were possible. To better quantify the impact of mitigation measures, a large amount of data on the building stock (i.e. the buildings thermal properties), the network and supply infrastructure is needed, since it is a major challenge to quantify and predict the urban energy demand [58]. As mentioned in Section 2.1.3, the two main modeling strategies for building energy consumption are top-down and bottom-up methods (that apply either statistical or physical models). The former has some limitations, like the need of a large sample group, and it does not specify the impact of the energy conservation measures, which is important for urban energy strategies. If data can be combined with simulation models of buildings and energy systems, very powerful analysis possibilities for an energetic and economic evaluation of scenarios arise.

In the present study, 3D data models in CityGML format of the entire building stock of a region with 34 municipalities in Germany were used (the same as the study in Section 2.2) and enriched with data of building's year of construction and their function, to allow an automatized simulation of the heating demand of each individual building in the region (both residential and non-residential buildings). Not only the

current heat demand, but also two refurbishment scenarios for each simulated building were calculated: medium (standard refurbishment level corresponding to the German Energy Saving Ordinance 2009) and advanced (a level of refurbishment which is similar to standards of passive houses, but without a ventilation system with heat recovery). In this study, the proposed integrated climate protection concept had three main goals:

- The first purpose was to determine potentials to reduce emissions and design innovative projects to decrease or even avoid CO<sub>2</sub> emissions. This required an energy status analysis to ascertain strengths and weaknesses. Laying the foundations for continuing CO<sub>2</sub> monitoring and determining the potentials of renewable energies should be ensured too.
- Another objective was to issue a realistic and viable package of measures forming a basis for a financing concept.
- Thirdly, the rural district of the case study strives to become climate-neutral before the year 2050 and to reduce the total CO<sub>2</sub> emission per capita in the county.

A validation of the results of the urban simulation was done by using aggregated consumption data from each community. In addition, the local solar photovoltaic potential was also determined, although it will not be shown here since it was present in the previous sections. Besides that, in this study new methodologies were described to better quantify the costs and benefits of CO<sub>2</sub> mitigation strategies on a local or regional level and to support decision making.

#### **2.4.2. Obtained results of heating demands**

The urban simulation platform SimStadt [59], which was also used for the studies in Sections 2.2 and 2.3, was used to investigate the current status of energy demand of the buildings in the region under study, evaluate prospective energy demand scenarios and serve as an advanced base to design concrete measures for action. Within the space heating calculation workflow, the thermal energy demand was calculated for each building, where some basic data like year of construction, building usage as well as proper 3D geometry was available. Geometry data were provided in the CityGML data format. The 3D model included 80% of the objects in LOD2 and 20% in LOD1. The monthly energy balance was calculated according to DIN 18599-2, a quasi-steady-state method. The simulation results were then classified in different building categories: residential, public and industry, trade, commerce and services. Municipal concession bills for total electricity and gas consumption were used to compare the simulated results with the real consumptions.

Once the energy demands were available, the approach to validate the results was to use gas supply bills from the municipalities and compare them with the space heating demand simulated in SimStadt (see Figure 24). The heat demand of non-residential buildings was not considered in this analysis as their use is very variable with a high uncertainty in the simulation results due to uncertain usage profiles. As Figure 24 illustrates, the deviation ranges between -20 % to +20 % for almost half of the municipalities. Higher errors might be due to inaccurate sources of information for the measured gas consumption. Also, each municipality is supplied by different types of energy carriers, one of which is gas, therefore only the gas proportion of the heat demand was compared with the measured gas consumption.

Lacking of adequate data is always a big issue in analysing urban demands. This study found out that even the statistical data from communal sources of information can sometimes be thoroughly different from various sources, which makes the simulation validations very difficult. Proper user-related attributes such as internal gains, ventilation rates, daily and annual operation time of the building could lead to more realistic heat demands for the buildings. In our study, the values for these attributes were taken from a German standard, DIN 18599-10: 2011-2, however they might be very specific for some non-residential buildings such as the industry.

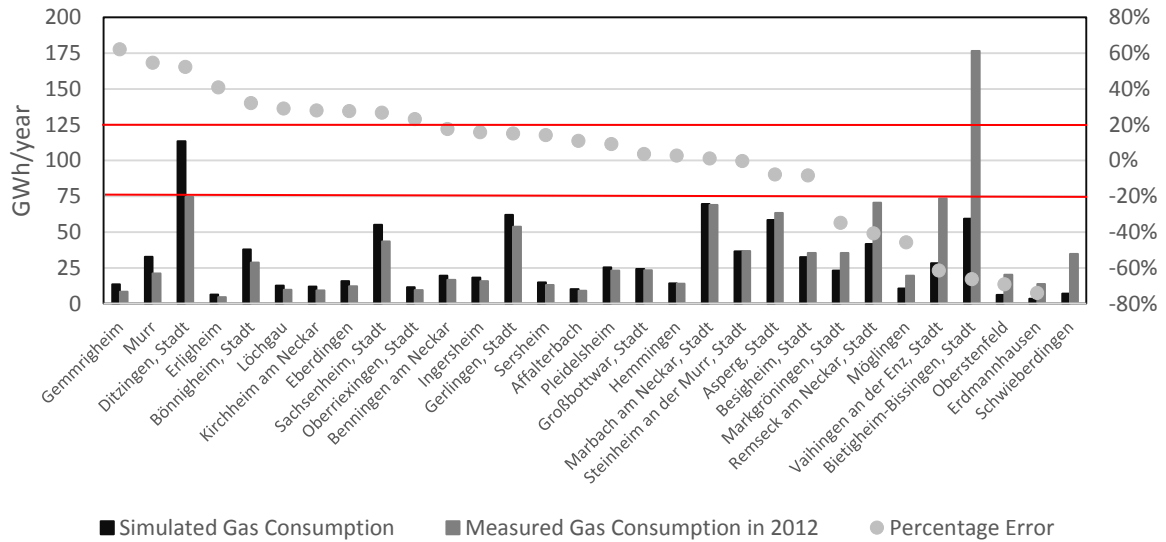


Figure 24: Comparison of simulated and measured aggregated heating consumption of residential buildings with gas heating.

Two refurbishment scenarios were also analyzed. The results showed that within the residential sector single family buildings had the highest efficiency potential, as their specific heating energy consumption was higher than for more compact multi-family apartment buildings (see Figure 25).

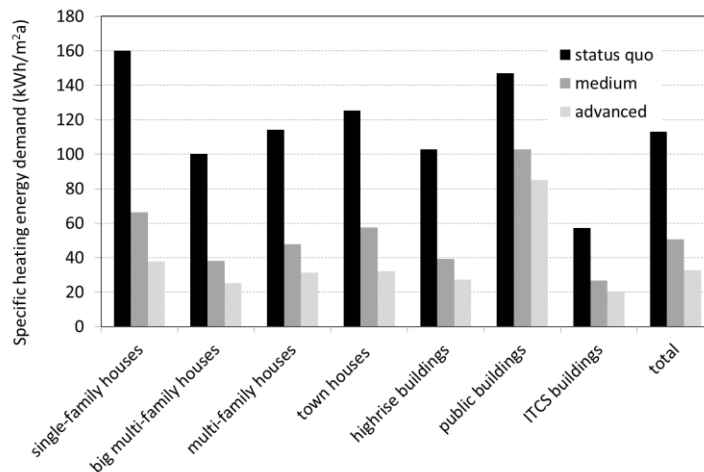


Figure 25: Specific heating demand for different building types in the municipality Hemmingen as a consequence of the refurbishment scenarios.

### 2.4.3. Conclusions of this study

Urban 3D models enriched with data on building’s construction, thermal properties and functions like residential or office offer excellent support for establishing climate protection concepts, allowing to quantify measures to improve energy efficiency and integrate renewables. In this study, SimStadt was employed for developing a climate protection concept for the case study of Ludwigsburg with almost 177,000 residential and non-residential buildings, quantifying CO<sub>2</sub> emission reductions, energy savings and energy cost savings for different measures and initiatives. The heat demands of the buildings were calculated building by building. This study indicated that it is very challenging to get detailed and reliable municipal consumption data to seriously validate simulation results, since sometimes the measured gas consumptions in a large scale

such as a municipality can even be not trustable. This problem bolds out the advantages of an automated platform for calculating heat demand in large scales such as cities, especially if there is no measured consumption data available or a prediction for a new scenario is needed.

It was shown that for this case study, on an aggregated municipal level, the deviations between measured and simulated gas consumption were between 20-30%, or sometimes higher where the input data like refurbishment data was not fully available. However, previous validation works at scale of building-blocks with good monitoring data quality demonstrated that the error between consumption and modeled yearly heating energy demand could be less than 10%. Therefore, it is recommended for the municipalities to pay greater attention on intelligent data collection with particular focus on the building's year of construction and refurbishment status in their databases. It was also shown that for Ludwigsburg, applying the highest standard refurbishment scenario reduced the heating energy demand of the building sector up to 58%, or by 46% applying medium level of insulation.

All in all, using the automated workflows for urban energy modeling makes it possible to establish and evaluate policies on a municipal and regional level. With reliable input data such as up-to-date 3D models as well as buildings construction and usage data, this work showed that building efficiency, refurbishment scenarios and renewable integration can be well quantified to support decision making for developing climate protection concepts. It is even more worthy where achieving current state of consumption of the buildings is challenging, or analyzing different scenarios (e.g. refurbishment scenarios) is of great interest.

## **2.5. New tool for modelling and estimating the energy performance of districts**

Nowadays, it is very common to find 3D models of cities all around the world. Tools such as SimStadt are able to calculate the energy demand of thousands of buildings in a district. However, they do so through simplified calculations such as static energy balances that only consider dynamic effects through correlation factors. The interconnection of 3D models with software tools that evaluate the thermal performance of buildings in an accurate and dynamic way is very rare, but such tools are necessary in order to evaluate the thermal performance of a district in which complex interactions take place (not considered in simplified models). Only in this way could time-dependent strategies such as demand side management be assessed properly on a large scale.

The proposal of this work is to introduce a new tool that has been developed and will allow to simulate the thermal behavior of whole districts in a user-friendly, accurate and simple way. In order to evaluate the thermal performance of all the buildings in a district, the first requirement is to know their geometry. In this work, using open-source software was considered compulsory, so that any potential user could employ it. The proposed method solves also the problems of scarce publicly available urban digital building information, since potentially, any district of the world could be modelled following this procedure thanks to the widespread availability of open-source geometric data such as Google Maps. However, it should be mentioned that this tool could also be eventually coupled with other 3D model formats such as CityGML, which would provide the necessary geometric information, or even models obtained from the cadaster of the municipality where the district is located.

### **2.5.1. HULCGIS**

After reviewing all the free and open-source Geographic Information Systems softwares that are available, QGIS [60] was considered as the most suitable option. QGIS is an application that supports viewing, editing, and analyzing geospatial data. QGIS also supports both raster and vector layers. In the latter, vector data are stored as either point, line, or polygon features. Most importantly, QGIS allows the integration of plugins written in Python, which can perform many geoprocessing functions.

A plugin named “HULCGIS”, due to its combination of HULC (Unified LIDER-CALENER software tool) and GIS, has been programmed in Python and integrated within QGIS. HULC is one of the official building energy certification tools in Spain, which allows to obtain the energy demands of individual buildings through detailed models and dynamic hourly simulations. The new plugin that has been developed allows to obtain an attribute table that contains the information of all the buildings of the district under study: geometry (coordinates of all the nodes), year of construction, number of floors, floor height, glazing, area and so on.

First of all, the user creates the polygons that represent the buildings of the district. This can be done in two ways: either the user uploads a file in which the polygons are already created (such as the Spanish cadaster), or the polygons are created manually by clicking on the screen for each node (using Google Streets, Google Satellite or Open Street Maps for example as background images to help in the process). Once each polygon is created, the user is asked to fill in the necessary information such as the year of construction, which could be obtained from the Spanish cadaster. In Figure 26, an example of the polygons created in a district in Southern Spain can be seen, as well as the HULCGIS user interface programmed in Python.

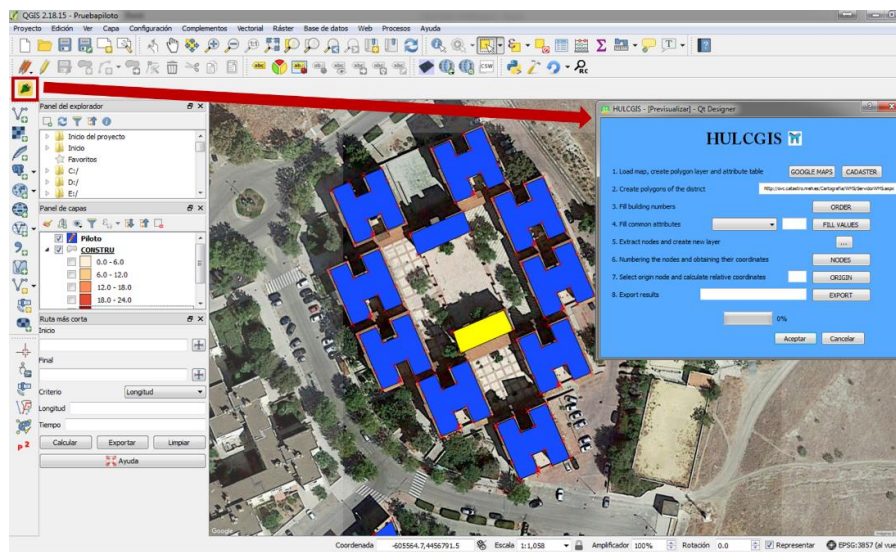


Figure 26: Screen capture of the HULCGIS plugin within QGIS.

After creating all the polygons of the district, the steps shown in the HULCGIS interface are followed: the polygons are converted into nodes, these nodes are then numbered, and finally their relative coordinates after choosing a reference node are obtained. Once the process is finished, the user exports the results, and an attribute table is saved as a text file. An example of attribute table is given in Table 4.

Building number	Year	Floors	Floor height	Glazing [%]	Area	Vertex	Coord_X	Coord_Y	X	Y
1	2000	2	3	15	302.52	1	-1503675.273	3405314.082	0.00	0.00
1	2000	2	3	15	302.52	2	-1503676.297	3405315.141	-1.02	1.06
1	2000	2	3	15	302.52	3	-1503681.206	3405320.256	-5.93	6.17
1	2000	2	3	15	302.52	4	-1503691.693	3405310.191	-16.42	-3.89
2	1980	5	3	15	843.13	21	-1503459.603	3404507.953	-8.89	35.20
2	1980	5	3	15	843.13	22	-1503480.709	3404467.99	-15.81	26.21
2	1980	5	3	15	843.13	23	-1503455.384	3404456.165	-4.48	14.40

Table 4: Example of attribute table in HULCGIS.

### 2.5.2. Creation of HULC models

The file with the attribute table of the district contains all the information that is necessary to create a model for each of its buildings. This file is read by a tool programmed in Visual Basic for Applications (VBA), which will use all the available information. HULC is not able to simulate more than one building at the same time. Therefore, this tool will generate one HULC file for each building individually, iterating between all the buildings included in the attribute table. In addition, if two buildings are adjacent this would be identified, and the corresponding walls would be modelled as adiabatic.

One of the most important steps towards a more accurate evaluation of the thermal performance of districts offered by this tool, apart from performing dynamic hourly simulations, is that the surroundings of each building are accurately considered, since the geometry of all the other buildings of the district is taken into account in every simulation. Nevertheless, in order to reduce the computational time, not every building of a district should be considered, since a building 1 kilometer away from the one that is being studied would produce no shading on it. To limit the distance of the surrounding buildings that should be considered, the outcomes of the study developed in Section 2.3 regarding city tiling strategies will be used. Therefore, in the case of a medium density district, a square tile size of 300 meters around the case study building would be enough. In case of high density districts, the size should be increased up to 500 meters.

For example, focusing on the information of one building in Table 4, we can see that the coordinates of all of its nodes as well as the number of floors and their height is known. This allows to convert this information into that which HULC needs to create all the geometry of the building, including the walls with different orientations, the component in contact with the ground and the roof of the upper floor. Then, the percentage of glazing is used to create a window in each wall of the building, located in the middle and with the corresponding area. Since it is not possible to discern the location of the windows in walls of different orientations in this simplification of the district, it will be considered that every wall of a building will have a window whose size depends on the percentage of glazing of the building and the area of the wall where it is located (unless it is adjacent to another building). Last of all, the year of construction allows to estimate the materials of the walls, roofs, types of windows and so on, assigning default values from typical buildings of the corresponding year. Eventually, the 3D model of the district could also include information about the use of the building, assigning different internal gains, operation schedule and so on. An example of a building model generated in HULC is shown in Figure 27, for the same district that was displayed in Figure 26. The current level of detail obtained by HULCGIS corresponds to approximately an LOD1, although it could potentially be used to create even more detailed multi-zone models if the information were available in the 3D models.

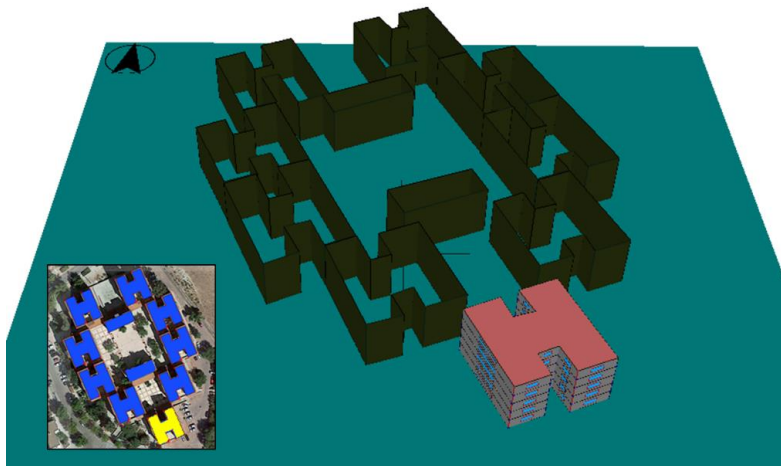


Figure 27: Example of HULC building model created by HULCGIS.

### 2.5.3. HULCGIS validation

For the purpose of determining the effectiveness of the developed tool when assessing the thermal performance of a building, a validation has been carried out. HULCGIS was used to obtain a simplified model of a building located in the province of Seville, in which the real plans, construction features and so on were known. A detailed model with the real geometry was developed and simulated in HULC. Then, the HULCGIS simplified model was created and simulated. A comparison of the geometry of both building models can be seen in Figure 28.

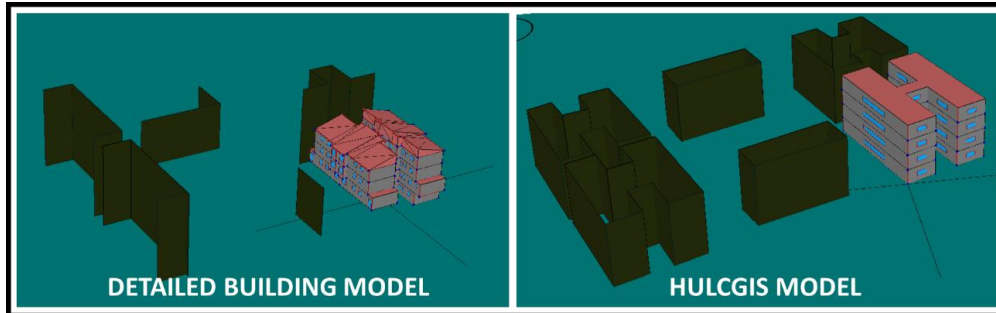


Figure 28: Comparison between the building models.

The hourly energy demand results in Wh are compared in Figure 29, where the positive values are hourly cooling demands, and the negative values are heating demands. As it can be seen, the values given by the HULCGIS model are a bit higher than those of the detailed model. However, it should be taken into account that there are many simplifications in the process: the shape of the roof, estimation and location of the glazing, allocation of the materials depending on the year of construction and so on. Despite this, the correlation between the results at building level is quite good.

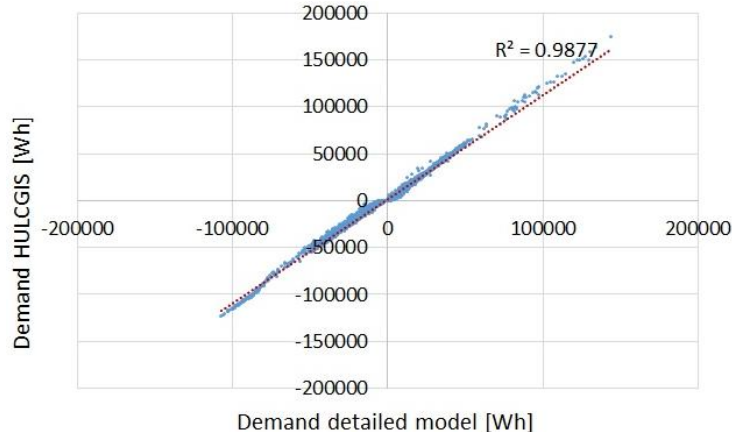


Figure 29: Comparison of the results between the detailed model and the HULCGIS model.

### 2.5.4. Tool for the estimation of demand reduction measures in districts

The tool that has been developed in the present work offers another potential approach. Since the information of the geometry of all the buildings of the district is already available, why not use it to simulate whole districts with different thermal mitigation or even DSM strategies? This is possible thanks to an additional tool that has been developed, which allows to select the values for certain parameters instead of using the default values assigned through the year of construction.



Tool for the estimation of demand reduction measures in districts				V 0.1			
Simulate district or building?	District	Climatic zone	A3	Use default values?	Yes	Consider shading between buildings?	Yes
Building number	1	Occupancy [m <sup>2</sup> /person]	33.33	ACHeq [1/h]	1.13	Distance [m]	1000
U_walls	1.77	Lighting [W/m <sup>2</sup> ]	4.40	Night ventilation [1/h]	4	Free floating?	No
U_roofs	1.37	Equipment [W/m <sup>2</sup> ]	4.4	Thermal bridges reduction [%]	0	Choose set-point temperatures?	No
U_floors	1.43	Solar factor in winter	0.85	Solar factor in summer	0.85	CREATE BUILDING	
U_windows	5.7					SIMULATE	

Figure 30: User interface of the tool for the estimation of demand reduction measures in districts.

In this way, it is possible to simulate a whole district with the base case scenario, and then simulate it with an improvement of the thermal insulation of all of its buildings for example. This provides a very powerful tool for an accurate assessment of the potential savings achieved by thermal mitigation strategies in whole districts. This tool allows to change the transmittance of walls, roofs, floors and windows, as well as the internal gains, solar factor of the windows, thermal bridges and ventilation. Furthermore, it is possible to carry out the simulations in free-floating, so that the effect on the thermal comfort of the occupants after applying different improvement measures can be evaluated, instead of evaluating the energy demands.

Last of all, it should be mentioned that there are open access plugins available in QGIS that allow the visualization of districts in 3D. Any of the parameters could be used to color the polygons of a district. Therefore, it would be possible for example to add a column to the attribute table with the result of the energy demand of each building calculated by HULCGIS, and visualize then the results in 3D. An example of this kind of illustration is shown for some buildings in La Graciosa Island in Figure 31.



Figure 31: Example of visualization of results for some buildings in La Graciosa Island (Las Palmas, Spain).

## 2.6. Review of clustering techniques for decision making in districts

### 2.6.1. General concepts of clustering approaches

As mentioned in Section 2.1.4, it is unfeasible to produce a very detailed model for every single building of a district in order to assess its overall energy performance in an accurate and dynamic way, mainly due to the intricate data gathering processes and the enormous computational power and time that would be needed. Even if a detailed tool such as HULCGIS is used, the characterization of a district should involve a domain reduction process afterwards, capable of reducing the sample of buildings so that even more detailed

modeling and monitoring has to be carried out only on just a few samples.

The use of representative buildings of a district permits the creation of benchmarking models, as well as the possibility to assess in detail different approaches that involve dynamic interactions such as demand side management. Also, by limiting audits and metering to representative buildings, data gathering challenges are mitigated and the use of data analytics coupled with building simulation has the potential to provide efficient solutions [61].

According to [61], most studies that select representative buildings use statistical approaches, but they usually analyze single building features only (e.g., total energy consumption) and do not focus on the analysis of multiple features in parallel. For this reason, the identification of representative buildings may be biased towards a particular feature and consequently other building characteristics that are important for building energy modelling may be underrepresented. In this context, statistical methods can exhibit a weakness in terms of providing holistic results for representative building identification. An alternative to statistical methods is clustering, a data-mining technique that allows the grouping of elements sharing similarities, identifying hidden structures in datasets and defining classes.

Clustering has been applied for different purposes in the building sector, summarized in five major areas of interest [61]: building benchmarking, energy profiling, representative building identification, predictive modelling and other areas mostly related to occupant behaviour. Once the clusters have been defined, it is possible to select the most representative object of a given group. Clustering techniques are well documented, and most common clustering algorithms include: k-means, model based clustering, hierarchical agglomerative clustering and k-medoids [30].

According to [34], determining the optimal number of clusters is not a trivial problem. For instance, the k-means method can generate as many clustering schemes as the numbers within the given range. For that reason, a criterion is required to identify the optimal number of clusters. Assuming that each cluster is to be represented through at least one building, the upper limit for the number of clusters depends on the computational resources and time available for the performance assessments. A lower limit can also be set to ensure a minimum of diversity in the resulting sample.

The distinction between a cluster centroid and medoid is also important, and it is well explained in [61]. A centroid is a hypothetical central point in a cluster, whereas a medoid is a specific element, i.e., a building. Cluster algorithms, such as k-means, are able to identify centroids. A further step is required to link centroids to medoids. This operation comprises first identifying centroids (using k-means) or group memberships (using a hierarchical algorithm) and then calculating a distance matrix of the elements in a cluster. From the distance matrix, the closest element to the centroid (using k-means) or the element with the smallest distances from all the other elements (using a hierarchical algorithm) is selected. This element is assumed to be the medoid of that cluster. Therefore, this technique uses the most representative point for a group of data (medoid) as a measure of the center of the cluster, ensuring that real data points are selected as prototypes for the clusters [36].

### **2.6.2. Studies based on clustering techniques**

Many research studies are focused on clustering techniques in the building sector, some of which are going to be mentioned due to their similarity to the approaches proposed in this Thesis. For instance, in [62] a new methodology based on the use of the principal components analysis was developed, selecting the representative buildings among a total of 1100 schools. The classification method was based on the application of k-means clustering techniques, proposing five robust energy classes for space heating. The methodology that was followed allowed to define accurately the typical building of each energy class, so as to perform analyses on the potential energy savings for each group. In addition, [61] outlines a novel methodology for identifying representative buildings, utilizing a combination of building classification, building clustering and predictive modelling.

The study in [36] presented a new method for developing typical residential reference buildings at district level for bottom-up energy modeling purposes. According to this study, apart from k-means techniques, k-medoids is also widely used. As a case study, this work employed k-means and k-medoids techniques, for determining the representative archetype buildings of a sample. The energy consumption of the studied stock calculated by using representative archetype buildings was analyzed and compared with that from the 'building-by-building' simulation approach. Their performance analysis indicated that the k-medoids clustering technique was more accurate than k-means, by showing a lower relative error of stock energy consumption compared with dynamic stock simulations of real building shapes.

## 2.7. Brief summary

The present Chapter has justified the selection of the district scale as the most optimal one to improve the energy performance of the built environment, increase renewable energy integration and carry out innovative approaches such as demand side management, which need to consider dynamic interactions. In addition, this chapter also allowed to reach important conclusions with regards to solar potential estimations and accurate energy demand calculations. The drawbacks of most current approaches for urban analyses which make use of simplified methods have been highlighted, and an alternative tool has been developed to couple 3D models with detailed dynamic simulations of the thermal performance of buildings. Due to the complexity of dealing with models that may contain even hundreds of buildings, the importance of reducing the study domain has also been brought forward, emphasizing the usefulness of clustering techniques for the purpose of choosing the most representative buildings of a district.

The next steps to address the challenges mentioned in Chapter 1 will be taken in the following chapters. First, Chapter 3 will enable us to figure out whether it would be beneficial to implement DSM approaches at district level. Once that is achieved, Chapter 4 will allow us to learn how to characterize a district properly.



# 3. SMART END-USE: DEMAND SIDE MANAGEMENT APPROACHES

In this era of uncertainty with regards to energy planning, consumer demand has emerged as a central figure, since it can be seen as a means of balancing the energy supply and demand of electricity by providing the system with a flexibility whose responsibility no longer falls only on the generation infrastructure. Unlike other energy resources, electricity has to be used when it is generated, since its storage on a large scale is still an intricate (and costly) task. Utility companies increasingly have to deal with peak demands in constrained networks, so regulating the electricity use is critical. This long-term increase of energy demand throughout the world requires new power utilities and transmission and distribution capacity additions, but building new capacity as back-up power is expensive and the new power plants could be used infrequently. The aim of Demand Side Management is to attenuate these requirements.

The previous chapters have highlighted the need to widen the scope of energy analyses and consider the district scale, which integrates many buildings and makes it possible to investigate their potential synergies. With this in mind, it becomes clear that looking into the possibilities that DSM can offer on a district scale is worth investigating. As a first step, this chapter will review the role of DSM in this context, exploring innovative approaches that have not yet been implemented in many countries such as Spain. First, Section 3.1 will include a brief introduction to DSM. For more information, ANNEX C presents an extensive review of issues related to DSM that aims to gather much of the information that is present in the literature but in a very disperse way, discussing its current state of deployment and giving some insights into how it can be implemented with the help of smart homes.

As a further step, this chapter also introduces two new applications to prove the benefits of DSM in buildings and districts. The first one is developed in Section 3.2, to demonstrate the benefits of using dynamic pricing and the structural thermal energy storage capacity of buildings for DR purposes, focusing on one specific plus-energy dwelling. As a continuation of this proposal the second application, presented in Section 3.3, increases the scale to a neighborhood level and focuses on proposing strategies where a cluster manager controls all the heat pumps of a district, providing flexibility and obtaining benefits from the participation in secondary reserve markets.

## 3.1. Introduction

### 3.1.1. The concept of DSM

Traditionally, the demand in the built environment has been addressed by requiring green-rated buildings and energy efficient equipment. However, retrofitting solutions to existing buildings can be a difficult and costly task [63]. In the power grid, the frequency is the indicator of the balance between supply and demand, dropping when the consumption exceeds the supply and increasing when generation exceeds consumption. Blackouts happen if the supply is incapable of meeting the demand, which can be solved either by investing in new power plants and transmission lines, or by reducing the electricity demand. However, the first option might not be economically feasible, since critical periods only occur a few hours per year and increasing the price of electricity would not easily solve the problem. With the increasing penetration of intermittent renewable generation, there is a growing need for ancillary services to absorb the related disruptions [64]. In order to relieve the electricity grids, it is of paramount importance to be able to reduce the peak demands or shift the loads during peak periods through Demand Side Management systems.

DSM, also known as Energy Demand Management, was defined in the 80's as “the planning, implementation and monitoring of those utility activities designed to influence customer use of electricity in ways that will produce desired changes in the utility's load shape” [65]. It can also be defined as the modification of consumer demands through several methods, with the intention of adapting the total energy consumption or moving the time of use to off-peak times. Generally speaking, all programs intended to influence the customer's use of energy are considered DSM and can be addressed to reduce the demand at peak times, reduce the seasonal consumption or alter the time of use [66]. In general, these programs encourage the end user to be more energy efficient, but DSM can also help to reduce network congestion and the need for investment in new generation equipment [67].

During the past years there has been a noticeable increase of interest in Demand Response strategies, which is reflected in the rise of scientific publications from 219 in the year 2000 up to 1418 publications in 2016 (own survey in the ScienceDirect database). The distinction between DSM and DR and their scope is addressed in ANNEX C in more detail, since it has been subject of discussions between researchers during the past years. Many different DSM approaches are being evaluated, for example by determining the potential of electric vehicles to provide reserve power as a vehicle-to-grid concept [68]. Nonetheless, incentives, dispatch methods and compensation of DR remain challenges that restrain system planners and operators from adopting these strategies [69].

According to [70], the status of EU Member States regulation concerning DR can be divided into three groups: those who have yet to seriously engage with DR reforms (Portugal, Spain, Italy, Croatia, the Czech Republic, Bulgaria, Slovakia, Hungary, the Baltics, Cyprus and Malta), those in the process of enabling DR through the retailer only (Germany, the Nordic countries, the Netherlands and Austria) and those who enable both DR and independent aggregation (Belgium, France, Ireland and the UK). Nowadays, Spain relies mostly on hydro and gas for its flexibility needs, and the regulatory development of DSM is at a very low level [71]. A very complete review of dynamic pricing programs in the U.S. and Europe was done in [72], stating that Europe has a strong focus on large-scale roll-outs of smart meter devices.

As mentioned in the introduction of the present Thesis, buildings are responsible for a large portion of the total electricity consumption in many countries, and they are critical in efforts towards attaining the much needed operational flexibility in the grid [16]. Among the different contributors, heating, ventilation and air-conditioning systems are the most influential. To reduce HVAC energy consumption, a very simple and effective way would be to improve the control strategies, allowing the use of DR instead of replacing the existing equipment. For more detailed information about DSM, including the techniques available, the role of the users, smart homes, sensors and actuators as well as the importance of energy storage, the reader is referred to ANNEX C.

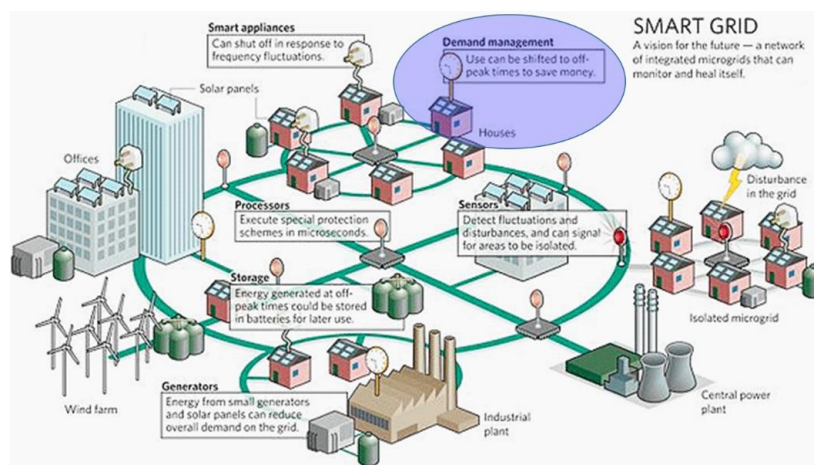


Figure 32: Demand Side Management within the Smart Grid environment [7].

### 3.1.2. Review of the existing literature on DSM

#### 3.1.2.1. Studies focused on pricing, renewable energies and storage

There are countless publications on DSM and there is a noticeable increase in recent years of the number of published papers on this issue. However, they emphasize different aspects. Many studies focus on price based DSM, quantifying the suitability and impact of DSM approaches under variable prices or real-time pricing [73–77]. Conversely, other publications emphasize the influence of DSM on Smart Grids, developing different frameworks for its integration into micro grids or Smart Grid environments [78–87]. According to [67], electric appliances consume around 62% of the electricity of a home in Spain, where unattended appliances such as washing machines are responsible for 13% of the total electricity demand. This means that being able to program these appliances to work at non-peak times could achieve considerable savings at no cost.

There are also many studies which stress the importance of storage within a DSM framework. For instance, the study presented by [88] assesses the impact of using Phase Change Materials (PCM) in buildings to leverage its thermal energy storage capability, claiming that significant advantages can be obtained for space heating applications. On the other hand, [89] analyzes the potential of Thermal Energy Systems, integrating conventional storage technologies like hot water tanks as well as the structural thermal energy storage capacity of a building. The study developed by [90] presents an existing installation of a TES system coupled with heat pumps, performing simulations to show the load shifting potential of the storage while assessing energy and cost savings. [91] also showed some interesting results regarding load shifting, arguing that the peak load of a dwelling can be reduced on average by 24% and 13.5% as a result of washing machine and dishwasher load shifting respectively. Last of all, the potential to improve the balancing between electricity used for heating and local production of a NZEB by active use of the structural thermal energy storage capacity of a building is analyzed by [92].

On the other hand, [67] make a comparison between renewable generation and DSM, suggesting that DSM exhibits the best performance in terms of economic efficiency and environmental sustainability, reducing peak loads and losses in the system. CO<sub>2</sub> emissions could also give customers an environmental motivation to shift loads during peak hours. It has been shown that the impact of Demand Response programs is significant and most appreciable at aggregated households than individual households [93]. This will be further investigated in this chapter and the ones that follow.

#### 3.1.2.2. DSM and optimization of energy consumption

A proposal of a control architecture focusing on the optimization of self-consumption over a DSM system with PV generation is given by [94]. The objective of its DSM system is to schedule different tasks commanded by the user throughout the day, modifying the time at which they are executed so as to optimize an energy criterion. As an alternative, the approach discussed by [95] consists on the determination of an optimal schedule of the operation of predictable devices. At the beginning of each day, the energy flows are forecasted, modifying the consumption of the house accordingly. Furthermore, significant savings can be achieved with actions such as changing the settings of the thermostats or retrofitting projects. Shiftable loads are heating, cooling air-conditioning, washing machines, dryers and dishwashers [91]. Command and control of heating and cooling systems is becoming a cost-effective viable option, particularly applicable to the existing building stock [63]. Further studies are the one presented in [96], that reviews various optimization techniques applied to DSM, or by [97], who affirm that the number of electric vehicles will grow considerably in the future, representing an opportunity as dispatchable energy sources.

On the other side, the time-scale of DSM methods could be either day ahead (sensitive to error in data forecasting) or real time (not so accurate but with a good performance if they complement day-ahead methods). However, day-ahead negotiations between different parties may not be feasible in many electricity grids, where such infrastructure is still not available [98]. Therefore, efforts are being made to find algorithms which react in real time, but there is a drawback that should be taken into consideration: there

has been insufficient attention to the possible energy losses incurred because of DR, since at fast time scales perturbations on the building controls may actually increase the energy consumption [99]. Therefore, a thorough knowledge of the overall behavior of the system is necessary so as to evaluate the energy cost savings in a realistic way.

### 3.1.2.3. Reported cost savings

Focusing on the use of the structural thermal energy storage capacity of buildings for DSM purposes, it should be mentioned that in some cases DSM may not achieve a significant reduction in the energy demand, but the electricity bills could be reduced as a result of the implementation of time-use tariffs and incentives. Few studies have been performed on optimal DR control to maximize cost savings by considering also the trade-off between peak demand reduction and the possible energy increase, which is highly nonlinear and complex [100]. For instance, [101] used a control strategy with a cooling storage system and stated that although the costs were reduced by 24%, the energy consumption increased 20% due to longer operation of the chiller and pumps compared to the base case.

Also, the study in [102] presents an algorithm to assign temperature set-points to price ranges based on discomfort tolerance indexes, with a controller based on Model Predictive Control (MPC) for HVAC usage. The authors of [102] showed that their strategy could lead to significant cost savings. Conversely, [103] developed an advanced controller by combining the use of TRNSYS and Matlab programs. This study proposed to reduce the cooling set-point temperature for precooling before the peak hours start, storing cooling energy in the building and keeping the HVAC system off during the peak hours to reduce energy costs. Another possibility is the one given by [104], in which a controller changes the set-point temperatures when retail prices are higher than customers preset price, providing up to 10.8% of energy cost savings. Moreover, [13] demonstrated that ground source heat pumps present a high potential as flexible loads when combined with the thermal storage capacity of the building, proposing a load shifting strategy by preheating the building and avoiding peak periods, leading to a reduction of electricity costs of up to 34 %. Another strategy was to apply longer preheating times to guarantee that the temperature is stabilized in the first peak period, turning it off during the duration of the peak and thus avoiding higher costs. This study also tested different preheating times, taking into account the outdoor temperature and achieving cost savings of 16-19 %.

Focusing on a combination of air-conditioning use and time-shiftable appliances, [105] develops a MPC scheme minimizing peaks and flattening the overall energy use profile by altering the thermostat set-points in individual homes, removing 10 % of the heating load without affecting the quality of service. The publication [106] devised an Energy Management and Control System to schedule electricity end-uses in a University campus, analyzing the effect of different schedules and using different control strategies for HVAC split systems. The results showed a high potential for peak reductions and economic benefits. Also, [107] presented a novel control algorithm for joint thermal comfort optimization and DSM in microgrids with RES and TES. Conversely, [108] focused on quantifying the potential energy savings in HVAC systems through set-point and deadband changes. This study also considered the effects of some influential factors on building HVAC energy consumption using building energy simulations. In summary, the study stated that increasing the deadband would result in an increase of energy savings. Alimohammadisagvand et al. [109] investigated DR actions on thermal comfort and energy costs in detached residential houses in a cold climate, reporting maximum annual savings in total energy costs of up to 10 %.

In [110], a residential DR context is described, using a multi-objective strategy for space heating and DHW production with heat pumps and a TES system. Chassin et al. [69] presented detailed simulation and performance studies showing how thermostatically controlled electrical loads can provide very valuable energy storage and how they could be prime candidates for fast DR. Also, [15] investigated how residential heat pumps which participate in load shifting can contribute to the reduction of emissions and operational costs. Last of all, [111] analyzed the performance of a dynamic thermostat controller of HVAC systems in homes that have dynamic price of electricity. The consumers in this case set a threshold price that the thermostat uses to set the temperature during peak power price periods. The results show that 12% of annual



energy cost savings for HVAC operation can be achieved without significantly changing thermal comfort.

#### 3.1.2.4. Reserve market opportunities

The growing share of renewable energies and the use of the potential of DR require power networks that intelligently link producers and consumers with the status and demands of energy transmission and distribution systems. Many studies related to the use of heating and cooling strategies for DR focus on dynamic pricing and time-of-use tariffs. Another option, however, is the participation in ancillary services markets. Integrating DR into ancillary services for electricity networks has received interest internationally and has to varying extents been integrated into national markets [112]. For Germany alone, depending on the technology, 18 to 27 GW of flexibly controllable load and 35 GW of negative controllable load could become available [113], which is comparable to the ramp-down or start-up of approximately 20 large-scale power plants [114]. In addition, Continental Europe has a need for 3 GW of Frequency Containment Reserve to stabilize the grid frequency automatically within seconds.

The provision of ancillary services to grid operators is organized differently across national power markets. [112] reviews and provides a comparison of national ancillary services markets in the context of DR in Europe. Participation in providing these grid services is contingent on various requirements on bidding generation plants and DR providers. Among other factors, this also includes a minimum power requirement needed to bid for participation in most countries. For example, in Germany, this requirement is a 1 MW symmetric flexibility band for Frequency Containment Reserve (FCR) and 1 MW (asymmetric positive or negative) for automatic Frequency Restoration Reserve. In addition to such country specific requirements, the European Network for Transmission System Operators for Electricity (ENTSO-E) establishes standards and common structures for the European market as a whole and aids the European Commission in establishing guidelines in the form of common regulations [115]. Thus, before participating in ancillary services, generators and DR assets must document and prove their suitability and fulfillment of the requirements. This is a challenge for small DR assets and in particular for assets such as household heat pumps whose suitability to providing these grid services is dependent on aggregating many small assets that individually would not otherwise, alone, qualify for participation.

Several model-based approaches are proposed in the literature. In [116] commercial building frequency regulation capability is estimated. [117] exploited HVAC and internal thermal storage systems to show the provision of DR by buildings, and concluded that the intraday market allowed for successfully meeting objectives of maintaining comfort while providing dependable DR capacity. An aggregated model of a fridge-freezer population is developed in [118], examining a price control strategy to quantify DR savings. In the study current ancillary service payments are analyzed and it is shown that they are insufficient to ensure widespread uptake by small consumers, and that new mechanisms need therefore to be put in place to make providing DR with consumer appliances such as refrigerators an attractive option. The challenges in distributed provision of FCR can even lead to undesirable rebound effects in system frequency if distributed algorithms for the control of small load shedding DR assets (such as refrigerators, HVAC systems or heat pumps) are not properly synchronized [119]. A case study for a battery energy storage system under the German regulatory framework is investigated with different operation strategies in [120].

Providing ancillary services in the context of microgrids is also the focus of some studies. For example, [121] proposed an optimal scheduling model for a microgrid which coordinates the aggregated prosumers net load in its connected distribution feeder. Furthermore, [122] developed an algorithm for the aggregation of flexible loads for DR applications at the substation level, while [123] developed a framework focusing on domestic storage heating DR capability in balancing markets. Simulation studies of building flexibility and, as particularly shown in the literature referenced above, studies about integrating heat pumps into flexibility markets and grid services have clearly received attention in the literature. Several demonstration projects of such systems have been set up in recent years, for example [124] demonstrated flexible DR provision with 54 residential heat pumps.

More recently, other studies that deal with the provision of Frequency Restoration Reserve (FRR) have been published. For example, [125] includes a very accurate description of the German Frequency Restoration Reserve market and presents an operating strategy for battery energy storage systems providing FCR. In [126] the benefits of combining PV-battery systems and the provision of FRR are assessed, concluding that prioritizing the provision of FRR over self-consumption enhancement results in even higher revenues, but significantly reduces self-consumption. Also, [127] proposes a distributed price-based optimization scheme for involving a population of consumers in day-ahead procurement of electricity and frequency containment reserves, while [128] introduces plug-in electrical vehicles as a way to store energy, taking part in both day-ahead and reserve markets. Last of all, a similar study to that which will be proposed in this chapter is given in [129], which focuses on the integration between the heating and the power systems by analyzing a heat pump supplying a district heating island system.

### **3.1.2.5. The importance of the interactions between buildings**

As highlighted in Chapter 2 of this Thesis, widening the scale and considering the synergies between buildings offers many advantages. This is also true for DSM and DR approaches. In [100] the importance of coordinating flexible DR assets to avoid undesirable side effects of DR at the distribution network level is shown, and the performance of conventional DR at the level of a group of buildings is evaluated. Control strategies that coordinate at the cluster level are important, especially for ancillary services such as FRR. [130] estimates the amount of energy storage and revenue that thermostatically controlled loads can provide in residences participating in ancillary service markets. The study presented in [131] developed a methodology to quantify the flexibility in buildings, which returns the amount of energy that can be shifted and the associated costs. The results are presented in cost curves, which allow the comparison between buildings and the aggregation of flexibility, and reveal large variations depending on time, weather, utility rates, building use and comfort requirements. Also, an aggregator controlling a cluster of residential heat pumps to offer direct control flexibility services is evaluated in [132]. In that study, heat pumps are required to supply hot water and space heating at certain times and are activated flexibly in order to do so. The results show a larger potential for upward modulations than for downward modulations.

Another example of such a study is [133], which considers HVAC and domestic electric water heaters for potential DR applications and an interaction between the system operator and consumers to facilitate managing cyclic operation of consumer heating loads. In this case, the system operator and the consumers signed a contract allowing the operator to control the operating cycle of HVAC loads without overriding the user preferences. In the algorithm proposed in [133], house modules submit operating proposals to a system-wide module, which judges the received proposals and accepts those in line with the objective, resulting in significant benefits.

### **3.1.3. Aim of this chapter**

The first sections of this chapter have shown the numerous possibilities offered by DSM. One of the most interesting ones is the exploitation of the buildings' thermal mass. In order to analyze the potential benefits that exploiting the structural thermal energy storage capacity of buildings can offer for DSM purposes, two applications will be proposed in the remainder of this chapter. The first application will focus on an individual building: a plus-energy dwelling. Here, the impacts of different dynamic pricing strategies by managing the activation of a heat pump in response to price changes will be evaluated, analyzing the influence on cost savings, indoor comfort, heat pump consumption, reduction of the Heat Pump (HP) use during peak hours and photovoltaic energy self-consumption ratio of the building. Different price thresholds will be used, fixed or variable, which either constrain the use of the heat pump during its normal operation or enforce its activation.

As a follow up, the second application will increase the scale and assess the benefits of allowing the direct control of the heat pumps in the dwellings of a district, in order to sell the flexible power on the market for Frequency Restoration Reserve. In this case, a cluster manager makes the decision whether the buildings that

are managed should activate their heat pumps or not when an activation call from the FRR is received. The main goal is to analyze the potential cost savings of different cluster manager strategies at district level, providing load flexibility through the use of the thermal mass while bearing in mind the thermal comfort of the occupants.

## 3.2. Contributions of heat pumps to Demand Response: a case study of a plus-energy dwelling

### 3.2.1. Introduction

Using a plus-energy dwelling located in Germany as a case study, the main purpose of the present work is to analyse the impact of different dynamic pricing strategies on several aspects: cost savings, indoor comfort, heat pump consumption, reduction of the HP use during peak hours and photovoltaic energy self-consumption ratio of the building. A controller is proposed, which can automatically manage the activation of the HP in response to price changes, so that cost savings can be achieved and the overload on the grid during peak periods can be diminished by shifting the loads from peak to off-peak periods. In order to do so the energy has to be stored in the building, which is possible thanks to the mass within the thermal envelope, offering a passive thermal storage to shift the electricity demand. As far as the author of this Thesis knows, no study such as the one proposed here has been previously done on the potential of dynamic pricing strategies in plus-energy buildings.

The aim is also to analyse the influence of changing set-point temperature bands (range around the set-point where room temperature oscillates) with regards to the previously mentioned aspects. Sixteen strategies were simulated for three set-point temperature scenarios. Different price thresholds are used, fixed or variable, which either constrain the use of the heat pump during its normal operation or enforce its activation. Temperature thresholds will also be considered to avoid overheating. Another interesting question is whether there may be a good compromise between cost savings, the increased energy consumption, the thermal comfort of the occupants and the contribution to the reduction of the grid's peak load. Several conclusions are drawn, and the optimal strategies for each set-point temperature scenario are presented.

The contents of this section have been extracted from the paper "*Contributions of heat pumps to Demand Response: a case study of a plus-energy dwelling*" [134], by *L. Romero Rodríguez et al* and published in the journal "*Applied Energy*". For more detailed information about the case study, the methodology followed and the obtained results, the reader is referred to that publication.

### 3.2.2. Case study: Modelling and Simulation

The case study is a real dwelling currently being intensively monitored, located in a new district in Wüstenrot (Germany) which consists of more than 20 plus-energy houses recently built with high insulation standard (KfW 55), PV arrays of different sizes as well as an electrical storage of 5 kWh. Heating is provided inside the dwellings by using underfloor heating, supplied by heat pumps which are connected to a cold district heating network located in the area. In addition, each building has thermal energy storage capacity through a space heating tank and a DHW storage tank. An illustration of the dwelling under study can be seen in Figure 33.



Figure 33: SketchUp model of the building.

Both the supply system and the building have been modeled in the TRNSYS 17 [135] environment, which allows to perform the planned simulations optimally in view of the fact that all parameters can be adjusted in a flexible way. The aim was to develop a model which could reflect the reality, so as to be able to validate it with experimental data and analyze the impact of the chosen dynamic pricing strategies. The building's geometry was created with the software SketchUp, the sizing of all the elements (thermal storage, battery, PV modules, heat pump characteristics, fluid flowrates, temperature of the cold district heating network etc.) corresponds to the reality and the chosen time-step for the simulations is 30 minutes, considered as a good compromise between simulation time and accuracy for the purpose of this study. A weather file was created by using available measurements at the location of the dwelling. A representation of the TRNSYS supply model and its connection to the building can be seen in Figure 34.

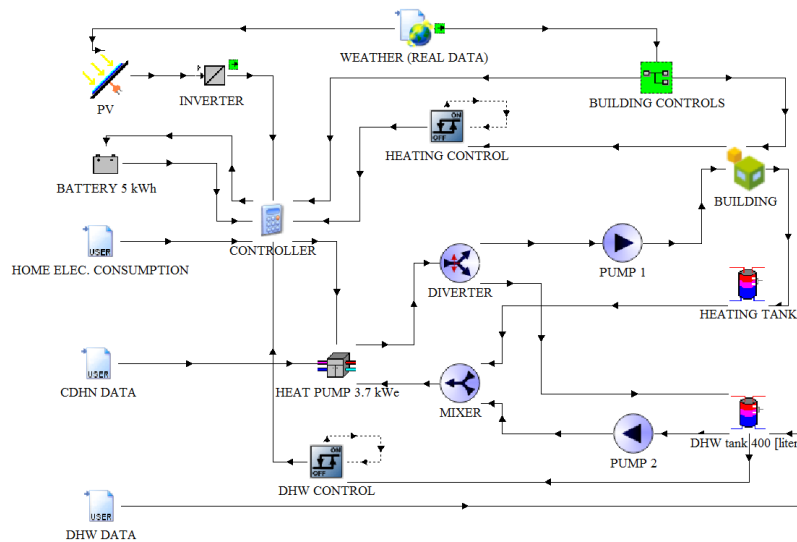


Figure 34: Simplified representation of the TRNSYS model.

Before proceeding to analyze different strategies of dynamic pricing, a validation of the model was considered appropriate so as to check that the behavior of the model was close to the reality. Once the model has been adjusted and validated, the results of the strategies that will be studied can be considered as more reliable and realistic. For more information about the validation of the model with regards to the heat pump consumption, PV production and indoor temperatures, the reader is referred to the publication by the author of this Thesis [134].

### 3.2.2.1. Proposed dynamic pricing strategies

Different dynamic pricing strategies will be compared with the situation in which there is no price restriction to use the energy, considered as the base case (strategy 1). The focus will be in the month of February, which is the period of the validation of the model. Some of the strategies proposed imply that the heat pump will

work whenever the requirements of the normal operation control are fulfilled, but with different price thresholds (upper limits). Other strategies will involve turning on the heat pump until that threshold is reached, but with varying indoor temperature ( $T_{air}$ ) limitations to avoid overheating. Three different scenarios with the same temperature set-point ( $20\text{ }^{\circ}\text{C}$ ) but different temperature bands ( $20 \pm 0\text{ }^{\circ}\text{C}$ ,  $20 \pm 1\text{ }^{\circ}\text{C}$ ,  $20 \pm 2\text{ }^{\circ}\text{C}$ ) will be considered. The list of the sixteen different devised strategies as well as set-point scenarios is presented in Table 1. The chosen indoor temperature thresholds are one or two degrees higher than the set-point temperature. Conversely, the price thresholds are: close to the average price of the whole period ( $0.21\text{ €/kWh}$ ), high so as not to be so restrictive with the HP operation ( $0.23\text{ €/kWh}$ ), the average price of the day, the lowest 25% of the day and with no specific price limitation but the HP operation is only allowed during the night, when prices are often lower.

Set-point controls	$20 \pm 0\text{ }^{\circ}\text{C}$	$20 \pm 1\text{ }^{\circ}\text{C}$	$20 \pm 2\text{ }^{\circ}\text{C}$
Strategy 1	No limit. Static price of $0.22\text{ [€/kWh]}$ . HP works whenever necessary.		
Strategy 2	No limit. Day-ahead dynamic prices. HP works whenever necessary.		
Strategy 3	HP works whenever necessary if the price is less than $0.21\text{ [€/kWh]}$		
Strategy 4	HP works whenever necessary if the price is less than $0.23\text{ [€/kWh]}$		
Strategy 5	HP works whenever necessary if the price is less than the average price of the day.		
Strategy 6	HP works whenever necessary, only during the night.		
Strategy 7	HP works always if the price is less than $0.21\text{ [€/kWh]}$ if $T_{air} < 21\text{ }^{\circ}\text{C}$ .	HP works always if the price is less than $0.21\text{ [€/kWh]}$ if $T_{air} < 22\text{ }^{\circ}\text{C}$ .	
Strategy 8	HP works if the price is less than $0.23\text{ [€/kWh]}$ if $T_{air} < 21\text{ }^{\circ}\text{C}$ .	HP works always if the price is less than $0.23\text{ [€/kWh]}$ if $T_{air} < 22\text{ }^{\circ}\text{C}$ .	
Strategy 9	HP works always if the price is lower than the average price of the day and $T_{air} < 21\text{ }^{\circ}\text{C}$ .	HP works always if the price is lower than the average price of the day and $T_{air} < 22\text{ }^{\circ}\text{C}$ .	
Strategy 10	HP works always during the night if $T_{air} < 21\text{ }^{\circ}\text{C}$ .	HP works always during the night if $T_{air} < 22\text{ }^{\circ}\text{C}$ .	
Strategy 11	HP works always if the price is less than $0.21\text{ [€/kWh]}$ if $T_{air} < 22\text{ }^{\circ}\text{C}$ .	HP works always if the price is less than $0.21\text{ [€/kWh]}$ if $T_{air} < 23\text{ }^{\circ}\text{C}$ .	
Strategy 12	HP works always if the price is less than $0.23\text{ [€/kWh]}$ if $T_{air} < 22\text{ }^{\circ}\text{C}$ .	HP works always if the price is less than $0.23\text{ [€/kWh]}$ if $T_{air} < 23\text{ }^{\circ}\text{C}$ .	
Strategy 13	HP works always if the price is lower than the average price of the day and $T_{air} < 22\text{ }^{\circ}\text{C}$ .	HP works always if the price is lower than the average price of the day and $T_{air} < 23\text{ }^{\circ}\text{C}$ .	
Strategy 14	HP works always during the night if $T_{air} < 22\text{ }^{\circ}\text{C}$ .	HP works always during the night if $T_{air} < 23\text{ }^{\circ}\text{C}$ .	
Strategy 15	HP works always if the price is among the lowest 25% of the day and $T_{air} < 21\text{ }^{\circ}\text{C}$ .	HP works always if the price is among the lowest 25% of the day and $T_{air} < 22\text{ }^{\circ}\text{C}$ .	
Strategy 16	HP works always if the price is among the lowest 25% of the day and $T_{air} < 22\text{ }^{\circ}\text{C}$ .	HP works always if the price is among the lowest 25% of the day and $T_{air} < 23\text{ }^{\circ}\text{C}$ .	

Table 5: Analyzed strategies using day-ahead electricity market prices.

In order to show how these strategies work, an example during a certain period will be given. In strategy 7, the heat pump will always work if the price is lower than 21c€/kWh and the temperature is lower than 21 °C, while in strategy 8 the price threshold is increased up to 23 c€/kWh. Conversely, strategy 15 maintains the same temperature threshold, but in this case the heat pump will always work if the electricity price is within the lowest 25 % of the day. Figure 35 depicts the operation mode of these options, showing the indoor temperatures of the simulations as well as the price thresholds and the times at which the heat pumps were activated in each case.

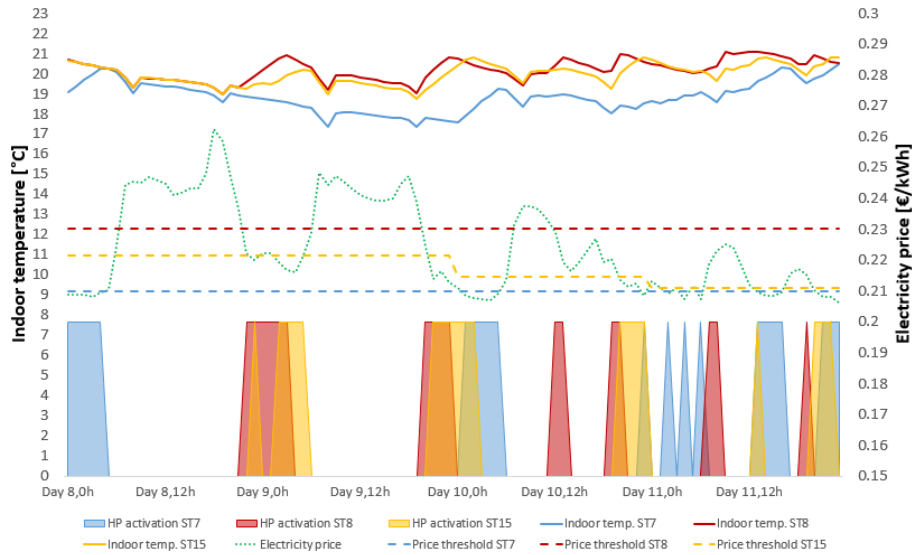


Figure 35: Example of different modes of operation depending on the strategy (ST).

### 3.2.3. Analysis of results

#### 3.2.3.1. Cost savings and thermal comfort

As regards to the costs of running the heat pump to provide heating for the building, the results for all the options considered are shown in Figure 36. As it can be seen, among the most cost-effective options for the three set-point scenarios are strategies 3, 5 and 7 with given fixed price limits for activation, achieving savings up to 21 % when each strategy is compared to their base case. In the case of set-point  $20 \pm 2$  °C, strategy 11 has an even lower cost. Conversely, strategies 12, 13 and 14 (in which the heat pump always works with certain temperature and price thresholds) are among the most expensive options.

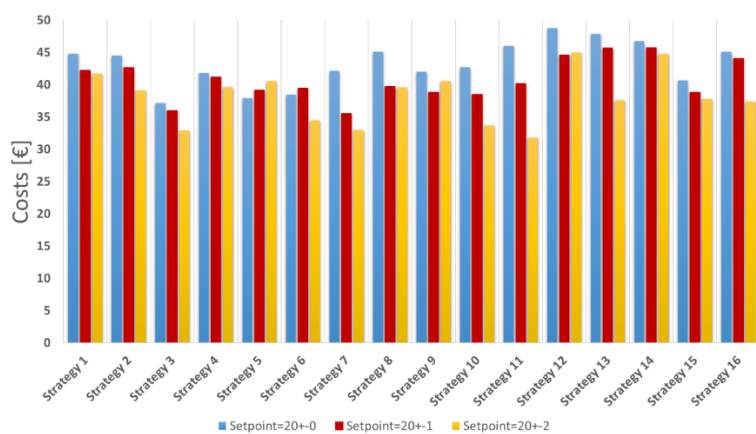


Figure 36: Comparison of heat pump monthly cost for heating electricity.

There is however a reason behind these results: due to the price thresholds, the heat pump might not be activated when needed, or it may be activated more often than necessary. Therefore, in order to choose the optimal strategies, the focus cannot be merely on costs, and it is of paramount importance to check the indoor temperatures achieved by each of the strategies to detect comfort problems. Figure 37 shows a comparison of the daily average temperatures for some strategies of the  $20 \pm 0^\circ\text{C}$  set-point scenario. It becomes apparent that for instance in strategy 3, among the best when focusing on costs, the heat pump is not activated often enough so as to keep an appropriate indoor comfort. The reason is that its price threshold is too low, so there are some periods in which the heat pump would not be activated at all. This could be expected because the limits for strategy 3 are only costs, and not temperature. Conversely, strategy 13 (HP works always if price is lower than average and  $T_{\text{air}} < 22^\circ\text{C}$ ) behaves in the opposite way: much higher indoor temperatures than in the base case are achieved, therefore increasing the heat pump consumption and costs. However, some strategies such as 4, 5 or 15 are capable of maintaining acceptable indoor temperatures.

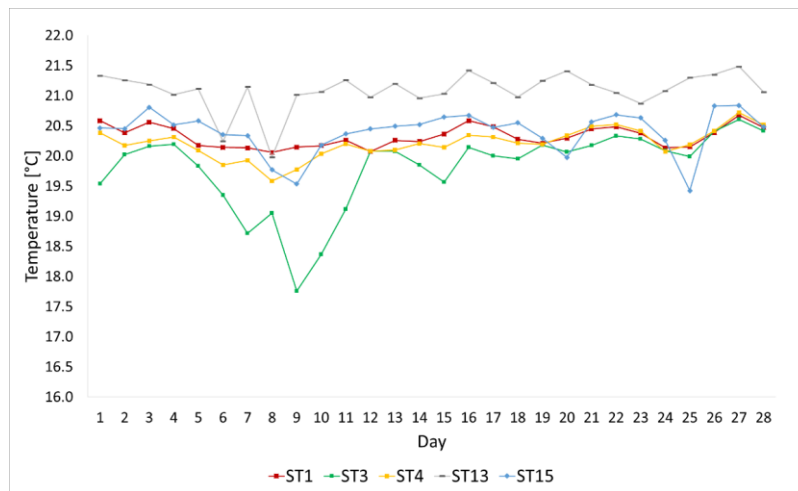


Figure 37: Comparison of the daily temperature of different strategies. Case  $20 \pm 0^\circ\text{C}$ .

Figure 38 presents the sum of excess of degree-hours during the whole month for every strategy and set-point scenario. Positive values mean the sum of excess degree-hours above  $20^\circ\text{C}$ , while negative values mean the sum below  $20^\circ\text{C}$ . It is evident that strategies 3, 7 and 11 (which have a low price threshold of  $21\text{ c}\text{€}/\text{kWh}$ ) are not capable of reaching  $20^\circ\text{C}$  during many hours of the month, while strategies 11, 12, 13, 14 and 16 (with less restrictions for the HP operation) produce too much overheating.

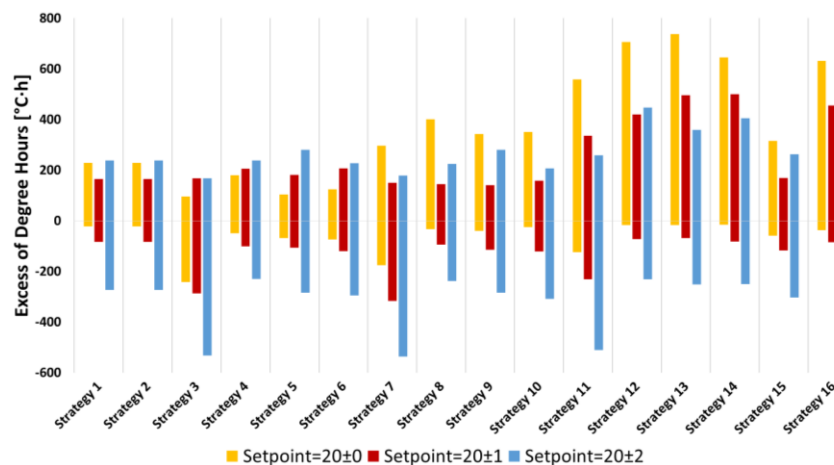


Figure 38: Comparison of the amount of excess degree-hours. Positive values show  $>20^\circ\text{C}$  and negative values  $<20^\circ\text{C}$ .

### 3.2.3.2. Heat pump consumption and self-consumption ratio

The heat pump consumption is strongly linked to the cost savings and the thermal comfort. One conclusion of the set-point scenario  $20 \pm 0$  °C is the fact that if no negative deviation from the set-point is allowed, i.e., nearly no  $< 20$  °C excess degree-hours, then the HP consumption is always increased. That is the case of using strategy 10 (HP works always during the night if  $T_{air} < 21$  °C) instead of the base case. The reason is that increasing the temperatures above its normal set-point temperature (from 20 to 21 or 22 °C) for these strategies results in an increase of the energy losses of the building. Therefore, although there may be cost savings, the heat pump consumption is increased.

On the other hand, the ratio of self-consumption of the household is influenced by the used HP strategy, the state of charge of the battery and the time-dependent match between PV production and HP consumption. In general, most of the strategies use the electricity during non-peak periods, which are not normally during the day (when there is PV production). Therefore, the heat pump (which is the main electricity consumption contributor) would be rarely used at the same time as the electricity is produced by the PV panels. As a result, the self-consumption ratio could decrease. The amount of decrease would then depend on the capacity of the electric battery. However, there are only slight variations, always lower than 8 % among all the different strategies.

### 3.2.3.3. Use during peak hours

One of the main reasons of the existence of DR is the benefits it can bring with regards to the reduction of peak demands, which might cause grid stress and entail an increase of the use of less efficient power plants. To illustrate the influence of the chosen strategies on peak reduction, Figure 39 shows the percentage of heat pump use during peak hours. As we can see, the base case strategies have the highest percentages of heat pump use during peak hours. The obvious reason is that there is no time restriction for their use, and no price thresholds. The strategies which have a price threshold of 23 c€/kWh (4, 8 and 12) are the ones with a highest percentage of use during peak hours among the proposed strategies, since the threshold is quite high and the heat pump is used during peak hours more often. On the other hand, strategies 3 and 7 (price threshold of 21 c€/kWh) use the heat pumps only rarely during peak times, and the same happens with strategies 6, 10 and 14, which only allow their use during the night. For the rest of the strategies, we can observe that the heat pump is never used during peak hours, showing how beneficial they could be when the focus is on peak reduction.

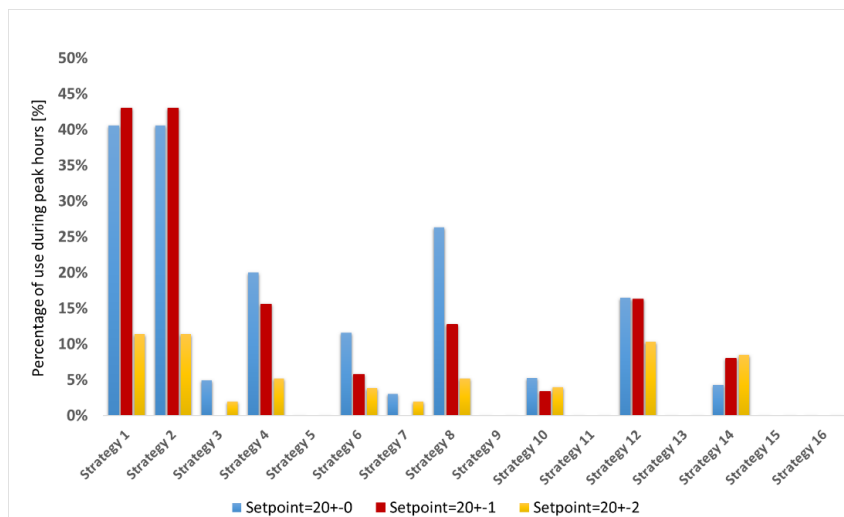


Figure 39: Percentage of HP use during peak hours [%].



### 3.2.3.4. Optimal strategies

A good compromise between thermal comfort and cost savings needs to be achieved so as to choose the most interesting strategies, which vary depending on the set-point scenario. Moreover, the reduction of the heat pump consumption, use during peak hours and increase of self-consumption ratio should be also borne in mind, since they entail environmental benefits. A summary of the best considered strategies for each set-point scenario is shown in Table 6. It should be noted that due to the interaction of different aspects, the criteria for choosing the optimal strategies are somewhat subjective.

		HP costs [€]	Cost savings [%] (compared to own base scenario)	Cost savings [%] (compared to 20±0 base scenario)	Sum of excess temperature degree-hours < 20°C	Sum of excess temperature degree-hours > 20°C	HP cons. Savings (compared to own base scenario)	Ratio of self-consumption [%]	Percentage of use during peak hours [%]
Set-point 20±0	Strategy 1 (base case)	44.8	0 %	0%	22.2	227.9	0.0%	33.6%	40.6%
	Strategy 5	37.9	15.3%	15.3%	69.3	104.1	9.2%	34.3%	0 %
	Strategy 15	40.7	9.2%	9.2%	58.6	315.8	1.4%	35.2%	0 %
Set-point 20±1	Strategy 5	39.1	7.3%	12.7%	107.3	181.4	2.1%	38.2%	0 %
	Strategy 8	39.7	5.9%	11.3%	94.4	144.1	2.5%	39.8%	12.7 %
Set-point 20±2	Strategy 6	34.4	17.5%	23.1%	295.0	227.3	10.9%	36.0%	3.9 %
	Strategy 10	33.7	19.2%	24.7%	309.2	207.2	12.8%	36.2%	4.0 %

Table 6: Selection of the optimal strategies.

Several conclusions can be drawn from the selection which has been made. Compared to the base case (the way in which the real household is controlled), it is possible to achieve around 15 % of cost savings for the energy used to heat the building, without changing the set-point temperature band, and without sacrificing noticeably the thermal comfort. This involves using strategy 5, in which the heat pump will work when necessary, but only if the price is below the average of the current day. As a result, the HP consumption is 9 % lower, the self-consumption ratio also increases by 1 % and there is no use of the HP during peak hours. Strategy 15 (turning on the HP always if the price is within the lowest 25 % of the current day and the indoor temperature is below 21 °C) can also achieve 9 % savings with almost the same heat pump consumption as the base case and no use during peak hours, although with a bit more of overheating. On the other hand, increasing the temperature band up to ± 1 °C would increase the self-consumption ratios and achieve around 12 % of cost savings by using strategies 5 or 8. However, this involves obviously an increase of the < 20 °C excess degree-hours. Last of all, using the set-point scenario 20 ± 2 °C would allow to use strategies 6 or 10, which achieve around 24 % of cost savings compared to the base case in 20 ± 0°C, also reducing the HP consumption and the use during peak hours, and increasing the ratio of self-consumption.

### 3.2.4. Conclusions

The present work has analyzed the benefits of DR strategies for heat pumps incentivized by day-ahead pricing signals. A recently constructed plus energy district in Southern Germany was taken as a case study, with monitoring data available for decentral heat pumps connected to a cold district heating network. Several dynamic pricing alternatives which depend on temperature and price thresholds were evaluated to control the operation of the heat pump in one of the buildings. This was done with the purpose of finding those strategies that could lead to significant cost savings while maintaining an acceptable thermal comfort.

Evidence has been obtained on the importance of choosing the correct price thresholds when using dynamic pricing strategies for DR purposes. The results show that fixed price thresholds are not the best option, since the high variations of the market could result in reduced activations of the heat pump, with the consequent thermal comfort losses. Instead, dynamic thresholds depending on the variations within the day are a better alternative.

Savings up to 25% were achieved by using optimal strategies, also resulting in increases of self-consumption ratios for the given photovoltaic systems and without sacrificing noticeably the thermal comfort of the occupants. Apart from the previously mentioned benefits, the proposed optimal strategies achieved significant peak reductions on the grid, since the heat pumps were mostly used during low-peak periods. These strategies also highlight the importance of knowing how much the users are willing to sacrifice their comfort to achieve savings. If the thermal discomfort tolerance is decided upon, the present study provides answers to estimate the savings which may be achieved, helping with decision-making. In addition, it is vital to take into account the heat pump energy consumption when choosing the best option, since overheating the building above its normal set-point temperature results in energy losses, therefore increasing the energy consumption unless the sum of excess degree-hours below the set-point temperature is also noticeable. In the case of having local renewable generation, the self-consumption ratios should always be considered, since their increase is also valuable to relieve the electricity grids.

The outcomes of the present study have shown the great impact that the use of heat pumps and the thermal storage capacity of buildings may have by using dynamic pricing strategies within a DR framework. The importance of looking at all the implications of these strategies was also demonstrated, since it was proven that the decisions to choose the optimal strategies should not rely solely on one of many potentially contradictory aspects. Bearing this in mind and once the benefits of using heat pumps for the provision of DSM has been proven for an individual building, the next application will expand the scope of action.

## 3.3. Heuristic optimization of clusters of heat pumps: a simulation and case study of residential frequency reserve

### 3.3.1. Introduction

As countries continue to implement support mechanisms for volatile renewable energy production, the systems and processes needed to maintain balance in power grids continue to increase in importance, and are consequential for the success of energy transitions. Methods for accommodating this volatile generation in the grid are being supported by new technologies (e.g., battery storage), regulatory measures such as strategic stability reserve plants, and innovation in the private sector with tariffs incentivizing flexible demand for electricity users [136,137]. The demand side has been acknowledged as an important part of ensuring this future stability in power grids more dependent on the fluctuations of renewables [138]. Especially, heating applications coupled with heat storage are promising in providing a significant contribution to power grid stability. Households with own onsite distributed generation augmented by electrical and thermal storage capacities (prosumers), can adjust energy use based on the current needs of the electricity grid and heat pumps, as an established technology for enhancing energy efficiency, are

increasingly seen as having potential for shifting electricity use and contributing to Demand Response.

The present work is carried out in the framework of the EU Horizon2020 project Sim4Blocks, and the application is based on a newly built plus-energy settlement in the rural municipality of Wüstenrot in Southern Germany, the same as in the previous application. Using a model developed and validated with monitoring data of one of the households, the technical and financial viability of utilizing household heat pumps to provide power in the market for Frequency Restoration Reserve are studied. The research aims to evaluate the cost savings and the flexible electrical load offered by a cluster of buildings whose heat pumps are activated depending on selected rule-based participation strategies, focusing also on other important factors such as the thermal comfort of residents, the heat pump consumption or the influence on the PV self-consumption ratios. In this way, the potential benefits offered by clusters of buildings that exploit their structural thermal energy storage capacity are evaluated on a district scale.

The contents of this section have been extracted from the paper “*Heuristic Optimization of Clusters of Heat Pumps: A Simulation and Case Study of Residential Frequency Reserve*”, by L. Romero Rodríguez et al and currently accepted for publication in the journal “*Applied Energy*”. For more detailed information about the FRR market, the case study, the methodology followed and the obtained results, the reader is referred to that publication.

### 3.3.2. Market integration: frequency restoration reserve

The provision of FRR to the electricity market can be either positive (to compensate excess demand) or negative (to compensate excess power supply). In this study, the focus will be on the provision of negative FRR. Negative utilization payments, which imply a cash flow from the electricity network operator to the customer, lead to short activation periods of typically less than two minutes. This is a problem for heat pumps operations, since such short cycles have a negative impact on lifespans. Figure 40 shows that FRR activations are typically very short (on the order of minutes) and that they decrease rapidly with decreasing (also negative) utilization price bids on the part of participants. Activations of participants bidding positive prices last significantly longer.

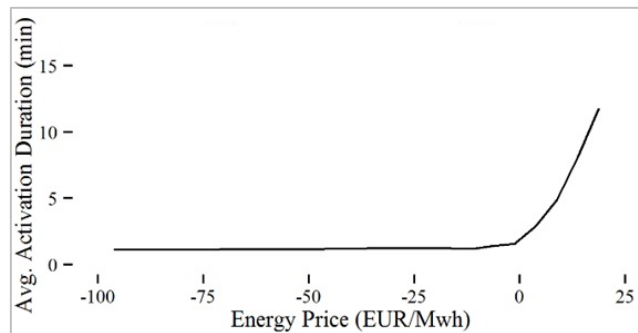


Figure 40: Example of the duration of the activation calls vs. energy price bid. Own analysis of data for calendar year 2015. Data published by Transmission System Operators (TSOs) and publicly available at [www.regelleistung.net](http://www.regelleistung.net).

The benefit that can be achieved in this process consists on the avoided supply of electricity purchased through the standard heat pump tariff (assumed based on local market conditions to be 22 cEUR/kWh, a flat tariff) and in the additional income from participation in the FRR market. However, several regulatory surcharges and taxes must be subtracted, and an additional fee for the participation and services of an aggregator must also be set aside.

### 3.3.3. Case study: Modelling and Simulation

#### 3.3.3.1. Description of the case study

The case study used in this work is based on a group of plus-energy dwellings located in a district of real inhabited houses in Wüstenrot (Germany). Six different building typologies were chosen for the study, with the same geometry (two floors of around 125 m<sup>2</sup>) and ventilation schedule but with different internal gains (people, equipment and lighting) as well as different infiltration rates and size of the heating tanks. Building 1 exists in the reality including the actual energetic parameters, and the rest of buildings are hypothetical, with different energetic parameters. In this way the sample is quite heterogeneous, which allows to draw conclusions for different building typologies. Since these dwellings have a significant thermal mass, their structural thermal energy storage capacity is used. It is this capacity that allows to store the heat inside the dwellings during a certain amount of time. The parts of the energy supply system which will be included for each building model are: PV modules, heat pump, heating water storage tank, DHW water storage tank and electricity storage. For the specifications of these elements, the reader is referred to the mentioned publication.

#### 3.3.3.2. Model description and selection of the time interval

Both the building model and the supply model have been developed by using TRNSYS 17 [135], trying to reflect the reality as closely as possible. The models will be the same for each building typology, but varying the parameters mentioned in the previous section. A representation of the TRNSYS model can be seen in Figure 34, and a validation of this model (building 1) was also carried out so as to ensure that the results of the simulations would be representative of the reality.

Although usually the minimum running time of heat pumps is between 10 and 15 minutes, in this study 30 minutes will be considered for the simulations. One of the reasons is that to preserve the life cycle of the heat pumps this timeframe should be increased, since the heat pumps will be activated much more frequently in this FRR framework than during a normal operation. In addition, our study looks into the ability of buildings to provide energy flexibility with their heating systems and focuses thereby on the limits of their participation in terms of energy restrictions. The decision to analyze 30 minute time steps of heat pump operation allows for abstracting away from the nontrivial issues of hardware failure and maintenance costs that are also associated with fast on-off reactive heat pump activations. We thus allow heat pumps to participate in the market in our simulation while assuming that the cluster manager and aggregator will compensate this minimum runtime restriction with internal balancing within their portfolios (compensating positive capacity reactions, battery capacity, etc.).

#### 3.3.3.3. Cluster manager: analyzed strategies

The main aim of the present work is to study the potential cost savings achieved by different strategies when a cluster manager controls the heat pumps of several buildings, by participating in the FRR market. For doing so, the cluster manager needs to know what would happen regarding the status of each building if the heat pump had to be activated, and decide whether a building is suitable to be used or not. The focus of the study has been on the month of February, and data from the FRR for that month in 2015 has been used. The cluster manager will deal with 6 buildings.

Figure 41 depicts the cluster manager framework in our study. First, there is an interaction between the TSO, which releases the activation calls, and the aggregator, who has a portfolio of customers willing to provide power to participate in the FRR. Then, there is an open option between the aggregator and the cluster manager, since they can agree to sign a private contract with different requirements.

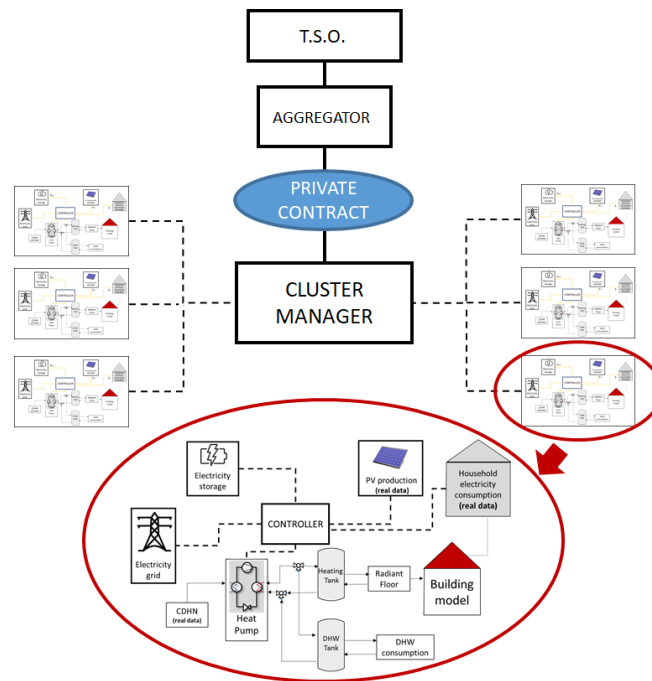


Figure 41: Overview of the cluster manager framework.

Our analysis studies two different configurations of such private contracts. The first one is an agreement which allows the cluster manager to provide the aggregator with as much flexible power as it has available by activating the flexibility of its portfolio of buildings. In this case, any building that fulfills several set conditions will activate their heat pumps at full power if the aggregator sends the cluster an activation request. Settlement between the cluster and the aggregator is then based on the total energy used by the heat pumps during the activation time period, irrespective of how much additional energy this turns out to be compared to the original baseline expected consumption of the heat pumps (up to the maximum possible power consumption of the devices). In the second type of contract studied, the agreement is such that the cluster manager always has to provide the aggregator with a specified (and constant) amount of power. In this case, the cluster must decide which subset of buildings to activate, in order to comply with the activation of only a fixed, limited amount of power. The assumption that our work tests is whether heat pumps, with dynamic and complex physical constraints but with nonetheless high degrees of flexibility, could benefit and/or be appropriate for participation in both types of market contractual arrangements.

Table 7 displays the considered bidding strategies for the cluster manager. We analyze bids of three different FRR prices including the case of a negative value (the customer is paid for consuming the energy), although in all cases, regulatory taxes and surcharges are still applied to the overall incurred costs of the dwellings. Strategies 2, 3 and 4 are simulations studying the variable power contract between the cluster manager and the aggregator (the cluster provides maximal flexible power, and the aggregator pays for all of it, irrespective of amount or variability). In this case, any building would activate its heat pump if the following conditions are met: an activation call is received, the building is electrically self-sufficient during the time step and the indoor temperature of the building is below a certain threshold. On the other hand, strategy 5 involves the contract which guarantees a constant power. In this strategy, the three buildings with the lowest indoor temperatures will always be chosen by the cluster manager to be activated. In this case, there are no self-sufficiency or temperature thresholds.

FRR	FRR(-50) Price: -50 EUR/MWh	FRR(0) Price: 0 EUR/MWh	FRR(+10) Price: +10 EUR/MWh
Strategy 1	Normal control, no activation calls.		
Strategy 2	Activate HP if electrically self-sufficient and $T_{air}$ below 21 °C.		
Strategy 3	Activate HP if electrically self-sufficient and $T_{air}$ below 22 °C.		
Strategy 4	Activate HP if electrically self-sufficient and $T_{air}$ below 23 °C.		
Strategy 5	Choose the 3 buildings with the lowest temperature.		

Table 7: Strategies and FRR price scenarios considered.

The acceptance level of the activation calls depends on the price: the more the customer is willing to pay, the more often he gets activated. Depending on the FRR bids (-50, 0, or +10 EUR/MWh), a different number and frequency of activations occur. The higher the FRR price, the longer the duration of the activations and the more often they occur. This is shown in Figure 42. These three very different scenarios have been chosen to consider different alternatives when participating in the German FRR market and to be able to check their influence in the obtained results.

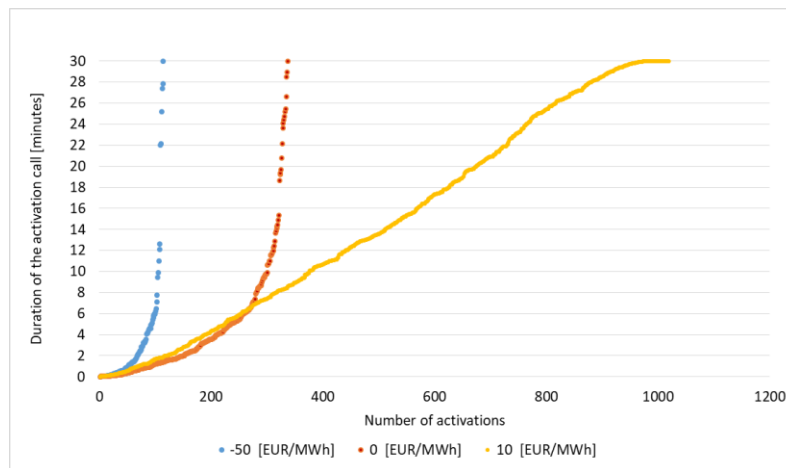


Figure 42: Comparison of the number of activation calls for the three scenarios depending on the duration. Real FRR data from February 2015.

### 3.3.3.4. Control strategy of the simulations

Whenever an activation call is received, a prediction of what would happen regarding the indoor temperature of the buildings if the heat pump is activated is necessary, since otherwise the activation of the heat pump could result in temperatures outside the comfort limits. However, predicting the state of each building after an activation call is a problem that incorporates many dynamic interactions, including solar and internal gains, climate, and the temperature of the thermal storage tanks. To overcome this, simulations with the control strategy shown in Figure 43 were developed for this work.

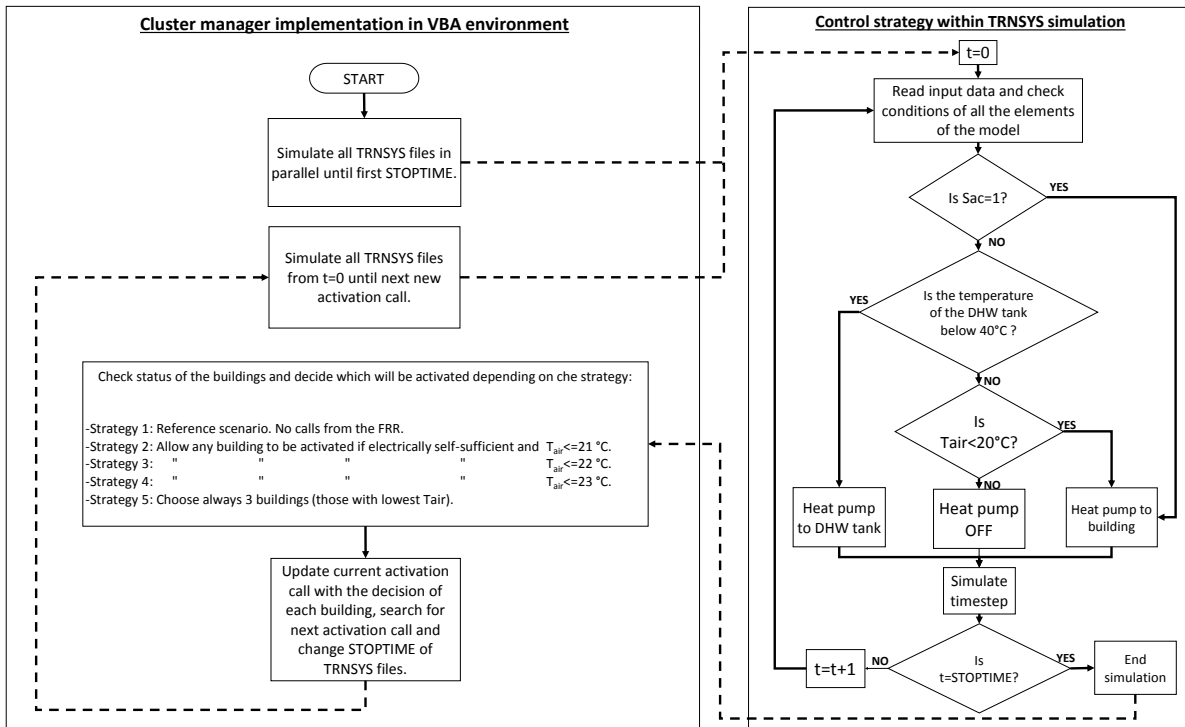


Figure 43: Flowchart of the simulations.

At the start of the simulation, the TRNSYS models of the six buildings are simulated in parallel through a batch file until the first FRR activation call is received. The control strategy during the simulation of each time step in TRNSYS can be seen on the right part of Figure 43, giving priority to activating the HP for the building if an activation call ( $S_{ac}$ ) is received, then to the DHW tank if there is no activation call but its temperature is below 40 °C (so that the provision of hot water is always guaranteed, which is the behavior in the real system), and last of all to the building to try to maintain a consistent temperature of 20 °C. It should be taken into account that the simulation in 30 minute intervals means that the HP will be either on or off during the whole time step. Note that a short duration of an activation call implies using the heat pump at the retail price of 22 cEUR/kWh for a long time, until completing the 30 minutes of its minimum running time.

Once the six buildings have been simulated until the first activation call (including it), the information flow is returned to the cluster manager, which checks the status of every building, and then makes a decision about the activation of each building depending on the strategy that is being followed. Then, the distribution of the activation calls among the buildings and the logging of the respective data are updated based on the decision. Then the simulations start again from the beginning, this time bypassing those activation calls where a decision has already been made.

### 3.3.4. Results: DR potential of a cluster of dwellings

#### 3.3.4.1. Overview of the strategies

In order to illustrate the way in which the different strategies work, Figure 44 shows an example of activation call decisions for the price scenario FRR (+10). In the graph, if an activation call is received and accepted its value is a 1. If it was received but discarded, it is shown as a 0.5. There were an observably large number of activation calls on this day for this price scenario. At the beginning of the day, none of the strategies accepts any activations. This is because the self-sufficiency constraints were not fulfilled for strategies 2, 3 and 4, and the building was not among the three with the lowest temperature in strategy 5. Later, some of the self-sufficiency constraints were fulfilled and the simulated building accepted some of the activations in the

different scenarios, reaching higher temperatures in those with higher temperature thresholds. Note that ventilation and solar gains also influence the temperature patterns in the simulation.

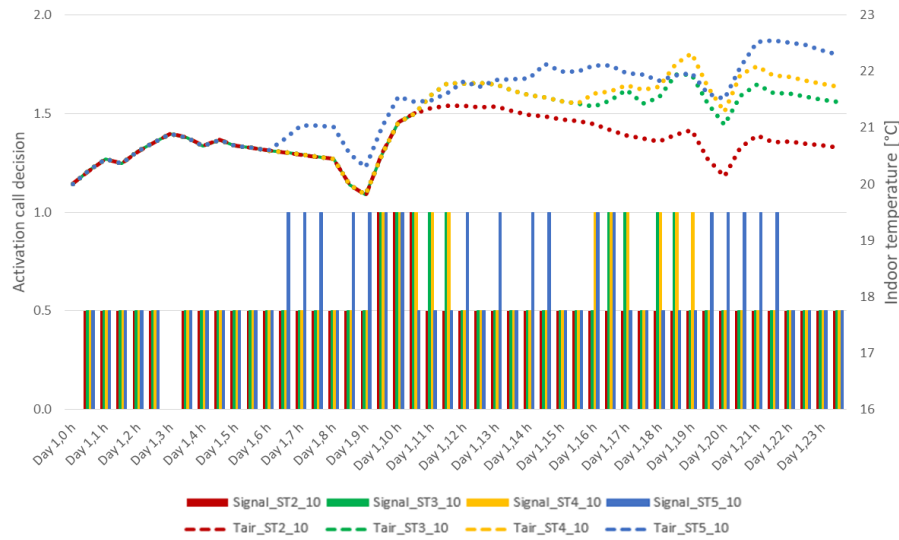


Figure 44: Example of activation call decisions and indoor temperatures.

### 3.3.4.2. Acceptance of the activation calls

In this section, we study the amount of times that each building accepted the activation calls for each strategy and for each price scenario. This is shown in Figure 45 as a percentage of activations. The nature of the data and experiment is such that there were a different number of activation calls in each price scenario, as higher price bids received more activations.

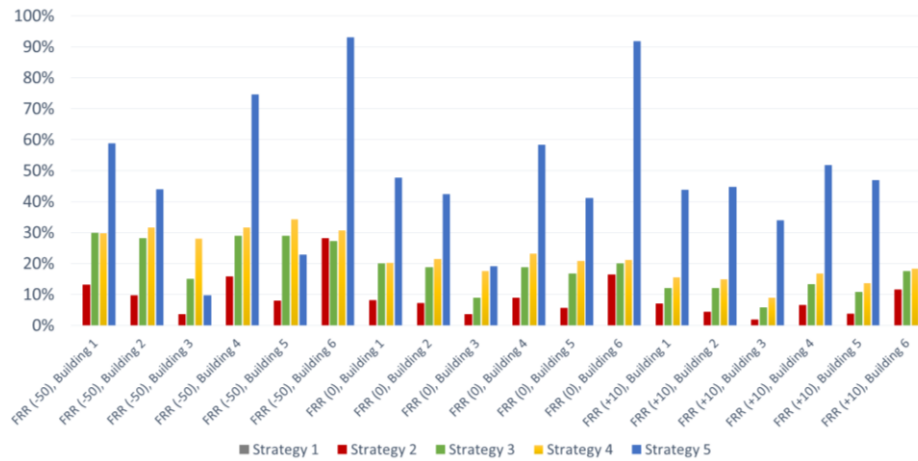


Figure 45: Percentage of accepted activations.

From the data we see, first, that strategy 5 results in the highest number of accepted activations. The reason is that there are no temperature constraints, and that three buildings are always chosen. Second, the higher the temperature threshold is, the higher the number of activations, which is a logical consequence of the building being allowed to be more overheated. However, the differences between strategies 3 and 4 are much smaller than between strategies 2 and 3. Third, the number of accepted activation calls is rather low due to the self-sufficiency constraint, which could be partially solved by having supplementing the heating systems with electric batteries with higher capacities. Fourth, these results allow for confirming that the number of activations generally increases in the price scenarios which have a higher number of activation calls. It is interesting to see that depending on the characteristics of the buildings, one participating in the price scenario FRR (+10) could be called less times than another one in the scenario FRR (-50). That is the case for example



of FRR (+10) Building 3 compared to FRR (-50) Building 6, even if the number of potential activation calls goes from around 100 to 1000. The reason is that building 6 has much higher energy losses, and so it would be able to accept the activation calls more often than building 3 which retains more thermal energy. The differences between the building typologies are further discussed in Section 3.3.4.7.

### 3.3.4.3. Thermal comfort

An important indication of the residents' levels of comfort, despite control of their heating systems, are the temperatures reached in the buildings during the different strategies' simulations. Figure 46 shows the total excess degree hours above 20 °C reached in the scenarios. By definition, this amount always increases with increasing temperature thresholds. However, we observe that the behaviour of strategy 5 is very different depending on the price scenario. In FRR (-50), the number of activation calls is low, so the amount of overheating is similar to that of the other strategies. In FRR (0) the excess degree-hours is already higher than in the other strategies and in FRR (+10) it is hugely increased. We also observe that there is not a noticeable difference when going from strategy 3 to strategy 4 in the case of building 6 for the price scenario FRR (+10). This is explained by the combination of there being a large number of activation calls, relatively high energy losses in the building and that the self-sufficiency requirement does not allow the building to reach the upper temperature limit of 23 °C.

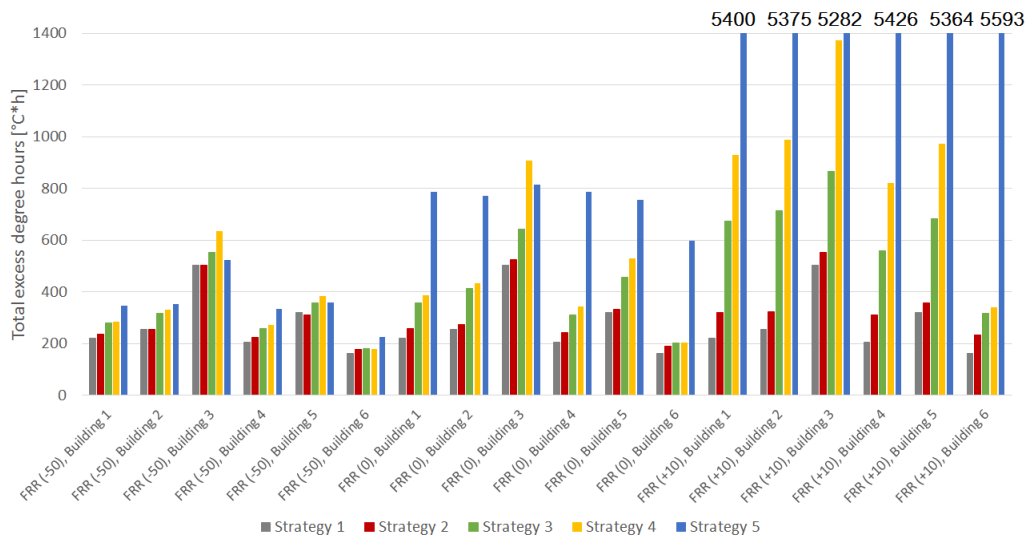


Figure 46: Total excess degree hours (> 20 °C).

All these observations allow us to conclude the following: if there is a contract requiring a constant power to be delivered by cluster manager to the aggregator, and the number of activation calls is rather high, then either temperature constraints should be imposed, or the amount of power offered should be decreased so that it is not necessary to activate large numbers of buildings. Otherwise, the overheating would result in unacceptable comfort levels for the residents.

### 3.3.4.4. Cost savings

The cost savings that can be achieved by the cluster manager when participating in FRR is one of the most important outcomes of the present work. The cost savings are calculated in each case by comparing each building with its own baseline case (strategy 1, no FRR participation). Figure 47 shows the results. As it can be seen, almost none of the proposed strategies are profitable, and those that are, produce practically negligible benefits. The main reason for such poor profit results is the following: as stated before, the assumption of the present work is that the heat pumps cannot be activated for less than 30 minutes to prevent a reduction of lifetime with many activation calls among other reasons. However, participating on the FRR market means that the heat pumps will be activated more often than in the original scenario, thus increasing their consumption and costs. Profits could still be made if the revenues from the FRR market were

considerably higher, but in the present context, these revenues (or cheaper electricity costs) do not compensate for the higher HP power use. Although the heat pumps benefit from lower prices during the activation calls, their duration may be short, and during the rest of the time that they are running until completing 30 minutes, the normal price will be charged. For this reason, there needs to be a large difference between the retail price and the energy price available on the FRR market if actors such as heat pump owners are to be motivated to participate in FRR. We discuss this further in Subsection 3.3.4.8.

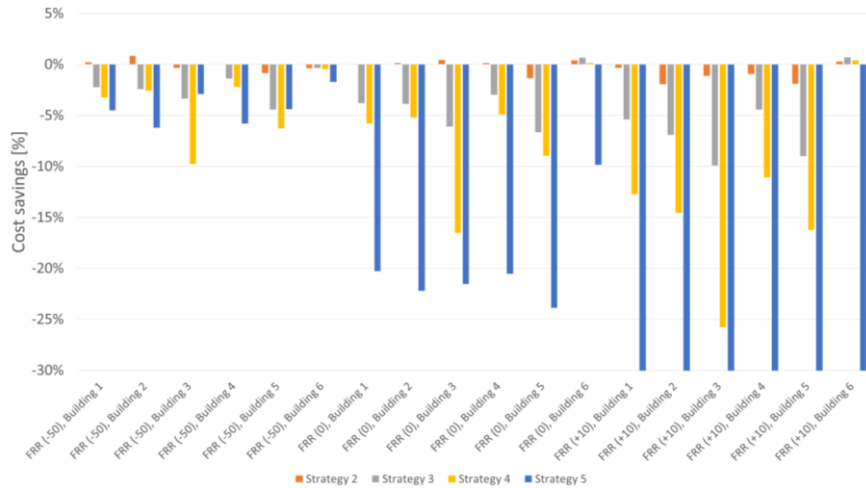


Figure 47: Cost savings [%] of the proposed strategies (negative values mean higher costs than their base case).

### 3.3.4.5. Self-consumption ratio and heat pump consumption

Changing the price scenarios does not significantly affect the ratios of self-consumption. Within this study, whenever an activation call is accepted, the negative power provided as FRR is that of the heat pump, and the rest of the system is isolated from this exchange. Since in the analysed strategies the heat pump consumption would in that case be assumed by the FRR, the ratio of self-consumption of the household is slightly increased. As regards to heat pump consumption, both increasing FRR price bids as well as increasing temperature thresholds increase the consumption of the HPs, which is as expected.

### 3.3.4.6. Power to the FRR

Depending on the strategy considered, a different amount of energy will be exchanged. The higher the HP consumption or the temperature threshold, the higher the exchange of energy between the cluster manager and the aggregator, therefore being able to provide more power as FRR. For the purpose of estimating the amount of energy obtained from the FRR market, we assume that there are 100 buildings of each of the 6 building typologies. When looking at the cluster results for FRR(0), the amount of power exchanged during the month can be seen in Figure 48. Strategies 2, 3 and 4 vary in the provided power, which can reach up to 2 MW in some cases but the activation calls are not always accepted. On the other hand, strategy 5 activates always the heat pumps of 300 buildings, providing in this way a more or less constant power of almost 1 MW, however with the thermal comfort issues stated in section 3.3.4.3.

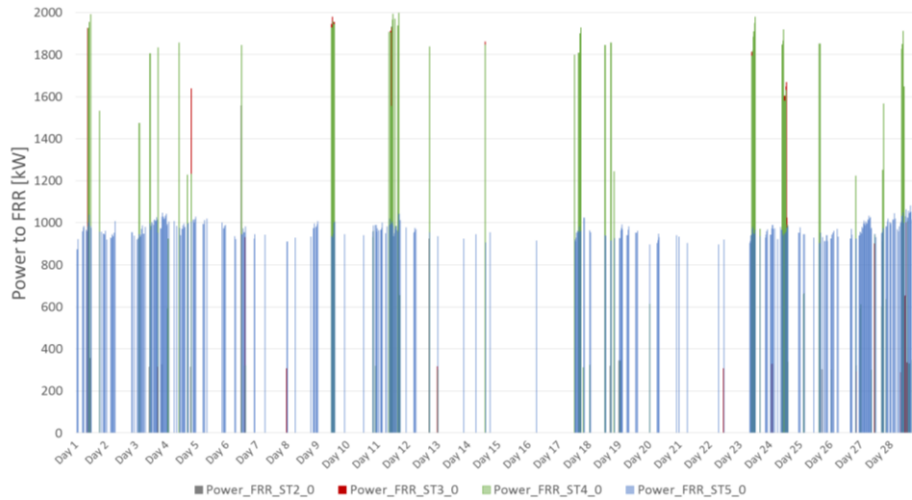


Figure 48: Power provided for price scenario FRR (0).

### 3.3.4.7. Comparison between building types

As shown in the previous sections, there are significant differences among the different building typologies. Regarding the number of activations, the buildings with higher energy losses (for example building 6) participate much more often on the FRR than those with fewer losses. The HP costs and consumption are obviously also higher, as well as the power exchanged with the FRR. The self-consumption ratio is also lower. The main conclusion is therefore that buildings with higher energy losses are more suited for participation in FRR than highly insulated buildings. These buildings can accept more activation calls, thus making their participation using these strategies more viable (although the thermal losses and the increase of HP consumption should also be carefully assessed).

### 3.3.4.8. Possible future price scenarios

Since the present study demonstrates that almost none of the proposed strategies are economically feasible with the current prices and taxes applicable to the DR participation in FRR in the studied German case, a sensitivity study based on different prices has been done to analyse the potential of these strategies if the market were to change. These prices would already include the taxes, so they are the final costs that the cluster manager would pay for the energy whenever an activation call is received. The rest of the time, the constant price of 22 cEUR/kWh is kept. Figure 49 shows the results, which consider different prices but keeping the same number of activation calls as well as duration of the previous scenarios.

As is apparent, there is a high influence of the number of activation times and their duration. The higher the number of activations and duration, the higher the profits. Strategy 5 is not profitable unless a very negative price is achieved, which seems unrealistic. The strategy 5 of FRR(+10) was discarded due to extreme overheating of the buildings. On the other hand, the profits of using the activation calls of price scenarios FRR(-50) and FRR(0) are mostly negative or negligible. In the case of using the activation calls of price scenario FRR(+10), the strategies start to be profitable when a final price around 10 cEUR/kWh is applied. Once that limit is reached, the lower the price, the higher the profits. Last of all, it can also be seen that the profits are higher for the number of activations and duration of the FRR(+10) price scenario when compared to FRR(-50) and FRR(0), even if the price for FRR(+10) is higher. All these outcomes highlight the importance of the number of activation times and their duration for heat pumps to participate in secondary reserve markets, as well as the need to reduce the taxes in order for them to be economically feasible.

Savings Cluster [%]	Price [€/kWh]	ST2_-50	ST3_-50	ST4_-50	ST5_-50	ST2_0	ST3_0	ST4_0	ST5_0	ST2_10	ST3_10	ST4_10
Price 1	0.20	-0.5%	-2.6%	-3.8%	-4.6%	-0.2%	-3.2%	-5.5%	-18.6%	-1.4%	-5.5%	-11.5%
Price 2	0.15	-0.2%	-2.1%	-3.2%	-4.1%	0.3%	-2.2%	-4.3%	-16.5%	1.2%	-0.5%	-5.1%
Price 3	0.10	0.0%	-1.6%	-2.7%	-3.5%	0.8%	-1.3%	-3.2%	-14.4%	3.7%	4.5%	1.3%
Price 4	0.05	0.3%	-1.1%	-2.1%	-3.0%	1.2%	-0.4%	-2.1%	-12.3%	6.3%	9.5%	7.7%
Price 5	0.01	0.4%	-0.7%	-1.6%	-2.5%	1.6%	0.4%	-1.2%	-10.6%	8.3%	13.6%	12.8%
Price 6	0.00	0.5%	-0.6%	-1.5%	-2.4%	1.7%	0.6%	-1.0%	-10.2%	8.8%	14.6%	14.1%
Price 7	-0.01	0.5%	-0.5%	-1.4%	-2.3%	1.8%	0.8%	-0.8%	-9.8%	9.4%	15.6%	15.4%
Price 8	-0.05	0.7%	-0.1%	-0.9%	-1.9%	2.2%	1.5%	0.1%	-8.1%	11.4%	19.6%	20.5%
Price 9	-0.10	1.0%	0.4%	-0.4%	-1.3%	2.7%	2.5%	1.3%	-6.0%	14.0%	24.6%	26.9%
Price 10	-0.20	1.5%	1.4%	0.8%	-0.2%	3.6%	4.3%	3.5%	-1.8%	19.1%	34.7%	39.7%
Price 11	-0.5	2.9%	4.4%	4.3%	3.0%	6.5%	10.0%	10.2%	10.7%	34.4%	64.8%	78.2%

Figure 49: Cluster cost savings depending on different price scenarios. Positive values mean the achievement of cost savings compared to the case with no FRR participation.

### 3.3.5. Conclusions and outlook

This work analyzed the role of heat pumps controlled by a cluster manager and equipped with both electrical and thermal storage systems for flexibility when providing FRR to the grid. Simulations with a time resolution of 30 minutes for a case study based on a plus-energy district built in southern Germany showed that the DR potential is significant, but for profits to be achieved, particular attention needs to be given to the number of activation times, and most importantly to their duration. Otherwise, it is very difficult for such a framework to be economically viable. As shown by an analysis of possible future scenarios, even if the prices paid by the grid operator were higher, the influence of the duration would be more important, since lower durations would entail a longer runtime billed at the normal price of electricity due to the minimum running time of the heat pumps.

For the reasons given in the previous discussions, some changes are necessary before these approaches that activate the heat pumps of a portfolio of buildings can be put into practice. If it is foreseen that households will participate in DR business models, then further control system algorithms at the cluster and aggregator levels need to be studied and applied to effectively manage and coordinate the availability of individual systems in and across households.

## 3.4. Summary of findings of this Chapter

In this chapter, evidence has been obtained on the contributions that demand side management approaches can bring to the energy system, with particular emphasis on the exploitation of the structural thermal energy storage capacity of buildings. In the first application that was shown in Section 3.2, several dynamic pricing strategies for DR purposes in a plus-energy dwelling were studied, concluding that savings up to 25 % could be achieved without sacrificing the thermal comfort of the occupants and achieving significant peak reductions on the grid. The importance of choosing the correct price thresholds when using dynamic pricing strategies was also highlighted, as well as that of knowing how much the users are willing to sacrifice their comfort to achieve savings. All in all, the outcomes showed the great impact that the use of heat pumps and the thermal storage capacity of buildings may have by using dynamic pricing strategies within a DR framework.

Widening the scale, the second application analyzed then in Section 3.3 the role of controlling the heat pumps in a district when providing FRR to the grid for flexibility. Simulations with a time resolution of 30 minutes showed that the DR potential is significant, but for profits to be achieved, particular attention needs to be given to the current economic incentives, the number of activation times, and most importantly their duration. Otherwise, it is very difficult for such a framework to be economically feasible. Also, buildings with higher energy losses are more suited for participation in FRR than highly insulated buildings, since they can accept more activation calls (although the increase of energy consumption should also be carefully

assessed). Some changes are therefore necessary before these approaches can be economically viable, but their benefits with regards to providing flexibility for reserve markets given the right conditions has been demonstrated.

Finally, we should bear in mind that even though building models such as the ones created for the purposes of this chapter can be quite precise, and allow to reach important conclusions regarding the benefits provided by demand side management approaches, they are not sufficiently adequate for evaluating real cases on a district scale. This is mainly due to the assumptions that are made in the process, related to the real characteristics of the buildings under consideration and their use patterns. In Chapter 2, it was highlighted that in order to assess innovative approaches that require dynamic interactions such as demand side management in a certain district, it is necessary to characterize its buildings in an accurate way that reflects their real characteristics and operation. Before addressing that issue, here in Chapter 3 we analyzed first the benefits that could be obtained from the implementation of demand response approaches on a district scale. Once this has been accomplished, the next step in this Thesis will be to define a methodology in Chapter 4 for a proper characterization of districts through monitoring, which will then be applied in Chapters 5 and 6 for further demand side management applications.



## 4. BASELINE MODELS FOR CHARACTERIZATION, FORECASTING AND DECISION-MAKING IN DISTRICTS

In the author's opinion, any district should be evaluated based on its real performance. Even though very precise simulation models can be developed, ideally a monitoring campaign should be carried out, which would provide the necessary information for an even more accurate assessment. The spatial and temporal variability of the conditioned spaces in a district make their operation very different from each other, and also from that of the standard uses of the normative. Depending on the climatic zone where a district is located, there may be cases of relatively benign climates in which the buildings operate in free-floating during most of the time, or other harsher climates in which the buildings use frequently the air-conditioning systems. As a consequence, the air-conditioning energy use in districts presents the following features:

- Difficulty when comparing the energy performance between dwellings (benchmarking), since their conditions are not homogeneous.
- Difficulty to distinguish the impact of energy saving measures.
- Difficulty to justify and prioritize the implementation of energy saving measures (if there is no consumption there are no savings).
- Difficulty to evaluate the efficiency of retrofitting measures by comparing the conditions before and after their implementation.

For these reasons, it is necessary to carry out measurements that provide precise knowledge of the real behavior and operation of the buildings under study. The methodology proposed in Chapter 2 to select the representative buildings of a district could be followed, monitoring those buildings in detail.

In this chapter, a novel proposal for obtaining energy baselines in residential buildings will be developed, which consists of transfer functions that are able to characterize any building based on measured data of its air-conditioning consumptions and indoor air temperatures. The procedure is also sensitive to the different operating conditions of buildings, which may vary through time, and will be validated both theoretically and experimentally. In addition, short monitoring campaigns would be sufficient. The proposed model solves the difficulties of characterizing a district in detail. This means a qualitative step forward, since most existing tools are simplified and are unable to reach such detailed analyses, mainly due to the high computational costs and time consumption.

Having a method to characterize buildings allows many possibilities. Among them is calibration, which would enable to calibrate simulation models. Also, another potential alternative would be to use the proposed baselines for forecasting purposes, using them in real time when integrated within an energy management system. Last of all, decision-making would also be possible, since for instance different approaches of demand side management could be evaluated simultaneously before deciding the optimal alternative.

In this chapter, Section 4.1 will include the fundamentals of baseline models. Then, Section 4.2 will develop the mathematical basis of the model. Section 4.3 will include a theoretical and experimental validation of the model, and last of all Section 4.4 will propose several alternatives for the integration of the proposed baseline models with DSM approaches.

## 4.1. Fundamentals of baseline models

One of the main issues related to existing buildings is to conduct accurate assessments of the energy savings achieved after implementing improvement measures. This process is known as Measurement and Verification (M&V) of energy savings [139], which is illustrated in Figure 50.

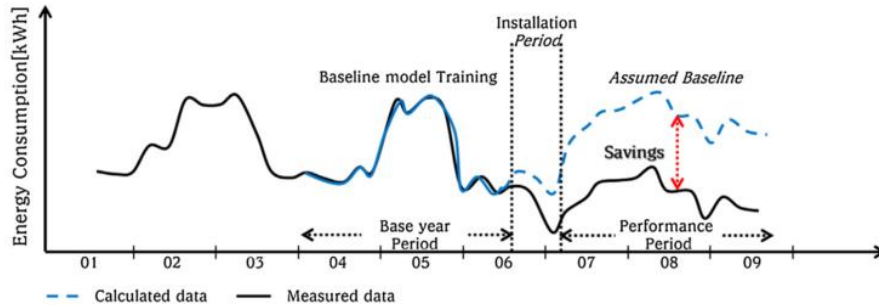


Figure 50: Baseline concept [140].

The M&V process can be summed up in four stages:

1. Measure the initial situation for its energetic characterization (baseline model).
2. Evaluate different alternatives for energy saving and efficiency, choosing the optimal one.
3. Implementing the optimal alternative and measuring the new energetic status of the building.
4. Guarantee the energy and economic savings, comparing the measurements from the previous stage with the baseline.

The proposed model derives from the need to have versatile and reliable energy baselines, which allow not only to evaluate the impact of energy saving measures in buildings, but also other alternatives. In the present Thesis, the baselines that will be proposed could be used as a tool for the characterization of the thermal performance of districts, the design of retrofitting strategies, software calibration or as a support for management algorithms that aim to forecast future energy consumptions or the impacts of improvement measures. Since one of the premises required from the proposed model was that the physical component of the characterization had to be predominant over the mathematical component, this guarantees a good extrapolation of the results when the conditions of climate or use of the building are different from the ones used for the adjustment of the model.

Forecasting energy consumptions is very important for the optimization of energy management, and it is also needed for energy storage. There is no single way to create a model to perform consumption forecasting, since each model presents different advantages and disadvantages. However, the most widespread line of research is based on neural networks. The following table shows a comparison between the models found in different publications.

Model	Complexity	Simplicity	Applicability	Inputs	Accuracy
Detailed	Very high	No	Low	Detailed	Very high
Simplified	High	Yes	High	Simplified	High
Statistical	Reasonable	Yes	Very high	Historic	Reasonable
Neural Networks	Very high	No	High	Historic	High
SVM Vector	Very high	No	Low	Historic	Very high

Table 8: Characteristics of the different models used in previous publications. Source: [141].



As could be seen in the previous table, the simplified alternative presents features significantly valid. Simplified models are used due to their low computational costs, which allow their implementation in tools such as those for the support of urban planning or the integrated management of districts. Both cases present similar requirements: high accuracy, but limited computational costs that allow their execution multiple times in real time.

Forecasting the variables related to energy consumption allows the estimation of their future evolution, with the aim of being able to anticipate peak demands or predict future consumptions. In the case of electricity consumptions, forecasting is an essential tool for an optimal management of energy production and consumption. The problem of electricity is that it cannot be stored in an efficient way. Therefore, knowing the future evolution of the consumptions would allow reducing the losses due to an excess of produced electricity.

The application of predictive algorithms for the estimation of the consumption in buildings is very convenient due to three main reasons:

- Long-term forecasting provides an advantageous position with respect to the electricity supplier, since knowing the estimated consumptions would allow to negotiate the terms of the contract.
- Knowing the demands beforehand and being able to program the activation of systems such as air-conditioning units would also allow to avoid peak demands.
- A reliable forecast with a one day time horizon would allow not only to schedule the consumptions, but also the possibility of benefitting from dynamic pricing markets or time-of-use tariffs.

The main objective of the present chapter is to develop and validate a novel proposal for obtaining energy baselines, valid for residential buildings. The model should be dependent on the indoor air temperature, as a thermal response of the building, and the air-conditioning consumption, as response to the air-conditioning systems. In addition, due to the high thermal inertia of buildings, the proposed models should contemplate dynamic effects, taking into account what is happening in the current time-step but also what happened in the previous ones. Furthermore, as explained above, the proposed procedure should be sensitive to the operating conditions of the building, since they may vary throughout the period of verification of energy savings. Within the framework of this Thesis, the prediction of energy consumption will be used for the evaluation of different strategies that operate the air-conditioning systems. This will be presented in Chapters 5 and 6.

## 4.2. Mathematical basis of the developed QT model

In this section, the model that has been developed will be explained in detail. The proposed model will be named "QT", due to its combination of thermal loads (usually represented by Q in heat transfer equations) and indoor air temperature (represented by T).

### 4.2.1. Initial hypotheses

The model presents the following assumptions:

- The time base is variable. During the development of the model, scenarios that consider ranges from 10 minutes to 1 day have been validated.
- The invariance of the models due to the fact that the coefficients are constant require to consider as many options as different operating modes. In this methodology, the heating and cooling periods are distinguished, particularizing the procedure in each of them.
- It is necessary to know the weather conditions, the times when the air-conditioning was operating as well as the corresponding set-point temperatures in order to make use of the baseline model.

- It will be considered that when the air-conditioning system is activated, the target variable will be the air-conditioning consumption, and the representative indoor air temperature during the operation would be known.
- The limitations linked to the invariance of the model or hard to measure excitations (such as internal gains variations, heat flows due to long wave radiations or the effects of the building's inertia) are implicit in the indoor air temperature model. This means that, if the building is retrofitted, the evolution of its indoor temperature when the air-conditioning system is activated can be an input for the calculation of the energy use through the characterized model. This is due to the fact that the temperature-humidity conditions can be compared to the ones of the building if it had not been retrofitted. However, the evolution of the indoor temperature of the building when the air-conditioning system is not activated is different for the retrofitted and non-retrofitted building, since it is as if they were different buildings. This difference of temperatures is linked to the energetic difference between the initial situation (monitored scenario used for the adjustment of the models) and the new situation that wants to be evaluated.

## 4.2.2. Development of the baseline models

The procedure that is going to be explained requires measured data of the heating or cooling consumptions for its application (through direct monitoring or through the estimation of the disaggregation of the total electricity consumptions) and indoor temperature data of the representative spaces. In addition, it is supported by the use of an energy performance of buildings assessment tool such as HULC, which allows to obtain the excitations of each relevant space. Therefore, a geometric, constructive and operational multi-zone definition is required, distinguishing the monitored spaces.

The procedure for the characterisation of the energy demand consists in developing and applying sequentially two baselines:

- Primary baseline: characterization of the full free-floating indoor temperature assuming that the user has been neutralized (no air-conditioning systems are operated).
- Secondary baseline: characterization of the air conditioning consumption with the real operation of the building.

### 4.2.2.1. Primary baseline

For the development of the model, an analysis of the fundamentals of buildings' thermal demands will be done. The calculation principles of these demands in a steady-state are included in the standard ISO 52016-1:2017 [142] and can be synthesized in the following equation.

$$D = Q_{LOSS} - \eta \cdot [Q_{GAIN-SUN} + Q_{GAIN-INT}] \quad \text{Eq. 1}$$

Where  $D$  is the thermal heating (+) or cooling (-) need.  $Q_{LOSS}$  refers to the heat losses of the building through its thermal envelope, as well as due to ventilation/infiltrations.  $Q_{GAIN-SUN}$  are the solar gains, and  $Q_{GAIN-INT}$  are the gains due to internal sources.  $\eta$  is the utilization factor.

If the functional dependency of each of them is analyzed in a simplified way:

$$Q_{LOSS} \approx (U \cdot A + \rho \cdot C_p \cdot ACH_{eq} \cdot V) \cdot (T_{IN} - T_{OUT}) \quad \text{Eq. 2}$$

$$Q_{GAIN-SUN} \approx AS \cdot RAD \quad \text{Eq. 3}$$

$$Q_{GAIN-INT} \approx \Phi \cdot t \quad \text{Eq. 4}$$

Where  $U$  is the thermal transmittance,  $A$  is the total area of the thermal envelope,  $\rho$  is the density of air,  $C_p$  is the specific heat,  $ACH_{eq}$  is the equivalent Air Changes per Hour of the ventilation,  $V$  is the volume,  $T_{IN}$  is the indoor temperature,  $T_{OUT}$  is the outdoor temperature,  $AS$  is the Solar Area of the space,  $RAD$  is the solar

radiation and  $\emptyset$  is the internal gains. All these variables are detailed in the cited standard, together with the particularities of its formulation.

Note that in the case of having no air-conditioning equipment, the air-conditioning consumption would be null, just as the real demand of the building. This allows relating the indoor temperature with climatic excitations, the use of the building through its internal gains as well as the characteristics of construction and geometry of the building.

$$T_{IN} = f(\text{TEXT}, \text{RAD}, \emptyset \cdot t, (UA + \rho \cdot C_p \cdot ACH_{eq} \cdot V)) \quad \text{Eq. 5}$$

This temperature is known as the full free-floating temperature, since it makes explicit reference to the indoor temperature that the building would have if it were never air-conditioned. The effect of air-conditioning is linked to the effects of the users, who turn on/off the air-conditioning units and establish their operating conditions.

As mentioned before, the proposed model has the same principles and formulation as transfer functions, whose mathematical formulation takes the form of:

$$f(t) = \sum_{i=1}^k \sum_{j=0}^m a_{ij} \cdot Y_i(t-j) - \sum_{j=1}^n d_j \cdot f(t-j) \quad \text{Eq. 6}$$

Where:  $f(t)$  is the target variable;  $Y_i$  are the  $k$  independent variables or excitations;  $a_{ij}$  are the  $m$  adjustment coefficients (numerators) of each variable  $Y_i$ ; and  $d_j$  are the  $n$  denominators or dependencies of the target variable with the past time-steps.

It should be noted that the target variable  $f(t)$  is a function of the excitations  $Y(t)$  in the current time-step but also in the previous ones, and also depends on the target variable itself in previous time-steps. These dependencies are linked to the inertia of the system. Therefore, the number of previous time-steps to be considered should be optimized depending on the characterized system.

The proposed methodology has also adopted the same nomenclature of numerators and denominators as transfer functions [143], which comes from their definition as the quotient between the Laplace transform of the response of the system  $Y(s)$  and the causative excitation  $U(s)$ .

The concrete expression of primary baseline takes the form of:

$$T_{FF}(t) = \sum_{i=0}^{N1} a_i \cdot T_{OUT}(t-i) + \sum_{i=0}^{N1} b_i \cdot SG(t-i) + \sum_{i=1}^{M1} d_i \cdot T_{FF}(t-i) + CONST \quad \text{Eq. 7}$$

$N1$  and  $M1$  are the number of numerators and denominators. These numbers depend on the time constant of the system that needs to be characterized as well as the period of observation [144]. The parameter  $CONST$  refers to the use of the building, which is considered invariant and therefore is included as a constant term of the model. On the other hand,  $SG$  represents the solar gains, which will be explained in more detail in the next section.

In real circumstances of operation, it is difficult to find continuous periods in which the building operates in free-floating during a sufficient amount of time (several days for example) during the heating and cooling periods. In this work, an innovative procedure that uses free-floating hours interspersed between conditioning periods has been used, developing a statistical base that allows to obtain the correlation coefficients of the primary baseline expression.

Last of all, it may be convenient to analyze the physical meaning of the coefficients of the proposed model. This physical meaning establishes the restrictions that should be taken into account in the process of identifying the coefficients.

1. The radiant exchange of the building with its surroundings is simplified to the effect of the outdoor air temperature by the coefficients  $a_i$ .

$$\frac{\sum_{i=0}^N a_i}{1 - \sum_{i=1}^M d_i} \sim 1 \quad \text{Eq. 8}$$

Values between 0.8 and 1 are accepted, where 1 implies that in steady-state the indoor air temperature would match the outdoor temperature if there were no internal or solar gains, and 0.8 implies that there would be a 20% difference between the indoor air temperature and the outdoor temperature due to the excitations that are contemplated implicitly such as the radiant exchange with the surroundings.

- The coefficients related to the solar gains allow to infer the net solar gains. This implies that the value of these coefficients in a steady-state should be lower than 1.

$$\frac{\sum_{i=0}^N b_i}{1 - \sum_{i=1}^M a_i} < 1 \quad \text{Eq. 9}$$

- The internal gains produce an increment of the indoor temperature. This increase is linked to the constant CONST, which should be higher than 0.

It must be stressed that modifications of the adjustments should be made differentiating the winter and the summer season due to the invariance of the model. The reason for this is that the behavior of the occupants is different in both seasons with regards to the use of the solar shading devices (such as blinds) or the opening of windows during the night.

#### 4.2.2.2. Solar gains

First of all, the net solar gains will be formulated as a function of the transmitted radiation (direct and diffuse) and that absorbed by the windows of the building.

$$SG(t) = \sum_{j=0}^{N3} Dg_j \cdot DC(t-j) + dg_j \cdot dC(t-j) + ag_j \cdot AR(t-j) + \sum_{j=1}^{M3} k_j \cdot SG(t-j) \quad \text{Eq. 10}$$

Where  $DC(t)$  and  $dC(t)$  are the direct and diffuse radiations respectively, transmitted to the interior of the building through the windows. Also,  $AR(t)$  is the radiation absorbed by these elements. The coefficients  $Dg_j$ ,  $dg_j$  and  $ag_j$  are obtained through simulations and they allow to convert the gross gains into net gains.  $N3$  and  $M3$  are the number of coefficients.  $M3$  normally takes a value between 1 and 2, whereas  $N3$  should be optimized in order to obtain a good adjustment of the model.

The following graph shows an example of direct and diffuse solar radiations in a certain building for the South orientation.

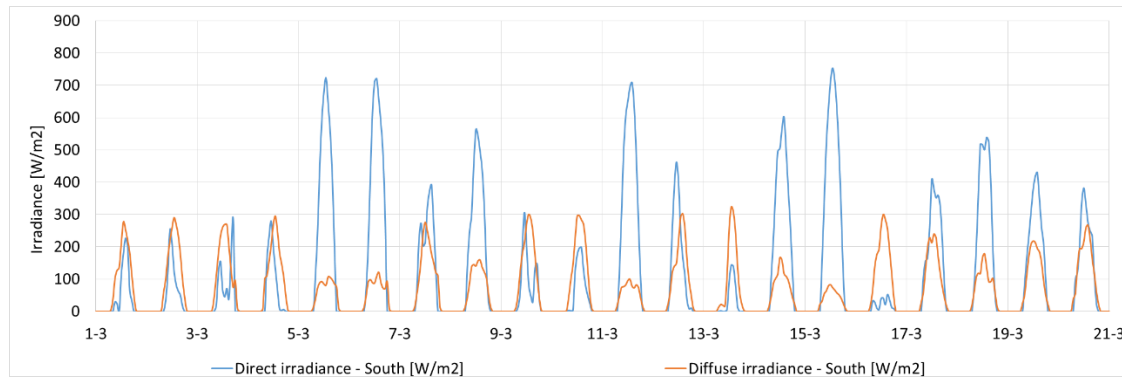


Figure 51: Example of direct and diffuse solar irradiance for the South orientation during several days.

The values of solar radiation for each orientation allow to obtain the transmitted direct and diffuse solar radiations, as well as the one absorbed, by using the following equations.

$$DC(t) = \sum_i A_{Vi} \cdot g_i \cdot DR_i(t) \quad \text{Eq. 11}$$

$$dC(t) = \sum_i A_{Vi} \cdot g_i \cdot dR_i(t) \quad \text{Eq. 12}$$

$$AR(t) = \sum_i A_{Vi} \cdot \alpha_i \cdot GR_i(t) \quad \text{Eq. 13}$$

Where the area of each window is known,  $A_{Vi}$  [ $m^2$ ], as well as their modified solar factors  $g_i$ , absorptivity  $\alpha_i$  and orientation. This allows to obtain the incident global radiation  $GR_i(t)$ , as well as the direct  $DR_i(t)$  and

diffuse  $dR_i(t)$  components. It should be highlighted that the modified solar factor refers to the amount of radiation transmitted through the window.

In the following graph, the magnitude of these gross solar gains on the building is shown. In this case, the building has a window of 3 m<sup>2</sup> oriented to the south, and another one of 2 m<sup>2</sup> oriented to the west.

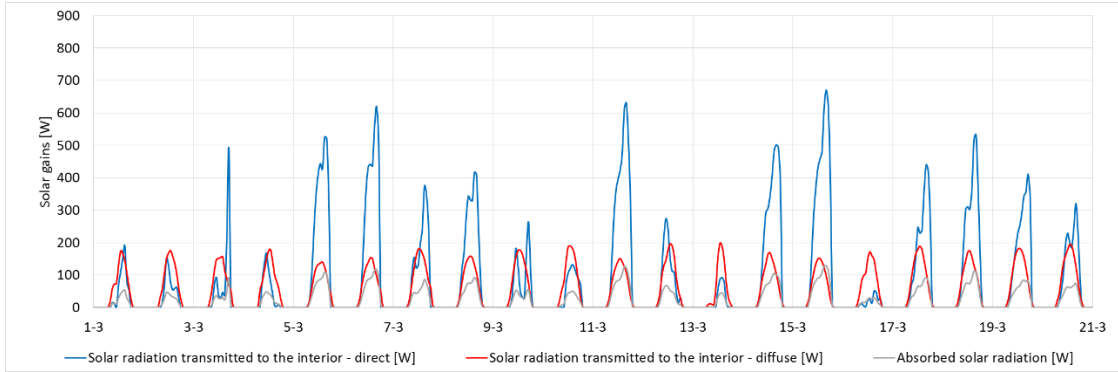


Figure 52: Example of gross solar gains on a building.

Finally, by using the previous equations it is possible to obtain the net solar gains through simulation, as well as the estimation carried out by using the proposed transfer function. In this case,  $M3$  takes a value of 1 and  $N3$  of 3.

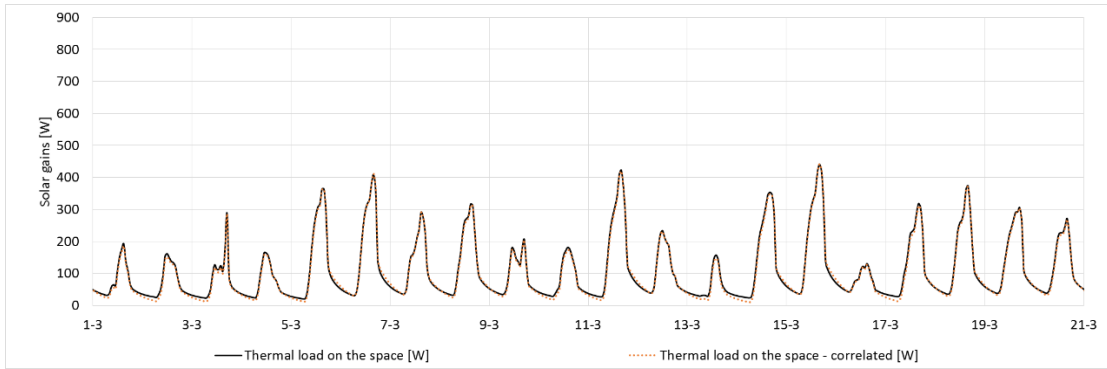


Figure 53: Thermal load on the space due to solar gains.

This graph shows the achieved accuracy and also how the gross solar gains, when converted into net solar gains (in other words the thermal load on the space), are delayed in time and even appear once the excitations have ceased.

#### 4.2.2.3. Secondary baseline

Once the primary baseline has been obtained, the energy consumption  $Q(t)$  in a certain timestep can be determined by observing the deviation that exists between the desired set-point temperature and the free-floating temperature obtained by the primary baseline. The formal dependency that regulates the previous relationship takes the following form:

$$Q(t) = \sum_{j=0}^{N2} C_j \cdot \Delta T(t-j) + \sum_{j=1}^{M2} D_j \cdot Q(t-j) \quad \text{Eq. 14}$$

Where  $\Delta T(t) = T_{IND}(t) - T_{FF}(t)$  is the difference between the desired set-point temperature in the building (using an air-conditioning system) and the indoor temperature that the building would reach spontaneously without air-conditioning systems (full free-floating temperature).

The Q model requires knowing the air-conditioning consumption as well as the indoor air temperature response of the space/building. In this way, when the air-conditioning system is not activated the energy consumption is zero, and the indoor air temperature is obtained from the previous expression. On the

contrary, if the air-conditioning system is activated, the electricity consumption would be obtained through the T model and the measured or desired (set-point) indoor temperature.

If the previous expression is considered in steady-state, and instead of knowing the air-conditioning consumption the thermal energy delivered to the building is known, the UA value of the thermal envelope of the building may be obtained.

$$UA = \frac{Q}{\Delta T} = \frac{\sum_{j=0}^{N2} C_j}{1 - \sum_{j=1}^{M2} D_j} \quad \text{Eq. 15}$$

Due to the approach followed for the secondary baseline, it is obvious that it is applicable when the set-point temperatures or the air conditioning periods are changed. Therefore, it proves its applicability as a method to obtain the energy demand in standard conditions for instance (reference climate and standard user).

### 4.3. Validation of the model

In this section, the proposed baseline models will be validated in two ways: first, a theoretical validation will be carried out through simulation, and then an experimental validation will be done by using temperature and air-conditioning consumption measurements obtained from the monitoring of a household.

#### 4.3.1. Theoretical validation

##### 4.3.1.1. Case study

A dwelling located in a social housing district in Seville (Spain) will be considered for the validation of the proposed models. This dwelling is located on the third floor of one of the building blocks of the district (see Figure 54).

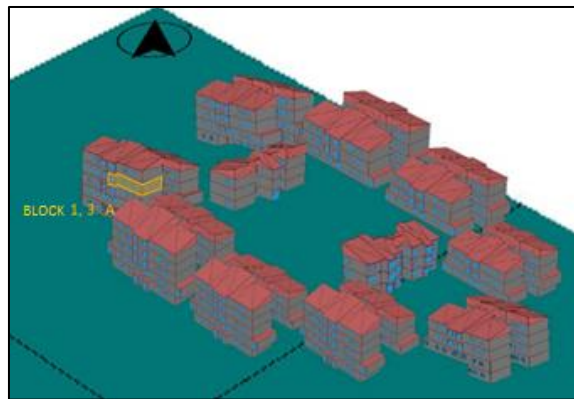


Figure 54: Location of the dwelling under study.

In order to carry out a detailed analysis of the thermal behavior of the dwelling, it is necessary to know the distribution of the different spaces, so a HULC multi-zone model was created to reflect the reality. In addition, it is necessary to include the shading effects due to the surrounding buildings, since these could have a great influence on the energetic behavior of the dwelling due to reduced solar access, particularly in the building under study. The building where the dwelling is located was built in 1983. The main facade is oriented to the South-West, and the quality of construction of its walls and windows is rather poor.



Figure 55: HULC model of the dwelling (left) and real image (right).

#### 4.3.1.2. Results of the theoretical validation

The main objective of this theoretical validation is to show the details of the application of the proposed baseline models. In order to do that, the first step is to simulate the HULC building model that was created, considering the real weather conditions. This is done by creating a weather file following the procedure explained in Annex A. The first simulation is performed without air-conditioning. That means that the full free-floating temperatures can be obtained, giving way to the primary baseline. An example of the temperatures that are reached inside the dwelling during the heating season is shown in the next figure.

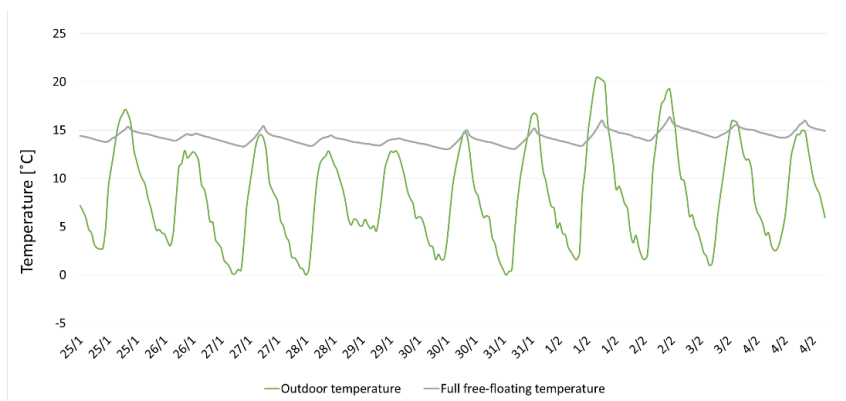


Figure 56: Illustration of the evolution of the indoor and outdoor temperatures.

If the whole year is shown (see Figure 57), the effect of the internal and solar gains can be observed. In average, the indoor temperature is higher than the outdoor temperature. Then, once the effect of the gains has been demonstrated they should be characterized. In order to do so, another simulation is performed in such a way that the thermal load due to solar and internal gains can be disaggregated.

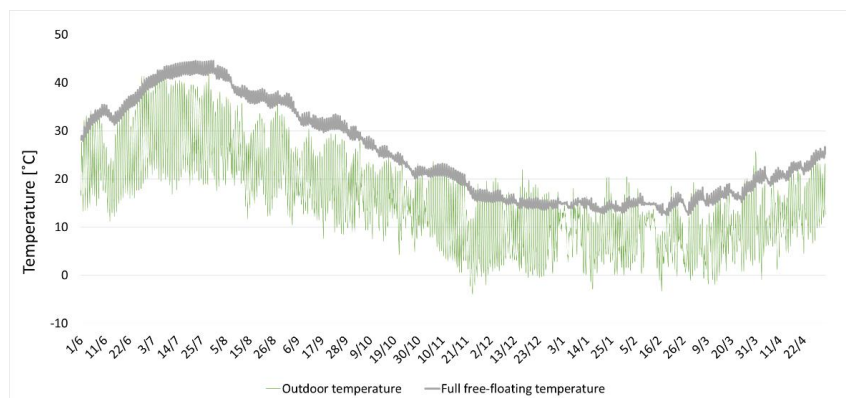


Figure 57: Effect of the internal and solar gains on the indoor temperature.

Finally, the proposed model for obtaining energy baselines will be obtained. To do so, first the primary baseline is identified, and then the secondary baseline with 6 numerators and 1 denominator. The primary baseline allows to estimate the full free-floating temperature, which combined with the secondary baseline model allows to estimate the thermal loads of the space when the air-conditioning equipment is activated, or the air temperature when the air-conditioning is not working. The following graph shows a comparison between the air-conditioning consumptions obtained by the simulation and the ones estimated through the proposed baselines, as well as a comparison between the temperatures obtained by the simulation and the ones estimated. The validity of the proposed procedure is demonstrated, as well as the goodness of fit offered by the physical sense that was forced in the identification of the coefficients of the proposed transfer functions.

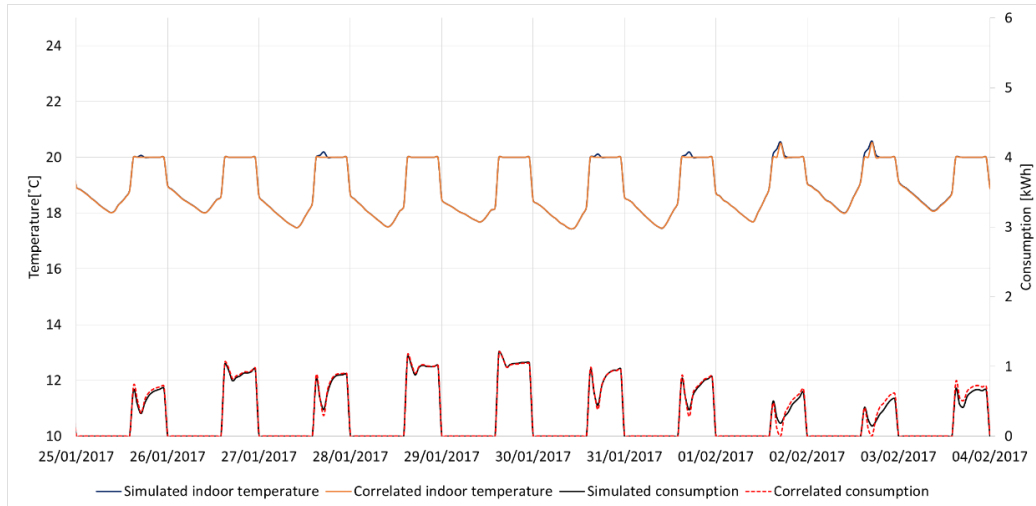


Figure 58: Comparison between simulated and estimated temperature and consumption measurements.

To illustrate the way the baselines work, we can see for example what happens at the end of March. Since the indoor air temperatures are over 20 °C and below 25 °C, there is no need for air-conditioning. As it can be seen in the figure below, although the indoor temperatures and the ones estimated by the primary baseline (full free-floating temperature) were very different during days when the air-conditioning system was working, after turning off the air-conditioning for some days they are very similar.

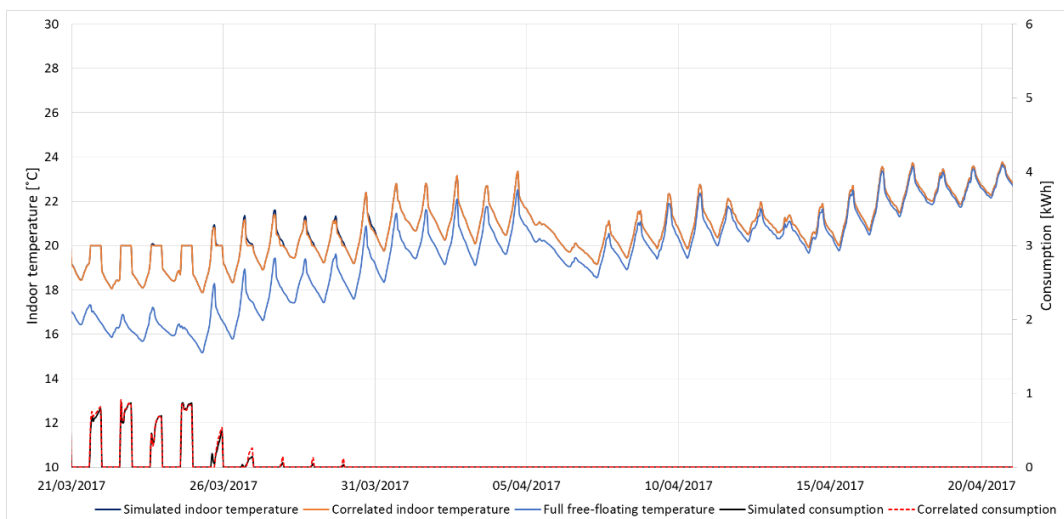


Figure 59: Evolution of the full free-floating temperature and the indoor temperature.



## 4.3.2. Experimental validation

### 4.3.2.1. Required monitoring

The first requirement in order to evaluate the real thermal performance of a district is to have temperature measurements of its representative buildings. This could be done by installing temperature sensors, preferably in the spaces that use the air-conditioning systems, but also in those which do not use them. More information about these sensors is given in Annex C.

On the other hand, an accurate assessment of a district would require data of the HVAC energy consumption of its representative buildings, which could be possible by installing a Smart Plug on the air-conditioning systems. However, if this were not possible, disaggregating these consumptions in residential buildings is an intricate task. The main reason is that even when there is access to the total electricity consumptions, they are very volatile and depend on the number of occupants, their behavior, income, size of the dwelling or climatic zone. Nevertheless, there are some ways in which this disaggregation of the air-conditioning consumption could be estimated: using the total electricity consumption combined with measurements of temperature, or using standard profiles. These alternatives are presented in Annex B in more detail and will be applied in Chapter 5.

### 4.3.2.2. Estimation of the matching climate

The energy consumption and thermal comfort of the dwellings in a district may be inferred by using data from a monitoring campaign, but the real weather conditions are also necessary for an accurate assessment. Ideally, a weather station should be installed in the district. However, if this were not possible (mainly due to budgetary constraints) there are other alternatives. Annex A describes the procedure developed in the present work to obtain a weather file at any location, modified through real measurements of outdoor temperatures, humidity and solar radiation that are typically obtained from weather stations that are located nearby. Once this new weather file is created, it can be used to perform simulations under real climatic conditions, or it can be applied for the baseline models developed in this chapter.

### 4.3.2.3. Case study

The same dwelling that was used in the previous section for the theoretical validation will be considered here. In this case, a temperature sensor was installed in the living room of the dwelling under study, and a Smart Plug was installed on the air-conditioning unit to measure its electricity consumption. A Smart Meter was also installed to check the total electricity consumption of the dwelling. The devices were operative from the 25<sup>th</sup> of July to the 15<sup>th</sup> of September 2017. The measurements obtained during this period can be seen in Figure 61.

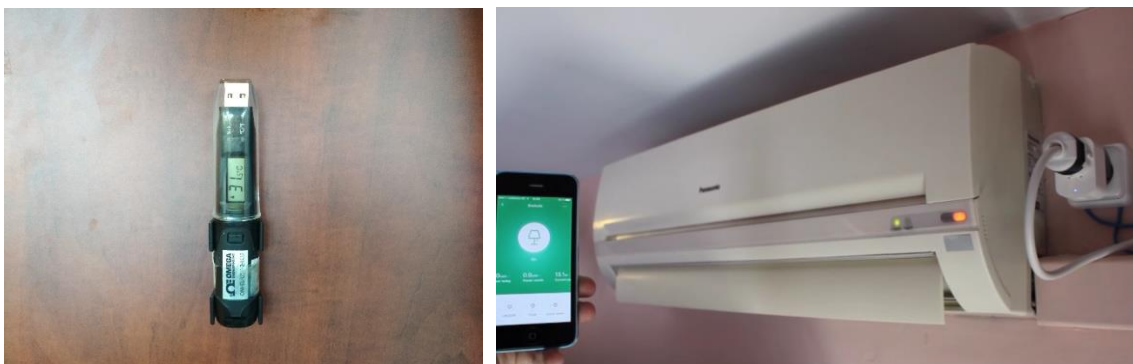


Figure 60: Installation of the temperature sensor (left) and smart plug on the air-conditioning system (right).

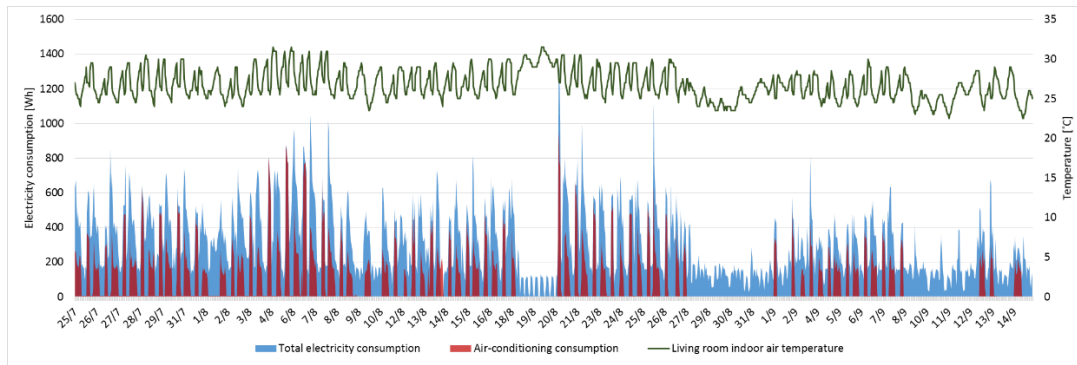


Figure 61: Measurements obtained from the monitoring campaign.

#### 4.3.2.4. Results of the experimental validation

In order to show the results obtained by using the proposed methodology of energy baselines, we will focus on 3 weeks in August 2017. Since the real air-conditioning consumptions were available (as well as the total household electricity consumptions), in this case there was no need to disaggregate the consumptions during this period. Once all the process for obtaining the baselines was carried out, it was possible to establish a correlation between the real air-conditioning consumption and the temperatures that were reached in this dwelling. The following figure shows the measured indoor temperature of the living room of the dwelling compared to the correlated values that were obtained, demonstrating the validity of the procedure.

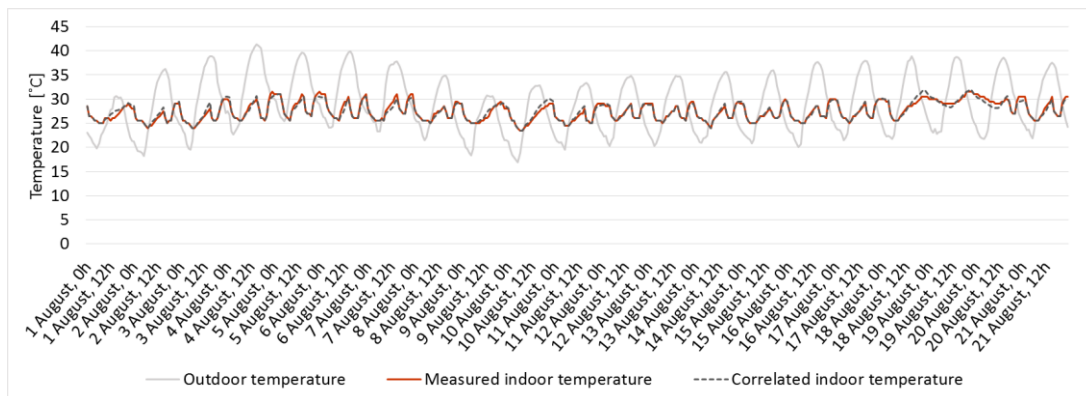


Figure 62: Comparison between the measured and estimated indoor temperatures.

In addition, the full free-floating temperature that the space would have had if the air conditioning system had not been used at all (obtained by using the primary baseline), as well as the total electricity consumption and the air conditioning consumption (measured and the one estimated in the previous section) can be seen in Figure 63.

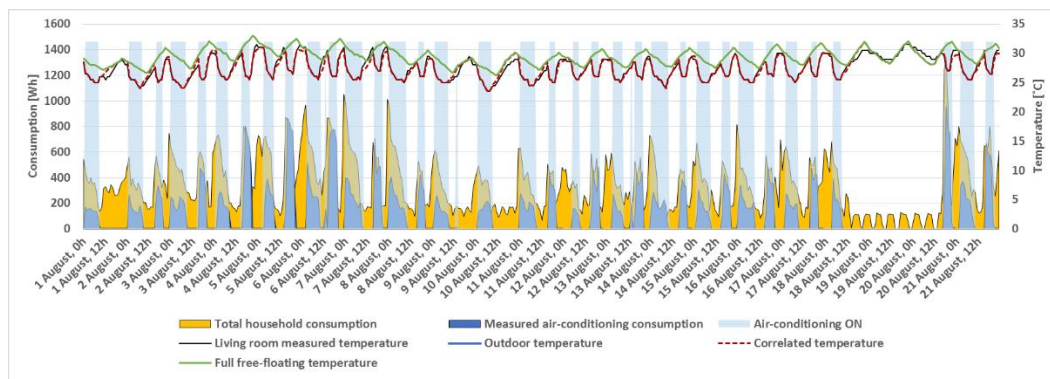


Figure 63: QT diagram of the dwelling during 3 weeks in August 2017.

#### 4.4. Integration of the QT model and DSM techniques

The present section focuses on the proposal of different DSM strategies, which were in the past usually considered only as traditional energy efficiency strategies: dynamic solar shading, ventilation and pre-heating/cooling. These strategies are based on the most essential parameters in order to achieve low-energy buildings, but they will be considered here within a DSM framework.

First of all, the proposed procedure can be synthesized in the following way:

1. The net solar excitations are obtained through simulation, as well as the order of the model (number of denominators M1, M2 and M3).

$$SG(t) = \sum_{j=0}^{N3} Dg_j \cdot DC(t-j) + dg_j \cdot dC(t-j) + ag_j \cdot AR(t-j) + \sum_{j=1}^{M3} k_j \cdot SG(t-j) \quad \text{Eq. 16}$$

$$DC(t) = \sum_i F_{SDi} \cdot A_{Vi} \cdot g_i \cdot DR_i(t) \quad \text{Eq. 16 A}$$

$$dC(t) = \sum_i F_{Sdi} \cdot A_{Vi} \cdot g_i \cdot dR_i(t) \quad \text{Eq. 16 B}$$

$$AR(t) = \sum_i F_{SGi} \cdot A_{Vi} \cdot (1 - g_i) \cdot GR_i(t) \quad \text{Eq. 16 C}$$

Where  $F_{SDi}$ ,  $F_{Sdi}$  and  $F_{SGi}$  are the shading factors. The rest of the variables were explained in Section 4.2.

2. Meanwhile, the previous simulation is not critical since the model will be corrected by using the real conditions obtained through measured experimental data.

$$T_{FF}(t) = \sum_{i=0}^{N1} a_i \cdot T_{OUT}(t-i) + \sum_{i=0}^{N1} b_i \cdot SG(t-i) + \sum_{i=1}^{M1} d_i \cdot T_{FF}(t-i) + CONST \quad \text{Eq. 17}$$

$$Q(t) = \sum_{j=0}^{N2} C_j \cdot \Delta T(t-j) + \sum_{j=1}^{M2} D_j \cdot Q(t-j) \quad \text{Eq. 18}$$

Also, the effect of the variation of the ventilation air flow with respect to the adjusted reference value is taken into account in the model in the following way.

$$\Delta Q_{VENT}(t) = \rho \cdot C_p \cdot V \cdot \Delta ACH(t) \cdot (T_{IN}(t) - T_{OUT}(t))/3600 \quad \text{Eq. 19}$$

$$\Delta ACH(t) = ACH(t) - ACH_{REF} \quad \text{Eq. 20}$$

$$Q(t) = \Delta Q_{VENT}(t) + \Delta Q_{HVAC}(t) \quad \text{Eq. 21}$$

Once the model has been identified, it is possible to use it for characterization or forecasting in real time. As shown in the table below, another possibility is to use it to support decision-making in any demand side management system.

Case	Modifications with respect to the conditions in which the baselines were obtained	Input	Unknown	Calculation process
1	Operation of the air-conditioning system: set-point temperatures and ON/OFF	$T_{IN}(t)$ (HVAC system activated with fixed set-points)	$Q(t)$	Eq. 17 to calculate $T_{FF}(t)$ and Eq. 18 to obtain $Q(t)$
2	Operation of the air-conditioning system: set-point temperatures and ON/OFF	$Q(t)$ is null (air-conditioning system not operating)	$T_{IN}(t)$	Eq. 17 to calculate $T_{FF}(t)$ and Eq. 18 to obtain $T_{IN}(t)$
3	Operation of the air-conditioning system: set-point temperatures and ON/OFF	$Q(t)$ is given a certain value.	$T_{IN}(t)$	Eq. 17 to calculate $T_{FF}(t)$ and Eq. 18 to obtain $T_{IN}(t)$
4	Solar control by using shading devices in certain windows, using Equations 16 A, 16 B and 16 C	$T_{IN}(t)$ (HVAC system activated with fixed set-points)	$Q(t)$	Eq. 16 A, 16 B and 16 C to obtain the new gross solar gains. Eq. 16 to obtain the new net solar gains. Eq. 17 to calculate $T_{FF}(t)$ and Eq. 18 to obtain $Q(t)$ . Note: Solar control could also be considered with the air-conditioning system inoperative, mixing these guidelines with those explained in Case 2.
5	Variation of the ventilation air flow for Indoor Air Quality (IAQ) Demand-Controlled Ventilation	$T_{IN}(t)$ and a variation of the ventilation air flow $\Delta ACH(t)$	$Q(t)$	Eq. 18 to obtain $Q(t)$ . With the new $\Delta ACH(t)$ (Eq. 20) calculate $\Delta Q(t)$ with Eq. 19. Calculate $Q(t)$ to obtain $\Delta Q_{HVAC}(t)$ as the energy that the air-conditioning system should deliver.
6	Night ventilation	$Q(t)$ is null and there is an increment of the ventilation air flow $\Delta ACH(t)$ as shown in Eq. 20	$T_{IN}(t)$	Eq. 17 to calculate $T_{FF}(t)$ without night ventilation. Obtain $T_{IN}(t)$ from Eq. 21, using Eq. 19 and Eq. 18.

Table 9: Possibilities offered by the proposed baselines for DSM purposes.

Cases 1, 2 and 3 refer to strategies that operate the air-conditioning system, while case 4 is variable solar control, case 5 would be the case of demand-controlled ventilation through presence detection, and case 6 is night ventilation for precooling during summer. In Chapter 5 of this Thesis several scenarios will be considered, applying the proposed energy baselines of case 3 of the previous table. Then, Chapter 6 will integrate the use of the baselines for cases 1 and 2. Finally, Annex D gives some insights into the use of cases 4 and 6.

#### 4.4.1. Conclusions

The model that has been proposed as an energy baseline for residential buildings presents a combination of two models: one to characterize the evolution of the indoor air temperature, and another one for the air-conditioning consumption. The model is based on transfer functions, but the physical information of the characterized building is implicit in the value of the coefficients. This provides the model with the capacities of an optimal baseline that can be executed under different climate and use conditions, offering robust and accurate results.

In addition, as a baseline, it allows to perform an accurate evaluation of the impacts of energy saving measures or demand side management strategies. Also, its physical component allows it to be used as a diagnosis tool or for an energy management tool.

The differentiating features of the proposed methodology are the following:

- Regarding its replicability, it is easy to identify the methodology with a reduced amount of monitoring data to adjust the model. It is also affordable, as demonstrated in the experimental validation.
- The duality of the QT model allows to obtain good results at short intervals with a discontinuous use of the air-conditioning systems, as is typical of residential buildings.
- The dynamic effects related to the inertia of buildings as well as operating conditions can be characterized by the model, even if they are variable.
- The characteristic parameters of the buildings are related to the coefficients of the models that have been developed. This allows to perform accurate estimations with different inputs than the ones used for adjusting the coefficients. In addition, it would eventually allow to calibrate simulation models, for example the ones proposed in Chapter 2 of this Thesis.

In addition, the work that has been developed in this chapter presents other highlights, such as:

- The indoor temperature model allows its implementation in an independent way for dwellings with a limited or null use of the air-conditioning systems, which could be sometimes at risk of energy poverty. In this case, since there are no significant air-conditioning consumptions in the buildings, the indoor temperature would be the variable used to estimate the effects of energy saving measures, through the calculation of comfort indices. This will be further elaborated in Chapter 5 of this Thesis.
- The proposed methodology could be used as a diagnosis tool, since its estimation may turn into a reference value with which other scenarios can be compared.
- Finally, this work could be incorporated within an energy management tool. This is due to the fact that the proposed baselines are able to perform precise forecasts of the energy needs of a building due to the physical information contained within their mathematical model. These baselines could be combined for instance with storage, energy production, or the optimization of electricity purchase from the grid (demand response). This will be further studied in Chapters 5 and 6.



# 5. CHARACTERIZATION OF DISTRICTS: APPLICATION FOR BUILDINGS WITH LIMITED USE OF AIR-CONDITIONING

---

The opportunities offered by the application of the models introduced in Chapter 4 are enormous. From the point of view of the author of this Thesis, one of the most outstanding ones is the characterization of districts. For this reason, the methodology that was previously described will be applied in this chapter in order to characterize a district in which temperature and total electricity consumption measurements are available, but with no data of the air-conditioning consumptions. Several applications will also be mentioned, such as buildings' diagnosis, benchmarking possibilities, or even demand side management. However, this chapter will introduce an innovative application of the developed methodology: buildings with a limited use of air-conditioning supported by renewable energy.

The motivation for that is that the high energy consumption of the building sector, climate change and energy poverty are the major problems encountered in the built environment in Europe [19], and the three sectors are strongly interrelated, presenting significant synergies. Energy poverty refers to the situation in which a household is unable to maintain a proper level of indoor thermal comfort as a consequence of a combination of three causes: low income, high energy prices or poor energy efficiency of housing [145]. This affects the capacity of the occupants to consume energy so as to keep the proper indoor environmental conditions, thus deteriorating their health and quality of life. The issue of energy poverty has devastating implications for the society, and it has been aggravated in the past years due to the economic crisis and the increase of energy prices. According to the study in [146], 5.1 million people in Spain, which means 11% of the households, claim that they are incapable of maintaining a proper indoor temperature in winter.

To improve the thermal comfort of buildings, for example in social housing, it is very common to carry out thermal mitigation strategies by rehabilitating the existing building stock: increasing the thermal insulation, improving the thermal bridges or reducing the air infiltrations (winter), as well as using solar control strategies or night ventilation (summer). However, this study seeks to offer a different alternative, which could either substitute or, even better, work hand in hand with traditional retrofitting strategies. This will be done by making use of energy baselines that will be obtained from the characterization of a social housing district, following the methodology proposed in Chapter 4. Together with the estimation of the PV potential, this study will innovatively introduce the possibility of using surplus electricity to power the heat pumps of the district, improving the thermal comfort conditions.

The content of the chapter is summarized as follows. First, in Section 5.1 the characterization of a district without monitored air-conditioning consumptions will be explained in detail for a case study. In Section 5.2, several applications based on the characterization of districts will be mentioned. Then, the novel application of the energy baselines for buildings with limited use of the air-conditioning systems will be included in Section 5.3.

## 5.1. Characterization of a district without monitored air-conditioning consumptions

### 5.1.1. Description of the case study

With the aim of demonstrating the proposed methodology for the characterization of districts through energy baselines, a social housing district in Seville (Spain) owned by the Agency for Housing and Rehabilitation in Andalusia (AVRA) will be considered as a case study. This district is composed of 235

dwellings, distributed among the buildings in the area. These dwellings are rather particular, since they belong to a category which makes a limited or null use of the air-conditioning systems, either because they don't even have such a system, or because their limited resources do not allow the occupants to use them. The city where the district is located has an average income of 12900 €/household per year, and the unemployment rate is very high (22.90% in January 2018). The climate is severe both in summer and winter and the thermal efficiency of the buildings is rather poor, thus the households that will be assessed are living in conditions of extreme energy poverty. Group A (Figure 64) is formed by 11 residential blocks built in 1981, while group B has 6 blocks built in 1983. Most of them have 3 or 4 floors with 2-4 dwellings in each floor, each of which has between 2 and 3 bedrooms.



Figure 64: District under study.

### 5.1.2. Monitoring of the district

In summer 2016, smart meters and temperature dataloggers were installed in some of the dwellings. After one year and a half, the collected data showed that good measurements of electricity consumption and temperature were available for the whole year of 2017 in several dwellings. Among them are the ones shown in Figure 65.

With the purpose of illustrating the usefulness of the proposed application of the energy baseline models, the case of one of the dwellings in the district is going to be analysed in more detail. This dwelling (highlighted in Figure 65) consists of two floors, and the monitored spaces in this case are the living room (in the ground floor) and 3 bedrooms (upper floor).

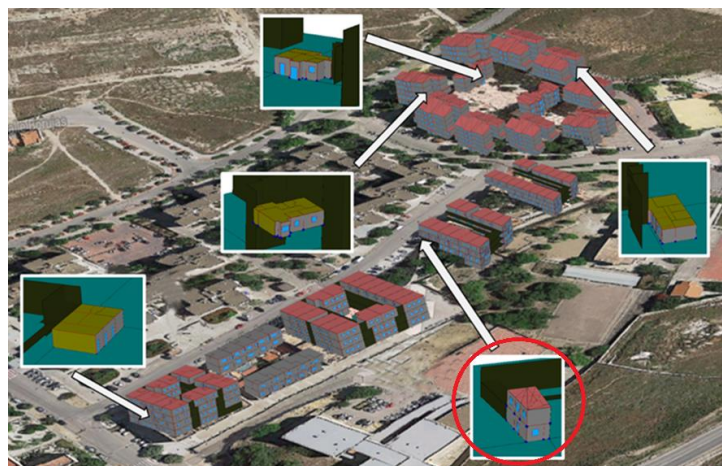


Figure 65: Location of some of the monitored dwellings and the developed models.





Figure 66: Plan of the dwelling and location of the temperature sensors.

If we compare the average daily indoor temperature in all the spaces of the dwelling during the monitoring period, we can clearly see that the temperatures are very similar in the intermediate months, a bit different in winter, and very different in summer, since the living room and the main bedroom have an air-conditioning unit.

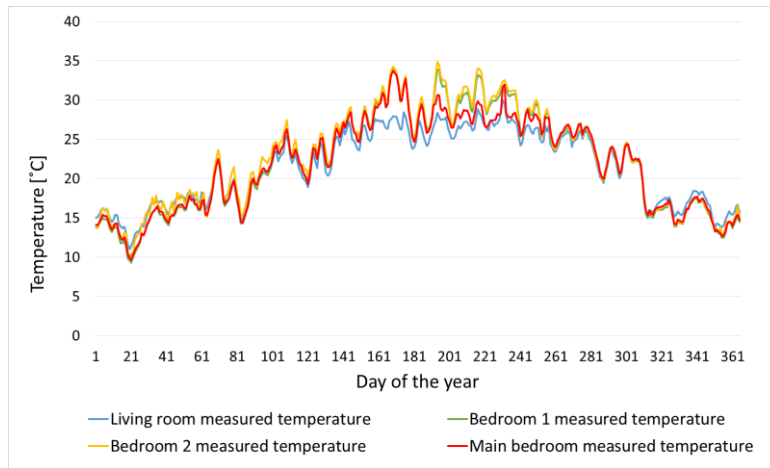


Figure 67: Comparison between the daily average indoor temperature measurements of the different spaces.

An example of indoor temperature and total electricity consumption measurements is shown below. During these 3 days, it can be observed that every indoor temperature drop coincides with peaks in total electricity consumption.

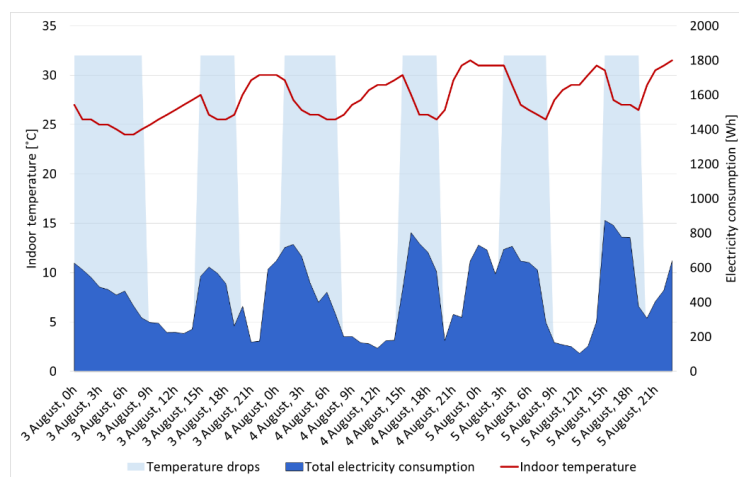


Figure 68: Example of temperature and consumption measurements in the dwelling under study.

### 5.1.3. Identification of air-conditioning consumptions

To discern the air-conditioning consumption from the total household electricity consumption data obtained from the Smart Meters, the best option is to observe the relationship between the total electricity consumption and the indoor temperature data. An example can be seen in Figure 69. Days in which there is clearly no air-conditioning can be used to estimate the household electricity consumptions. Once the patterns of use are known, the air-conditioning consumption can be obtained by calculating the difference between the total consumptions and the household electricity consumptions in hours were a difference can be observed between the measured temperature and the primary baseline temperature. For more information about the disaggregation of electricity consumptions, the reader is referred to Annex B.

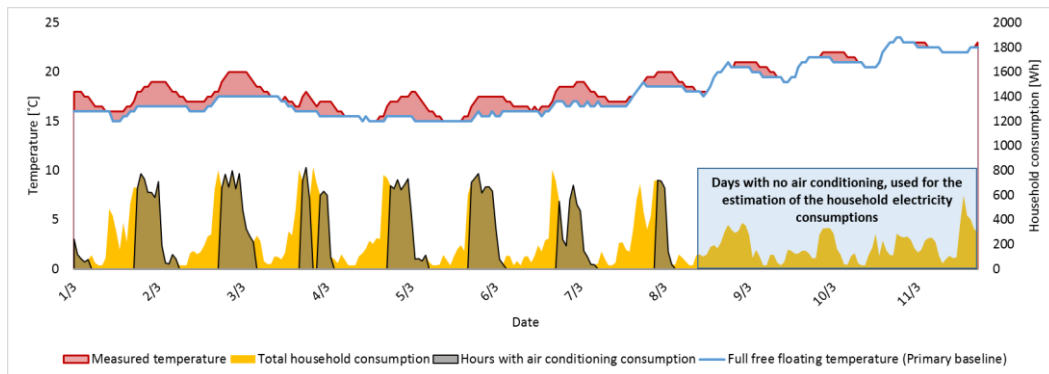


Figure 69: Example of days with and without air-conditioning.

### 5.1.4. Estimation of the matching climate

The real climate was obtained from the measurements in the closest weather station where data of outdoor temperature, humidity and solar radiation for the monitoring period were available (see Figure 70) for the district. Afterwards, the process explained in Annex A may be followed in order to produce a weather file with the real climatic data.



Figure 70: Chosen weather station in La Puebla de Cazalla, Seville, Spain.

### 5.1.5. Primary baseline

Once the matching climate was available, a HULC model of the dwelling was created and used to carry out a simulation with the real weather file. As a result, the solar gains of the different spaces and the monthly Equivalent South Solar Area (ESSA) per m<sup>2</sup> of the dwelling were obtained. In Figure 71, the solar gains of the dwelling obtained by the simulation can be compared to the horizontal radiation given by the weather station. As it can be observed, the solar gains of the dwelling are higher during the last hours of the day,

which is logical due to its orientation. The average value of the internal gains obtained through the calculation of the household electricity consumptions is 2.43 W/m<sup>2</sup>.

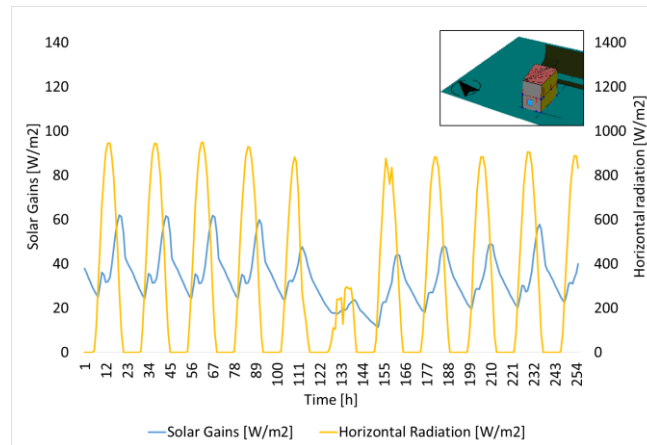


Figure 71: Comparison of horizontal radiation and solar gains. The black arrow points to the North.

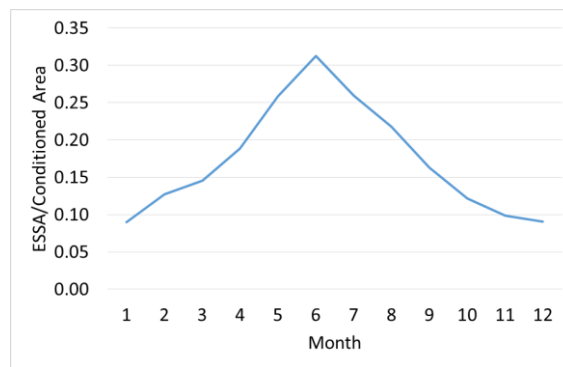


Figure 72: Monthly ESSA of the living room per m<sup>2</sup> of conditioned area. Real climate.

Then, the primary baseline was obtained by using indoor temperature measurements during periods of no air-conditioning use. Once the proposed procedure is finished, the coefficients obtained for the primary baseline are obtained. The experimental UA value of the dwelling was in this case 81.56 W/K. When the coefficients of the primary baseline are known, it is possible to obtain the full free-floating temperature (no air-conditioning systems are ever used). Assuming such neutralized users, the estimated temperatures by the primary baselines can be compared with the measurements in the two monitored bedrooms that have no air-conditioning system. As it can be seen in the next figure, the estimations are quite accurate.

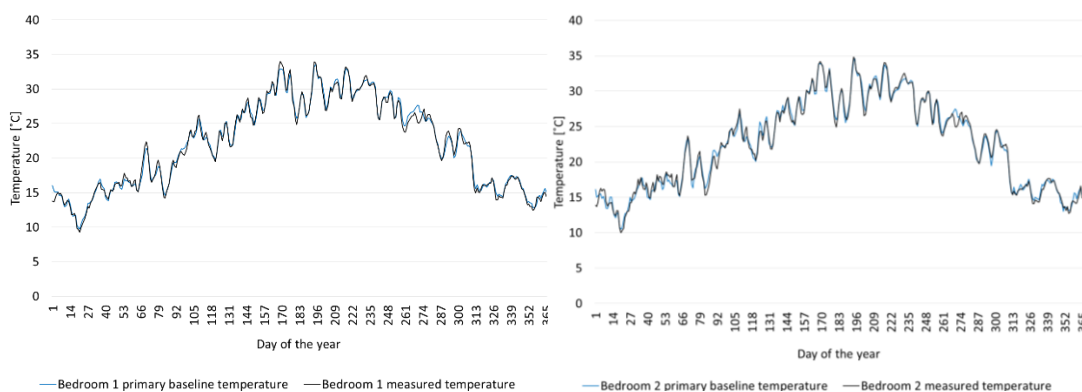


Figure 73: Comparison between the estimated and the real daily average indoor temperatures in two of the bedrooms.

However, when we compare the hourly measurements in the living room (which is air-conditioned) with the temperatures given by the primary baseline in typical days of winter, summer or intermediate months, we can see that in intermediate months the estimation is very accurate, but in winter and summer, when the air-conditioning unit is used, there are differences of temperature.

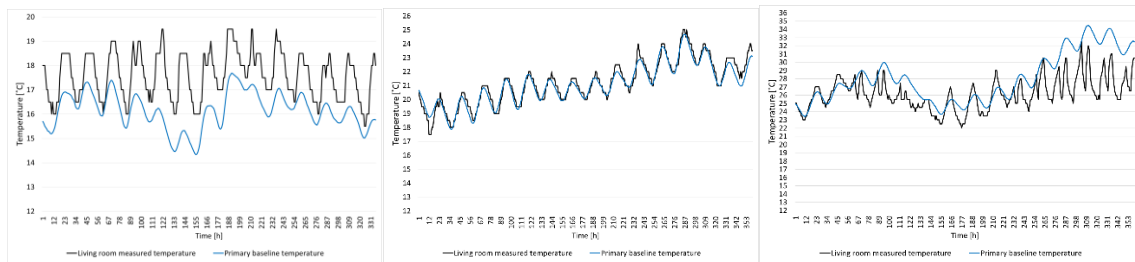


Figure 74: Comparison between the temperatures estimated by the primary baseline and the real measurements in February (left), April (center) and July (right).

The fit between the estimations and the real measurements in the 4 monitored spaces can be seen in the next figure. As expected, the fit of the primary baseline is obviously better in the bedroom, which has no air-conditioning system.

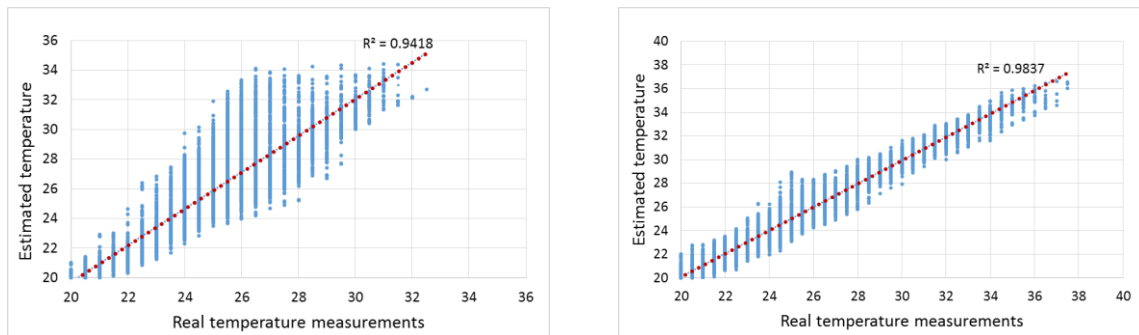


Figure 75: Fit between the measured temperatures and the estimated ones at hourly time-steps. Living room (left) and bedroom (right).

### 5.1.6. Secondary baseline

Last of all, the secondary baseline was obtained by looking at the consumptions that produce differences between the measured indoor temperatures and the full free-floating temperatures. An example of such differences is shown in Figure 76.

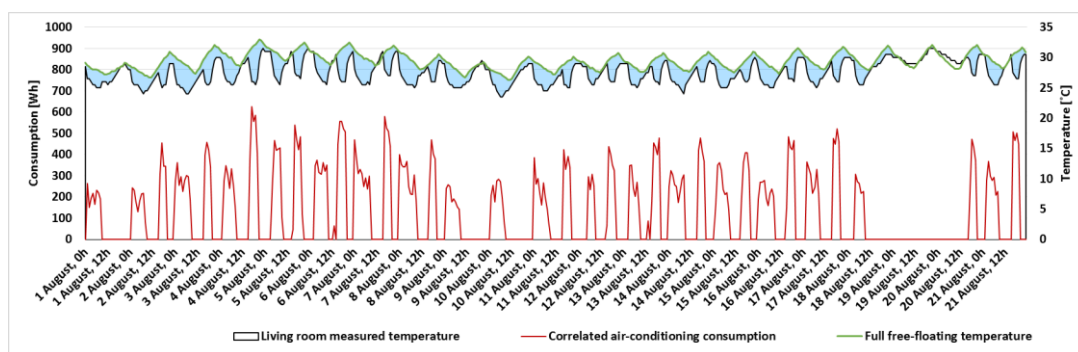


Figure 76: Example of a comparison between measured indoor temperatures, full free-floating temperatures and their associated consumptions.

After completing the process explained in Chapter 4, the coefficients of the secondary baseline are obtained. The following figure shows the relationship between the correlated air-conditioning consumption and the indoor temperature in the living room of the case study, both measured and estimated by using the secondary baseline. As it can be seen, the correlated temperature and the measured temperatures are very similar, and there is a clear relationship between air-conditioning consumptions and temperature decreases. Also, as soon as there is no air-conditioning the temperatures tend to be similar to the full free-floating temperatures. It can also be observed that during the 19<sup>th</sup> and 20<sup>th</sup> of August 2017, which was a weekend, the occupants were away and the air-conditioning system was not used, which is why the temperatures were similar to the full free-floating temperatures. In addition, during these two days the only electricity consumptions were those of the compressor of the fridge, with a cyclical behavior.

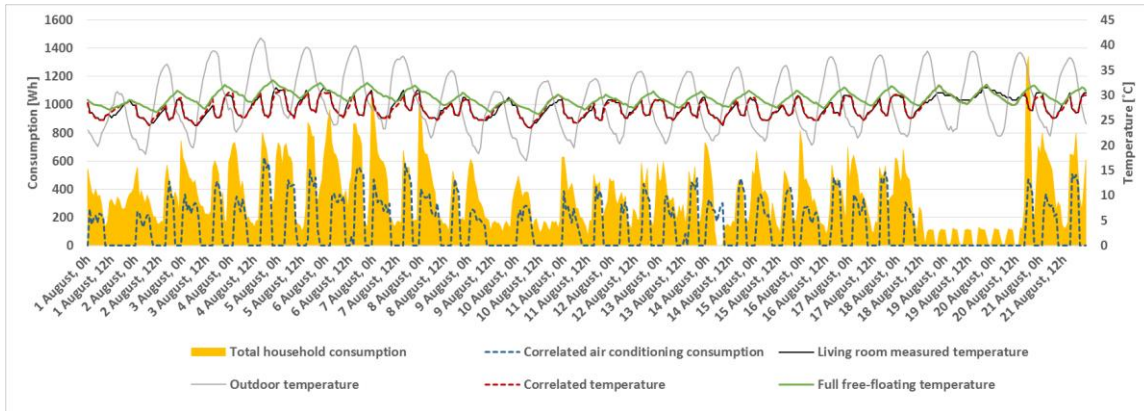


Figure 77: Comparison between the indoor temperature/consumption estimations and measurements and full free-floating temperatures.

In order to validate the obtained disaggregation of air-conditioning consumptions, the following figure shows the comparison between the correlated air-conditioning consumption in this case, and the one that was measured through a Smart Plug in Chapter 4 for the same period. As can be observed, the obtained results are very satisfactory, and it can be concluded that the estimation of the air-conditioning consumption carried out in this section is not very far from the reality.

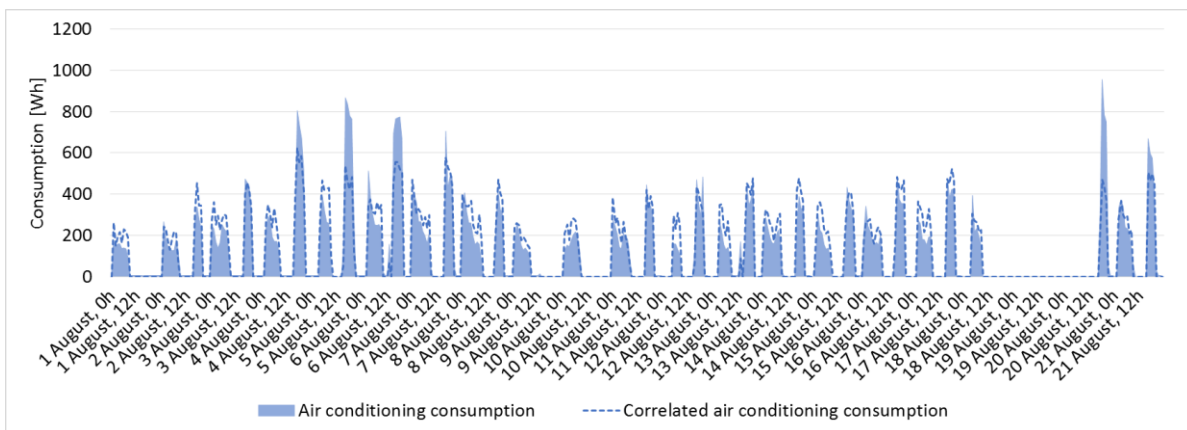


Figure 78: Comparison between the measured air conditioning consumption and the one estimated.

## 5.2. Applications based on the characterization of districts

### 5.2.1. Calculation of comfort indices

One of the possibilities offered by the characterization of districts through the application of primary and secondary baselines is the ability to calculate comfort indices that evaluate the thermal comfort of the occupants of the different buildings. By performing this under the same conditions of weather and use of the HVAC systems, benchmarking studies under real conditions become possible, comparing the results for all the dwellings of a district. This could be done for cases with air-conditioning consumptions, but also in scenarios with a limited or null use of air-conditioning.

As an example, Table 10 shows the results of thermal comfort in different spaces of some dwellings located in the same district that was presented in Section 5.1.1. In this case, the analysis is performed under real climatic conditions and the users were neutralized through the primary baseline, so there is no use of the air-conditioning systems. Without going into too much detail, the following magnitudes were considered to measure thermal comfort, distinguishing between summer and winter:

- Accumulated annual excess degree-hours.
- Accumulated annual excess degree-hours considering the Percentage of People Dissatisfied (Fanger).
- Hours in which the indoor temperature is outside the thermal comfort limits.
- Percentage of ours in which the indoor temperature is outside the thermal comfort limits.
- Hours in which the indoor temperature is outside the thermal comfort limits considering the Percentage of People Dissatisfied (Fanger).

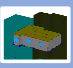


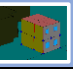

	Winter					Summer					
	[°C h]	[°C h PPD]	[h]	[% h]	[h PPD]	[°C h]	[°C h PPD]	[h]	[% h]	[h PPD]	
	Σ Temp. dif	Σ Temp. dif x PPD (Fanger)	Comfort W	Comfort W	Comfort W x PPD (Fanger)	Σ Temp. dif	Σ Temp. dif x PPD (Fanger)	Comfort S	Comfort S	Comfort S x PPD (Fanger)	
D1, room 1	9541	6658	2713	93	1523	12550	10454	2880	98	1962	
D1, room 2	7665	4794	2606	90	1186	13458	11702	2817	96	2021	
D1, living room	11013	8760	2663	92	1706	14029	12322	2839	97	2070	
D2, room 1	7744	5072	2496	86	1206	12998	11014	2871	98	2020	
D2, room 2	10356	7827	2685	92	1654	10431	7172	2928	100	1722	
D2, living room	9065	6420	2622	90	1439	12607	10842	2688	92	1819	
D3, room 1	9162	6511	2624	90	1447	12362	10330	2843	97	1933	
D3, room 2	10544	8000	2710	93	1712	7149	3991	2709	93	1097	
D3, living room	8999	6328	2617	90	1426	11932	9728	2849	97	1868	
D4, room 1	14158	12448	2811	97	2194	15301	13679	2917	100	2261	
D4, room 2	13625	11817	2791	96	2149	14563	12855	2900	99	2156	
D4, living room	15996	14828	2787	96	2362	14405	12590	2928	100	2273	
D5, room 1	13506	11514	2818	97	2116	12170	10109	2846	97	1898	
D5, room 2	11474	9259	2675	92	1801	13122	11375	2774	95	1952	
D5, living room	14224	12582	2778	96	2188	9888	7840	2591	88	1554	

Table 10: Comfort indices in some spaces of dwellings of the district for neutralized users, considering the real climate.

As it can be seen, it is possible to compare the results of thermal comfort of the different buildings, and the differences are rather high in some cases (see also Figure 79).

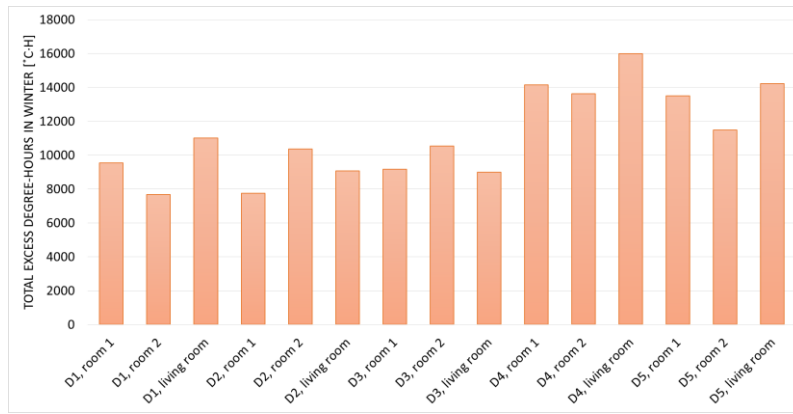


Figure 79: Comparison of total excess degree-hours in winter of the considered spaces.

### 5.2.2. Energy needs

Apart from enabling the comparison of the thermal comfort conditions of different buildings in a district, once the primary and secondary baselines are available it is also possible to characterize the relationship between the energy demands and the desired set-point temperatures. Therefore, the possibilities are endless, since this can be done without having to rely on complex simulation tools.

The application of the models proposed in Chapter 4 allows for example the calculation of the heating or cooling demands under different operating schedules, including also for instance the effect of night ventilation in summer. In addition, different climates can be considered. This also allows diagnosis making, benchmarking possibilities, energy savings assessment (the energy baselines could be generated before and after retrofitting a district), and the possibility to check the compliance of the buildings with current regulations regarding the thermal performance of existing buildings. As an example, the following figure shows a comparison of the heating demands of several dwellings of the district, both for the real and the standard climate (which was milder), considering the standard user of the Spanish regulation.

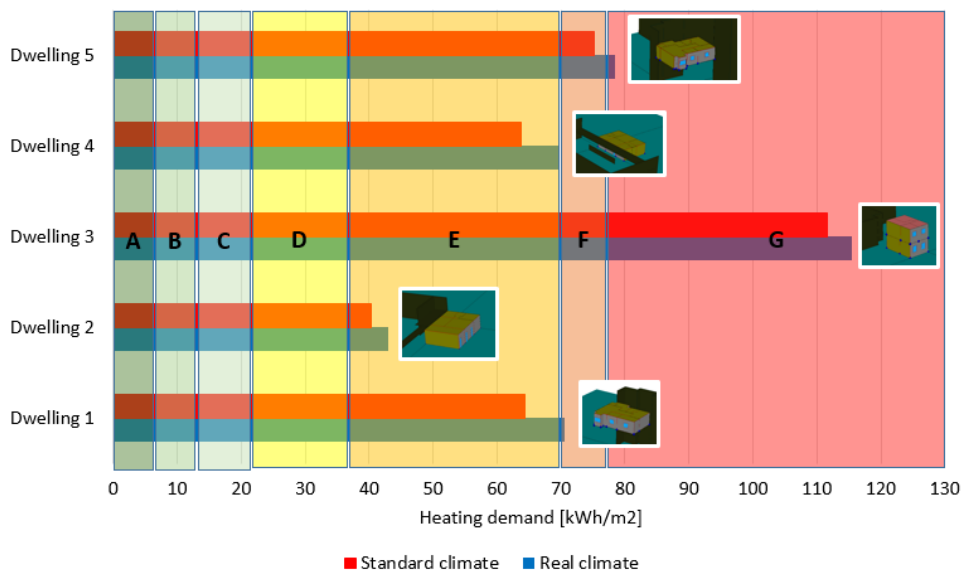


Figure 80: Comparison of heating demands obtained by the application of the energy baselines for the real and the standard climate.

Apart from the mentioned benefits of the proposed energy baseline models, other interesting possibilities arise as a result of the accurate characterization of the relationship between indoor temperatures and air-conditioning energy use. The last section of this chapter will introduce a novel application of the proposed energy baseline models, directed at mitigating energy poverty by providing electricity to the heat pumps of a district which has a limited use of the air-conditioning systems due to financial constraints.

### **5.3. Novel approach for benefitting from PV potentials**

#### **5.3.1. Aim of the study**

In this section, the methodology for the characterization of districts through energy baselines will be applied in the social housing district presented in Section 5.1.1. The main purpose of the study that will be proposed is to assess the benefits of exploiting the rooftop PV potential of the district so as to improve the thermal comfort of the occupants and mitigate extreme low and high indoor temperatures, and at the same time reduce their energy bills. This will be done by using the solar PV generation to cover part of the district's energy consumption, and the rest of the electricity (which would otherwise be exported) to supply power for the heat pumps of the households in the district instead. In this way, rather than using electrical storage as is frequent in most studies, the present study takes advantage of the thermal energy storage capacity of the buildings themselves and at the same time improves the thermal comfort levels of the occupants. The thermal behavior of the buildings will be characterized by using simulation models and the energy baselines obtained for the 37 typologies in which the 235 dwellings of the buildings were categorized.

Several alternatives will be analyzed in energy and economic terms for exploiting the PV potential of the district, changing the orientation and inclination of the PV panels as well as the separation between adjacent rows. This will be done with the purpose of determining the optimal options regarding maximum PV production, maximum self-sufficiency ratio and minimum investment costs. Once the optimal PV strategies are detected, 5 different alternatives to share the available electricity surplus of the district will be considered to improve the thermal comfort of the occupants. The current application aims to shed some light into whether it might be beneficial to install large PV systems in order to improve the thermal comfort in districts.

#### **5.3.2. Justifying the need for intervention in the district**

The monitoring campaign performed in the district revealed the unbearable temperatures that the occupants have to endure both in summer and winter, and the need for thermal comfort improvement measures. This section will focus on the measurements in 10 representative dwellings of the district, which recorded the indoor air temperature every hour during the whole year 2017. The characteristics of the chosen dwellings can be seen in Table 11.



Dwelling	Area [m2]	Number of occupants	Installed sensors
D1	78	3	-Smart meter.  -Living room temperature.  -Bedroom temperature.
D2	78	5	
D3	56	4	
D4	56	1	
D5	75	4	
D6	73	4	
D7	56	3	
D8	73	3	
D9	66	1	
D10	73	7	

Table 11: Characteristics of the monitored dwellings.

Since most of the studied dwellings were not air-conditioned, the indoor temperatures were persistently high or low for many days in a row. Door-to-door surveys revealed that some of the occupants even moved their cushions to the living room floor in summer, due to the unbearable temperatures in their bedrooms during the night which made it impossible to fall asleep.

Even though all the dwellings have a split air conditioner in the living room, most of them also have an electric stove under the living's room table, which is very frequent in Spain. Under the wrong assumption that using the stove incurs in lower costs, most of the dwellings do not make use of the split air conditioners in winter: either they don't use heating at all, or they only use the electric stoves. The hourly measured temperatures of the living rooms in the monitored dwellings can be seen in Figure 81. As shown, the indoor temperatures in all the dwellings are certainly far beyond the comfort zone most of the time, even though some of them make use of the split air conditioners for short periods.

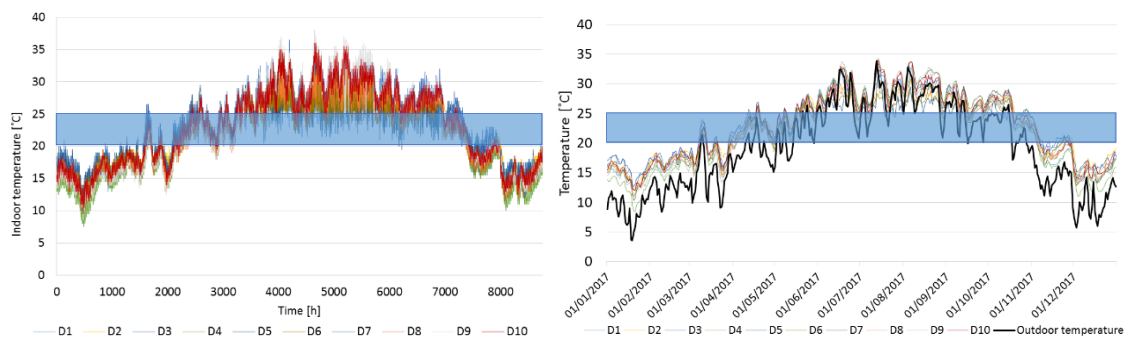


Figure 81: Hourly temperatures of the living rooms in the monitored households (left) and average daily temperatures (right).

On the other hand, the temperature of one bedroom in each monitored dwelling was also measured. In contrast with the measurements of the temperatures in the living rooms, it can be seen that none of the bedrooms in the dwellings are air-conditioned (see Figure 82). The differences between dwellings are mainly due to orientation (solar gains) and internal gains. The percentage of time outside the comfort zone in all the dwellings can also be seen in Figure 83. The results reveal the poor conditions in which the occupants of these households live, with several months in a row where the thermal comfort is violated 100 % of the time.

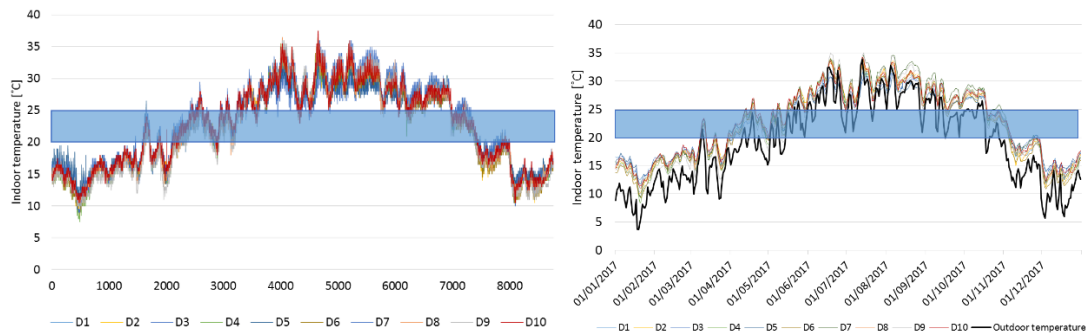


Figure 82: Hourly temperatures of the bedrooms in the monitored households (left) and average daily temperatures (right).

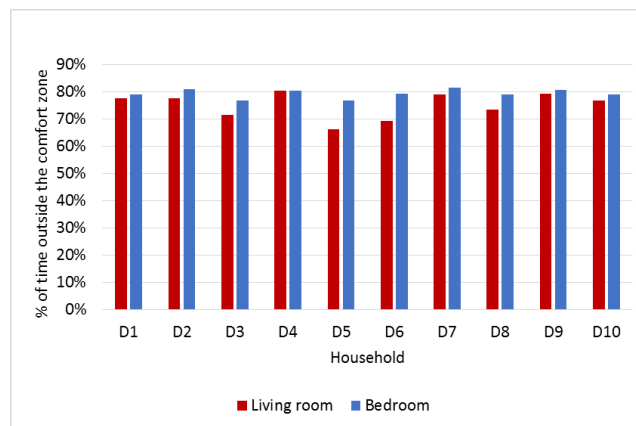


Figure 83: Percentage of time outside the comfort zone of all the households.

If we focus on individual dwellings, a clear difference can be observed between those whose living room is air-conditioned, and those that make no use of heating or cooling. This can be seen in Figure 84, which shows the difference of temperatures between the living room and the bedroom in dwellings D6 and D7. While D6 uses the split air-conditioning unit, D7 uses no heating or cooling whatsoever, which translates into very similar temperatures in both of its rooms.

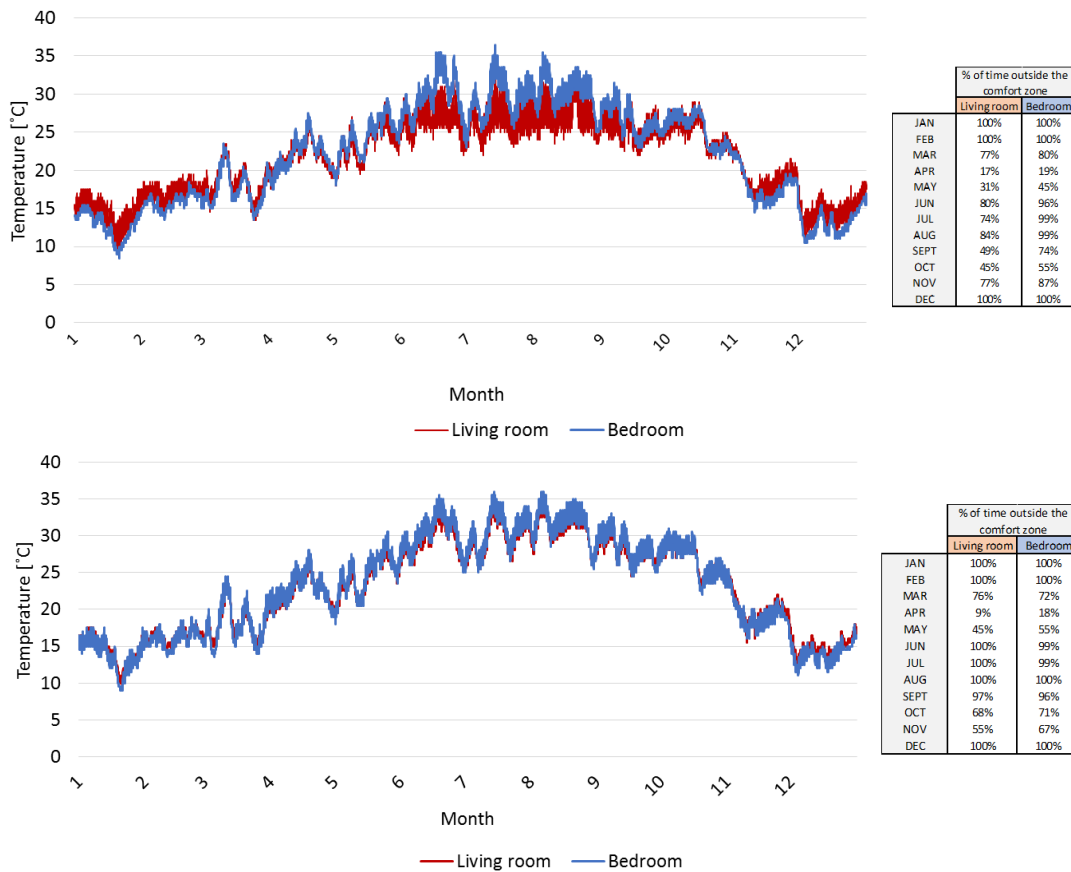


Figure 84: Comparison of temperatures in the conditioned household D6 (up) and the non-conditioned household D7 (down).

### 5.3.3. Electricity consumption of the district

Household electricity consumption has a very strong temporal variation not captured with consumption data from monthly bills, so high-resolution data from smart meters is paramount. The monitoring of 10 representative dwellings allowed to estimate the total electricity consumption of the district in an accurate way. As we aggregate different household electricity consumption profiles, the result for the district is a smoother profile whose shape will match better the PV generation. In order to show the measurements of the 10 dwellings, an average daily energy consumption profile per household in the district (which accounts for all appliances and lighting consumptions in the dwellings) has been produced, distinguishing between each month (see Figure 85). Peaks can be observed at lunch (around 15h) and dinner time (21-22h). These average profiles have been obtained considering only the consumption measurements in each individual dwelling when the difference between the temperatures in its two monitored rooms is lower than 1°C, so as not to take into account hours with air-conditioning consumptions.

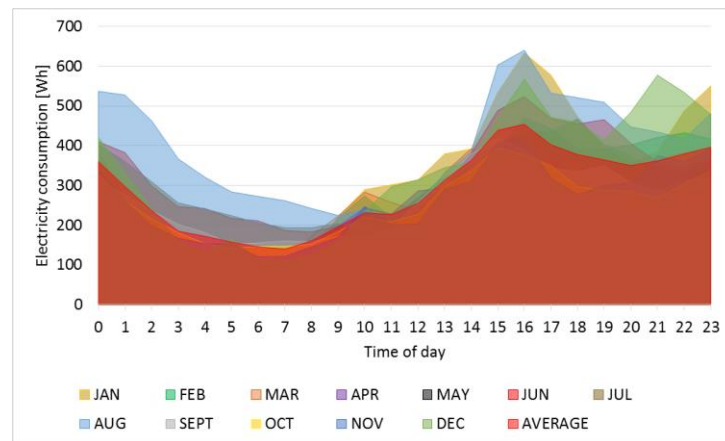


Figure 85: Average monthly energy consumption per household in the district.

In order to calculate the total electricity consumption of the district (without taking air-conditioning into account), the average consumption of the 10 monitored dwellings has been calculated for each hour of the year, discarding those consumptions when the difference of temperature between the monitored rooms of the household was higher than 1°C. Once the average consumption is calculated each hour, the total consumption has been estimated by extrapolating the result to the whole district, composed of 235 dwellings. The resulting hourly consumption profile of the district for the whole year is shown in Figure 86.

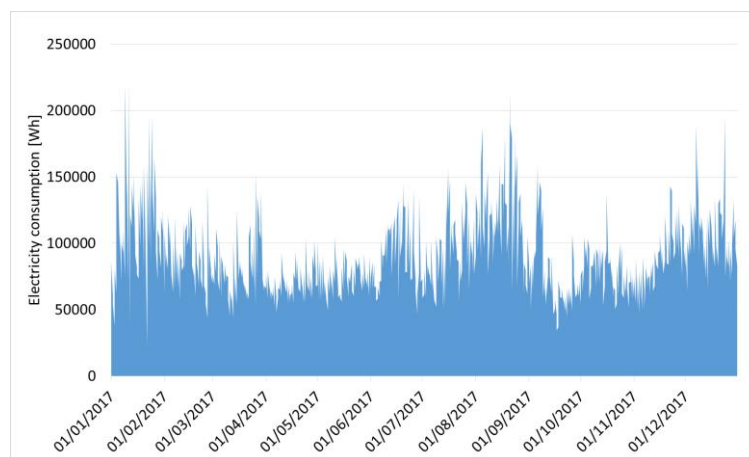


Figure 86: Electricity consumption of the district for every hour of the year.

### 5.3.4. Building typologies

To simplify the process, the district of 235 dwellings has been divided into 37 different typologies. This means that every dwelling in the district belongs to one of the typologies, which have been distinguished according to geometry of the dwelling, orientation and floor number. Table 12 shows a summary of the considered typologies. Ideally, the methodology explained in Chapter 2 could have been followed, determining the representative dwellings of the district through clustering techniques. However, this was not possible due to the fact that the monitoring campaign was already under way when the present study began, so it was not possible to choose which dwellings should be monitored. Nevertheless, the typologies proposed in this study were also very carefully chosen and are representative of the district's behavior.

TYOPOLOGY	ORIENTATION	AREA [m <sup>2</sup> ]	FLOOR	NUMBER OF DWELLINGS IN THE DISTRICT
1	SOUTH-WEST	66	GROUND FLOOR	7
2	NORTH-WEST	66	GROUND FLOOR	9
3	NORTH-EAST	61	GROUND FLOOR	4
4	SOUTH-EAST	61	GROUND FLOOR	2
5	SOUTH-WEST	78	INTERMEDIATE	8
6	NORTH-WEST	78	INTERMEDIATE	6
7	NORTH-EAST	78	INTERMEDIATE	6
8	SOUTH-EAST	78	INTERMEDIATE	9
9	SOUTH-WEST	66	INTERMEDIATE	13
10	NORTH-WEST	66	INTERMEDIATE	14
11	NORTH-EAST	66	INTERMEDIATE	15
12	SOUTH-EAST	66	INTERMEDIATE	14
13	SOUTH-WEST	66	UPPER FLOOR WITH ROOF	9
14	NORTH-WEST	66	UPPER FLOOR WITH ROOF	9
15	NORTH-EAST	66	UPPER FLOOR WITH ROOF	4
16	SOUTH-EAST	66	UPPER FLOOR WITH ROOF	4
17	NORTH-WEST / SOUTH-WEST	56	GROUND FLOOR	2
18	NORTH-EAST / SOUTH-EAST	56	GROUND FLOOR	2
19	NORTH-WEST / SOUTH-WEST	56	INTERMEDIATE	2
20	NORTH-EAST / SOUTH-EAST	56	INTERMEDIATE	2
21	NORTH-WEST / SOUTH-WEST	56	UPPER FLOOR WITH ROOF	2
22	NORTH-EAST / SOUTH-EAST	56	UPPER FLOOR WITH ROOF	2
23	NORTH-WEST	75	GROUND AND FIRST FLOOR	3
24	NORTH-WEST	75	GROUND FLOOR	2

25	NORTH-EAST	57	GROUND FLOOR	2
26	NORTH-EAST	65	GROUND AND FIRST FLOOR	2
27	NORTH-WEST	75	INTERMEDIATE FIRST FLOOR	4
28	SOUTH-EAST / NORTH-EAST	51	INTERMEDIATE FIRST FLOOR	2
29	SOUTH-EAST / NORTH-EAST	52	INTERMEDIATE SECOND FLOOR	2
30	NORTH-WEST	56	INTERMEDIATE FIRST FLOOR	6
31	NORTH-EAST	75	INTERMEDIATE FIRST FLOOR	9
32	NORTH-WEST	73	INTERMEDIATE + UPPER FLOOR WITH ROOF	23
33	NORTH-EAST	73	INTERMEDIATE + UPPER FLOOR WITH ROOF	27
34	NORTH-WEST / NORTH-EAST	64	INTERMEDIATE + UPPER FLOOR WITH ROOF	2
35	NORTH-WEST / SOUTH-EAST	64	INTERMEDIATE + UPPER FLOOR WITH ROOF	2
36	SOUTH-EAST / NORTH-WEST	64	INTERMEDIATE + UPPER FLOOR WITH ROOF	2
37	SOUTH-EAST / SOUTH-WEST	64	INTERMEDIATE + UPPER FLOOR WITH ROOF	2
				235

Table 12: Characteristics of all the dwelling typologies in the district.

### 5.3.5. Methodological description

From the point of view of the author of this Thesis, the PV potential of the district could be used to mitigate the consequences of low income and high energy prices on its inhabitants, which restrict their energy consumption especially when it comes to heating or cooling the dwellings. In this case, the solar power generation will be used to cover partially the electricity demand of the district. No electrical storage will be considered.

If the PV generation is lower than the demand, then all the PV generation will be used and the rest of the electricity necessary to cover the demand of the district will be obtained from the grid at its regular price. Conversely, if the PV generation exceeds the demand, there will be exported energy. Traditionally this is handled by using net metering, which allows users with surplus electricity to feed the electricity that they do not use back into the grid, obtaining benefits in the process. Given the intricate regulatory and practical

situation in Spain in this respect, the proposal of this study is to use the electricity surplus to feed the heat pumps in the district instead. In this way, the thermal storage capacity of the buildings is used and the thermal comfort of the occupants can be improved. The control strategy of the proposed system is summarized in Figure 87.

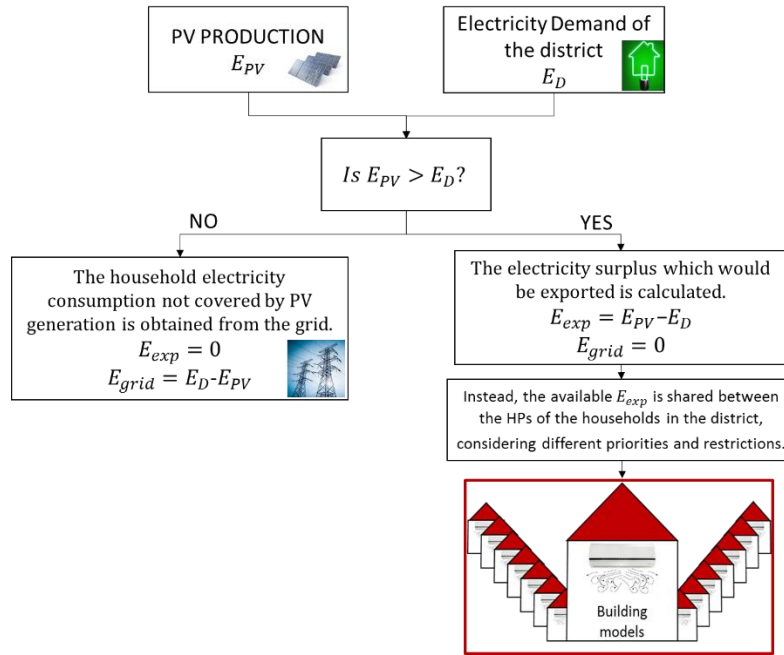


Figure 87: Control diagram of the proposed strategies.

On another note, two indicators will be used to analyze the match between the district's electricity consumption and the PV generation:

-Self-consumption ratio: share of the solar supply that is directly consumed in the district.

$$SCR = \frac{\sum PV_{production} - \sum PV_{exported}}{\sum PV_{production}}$$

-Self-sufficiency ratio: share of the district demand covered by the solar supply.

$$SSR = \frac{\sum PV_{production} - \sum PV_{exported}}{\sum E_D}$$

To determine the Life Cycle Costs (LCC) of each analyzed scenario, a time span which includes the capital investment, operation and maintenance costs was considered. The following parameters are used: investment period of 25 years, inflation rate of 3% and maintenance and costs of 1% of total investment of the project. The electricity cost from the grid is 0.209 €/kWh. The total investment costs are calculated by considering the price of the installed PV modules and inverters in each case. In addition, an increment of 40 % will be considered so as to take into account other costs such as wiring or installation.

The values for the LCC were obtained with the following equation:

$$LCC = Initial_{investment} + (Costs_{operation} + Costs_{maintenance}) \cdot \sum_{t=1}^{25} \frac{1}{(1+r)^t}$$

Where "t" is the year, and "r" is the inflation rate.

The PV modules chosen for the present study are the model Atersa A-250P (250W), and the inverters are Fronius Eco 25.0-3-s (25 kW), with costs of 182 Euros and 3690 Euros respectively.

### 5.3.6. PV potential simulation

Although the PV potential of a district is frequently estimated through the use of 3D models for example, the relatively simple layout of the case study in the present study allowed to design the PV system in a simpler but also detailed way. This was done by using *Helioscope* [147], a web-based PV system design tool that integrates shading analysis, simulation and CAD in one package. It allows to estimate the yearly energy production taking into account losses due to weather, shading, wiring, component efficiencies, panel mismatches and aging. It provides recommendations for equipment and array layout, and the discrete number of PV modules that can fit into a solar field is calculated, considering parameters such as the orientation and inclination of the modules or the separation between adjacent rows.

It should be mentioned that the buildings of the district which have tilted roofs will not be used to install PV modules, since the presence of solar thermal panels as well as other obstacles does not allow it. Considering, only the flat roofs, an example of a PV layout in the district under study using *Helioscope* can be seen in Figure 88. Since all the buildings have the same height, shading due to distant objects was not considered, only shading between the own PV modules. The total roof area of the district is 2300 m<sup>2</sup> approximately.



Figure 88: Example of layout of the district in *Helioscope*: south orientation in the flat roofs.

Although the PV modules are usually oriented to maximize the annual solar power supply, this may not optimize other indicators such as self-consumption, grid imported electricity or revenue. Thus, the present study varies the tilt and azimuth of the PV modules installed in the horizontal rooftops of the district, so as to assess in detail the match between the solar power supply and the electricity consumption of the district as well as evaluate different alternatives that will entail different PV yields in summer and winter (which will in turn influence the improvement of the thermal comfort of the occupants). Apart from varying the tilt and orientation of the PV modules, it is also interesting to evaluate the influence of the separation between rows in the horizontal rooftops of the district. This is done in *Helioscope* through the use of the span-to-rise ratio, which is based on the front-to-back distance between modules divided by the height at the back of the module bank. Therefore, this ratio is sensitive to whether the bank has multiple modules and the tilt of the module, since either of these will increase the rise distance. Raising the span-to-rise ratio increases the distance between rows, thus less PV modules will be installed, reducing the PV yield. However, increasing the ratio also reduces the shading losses, so various alternatives should be analyzed when focusing on maximizing the PV potential.

### 5.3.7. Thermal behaviour of the dwellings

In order to analyze the thermal behavior of the district in detail, a building model for each of the 37 typologies was developed. This means that a model with an accurate consideration of the geometry, materials, orientation, exposed surfaces of ceilings, walls, and floors is available for each of the 235 dwellings. The



dwelling models were developed in the HULC software, using the real constructive solutions. Then, the energy baselines were obtained for the 10 dwellings with good measurements available, allowing to calibrate the simulation models of the 37 typologies by following the procedure described in Chapter 4 and extrapolating the obtained baselines. This calibration was possible thanks to the physical meaning of the coefficients of the energy baselines' correlations.

As an example, a validation of the model of dwelling D4 (which corresponds to Typology 22) is presented in Figure 89, which compares the real measurements of the dwelling in 2017 with the simulation results of its free-floating temperature (no air-conditioning system) when using the real climatic data. As it can be seen, the results obtained are highly accurate.

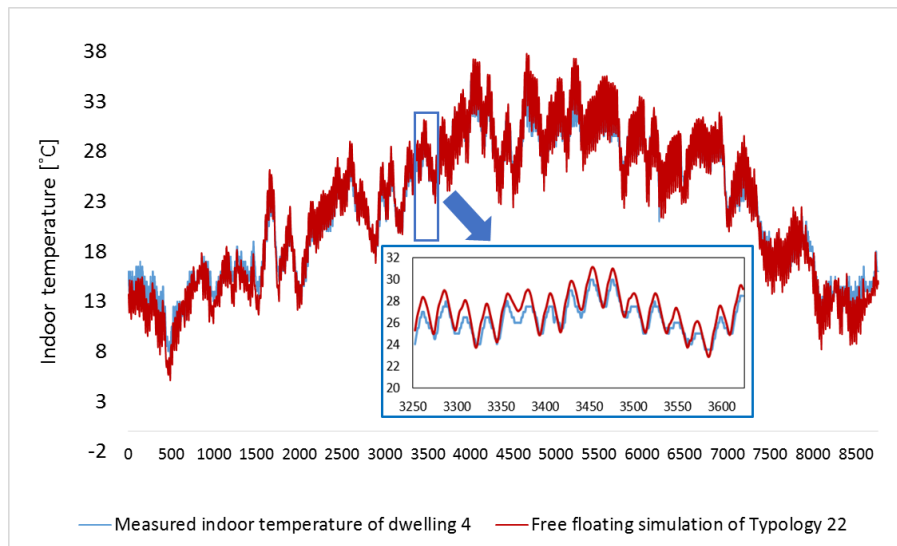


Figure 89: Validation of the simulated and measured indoor temperature of dwelling 4 for the whole year.

### 5.3.8. Description of the proposed strategies

#### 5.3.8.1. Optimal PV potential strategies

In this section, different alternatives that influence the PV production will be analyzed using the buildings with horizontal roofs. Many studies carry out a very detailed analysis for the optimization of the orientation and the tilt angle of the PV modules. For example, a very interesting review of tilt and azimuth angles considering design parameters, simulations and mathematical techniques for different applications can be seen in [54]. Other studies such as [148–151] determine the optimum tilt angles and orientation for solar photovoltaic arrays, in order to maximize incident solar irradiance for specific periods or latitudes. However, the amount of possibilities considered were reduced to 3 different tilt angles and 4 different orientations, since a detailed optimization was not its primary objective.

The options considered for the inclination of the PV modules are: latitude  $-10^\circ$ , latitude  $+0^\circ$  and latitude  $+10^\circ$ . For the PV module orientation, the following options (which adapt to the shape of the roofs) will be studied:

- North-East orientation of the PV modules ( $66^\circ$ ).
- South-East orientation of the PV modules ( $156^\circ$ ).
- South orientation of the PV modules ( $180^\circ$ ).
- South-West orientation of the PV modules ( $246^\circ$ ).

Two alternatives for module spacing will be also used: span-to-rise=1.5 and span-to-rise=2, to check whether it is better to increase the distance between rows (less PV modules installed but reduced shading losses) or not. The proposed alternatives will be analyzed with the aim of estimating their effect on the following variables:

- Number of panels that can be installed.
- Annual/winter/summer solar energy supply.
- Matched electricity consumption.
- Self-consumption ratio.
- Self-sufficiency ratio.
- Life Cycle Cost.

Once all the alternatives have been examined, three of them will be chosen regarding the following criteria: maximization of self-sufficiency (SSF), maximization of exported PV production (SUPPLY) and minimization of the investment costs (INV). This will be done focusing only on the PV production and electricity demand of the district.

### 5.3.8.2. Thermal comfort strategies

The previously mentioned chosen strategies will be then used for the thermal comfort improvement analysis of the dwellings, using weather data of a representative year. However, one question that should be answered is the following: if there is surplus production (exported energy), who should benefit from the available electricity? This study does not seek to propose a detailed course of action regarding this issue (just like sharing in the reality the PV production between dwellings with different electricity consumptions), since it would be a task for studies with different purposes.

Bearing in mind that the focus is on quantifying the improvement of the thermal comfort of the occupants in the district, the following strategies are proposed:

- All the 235 dwellings in the district receive the same amount of electricity to feed their heat pumps (proportional). An indoor temperature restriction is considered: the heat pump of a dwelling can only be used at any time of the simulation if the thermal comfort of the occupants is guaranteed (20-25°C). If this condition is not fulfilled, the energy that this dwelling would receive is shared by the remaining dwellings instead. If all the 235 dwellings have already been considered in a certain time-step and there is still a surplus, it will be quantified. This strategy will be named as “Prop”.
- A fixed amount of electricity (500 Wh or 1000 Wh) is used to feed the heat pump of each dwelling. In this case, the number of dwellings  $n_{HP}$  that can be fed considering the available electricity is calculated at the beginning of each time-step, and the  $n_{HP}$  buildings with the lowest indoor temperature (in winter) or highest indoor temperature (in summer) will activate their heat pumps. The same indoor temperature restrictions as for the first strategy are considered. These strategies will be named as “Q=500” and “Q=1000”.
- The indoor temperature of all the dwellings in the district is checked at the beginning of the time-step. First, the dwelling with the lowest indoor temperature in winter (or highest in summer) is heated until reaching a certain set-point temperature. The necessary consumption in order to do so is accounted for. Then, the next dwelling is chosen and so on, until all the exported PV electricity has been used. Two options will be considered: one with a set-point temperature of 25 °C in winter and 20 °C in summer, and another one with 22.5 °C for both summer and winter periods. These strategies will be named as “T=20/25” and “T=22.5”.

In summary, these 5 thermal comfort improvement strategies will be simulated for each of the chosen optimal PV strategies (maximization of self-sufficiency, maximization of exported PV production and minimization of the investment costs), making a total of 15 alternatives. An average Coefficient of Performance (COP) of 2 will be considered for all the heat pumps in the district, which is a rather conservative value. Then, several indicators will be shown so as to make a proper performance assessment and comparison between the different options. The total excess degree hours for example will account for the sum of temperature differences in the whole season between the indoor temperature and the comfort temperature (below 20 °C in winter and above 25 °C in summer).

### 5.3.9. Analysis of results

#### 5.3.9.1. PV potential calculations

Once all the PV potential calculations proposed in the previous section have been completed in Helioscope, the next step is to calculate all the variables involved. The number of PV modules that can be installed in the district is provided by the software, as well as the installed power and the solar power supply, calculated for every hour of the year. The annual results can be seen in Figure 90, with colors that highlight the best alternatives in each column independently.

ALTERNATIVE	PV MODULE ORIENTATION IN FLAT ROOFS	PV MODULE INCLINATION IN FLAT ROOFS	SPAN-TO-RISE RATIO	Number of PV modules	Installed power [kWp]	Investment [Euros]	Cost/kWp	Annual solar power supply [MWh]	Grid import [MWh]	Matched electricity [MWh/yr]	Annual exported electricity [MWh]	Winter exported electricity [MWh]	Summer exported electricity [MWh]	LCC [k€]	Self-cons. ratio	Self-suff. ratio
Base case	-	-	-	0	0	0	0	0	600	0	0	0	0	2185	0.0	0.0%
1	NORTH-EAST	LATITUDE + 10	1.5	885	221	261923	1184	204	477	124	81	36	44	2043	60.5%	20.6%
2	NORTH-EAST	LATITUDE + 10	2	824	206	246411	1196	223	467	133	90	37	53	1989	59.8%	22.2%
3	NORTH-EAST	LATITUDE	1.5	939	235	280862	1196	271	445	155	116	50	67	1950	57.2%	25.9%
4	NORTH-EAST	LATITUDE	2	839	210	250187	1193	244	452	149	95	41	54	1937	61.0%	24.8%
5	NORTH-EAST	LATITUDE - 10	1.5	1053	263	309946	1177	340	418	182	149	70	79	1886	53.6%	30.3%
6	NORTH-EAST	LATITUDE - 10	2	861	215	255800	1188	262	436	164	98	45	52	1888	62.7%	27.3%
7	SOUTH-EAST	LATITUDE + 10	1.5	848	212	252534	1191	326	406	194	132	78	54	1775	59.5%	32.3%
8	SOUTH-EAST	LATITUDE + 10	2	720	180	214716	1193	289	414	186	103	62	41	1759	64.5%	31.0%
9	SOUTH-EAST	LATITUDE	1.5	723	181	220593	1220	336	400	201	135	82	53	1714	59.7%	33.4%
10	SOUTH-EAST	LATITUDE	2	723	181	215430	1192	295	409	191	104	64	39	1743	64.8%	31.8%
11	SOUTH-EAST	LATITUDE - 10	1.5	945	236	282393	1195	392	387	213	179	98	80	1740	54.4%	35.5%
12	SOUTH-EAST	LATITUDE + 10	2	835	209	249167	1194	353	394	207	146	81	64	1725	58.7%	34.5%
13	SOUTH	LATITUDE + 10	1.5	797	199	239472	1202	326	398	202	125	71	54	1731	61.8%	33.6%
14	SOUTH	LATITUDE + 10	2	661	165	199613	1208	285	408	192	93	52	41	1720	67.5%	32.0%
15	SOUTH	LATITUDE	1.5	852	213	253555	1190	342	392	208	134	77	57	1726	60.9%	34.6%
16	SOUTH	LATITUDE	2	852	213	248392	1166	299	401	200	99	59	41	1749	66.8%	33.3%
17	SOUTH	LATITUDE - 10	1.5	884	221	261719	1184	344	388	212	132	81	51	1719	61.7%	35.4%
18	SOUTH	LATITUDE - 10	2	775	194	233859	1207	346	392	209	137	73	64	1700	60.3%	34.8%
19	SOUTH-WEST	LATITUDE + 10	1.5	903	226	271678	1203	293	402	199	94	51	43	1782	67.8%	33.1%
20	SOUTH-WEST	LATITUDE + 10	2	828	207	247432	1195	254	410	190	64	39	24	1784	74.8%	31.6%
21	SOUTH-WEST	LATITUDE	1.5	777	194	244695	1260	304	393	208	96	61	35	1716	68.4%	34.6%
22	SOUTH-WEST	LATITUDE	2	777	194	234370	1207	282	399	202	80	47	33	1727	71.5%	33.6%
23	SOUTH-WEST	LATITUDE - 10	1.5	1064	266	312803	1176	376	380	220	156	84	71	1751	58.6%	36.7%
24	SOUTH-WEST	LATITUDE - 10	2	872	218	258657	1186	291	393	207	84	51	33	1735	71.2%	34.5%

Figure 90: Obtained results in all the analyzed strategies. In each column, green cells represent the best options while red cells represent the worst ones. The marked alternatives are those chosen for the thermal comfort study.

First of all, it should be mentioned that choosing the optimal parameters is paramount in order to maximize the solar supply, which varies up to 48 % among the studied alternatives. On the other hand, the differences between them regarding grid import, matched electricity and self-sufficiency ratio are not very significant. The reason behind this is that the electricity consumption of the social housing district is low, especially when compared to the PV generation obtained during sunshine hours after the installation of the PV modules. Remembering that the exported energy and its potential revenue is not being computed in these calculations for the reasons noted above, the considered alternatives still show payback periods around 7 years. Other conclusions that may be reached are mentioned below:

- The base case, which considers the provision of all electricity from the grid, is the one with the highest LCC.
- A lower inclination angle of the PV modules leads to more modules being installed, since the separation between rows is less restrictive. The North-East and South-West orientations also favor the number of modules that can be installed due to the shape of the roofs. The same happens with the span-to-rise ratio: the simulations with a value of 1.5 allow the installation of more modules. In most cases this results in an increase of the solar power supply, but also an increase on the LCC. The reason is that although more PV panels are installed, the shading losses increase if a span-to-rise ratio of 1.5 is used. Therefore, the results need to be carefully analyzed in order to choose the optimal options.
- In most cases, the maximum power supply in summer and annually is achieved with an inclination of latitude-10°.

- In general, using the PV layouts with the North-East orientation results in less annual solar power supply as well as matched generation, exported electricity and self-sufficiency ratio. In addition, they are the ones with worse LCCs.
- The matched electricity and self-sufficiency ratio is higher when the South-West layout orientation is used (thus the grid import is lower in these cases). The reason is that the electricity demand of the district is higher after midday, favoring the South-West orientations which generate more energy during those periods.

After considering in detail all the results from the PV alternatives that have been analyzed, three of them have been chosen for the thermal comfort study (see Figure 90):

- Alternative 11: it was selected since it offers the highest solar power supply both in summer and winter.
- Alternative 14: it has the lowest investment cost and almost the lowest LCC, since it is the alternative with the lowest number of PV modules installed. This option is optimal from an economic point of view, but offers a lower solar power supply.
- Alternative 23: it shows the highest self-sufficiency ratio and matched electricity, as well as the lowest grid import. This is due to the fact that it is the option with more PV modules installed (and higher investment costs).

### 5.3.9.2. Thermal comfort improvement of the chosen strategies

As mentioned before, the three optimal PV strategies that have been selected will be now used to analyze the potential benefits of using their exported PV production so as to improve the thermal comfort of the occupants, considering five different alternatives. Therefore, a total of 15 simulations will be conducted. Each simulation analyzes on an hourly basis the thermal behavior of each of the 235 dwellings during the 8760 hours of the year. The decision of which heat pumps should be activated, which depends on the strategy, is taken every time-step. As an example, Figure 91 illustrates simulated indoor temperatures and consumptions in dwelling 130 for some of the analyzed strategies in the PV optimal case that maximizes the exported PV production (SUPPLY). It can be seen how during the day, the exported PV production (Q) given to this dwelling is used to supply heat, which results in an increase of the indoor temperatures. It can also be seen how on the 21 of March this dwelling was not chosen for the strategy T=20/25, since other dwellings of the district had a higher priority due to their lower indoor temperatures. Once all the alternatives have been simulated, several indicators are calculated.

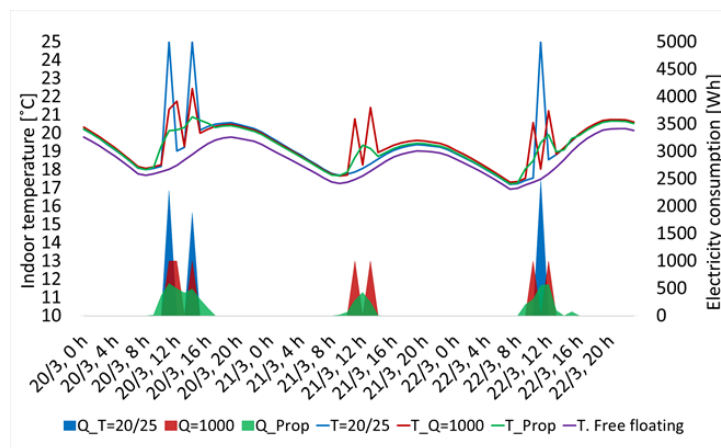


Figure 91: Example of simulated indoor temperatures and consumptions in the dwelling 130 for some of the analyzed strategies (case maximization of exported PV production).

The energy storage capacity of the structural mass becomes clear (see Figure 92) when the indoor temperature fluctuation under full free floating conditions (purple curve) and the indoor temperature

fluctuation when the heat pump operates (green curve) are compared. The effect of the thermal mass is proportional to the difference between both curves when the heat pump is switched off (shaded area). It can be seen how this difference is obviously higher in hours immediately after the heat pump operation.

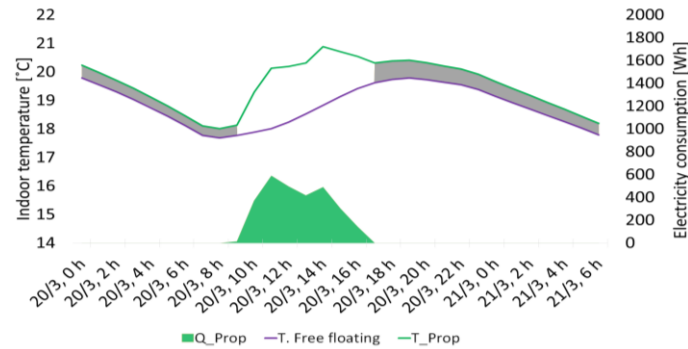


Figure 92: Example of thermal energy storage before and after the heat pump operation in the dwelling 130.

The results of all the strategies are given in Table 13, which shows among others the average total excess degree hours and average percentage of time outside the comfort zone of the dwellings in the district for each alternative. First of all, as we can see the three PV optimal strategies (SUPPLY, INV and SSF) have a different amount of available electricity, which influence the thermal comfort improvements. The percentage of energy used is computed in each simulation. This indicates the amount of available electricity that has been used during the whole year in the heat pumps of the district. A 100 % is never achieved, since it could happen that during a certain time-step all the buildings have already been heated/cooled and there is still surplus electricity, for example if  $Q=500$  Wh and the PV production is higher than 117500 Wh, or if the temperature requirements of the strategies are not met so the dwelling cannot be used. The number of activated dwellings varies depending on the followed strategy, and the highest values can be found for the strategy "PROP", since there are no priorities to heat/cool the dwellings and the same amount of energy is given to each of them.

	Available exported electricity [MWh]	Percentage of the energy used [%]	Average number of activated dwellings	Winter				Summer			
				Excess degree hours [°C·h]	Reduction [%]	Percentage of time outside the comfort zone [%]	Reduction [%]	Excess degree hours [°C·h]	Reduction [%]	Percentage of time outside the comfort zone [%]	Reduction [%]
BASE CASE	-	-	-	17405	0.0%	76.3%	0.0%	11369	0.0%	72.3%	0.0%
SUPPLY_PROP	178.8	92.19	222	15448	11.2%	68.8%	7.5%	8402	26.1%	61.7%	10.5%
SUPPLY_Q=500		90.02	133	15475	11.1%	69.3%	7.0%	8479	25.4%	62.2%	10.1%
SUPPLY_Q=1000		85.42	65	15530	10.8%	69.6%	6.7%	8459	25.6%	62.7%	9.6%
SUPPLY_T=20/25		96.81	45	15812	9.2%	69.9%	6.4%	8671	23.7%	62.1%	10.2%
SUPPLY_T=22.5		88.23	64	15760	9.4%	69.5%	6.8%	8646	24.0%	62.0%	10.3%
INV_PROP		92.6	95.54	226	16197	6.9%	72.5%	3.8%	9772	14.0%	66.9%
INV_Q=500	95.33		92	16206	6.9%	72.7%	3.6%	9719	14.5%	66.8%	5.5%
INV_Q=1000	89.81		45	16262	6.6%	73.0%	3.3%	9751	14.2%	67.1%	5.2%
INV_T=20/25	97.5		26	16452	5.5%	73.2%	3.1%	9896	13.0%	66.8%	5.4%
INV_T_225	89.22		40	16405	5.7%	72.8%	3.5%	9874	13.2%	66.8%	5.5%
SSF_PROP	155.7		92.66	222	15884	8.7%	69.9%	6.4%	8669	23.7%	62.9%
SSF_Q=500		90.78	130	15903	8.6%	70.3%	6.0%	8711	23.4%	63.2%	9.1%
SSF_Q=1000		86.07	64	15951	8.4%	70.7%	5.6%	8693	23.5%	63.4%	8.9%
SSF_T=20/25		97.32	61	16146	7.2%	70.7%	5.6%	8941	21.4%	63.2%	9.0%
SSF_T=22.5		85.47	43	16112	7.4%	70.5%	5.8%	8883	21.9%	62.8%	9.5%

Table 13: Overview of the average obtained results in the district.

The highest reduction of total excess degree hours is found for the case “SUPPLY\_PROP” (optimal PV case that maximizes the exported PV production, and shares the available energy between all the dwellings equally). The reason is that compared to the other strategies, the increase of temperatures produced by the heat pumps in the dwellings is lower, which translates into lower thermal losses. If a dwelling is heated/cooled only sporadically, the energy will be wasted rapidly. But, if a dwelling is repeatedly used, its thermal inertia allows to store the energy in a more adequate way. A 11.2 % reduction of the total excess degree hours in winter and 26.1 % in summer (more available electricity) may be achieved, reducing the percentage of time outside the comfort zone in 7.5 % and 10.5 % respectively. Although these results may not seem very appealing, the influence that these reductions of total excess degree hours have on the health of the occupants should be taken into account, since illnesses are associated with higher thermal comfort violations.

Besides, these results could be rather misleading. Although it is true that the strategy “PROP” is the best alternative when looking at the whole district, the electricity in this case is shared equally between all the buildings. This means that for example a dwelling with better solar access than another one is given the same amount of energy. Therefore, although when looking at the whole district the average total excess degree hours is lower in “PROP”, the dwellings with worse indoor conditions do not have a higher priority. Figure 93 shows the range of total excess degree hours of all the dwellings in the district for each strategy in the case “SUPPLY”, as well as their distribution, which is similar in the studied alternatives. As it can be seen, although the average of the district in the case “PROP” is lower, there are buildings with much higher total excess degree hours compared to the other alternatives. For this reason, the alternative T=20/25 is considered as a more suitable option, since it is also able to reduce the differences of thermal comfort between the dwellings of the district, favoring those which have worse indoor conditions.

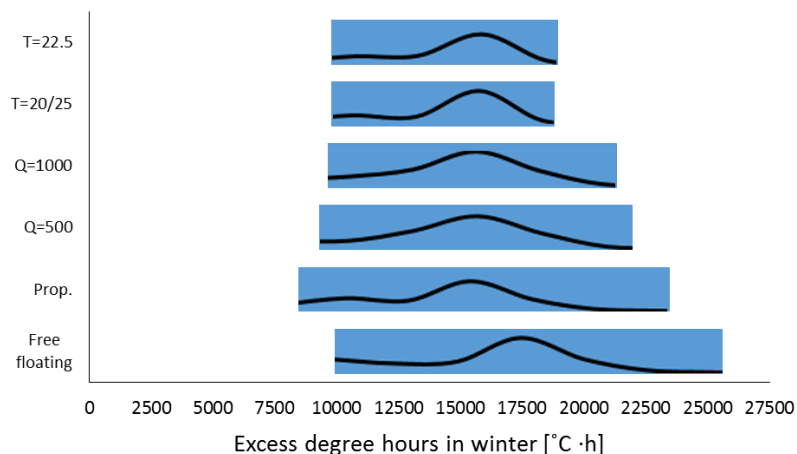


Figure 93: Comparison of total excess degree hours of the households for each strategy (case maximization of exported PV production).

Last of all, another interesting outcome of the present study is to know what the results of thermal comfort improvement would be, had the assumptions been different. The strategy T=20/25, considered as a consequence of the previous results as the most appropriate one to reduce the differences of thermal comfort in the district, will be used in the following scenarios:

- Only the living rooms will be considered, instead of heating/cooling the whole dwellings. The PV production still covers the district demand partially just like in previous cases.
- All the electricity generated by the PV modules will be used for the heat pumps instead of covering partially the electricity demand of the district, heating or cooling the whole dwellings.
- The potential PV generation if the buildings with tilted roofs had been used will also be considered, increasing the available electricity (still covering partially the electricity demand of the district and heating/cooling the whole dwellings).

The results (see Table 14) show that if only the living rooms of the district are considered, the comfort improvements are much higher (reductions of average excess degree hours of 34 % in winter and 72.6 % in summer). The reason for this is the lower amount of energy necessary to heat/cool the living rooms compared to the whole dwellings, which also decreases the percentage of energy used. An example of the hourly indoor temperatures achieved in the living room of a dwelling compared to its free-floating temperature is illustrated in Figure 94, showing the benefits of such a strategy. As for the case that doesn't partially cover the demand of the district, higher reductions are also achieved (from 9 % to 24 % in winter and from 24 % to 44 % in summer). Last of all, if the PV potential of the buildings with tilted roofs had been used, a reduction of almost 33 % could be achieved in winter and 67 % in summer, heating or cooling the whole dwellings.

	Available exported electricity [MWh]	Energy used [%]	Average number of activated dwellings	Winter				Summer			
				Excess degree hours [ $^{\circ}\text{C}\cdot\text{h}$ ]	Reduction [%]	Time outside the comfort zone [%]	Reduction [%]	Excess degree hours [ $^{\circ}\text{C}\cdot\text{h}$ ]	Reduction [%]	Time outside the comfort zone [%]	Reduction [%]
Base Case	-	-	-	17405	0.0%	76.3%	0.0%	11369	0.0%	72.3%	0.0%
Whole district (previous case)	178.8	96.8	45	15812	9.2%	69.9%	6.4%	8671	23.7%	62.1%	10.2%
Only living rooms	178.8	67.6	153	11428	34.3%	55.5%	20.8%	3117	72.6%	34.7%	37.6%
All PV generation is used	392.2	94.1	62	13263	23.8%	63.1%	13.2%	6370	44.0%	51.8%	20.5%
Including generation of tilted roofs	698.4	80.7	123	11680	32.9%	56.9%	19.4%	3774	66.8%	38.2%	34.1%

Table 14: Results of the analyzed options.

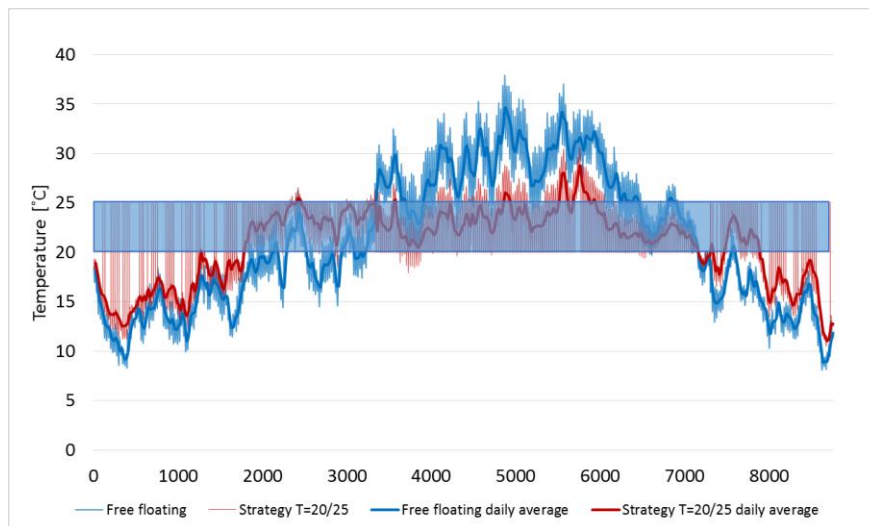


Figure 94: Hourly and daily free floating temperature of the living room in dwelling 147 vs. temperatures achieved with strategy T=20/25.

### 5.3.10. Conclusions

In this chapter, a novel approach in order to improve the thermal comfort of the occupants in a district at risk of energy poverty has been developed. Taking advantage of the rooftop PV potential of the area, the solar supply is used to cover part of the electricity consumption of the households during the day, reducing their energy bills. Then, instead of using electric storage, the proposal is to use the surplus electricity to supply energy for the heat pumps in the district, heating or cooling the whole dwellings.

First, the optimal strategies from an electrical and economical point of view were chosen, changing the orientation and inclination of the PV modules as well as their separation in order to maximize the solar supply, minimize the investment or maximize the self-sufficiency ratio of the district. The results showed that the solar power supply was maximized by using a South-East orientation, while using a South orientation with less PV modules installed led to the lowest investment, due to the relatively low consumption of the district compared to the PV generation. The self-sufficiency ratio was maximized using a South-West orientation, which favors the solar power supply when the consumption of the district is higher.

After choosing the PV optimal strategies, the surplus electricity in those alternatives was used to share the electricity between the heat pumps of the 235 dwellings of the district. Heating or cooling the whole dwellings, the results showed that the thermal comfort of the occupants could be improved in average up to 11 % in winter and 26 % in summer. If all the PV generation was used, a reduction of 24 % in winter and 44 % in summer could be obtained. On the other hand, if more buildings could be employed to install PV modules, improvements up to 33 % in winter and 67 % in summer could be expected. If only the living rooms of the district were heated, up to 34 % and 73 % reduction in winter and summer respectively could be achieved. In all the cases considered, the thermal comfort differences among the dwellings of the district are reduced significantly, particularly in some of the proposed strategies.

The outcomes of this study show the potential benefits of the approaches that have been introduced when it comes to tackling energy poverty, even without considering a previous implementation of traditional thermal mitigation strategies. In future work, the synergies between the approaches shown in the present study and traditional retrofitting strategies could be further analyzed. The reason for this is that the results of thermal comfort improvement shown here would most probably improve if thermal mitigation strategies were previously implemented, due to the reduction of the thermal losses of the buildings which allows to store the energy inside the buildings for longer periods. These proposed alternatives could be used by policy-makers in the future, reducing the energy bills of occupants with monetary restrictions and at the same time improving substantially their thermal comfort.

The contents of this section have been included in the paper *“Mitigating energy poverty: Potential contributions of combining PV and building thermal mass storage in low-income households”* [152], by L. Romero Rodríguez et al and published in the journal *“Energy Conversion and Management”*.



# 6. APPLICATION FOR A SMART MANAGEMENT OF MICROGRIDS

The previous chapters of this Thesis have demonstrated the potential of large scale energy analyses when it comes to achieving highly energy-efficient districts. Much emphasis was placed on giving insights into how to obtain accurate energy demand and solar potential estimations for whole regions, as a means of enhancing the integration of renewable energies, achieving higher self-sufficiencies and decreasing energy costs. The potential of using the structural thermal energy storage capacity of buildings for DR purposes was also established, and accurate and versatile energy baselines that characterize the buildings of a district were developed. As a last step, the present chapter aims to integrate several of those elements and findings of the previous sections, applying for instance the HULGIS tool presented in Chapter 2 and the baseline models that were shown in Chapter 4, in order to carry out preconditioning strategies which were introduced in Chapter 3. The final question to be answered in this Thesis is the following. Instead of looking at buildings as independent entities, could it be possible to enhance even more the economic savings and integration of renewable energies if the synergies between buildings are considered and DSM strategies are implemented on a district scale?

In this application, a district in La Graciosa Island in Spain will be proposed as a case study, considering PV production, electrical batteries, the structural thermal energy storage capacity of the buildings as well as the possibility to share the electricity surplus between different buildings. This will be done performing simulations supported by experimental measurements of the real electricity consumptions of the district. A novel rule-based control that is applied at 15 minutes intervals will be considered so as to decrease the energy costs of the district as well as increase the self-consumption and self-sufficiency ratios due to the reduction of electricity imports/exports. Compared to the traditional situation in which each building self-manages its own importation and exportation of electricity helped by electrical batteries, the proposed alternatives prioritize sharing the electricity surplus with other buildings of the district instead. As opposed to previous studies on this subject, this will be done in conjunction with different precooling strategies, which will be proposed as a means of achieving economic savings through indirect energy storage, available at no additional costs.

## 6.1. Introduction

The last few decades have shown that traditional energy improvement approaches are insufficient to ensure a sustainable future for all, even with the notorious emergence of renewable energies. The increasing energy demands, uncertainties due to intermittent renewable energy generation and constrained power systems call for an active participation of the consumers, which could play a vital role. Due to their major contribution to global energy consumption, buildings offer many potential advantages thanks to the varying nature of their many energy uses: from appliance load-shifting to thermal mass storage approaches. Even though the load management that could be provided by a single household is rather small, their aggregation creates many opportunities for innovative approaches at larger scales. However, as previously highlighted in this Thesis, the advantages for individual buildings have been widely studied, but there is still little understanding of the potential benefits of an urban scale implementation of such systems.

There are several approaches to integrate district energy systems, such as microgrids or virtual power plants (many micro-generators not necessarily located nearby). Integrated community energy systems could be accepted by many actors such as local governments, communities, energy suppliers or system operators, which see them as an effective means to achieve sustainability as well as consider their importance in future energy systems [153]. Sharing the energy among different users involves two key elements: ICT, and

optimization techniques [154]. The latter is due to the fact that an optimal management of a microgrid requires to investigate in detail the control strategies that should be implemented, since the large amount of bi-directional energy flows allows for multiple dispatching strategies.

## 6.1.1. Literature review

### 6.1.1.1. Distributed Energy Resources

Distributed Energy Resources (DER) are believed to be one of the great pillars for achieving a sustainable future. DER include, among others, small-scale electricity-producing units connected directly to the local distribution system or building where they are located (distributed generation), plug-in electric vehicles, distributed energy storages and responsive loads [155]. The proliferation of DER poses many challenges such as reverse power flows or overvoltage issues, but also brings increasing flexibility due to energy storage systems and flexible demands [156]. Thanks to the widespread use of DER, users that both consume and produce energy are emerging: prosumers.

To promote the use of renewable energies and DER, Feed-in Tariffs emerged as an economic incentive. However, the reduction of these Feed-in-Tariffs in many countries during the past years has encouraged an increase of self-consumption as well as the share of energy between nearby prosumers. Therefore, there have been increasing interests in investigating how to manage DER in an optimal way [156]. In this context, the microgrid concept allows prosumers to participate in an energy sharing zone, sharing the electricity instead of exporting it to the grid. Since the generation of DERs is unpredictable and intermittent, prosumers who have surplus energy could either store it with storage devices or supply others who are in energy deficit: this energy trading among prosumers is called Peer-to-Peer (P2P) energy trading [157].

### 6.1.1.2. Microgrids

Conventionally, prosumers exchange electricity with the grid: purchasing it from the wholesale electricity market and selling it in the retail market. A microgrid can be defined as a group of interconnected DER and prosumers with definable boundaries that could operate independently or not from other power grids. In this context, the surplus electricity from the prosumers of a microgrid could be shared with others (even with consumers that are not able to produce electricity), since some of them may have an energy surplus when others are in deficit and a cooperative distribution among them could improve the balance of energy supply [158]. At present such energy trading is mostly performed on very large scales, so new mechanisms for small scale trading are needed. The purpose of integrated systems on a district scale is to consider the requirements of the whole community, achieving better synergies between prosumers.

Many studies have been published on these topics. For instance, [159] considers an aggregator that controls a population of residential prosumers that own flexible Thermostatically Controlled Loads (TCL) and RES, studying the optimal scheduling method to maximize the economic benefits of the whole population and helping to balance supply and demand. The study in [158] proposed a method of autonomous cooperative energy trading in a microgrid with RES, storage and prosumer-to-prosumer energy exchange, showing that their proposed energy trading could increase the utilization of RES and reduce costs. The increasing utilization of RES could also result in CO<sub>2</sub> emission savings. Furthermore, in [154] a detailed review of prosumer based energy management and sharing is presented, claiming that there is an enormous potential for cost savings, energy conservation and peak load balancing, leading to a specific future research direction. The amount of projects in this area has also significantly increased all around the world, and [157] elaborates main focuses and outcomes of many of such projects, comparing their similarities and differences.

The number of participants in a microgrid is also important. According to [14], which evaluates the benefits of DR programs, the increasing number of participants increases the flexibility of the system and reduces the overall operational costs, but the benefits per individual decreases in the presence of more consumers since a reduced effort from each of them is needed. In addition, [160] showed that the more customers participate in P2P sharing and the bigger the battery size, the smaller the community's average annual energy costs of

each participant and the higher the community's self-sufficiency.

In the management of DERs, there are mainly two types of entities [156], operators and prosumers, and research on the management of DERs is categorized into two main streams that depend on their relationship. In the first one, the operators coordinate all the DERs to maximize the overall economic benefits or provide ancillary services (additional incentives would be needed). In the second one, the operators only provide a local market platform so that the prosumers share the energy with each other to maximize their own benefits individually (no additional incentives are needed). The latter is the so called peer-to-peer energy sharing concept, which will be analyzed in more detail in the next section. Energy sharing models specify how prosumers exchange and trade energy with each other, and the studies made in this field can be divided into 3 categories [161]: energy sharing conducted by one centralized authority, energy sharing achieved by the interaction between an operator and a group of prosumers, and energy sharing achieved by the interaction of a group of prosumers (P2P energy sharing).

#### **6.1.1.3. Peer-to-peer energy sharing**

Peer-to-peer energy sharing allows the surplus electricity from DERs to be traded between prosumers in a community microgrid [160]. P2P trading is also defined as flexible energy trades between peers, where the excessive energy from many small-scale DERs is traded among local customers [162]. P2P energy trading is one of the promising paradigms of smart grids in the near future, and it could not be implemented without smart grid technologies such as ICT, monitoring and control functions [163]. In [160] a P2P method was investigated allowing surplus DERs to be shared among the prosumers of a neighborhood, concluding that their method was able to reduce the energy costs of the community by 30 % compared to conventional peer-to-grid trading. According to [160], P2P energy sharing has a similar impact on raising a community's self-consumption, self-sufficiency and reducing energy costs as batteries, but at significantly less capital costs. Therefore, they provide a great potential for profitable applications in the near future.

It should be mentioned that for different studies the corresponding frameworks of P2P trading may be slightly different. For instance, [156] considers that in P2P energy sharing prosumers directly trade energy with each other to achieve a win-win outcome. On the other hand, [160] claims that the research on P2P energy sharing can be categorized by energy trade with and without an intermedia, and that although strictly speaking P2P means energy trade without an intermedia, it does not necessarily mean that the prosumers directly control their DERs, since they may get use of a third party entity to manage their resources: an aggregator, whose role is described below.

#### **6.1.1.4. Energy Sharing Coordinator**

To allow multiple prosumers to participate in the market (their low energy exchanges would not allow them to participate individually) and facilitate the control when sharing energy in a district, a coordinator is required. These coordinators have different names in the literature, the most common of which are: aggregator, energy sharing provider and Energy Sharing Coordinator (ESC), which is the name that will be used in the present work. They provide P2P sharing services and act as a local market operator, and their role is to respond to the requests made by the prosumers in an optimized way.

Generally, the ESC belongs to the microgrid operator or an independent third party that provides energy sharing service for all the prosumers that participate and is in charge of purchasing/selling electricity from/to the grid [164]. If the community needs electricity, the ESC buys it from the grid, and when there is electricity surplus, it sells it. It is likely that the role of the aggregator will continue to grow in importance, boosting the introduction of DER and smart grid technologies [165]. For instance, the study in [166] focuses on the design of a central energy management system in order to reduce the costs and emissions, relying on a day-ahead operational planning and an online adjustment procedure during the operation.

As regards to benefits allocation, it should be mentioned that the economic benefits obtained by trading electricity among the buildings of a district poses the question about how to share the savings fairly. The district as a whole may achieve cost savings, since a smaller amount of energy will be imported/exported to

the grid and the export prices are lower than import prices. However, the district may be composed of both prosumers and consumers (who are not able to produce electricity), which could eventually lead to a situation in which certain prosumers achieve less benefits when sharing their production, and thus see no motivation to participate on energy sharing approaches. Therefore, the design of models that consider incentives is very important so as to distribute the benefits in a fair way and increase the involvement of all potential parties involved. Some examples to approach this can be seen in the literature. One of the proposed solutions is to utilize auction models and multi-agent theory, defining a dynamical internal pricing model that treats the microgrid as a small energy market [164]. Another solution proposed by [167] is to provide energy credits to the prosumers according to their excess renewable production, shifting their self-production to high-price periods. Conversely, in [168] a model is proposed to address unfair cost distributions by ensuring Pareto optimality.

#### 6.1.1.5. Demand Response through Thermostatically Controlled Loads

Demand Response in districts can be carried out by using different types of loads: appliances, plug-in vehicles, Thermostatically Controlled Loads and so on. However, although providing energy flexibility in buildings by controlling appliances may be beneficial, from our point of view TCLs should be considered as a higher priority due to their much larger energy consumptions and thus potential contributions. TCL are able to provide flexibility thanks to the thermal mass and inertia. They may be seen as a storage solution that can be controlled as long as certain constraints are considered. Examples of TCL are some appliances, water heaters or heat pumps.

The contribution that an individual user can make to the power system by using TCL is minimal, so load aggregation should be applied to make the total capacity large enough. As mentioned in previous chapters, this could be done in the context of microgrids. Previous research that investigated the thermal mass potential used various approaches depending on the level of analysis, but when the focus is on the grid characterization and the scales are large, building models are often quite simple and do not capture the fine dynamics of buildings [169]. In [170] a framework for developing optimization-based control strategies to shift the heating loads in buildings was introduced, however, only one building was evaluated. Conversely, [171] proposed a model that analytically characterizes the aggregate power response of a population of air-conditioning units to a simultaneous step change in temperature set-points. The results given in [172] showed that enabling TCL to participate in real-time retail electricity markets could reduce consumer costs by over 10 % compared to an uncoordinated operation.

Different TCL have been evaluated in the literature considering large scales. The approach followed by [173] is based on a centrally optimized thermostat set-point signal that controls an aggregated detached house building stock, rewarding consumer participation with flexibility or comfort based bonuses. On the other hand, [159] chose electric water heaters as a representative technology to demonstrate the modeling and scheduling method of TCL, while [174] investigated the impact of DR activation using the aggregated power consumption of domestic refrigerators. However, the average aggregated power of the population of 25 fridges in this case was 1875 W, which is close to the power of a single heat pump in a building. Therefore, the author of this Thesis believes that using heat pumps is a more attractive alternative. In fact, an interesting method to quantify the equivalent storage capacity for 4 common domestic TCLs (electric space heating system, freezer, fridge and electric water heater) was carried out in [175], showing through simulations that the resource with the highest equivalent capacity is the electric space heating system (although with a significant seasonal variability compared to other solutions such as electric batteries). Also, [176] reviewed different thermal storage options, concluding that the built-in thermal mass was more cost-effective than water buffer tanks.

It is also important to consider the building characteristics in order to make use of the thermal mass storage capacity of buildings. The objective in [169] was to assess the potential of buildings to modulate the heating power and define simple control strategies to exploit the flexibility potential. Considering two residential buildings with different levels of insulation and air-tightness, this study concluded that contrary to other storage solutions such as batteries or hot water tanks, the modulation potential of the thermal mass varies

depending on the season. Also, the autonomy of a poorly insulated building is relatively short, while passive houses have a long time constant that leads to a larger autonomy but are able to store a smaller amount of energy. According to [14], which evaluated the value of flexibility of thermal inertia in buildings and active TES in DHW tanks, a higher participation of users would require smaller deviations from the minimum electricity demand profile per dwelling to achieve the same amount of load shifting, leading to lower thermal losses per dwelling. Also, the study in [176] presents a review of the existing literature on supervisory control for improving the energy flexibility provided by heat pumps in buildings.

#### 6.1.1.6. Studies on the optimal control of DER

The literature review that has been carried out revealed the large amount of studies that are being developed on the optimal control of distributed energy systems. A very interesting review is given in [177], which provides a very recent description on the progress in the field of DSM, DR programs and distributed generation. In addition, it is stated that in most studies the optimal scheduling is done for single users, and very few have expanded their work for multiusers energy scheduling. This assertion motivates the aim of the present work, which intends to find optimal dispatching strategies in a district composed of different prosumers.

Control strategies in microgrids can be classified into two categories: rule-based controls, and model predictive control [176]. Rule-based controls are simple heuristic methods (“if-then”) that rely on trigger parameters, but they can achieve a significant performance in a simple way, which facilitates their implementation. Conversely, model predictive controls present many advantages to optimize the management of a system, but they are more complex (an optimization problem) and require more investments.

Regarding the results of the optimal control strategies found by previous publications, the study in [178] focuses on a hybrid system in which the optimal control under a Time-of-Use (TOU) tariff is found. They conclude that in their case the imports of electricity from the grid are avoided during peak periods, using PV or wind energy instead, and the fuel cell system is only charged when there is an excess of renewable energy. In [179], which also analyses the optimal operation of a system under TOU tariff, it is concluded that the electric batteries are discharged at peak periods and charged from cheap grid and PV, while PV is only exported if the batteries are full. In addition, [180] considers a system with PV, CHP, storage and responsive loads with 5 minute time-steps, and concludes that the storage is charged during the night and discharged during high prices.

On the other hand, [181] uses a time series mixed integer linear program with an extension of the REopt model, considering hourly time-steps during a whole year. The authors state that the PV surplus is best delivered to the batteries, and then to the grid as a last resort. Also, [182] minimizes the costs of a system that includes PV, electric heaters, batteries, appliances, thermal storage and space heating demand over sequential 24-hour horizons for a whole year. In this case, the electricity is only exported to the grid during peak periods and if no more storage is available, since they affirm that maximizing PV self-consumption can be expected to decrease total costs, due to the fact that the feed-in prices are lower.

Another interesting study can be found in [183], which uses evolutionary algorithms and different time horizons of 6h, 12h and 24h to find the optimum control of a system that includes PV, wind, CHP, thermal and electrical storage. In this case, they conclude that the batteries supply power at peak periods and the electricity is exported to the grid only if the price is high. They also state a very important fact that will be further analyzed in the present study: according to them, considering a long time horizon would help to reach lower operation costs.

### 6.1.2. Aim of the study

The literature review that has been carried out in this chapter revealed the great interest of the research community in the issue of energy sharing in microgrids, since the interconnection between prosumers (mainly through peer-to-peer energy trading) is regarded as a very interesting alternative for improving cost savings at district level. On the other hand, it is also very frequent to find studies that perform demand side management strategies through thermostatically controlled loads. One of the most popular alternatives in this respect is to consider models that analytically characterize the aggregate power response of a population of appliances, but the author of this Thesis believes that, in order to achieve significant benefits at district level, other more important contributors to energy consumption such as air-conditioning should be considered. In addition, it is very unusual to find studies that combine both energy sharing and demand response approaches through thermostatically controlled loads. The present study intends to address that knowledge gap.

Using as a case study a microgrid composed of several prosumers in a district located in La Graciosa Island (Spain), this chapter aims to propose a novel strategy that encourages sharing surplus electricity between different prosumers, in order to maximize the overall cost savings and the utilization of renewable energy in the district. In this case, the prosumers are equipped with thermostatically controlled loads (heat pumps) and renewable generation (PV modules). A central controller (named Energy Sharing Coordinator) will manage all the resources in order to maximize the cost savings of the district, prioritizing sharing the electricity between prosumers instead of using the batteries or relying on the power grid. It should be mentioned that our study will focus on the achievement of cost savings on a district scale. Therefore, we abstract from taking into account the issue of the allocation of the obtained benefits among the prosumers of the district, which is an issue already discussed very frequently in literature as commented in previous sections.

In addition, a comparison between different preconditioning strategies will be carried out, determining the optimal strategies during a whole year and reaching important conclusions. To check the influence of considering different time horizons for the optimization of these preconditioning strategies, three time horizons will be examined: one day, two days and three days. Apart from analysing the cost savings, the self-consumption and self-sufficiency ratios will be estimated and compared to the traditional situation in which each building is self-managed, together with the evaluation of several variables such as the air-conditioning consumption or the energy lost when the electrical batteries are used. Last of all, a sensitivity analysis regarding the feed-in tariffs will be carried out.

## 6.2. Description of the case study

### 6.2.1. Characteristics of the district

The island of La Graciosa is located to the north of Lanzarote, in the Canary Islands (Spain). With a surface area around 29 km<sup>2</sup> and a population of 660 inhabitants, the island is vouching for a more sustainable future by investing in novel self-sufficient systems that are able to produce, store and distribute their own energy from renewable energy sources. A microgrid is being put into place, which will integrate the distributed generation using electrical storage that will help to manage the energy flows. In this way, the reliability of electricity supply will be enhanced, due to the fact that until recently the island relied only on the electricity that came from the island of Lanzarote through a submarine cable of 20 kV. In addition, economic savings could be achieved by exploiting the synergies between the prosumers in the island, and the CO<sub>2</sub> emissions could be reduced thanks to the better integration of renewable energies.

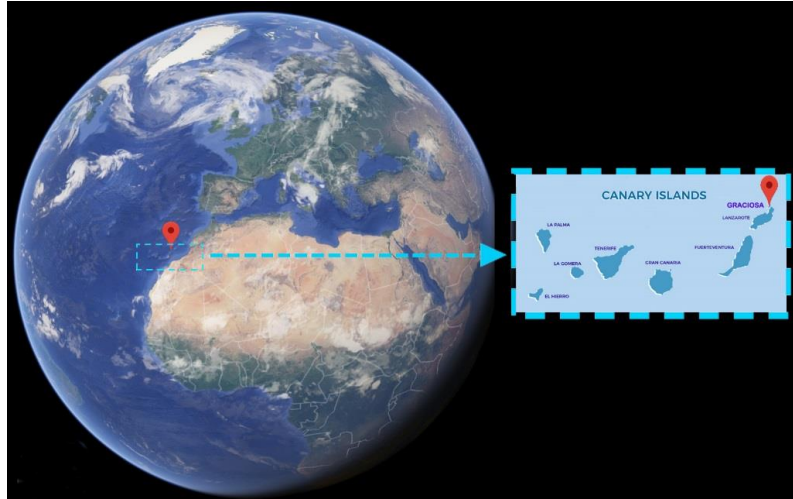


Figure 95: Location of La Graciosa Island.

The present study will be focused on a district fed by one of the electrical power transformers located in the island, since measurements of electricity consumption at 15 minutes time-steps are available for these buildings. This district is composed of 25 dwellings as well as the local school. All the dwellings and the school have PV modules installed, turning the system into a microgrid composed of prosumers with different load patterns. The location of the district under study is shown in Figure 96, and the interconnections between the buildings of the microgrid are shown in Figure 97.



Figure 96: Location of the case study district within the island of La Graciosa (left) and IDs of its buildings (right).

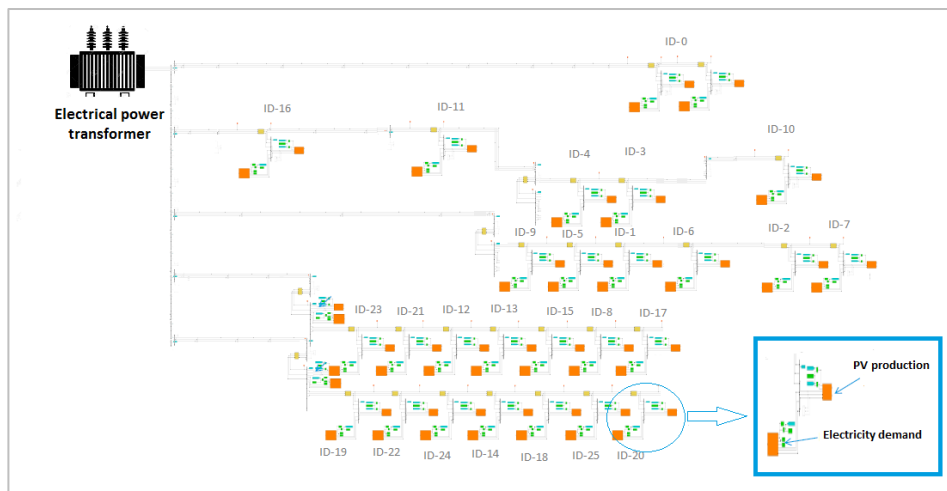


Figure 97: Interconnections between the buildings of the district.

Several visits were made to the island, carrying out surveys with the occupants of the dwellings under consideration and inventorying the energy systems. As regards to the installations that may be found in the dwellings, all the households have gas water heaters for the DHW and a heat pump located in the living room. All the buildings are equipped with several PV modules of 256 W nominal power and 16.27 % efficiency, located in their rooftops with a 15° tilt angle and varying orientations. In the case of the school, there is a total installed power of 10,445 W. The inverters that are installed, with 4.6 kW each, also have an integrated electrical storage of 2 kWh nominal capacity per household.



Figure 98: Example of PV modules installed in the island.

## 6.2.2. Monitoring and modelling of the district

### 6.2.2.1. Electricity consumption

A monitoring campaign was designed to investigate the electricity consumption of the buildings of the district at 15 minutes intervals. The monitoring involved all the 25 dwellings as well as the school, during the whole year 2016. In Figure 99 the annual electricity consumption measured for the different households as well as the school is shown. As it can be seen, the differences among dwellings are quite pronounced (for instance, ID 15 consumes 5 times more than ID 18). These differences will allow us to exploit the synergies between buildings with different energy consumptions.

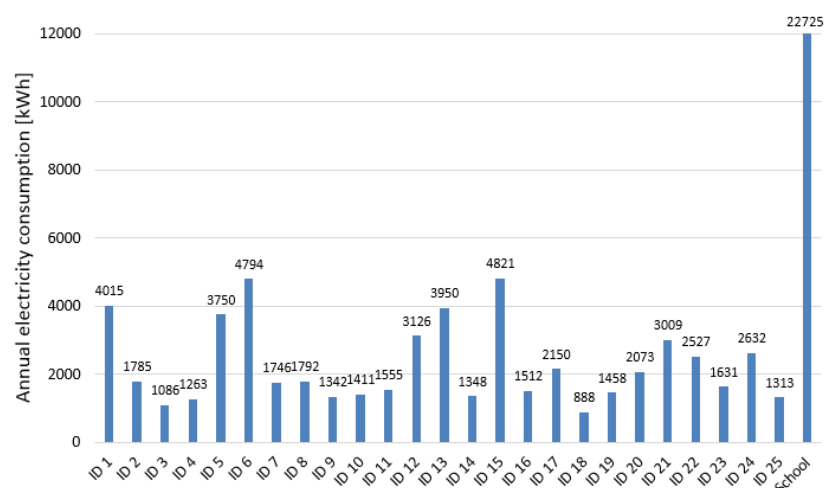


Figure 99: Annual electricity consumption of every building in the district.

### 6.2.2.2. PV production and electrical balance of the district

As for the PV production, a web-based PV system design tool that integrates shading analysis, simulation and CAD in one package was used to calculate it: *Helioscope* [147]. This tool allows to estimate the electricity production of the PV modules installed on the rooftops of the district, taking into account losses due to



weather, shading, wiring, component efficiencies, panel mismatches and aging. It also provides recommendations for equipment and array layout, calculating the discrete number of PV modules that can fit into a solar field and considering parameters such as the orientation and inclination of the modules or the separation between adjacent rows.

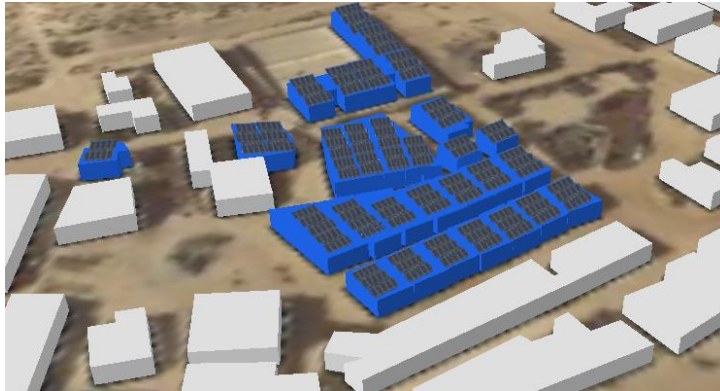


Figure 100: Depiction of the PV modules installed in the district.

For the whole period of the study, weather data was available through a nearby weather station, providing hourly values of outdoor temperature, humidity, and solar radiation. The simulation of the PV potential (using a weather file that contained the real data of the monitoring period, following the procedure in Annex A) allowed to estimate the electricity production of the district, obtaining the results shown in Figure 101. These results are also compared to the monthly real electricity consumption of the district. As is apparent, the amount of electricity that could be produced by the PV modules in the district is higher than the monthly electricity consumption. However, this assertion is rather misleading, since one might think that no electricity would need to be imported. Since there might be times with electricity surplus and times (for example during the night) where electricity would have to be imported once the batteries are depleted, the adjustment between supply and demand at short time scales should be considered.

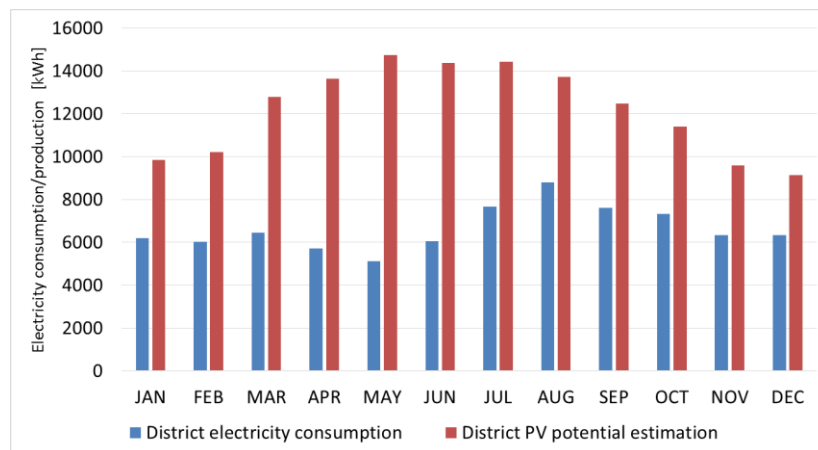


Figure 101: Monthly PV production of the district.

Adopting a 15 minutes time scale for analyzing the balance between the electricity consumption and the estimated PV production of each building provides interesting insights. Let us take a couple of days in January as an example (see Figure 102), focusing on two specific dwellings: ID 11 and ID 14. In this case, ID 14 is a dwelling occupied by one person who was away on holidays. For that reason, its PV production during the day would allow to charge the batteries, reaching a 100 % State of Charge (SOC) early in the morning. This means that this dwelling would have to sell the electricity on the retail market during this period (or get rid of it if that were not possible). Due to the low electricity consumptions (standby and fridge) during the day, the battery SOC drops only around 20 %, until it is charged again the following day. On the other hand, ID 11 is a dwelling occupied by two people who were present during the holidays. Their high

electricity consumption meant that electricity had to be taken from the batteries even during daylight hours with own PV production, and then from the grid once their battery was depleted.

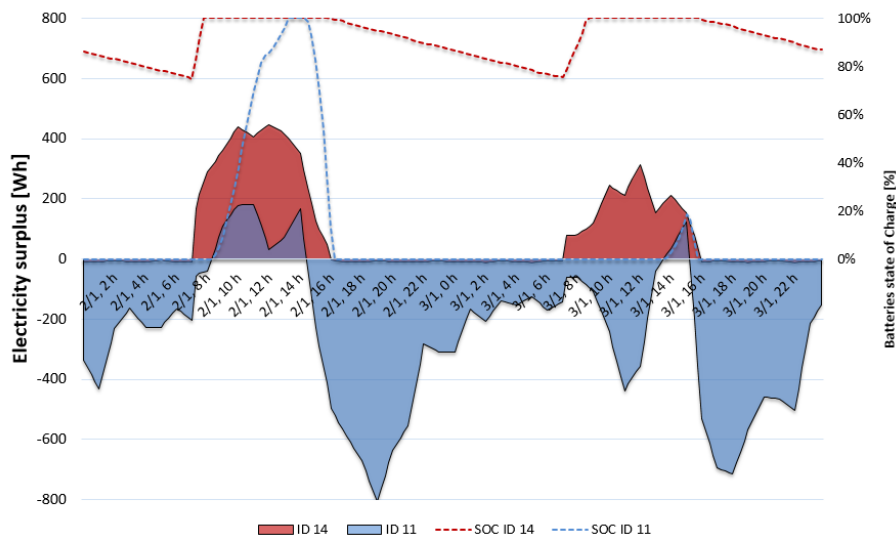


Figure 102: Electricity surplus of the two dwellings under study, calculated through the difference between PV production and electricity consumption. Positive values mean an electricity surplus, while negative values mean the need to import electricity.

Figure 102 reveals the importance of the strategies that will be proposed in the present work. In times were the battery of a dwelling is fully charged while at the same time other dwellings are in need of importing electricity, this electricity could be shared between them. This could bring economic benefits, due to the fact that the selling price for exported electricity is lower than that for the imported electricity (or even there might be no Feed-in-Tariff available). Furthermore, even if the battery of a dwelling is not full, it might be more beneficial to share the electricity with a household who needs to import it, since the electricity losses when charging and discharging the batteries would be avoided. Preconditioning strategies as well as a dynamic pricing framework could also help to detect optimal dispatching strategies. The present work aims to answer these questions.

### 6.2.2.3. Electricity prices

For the purposes of this study, a two-period tariff will be considered. The hourly real prices of the electricity market in Spain in 2016 (coinciding with the monitoring period) for this tariff were taken from a public organism of the Spanish government (<https://www.cnmc.es>). An example of these variable prices is shown in Figure 103 for the 1<sup>st</sup> of July.

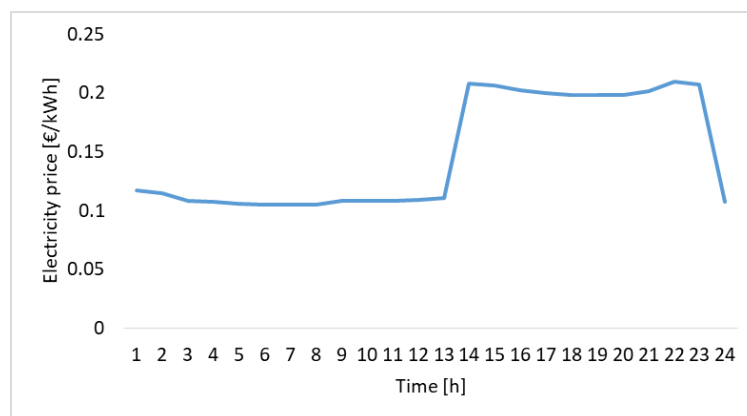


Figure 103: Variation of the electricity prices of the considered two-period tariff. 1<sup>st</sup> of July 2016.

#### 6.2.2.4. Thermal characterization of the buildings of the district

Finally, in order to analyse the thermal performance of the district a building model was developed for each of the 25 dwellings and the school by using HULCGIS, the tool developed in the present Thesis and explained in detail in Chapter 2. Once the simplified representations of the buildings were available, 3 main typologies were identified. The visits made to the district allowed to collect the necessary data of their real construction, geometry, occupancy and internal gains, which were then used for modelling them in detail (see Figure 104). Then, simulations were performed using the real climatic data during the monitoring period, allowing us to obtain the full free-floating temperatures.

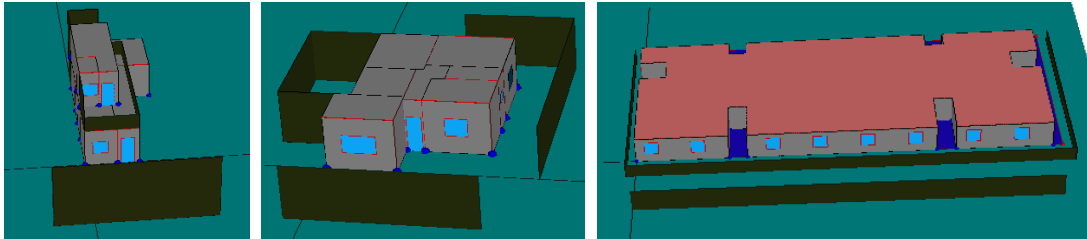


Figure 104: HULC detailed models of dwelling 1 (left), dwelling 2 (center) and the school (right).

Once the building representations were available, the model explained in Chapter 4 for obtaining the energy baselines was applied. Due to the lack of empirical data that would allow us to obtain the real primary and secondary baselines, in this case they were obtained numerically, considering short time-steps of 15 minutes. After completing the process, the full free-floating temperatures as well as the secondary baselines for each building were available, which were essential to implement the precooling strategies proposed in the present work.

### 6.3. Calculation methodology

#### 6.3.1. Scenarios

In this work, several scenarios will be proposed for comparison purposes. These scenarios are shown in Table 15, and consider two possibilities for the management of the district: “self-consumption” (where each building manages their own batteries and PV production as in the current real case), or “ESC” (where an energy sharing coordinator manages the energy flows within the district). The rule-based control for the latter will be explained in detail in next sections. The scenarios 0 and 0' were added to show the readers what the costs would be if there were no PV systems installed in the district. Also, different options regarding the air-conditioning will be taken into account: no air-conditioning, normal schedule (see Table 16), and precooling strategies with a time horizon of either 1 day, 2 days or 3 days. A time horizon of 3 days for example means that the same precooling strategy is applied during 3 days, after which the total cost for the district is computed, and the strategy with the lowest cost is chosen for the first day. The considered precooling strategies will be explained in the next section.

Scenario	Management	PV Self-consumption	Air-conditioning	Precooling	Time Horizon	Description
0	Individual	No	Yes	No	-	Self-managed buildings, no PV
0'	Individual	No	No	No	-	Self-managed buildings, no PV, no air-conditioning
1 (base case)	Individual	Yes	Yes	No	-	Self-consumption with PV
1'	Individual	Yes	No	No	-	Self-consumption with PV, no air-conditioning
2	Individual	Yes	Yes	Yes	1 day	Self-consumption with PV, precooling strategies with 1 day time horizon
3	Individual	Yes	Yes	Yes	2 days	Self-consumption with PV, precooling strategies with 2 days time horizon
4	Individual	Yes	Yes	Yes	3 days	Self-consumption with PV, precooling strategies with 3 days time horizon
5	District	Yes	Yes	No	-	ESC, with PV
5'	District	Yes	No	No	-	ESC, with PV, no air-conditioning
6	District	Yes	Yes	Yes	1 day	ESC, with PV, precooling strategies with 1 day time horizon
7	District	Yes	Yes	Yes	2 days	ESC, with PV, precooling strategies with 2 days time horizon
8	District	Yes	Yes	Yes	3 days	ESC, with PV, precooling strategies with 3 days time horizon

Table 15: Considered scenarios.

### 6.3.2. Preconditioning alternatives

Apart from prioritizing the distribution of surplus electricity among the buildings of the district, this study also aims to analyse whether preconditioning approaches could help to achieve cost savings in the district, along with other benefits. This will be done by taking advantage of the price differences in the two-period tariff presented in Section 6.2.2.3, which would eventually allow to preheat or precool the buildings at times where the electricity prices are lower. In this study, for the normal schedule of the air-conditioning systems temperature set-points of 20 °C in winter and 25 °C in summer will be used, considering the operating schedules presented in Table 16.

Time	Dwellings		School	
	Working day	Weekends and holidays	Working day	Weekends and holidays
0	0	0	0	0
1	0	0	0	0
2	0	0	0	0
3	0	0	0	0
4	0	0	0	0
5	0	0	0	0
6	0	0	0	0
7	0	0	1	0
8	0	0	1	0
9	0	1	1	0
10	0	1	1	0
11	0	1	1	0
12	0	1	1	0
13	0	1	1	0
14	1	1	1	0
15	1	1	1	0
16	1	1	0	0
17	1	1	0	0
18	1	1	0	0
19	1	1	0	0
20	1	1	0	0
21	1	1	0	0
22	1	1	0	0
23	1	1	0	0

Table 16: Operating schedules of the air-conditioning systems for the dwellings and the school of the district.

Seeing the operating schedules in Table 16 as the scenario with no preconditioning, new precooling strategies will be studied. These strategies modify either the amount of precooling time or the set-point temperature, which will allow us to reach important conclusions. Nevertheless, it should be mentioned that the outdoor air temperatures in La Graciosa Island are relatively high during the year, which means that there is virtually no heating consumption in the buildings. For this reason, only precooling strategies will be analysed in the present study, carrying them out in the living rooms of the dwellings (where the heat pumps are located) as well as the school. An example of the effects of different precooling strategies is shown in Figure 105. As it can be seen, performing precooling during times of low electricity prices increases the total energy use, but diminishes it during times of high electricity prices compared to the normal schedule (shown in red).

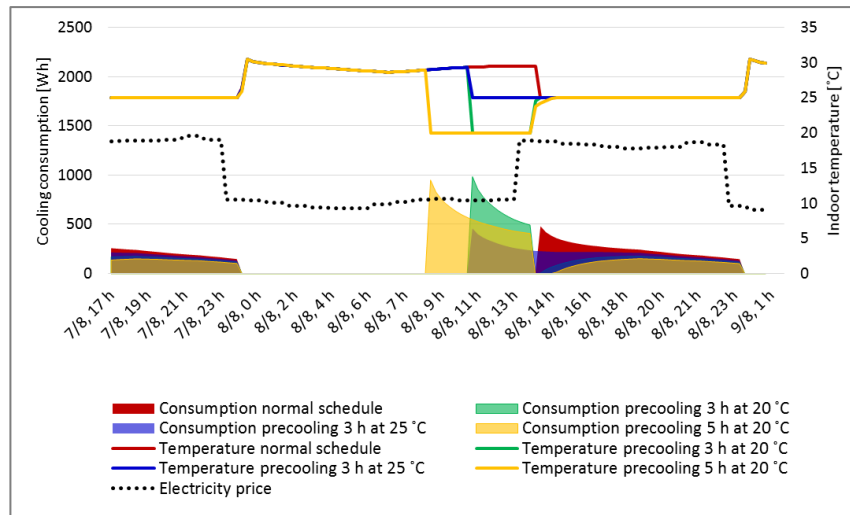


Figure 105: Effect of a precooling strategy on the indoor temperature and cooling consumption.

A total of 9 precooling scenarios will be considered in this study, plus the scenario with no precooling (see Table 17): 3 options for the precooling time and 3 options for the set-point temperature. For instance, the scenario with 3 hours of precooling and 23 °C set-point temperature on a working day in a dwelling would mean that the heat pump would precool its living room from 11 p.m. to 14 p.m. at 23 °C, and then use 25 °C from 14 p.m. to 0 a.m. (the normal operating schedule shown in Table 16).

Precooling strategies	Description
PR_ST1	No precooling
PR_ST 2	1 hours 25 °C
PR_ST 3	1 hours 24 °C
PR_ST 4	1 hours 23 °C
PR_ST 5	2 hours 25 °C
PR_ST 6	2 hours 24 °C
PR_ST 7	2 hours 23 °C
PR_ST 8	3 hours 25 °C
PR_ST 9	3 hours 24 °C
PR_ST 10	3 hours 23 °C

Table 17: Precooling strategies considered.

### 6.3.3. Proposed rule-based control strategy

As discussed earlier, the main goal of the present study is to investigate the benefits of exploiting the synergies between buildings by sharing the surplus electricity between them. This situation will be compared to that where each building is self-managed, which means that they use their own PV production, storing the electricity or exporting it to the grid in case of surplus and taking the electricity from their batteries or importing it from the grid in case of need.

In order to carry out this comparison, the first step is to define a new control strategy that encourages sharing the electricity in the district instead of charging the batteries or exporting the electricity. This will be done through an ESC. As mentioned before, the simulations will be carried out considering 15 minutes time-steps and 3 options for the time horizon: 1 day, 2 days and 3 days. In addition, the consideration of several preconditioning strategies will introduce the use of the structural thermal energy storage capacity of the

buildings, serving as a means of indirect energy storage. After each time horizon, the precooling strategy with the lowest cost for the district (in scenarios 2, 3, 4, 6, 7, and 8 as seen in Table 15) will be selected.

For the proposed ESC simulations of the whole district, the control strategy shown in Figure 106 has been developed. In this figure,  $i$  corresponds to the building number,  $j$  corresponds to the time-step,  $Pelec$  is the measured electricity consumption of the building,  $PV$  is the PV production,  $HP$  is the heat pump consumption,  $Eavl$  is the electricity surplus available and  $SOC$  is the state-of-charge of the batteries.  $Stoptime$  means the last time-step of the simulation, which considering 15 minutes time-steps would be 35,040 for a whole year.

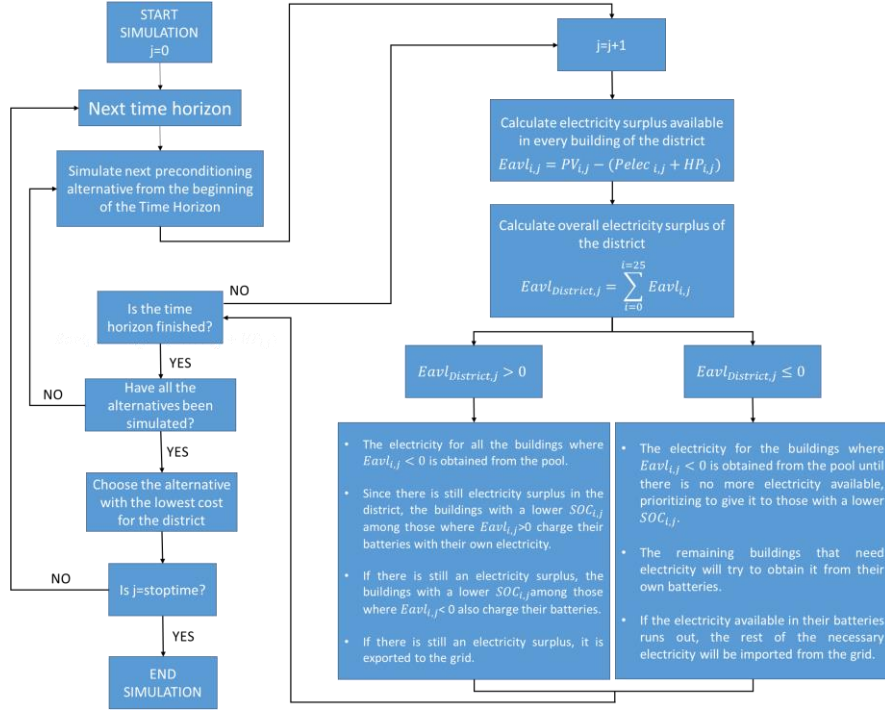


Figure 106: Proposed rule-based control strategy for each time-step.

To understand the procedure, an example for a time horizon of one day is going to be explained. At the beginning of the simulation, the first time horizon (1<sup>st</sup> of January) is analyzed, considering the first preconditioning strategy. In the first time-step of 15 minutes, the electricity surplus of each building in the district is calculated by taking into account their PV production, electricity consumption and air-conditioning consumption. This electricity surplus could be either positive (meaning that the building could export electricity) or negative (meaning that it would need to import electricity). Then, the overall electricity surplus of the whole district is calculated, and two situations could happen in this time-step.

- If  $Eavl_{District,j} > 0$ , it means that the district as a whole has an electricity surplus, which is managed by the ESC. Therefore, the district would be self-sufficient. In this case, those buildings that would need to import electricity obtain it from the ESC, but there would be still electricity available. Then, the buildings with the lowest  $SOC_{i,j}$  among those where  $Eavl_{i,j} > 0$  charge their batteries. In this way, the electricity that is shared with other buildings is taken from those whose batteries are fuller. After doing so, if there is still an electricity surplus, buildings where  $Eavl_{i,j} < 0$  will also charge their batteries, again prioritizing to give the electricity to buildings with lowest  $SOC_{i,j}$ . As a last resort, if all the batteries of the district are full then the electricity is exported to the grid.
- If  $Eavl_{District,j} < 0$ , it means that the district as a whole needs more electricity than that which the PV modules produce. First, all the electricity from the buildings with a surplus is used for those where  $Eavl_{i,j} < 0$  until there is no more electricity available, prioritizing to give the electricity to those with lowest  $SOC_{i,j}$ . Then, the remaining buildings that need electricity try to obtain it from their batteries, and if this were not possible, they would import it from the grid at the retail price.

At the end of this first time-step, the total cost for the district is computed, and the next time-steps are simulated in the same way until the end of the time horizon. Then, the total cost for this time horizon of the considered preconditioning strategy (which influences the HP consumptions) is calculated, and the simulation starts again from the first time-step of the current time horizon, simulating another preconditioning strategy. Once all the preconditioning strategies for the 1<sup>st</sup> of January have been simulated, the one with the lowest cost is chosen. Then, the simulation continues doing the same procedure on the 2<sup>nd</sup> of January, 3<sup>rd</sup> of January and so on, until the 31<sup>st</sup> of December. As a result, the outcome of the whole simulation will be the selection of the optimal preconditioning strategy for every day of the year, as well as the calculation of the total costs of the district, total energy consumption, self-consumption ratio, self-sufficiency ratio and so on, which will then be compared with the rest of scenarios shown in Table 15.

### 6.3.4. Simulation framework

The proposed rule-based control was programmed in such a way that it was possible to simulate the 12 scenarios that were proposed, where 6 of them involved finding the optimal precooling strategy among 10 possibilities in each time horizon (3 alternatives). In addition, in each time-step (35,040 in total) many energy flows are involved, and the model needs to check the status of every building of the district before making decisions. Therefore, a very complex, flexible and modular model was needed. A new tool was consequently developed in Fortran language, which after optimizing the programming produced the desired outcomes in a relatively fast way. The output files include the selection of the optimal precooling strategy for each time horizon, as well as data at 15 minutes intervals of electricity imports, exports, air-conditioning consumption, use of the batteries, costs, and all the variables that were necessary to carry out this study. An illustration of the developed simulation framework is shown in Figure 107.

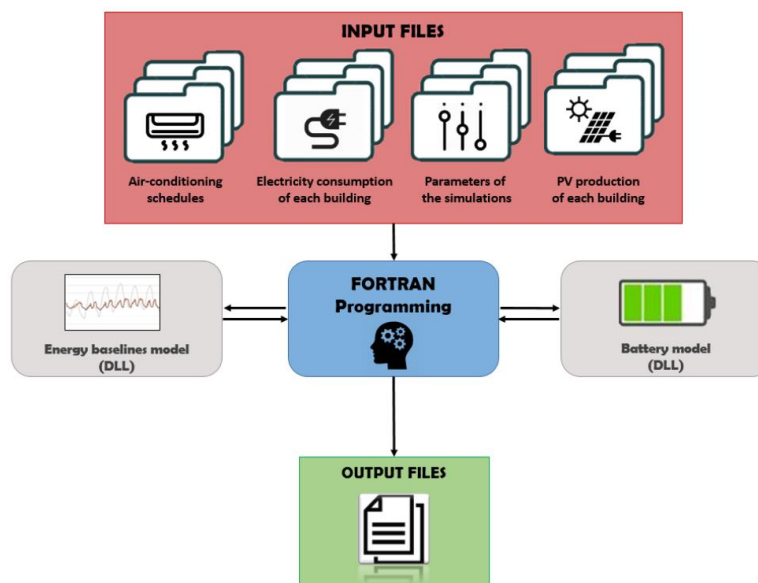


Figure 107: Illustration of the simulation framework.

#### 6.3.4.1. Input files and models

With regards to the PV production, as mentioned in Section 6.2.2.2, it was estimated by using Helioscope, so the PV production of each building was implemented in the Fortran model through input files. The electricity consumption of the district was also included through input files for each building, with the real consumption data of the whole year obtained from the monitoring campaign. The feed-in tariff that will be considered for the simulations when electricity is exported to the grid will be 0.05 €/kWh. On the other hand, the application of the energy baselines model proposed in Chapter 4 was done through a Dynamic Link Library (DLL). The same is true for the model of the batteries.



The model that has been used for the electric batteries, of lithium-ion technology, considers both charging and discharging efficiencies as well as the deterioration due to the utilization cycles. It is based on performance curves obtained from a representative sample of manufacturers. The first performance curve characterizes the charging/discharging efficiencies, allowing to calculate the real capacity of the battery, whereas the second one characterizes the deterioration of the battery as a function of the number of discharge cycles. Several restrictions are also included, such as the limitation of the depth of discharge.

### 6.3.5. Self-consumption and self-sufficiency ratios

The self-consumption (share of the solar supply that is directly consumed in the district) and self-sufficiency (share of the district demand covered by the solar supply) ratios were calculated in the following way:

-Self-consumption ratio:

$$SCR = \frac{\sum PV_{production} - \sum PV_{exported}}{\sum PV_{production}}$$

-Self-sufficiency ratio:

$$SSR = \frac{\sum PV_{production} - \sum PV_{exported}}{\sum E_D}$$

## 6.4. Results and discussion

### 6.4.1. Comparison of management alternatives

Both the traditional situation where every building of the district is self-managed and the innovative rule-based control strategy proposed in the present work were first simulated without considering precooling strategies, allowing us to reach important conclusions with regards to the benefits that can be derived from exploiting the synergies between buildings. As previously mentioned, the real district under consideration is equipped with PV modules, each building is individually managed and uses the air-conditioning schedules shown in Table 16, with no precooling. Therefore, the real case is scenario 1, which will be considered the base case from now on to compare the results. For comparison purposes, the scenarios 0 and 0' are also shown. The results are presented in Table 18, and will be explained in detail in the next sections.

SCENARIO	ELECTRICITY IMPORTS [kWh]	ELECTRICITY EXPORTS [kWh]	ANNUAL COSTS [€]	AIR-CONDITIONING CONSUMPTION [kWh]	ENERGY LOST IN BATTERIES [kWh]	REDUCTION COSTS [%]	SELF-CONSUMPTION [%]	SELF-SUFFICIENCY [%]
Scenario 0	85588	0	14363	7716	0	-	0%	0%
Scenario 0'	77872	0	13372	0	0	-	0%	0%
Scenario 1 (base case)	48471	88721	3462	7716	2813	0%	31%	47%
Scenario 1'	44127	92030	2470	0	2875	29%	29%	47%
Scenario 5	34050	74152	1919	7716	2960	45%	42%	64%
Scenario 5'	29375	77210	873	0	2942	75%	40%	66%

Table 18: Results of different management alternatives for the district.

### 6.4.1.1. Cost savings

First of all, we can see that the installation of the PV modules in the district under study led to a significant cost reduction. If we consider scenario 1 as the current real case, introducing the proposal of the ESC in the district would allow to reduce the costs around 45 % (see Figure 108). In this case, no precooling strategies are yet considered so the air-conditioning consumption remains the same.

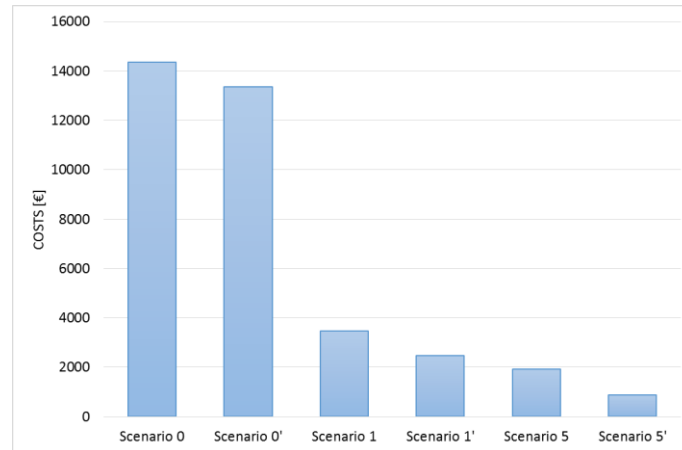


Figure 108: Comparison of annual costs for different management scenarios.

### 6.4.1.2. Electricity imports/exports

As for the electricity exchanges with the power grid, it can also be seen that the ESC scenario 5 reduces both the electricity imports and exports, since more electricity is retained within the district. This can be seen on a monthly basis in Figure 109.

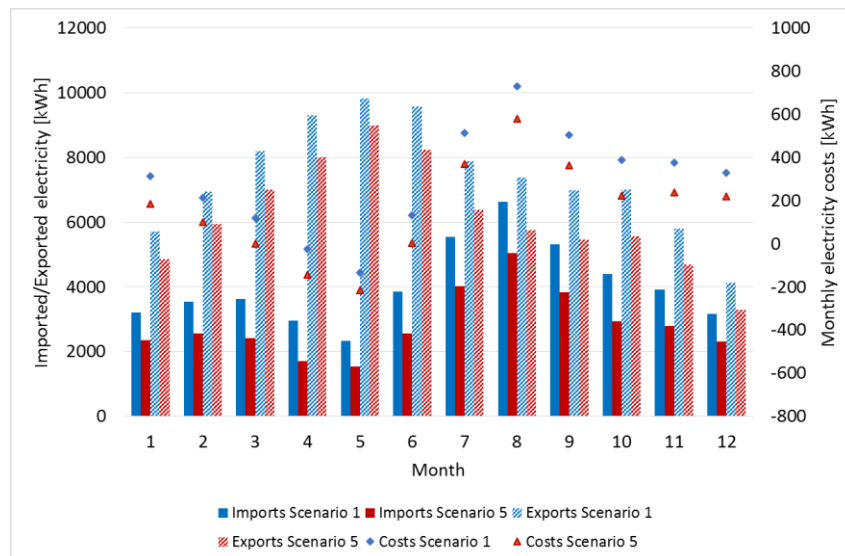


Figure 109: Comparison of monthly imports, exports and costs for the self-consumption and district scenarios.

### 6.4.1.3. Energy lost in batteries

With regards to the energy lost in the batteries, the proposed ESC concept involves a small increase, since the batteries of the district are more frequently used. This is due to the fact that the proposed concept prioritizes that every electricity surplus of the district is used for other buildings of the district and then to charge their batteries, instead of exporting it to the grid if the battery of the building is full as is the case in scenario 1. In other words, as justified in Section 6.2.2, in the proposed ESC concept it is probable that even

though the battery of a building with surplus is full, other buildings of the district might be able to charge their batteries with the available electricity.

#### 6.4.1.4. Self-consumption and self-sufficiency ratios

Apart from achieving cost reductions, the ESC proposal would allow to increase the self-consumption ratio from 31 % to 42 %, and the self-sufficiency ratio from 47 % to 64 %. This entails many benefits both for the district and the power grid, such as mitigating grid balancing and ramping issues as discussed in many studies. Although the degree of self-sufficiency is greatly affected by the battery capacities, the proposed framework allows the district to be more self-sufficient without investing in additional electrical storage.

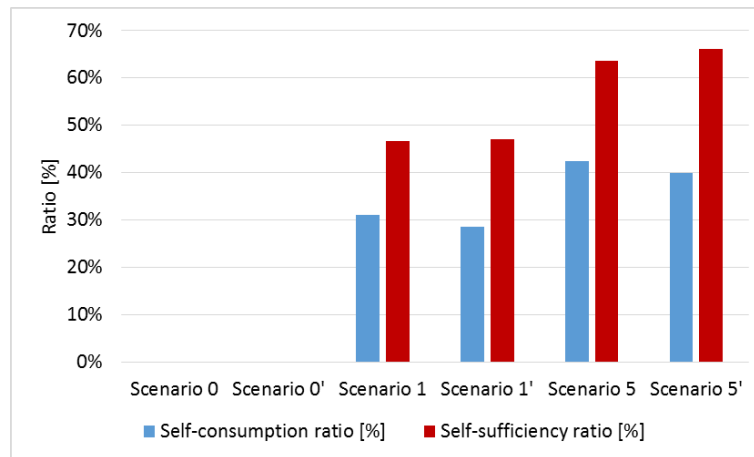


Figure 110: Comparison of the self-consumption and self-sufficiency ratios in different management alternatives.

#### 6.4.2. Comparison of precooling strategies

Once we have looked into the benefits that can be obtained from the introduced ESC concept at district level, we will now focus on the influence of implementing precooling strategies. As stated in previous sections, scenarios 2, 3 and 4 (self-consumption) and 6, 7 and 8 (ESC concept) will choose for each time horizon the most profitable precooling strategy among the 10 alternatives that were proposed. An example of this procedure is shown in Figure 111 for a case of a 1 day time horizon. As is apparent, every precooling strategy is evaluated each day, and the strategy with the lowest cost (or highest benefit) is chosen.

Day	Cost_ST1	Cost_ST2	Cost_ST3	Cost_ST4	Cost_ST5	Cost_ST6	Cost_ST7	Cost_ST8	Cost_ST9	Cost_ST10	Strategy chosen
166	-7.559	-7.428	-7.427	-6.932	-7.227	-7.256	-6.167	-7.042	-7.061	-5.463	1
167	7.699	7.974	8.031	9.195	8.036	8.304	10.093	7.930	8.531	10.542	1
168	2.485	3.041	2.755	3.714	3.084	3.027	4.553	2.948	3.248	5.046	1
169	-4.782	-4.804	-4.835	-4.784	-4.796	-4.800	-4.384	-4.624	-4.759	-3.798	3
170	-2.695	-2.821	-2.846	-2.902	-2.899	-2.943	-2.864	-2.880	-2.883	-2.884	6
171	10.815	10.704	10.511	10.500	10.551	10.445	10.455	10.521	10.470	10.653	6
172	-1.343	-1.357	-1.326	-1.327	-1.325	-1.362	-1.355	-1.289	-1.361	-1.311	6
173	7.485	7.427	7.429	7.454	7.475	7.270	7.602	7.562	7.274	8.020	6
174	7.389	7.527	7.757	8.464	7.494	7.942	9.453	7.366	8.318	10.698	8
175	37.829	37.836	38.455	41.780	36.805	40.677	43.441	37.466	41.299	44.578	5
176	5.306	5.950	5.585	6.721	6.543	5.869	7.694	7.221	6.117	8.158	1
177	-1.406	-1.620	-1.632	-1.416	-1.487	-1.584	-0.692	-1.042	-1.470	0.211	3

Figure 111: Example of selection of the best strategy that minimizes daily costs (positive values) or maximizes the benefits (negative values).

The results that were obtained for the whole year can be seen in Table 19. If we focus only on the ESC scenarios (5, 6, 7 and 8), we can establish that the differences are not very pronounced. As expected, the air-conditioning consumption increases after implementing precooling strategies, due to the increase of energy losses in the buildings. However, since the precooling strategies are performed during times of low electricity

prices, they are able to produce economic savings (although quite small in this particular case), achieve greater self-consumption and self-sufficiency ratios and diminish the energy lost in the batteries since they are less frequently used.

SCENARIO	ELECTRICITY IMPORTS [kWh]	ELECTRICITY EXPORTS [kWh]	ANNUAL COSTS [€]	AIR-CONDITIONING CONSUMPTION [kWh]	INCREASE AIR-CONDITIONING CONSUMPTION [%]	ENERGY LOST IN BATTERIES [kWh]	REDUCTION COSTS [%]	SELF-CONSUMPTION [%]	SELF-SUFFICIENCY [%]
Scenario 1 (base case)	48471	88721	3462	7716	0.0 %	2813	0.0%	31.04%	46.65%
Scenario 2	48114	87735	3437	8349	8.21%	2808	0.7%	31.80%	47.45%
Scenario 3	48150	87766	3443	8351	8.24%	2810	0.5%	31.78%	47.42%
Scenario 4	48182	87821	3447	8329	7.95%	2810	0.4%	31.74%	47.36%
Scenario 5	34050	74152	1919	7716	0.00%	2960	44.6%	42.36%	63.68%
Scenario 6	33547	72885	1881	8547	10.77%	2893	45.7%	43.35%	64.53%
Scenario 7	33605	72968	1888	8503	10.20%	2912	45.5%	43.28%	64.47%
Scenario 8	33680	73110	1896	8432	9.29%	2916	45.2%	43.17%	64.35%

Table 19: Results of the considered precooling scenarios.

#### 6.4.2.1. Optimal precooling strategies

Let us analyze which precooling strategies were chosen in each scenario (see Figure 112). Obviously, scenario 5 (which does not consider the selection of the optimal precooling strategies) always chose no precooling. On the other hand, the rest of scenarios chose to carry out precooling strategies in around 66 % of the summer days. Among the different options, PR\_ST9 (3 hours precooling at 24 °C) was the preferred alternative, followed by PR\_ST8, PR\_ST6, PR\_ST5 AND PR\_ST2. The differences between different time horizons are small, although in general it can be said that longer time horizons use more often the precooling strategies and prefer shorter precooling times.

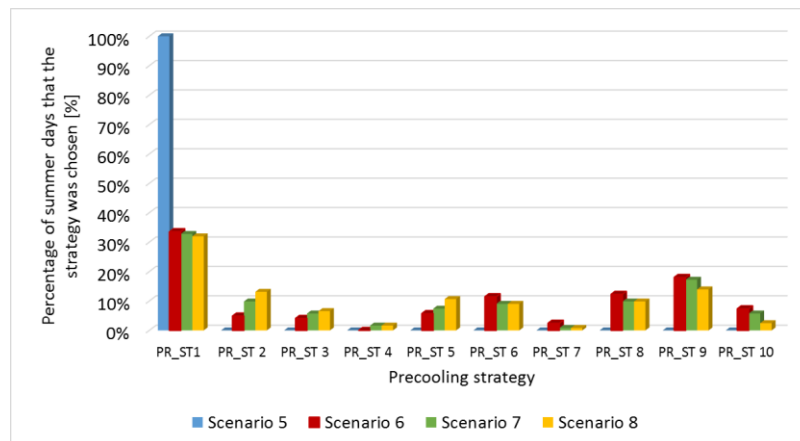


Figure 112: Percentage of days during summer that each precooling strategy considered was chosen for different scenarios.

#### 6.4.2.2. Cost-savings achieved by the precooling strategies

The results in Table 19 showed that only an additional 1.1 % cost savings could be achieved by implementing precooling strategies when considering the ESC concept, involving an increase on the air-conditioning consumption of 10.8%. If we only considered the air-conditioning costs, scenario 6 would achieve 3.7 % cost

savings compared to the air-conditioning costs of scenarios 1 or 5. Although it is true that the obtained benefits could seem relatively low, two issues should be taken into account. Firstly, that the characteristics of the considered climate are very particular, and the heating and cooling demands are rather low. And secondly, that the proposed precooling strategies can be implemented at no cost.

### 6.4.2.3. Reduction of cooling consumption during peak periods

Another benefit that can be obtained from the proposed preconditioning alternatives is that the peaks of cooling consumption are always produced during times of low electricity prices whenever a precooling strategy is chosen, as could be observed in the example given in Figure 105. In our case, since precooling strategies were selected in two thirds of the summer days in the new proposed scenarios, approximately 66 % of the days would avoid peak cooling consumptions during times of high electricity prices. This entails benefits for the grid if electricity needs to be imported, owing to the fact that these peaks should be avoided as much as possible due to the constraints in the power grids. Although the total energy consumption is increased around 10% due to the increased energy losses of the buildings, the environmental impact will remain similar due to the operation of the heat pumps at times with lower electricity prices where CO<sub>2</sub> emission rates are lower.

### 6.4.3. Sensitivity analysis: feed-in tariff

The proposal of an ESC made in this work allowed to prioritize sharing surplus electricity within the district, achieving less interactions with the power grid either to import or export electricity. However, the feed-in tariff plays an important role. A fixed price of 0.05 €/kWh for the feed-in tariff was considered in the previous simulations, but now we are going to look into its influence on the cost savings achieved in the district. Since this selling price would affect the selection of the optimal precooling strategies in several of the previous scenarios, we will focus only on scenarios 1 and 5 in this section, comparing the current real case with the ESC concept that implements no precooling strategies. This is possible due to the fact that in this case the electricity imports and exports would remain the same, regardless of the feed-in tariff. The comparison is shown in Figure 113 for different feed-in tariffs.

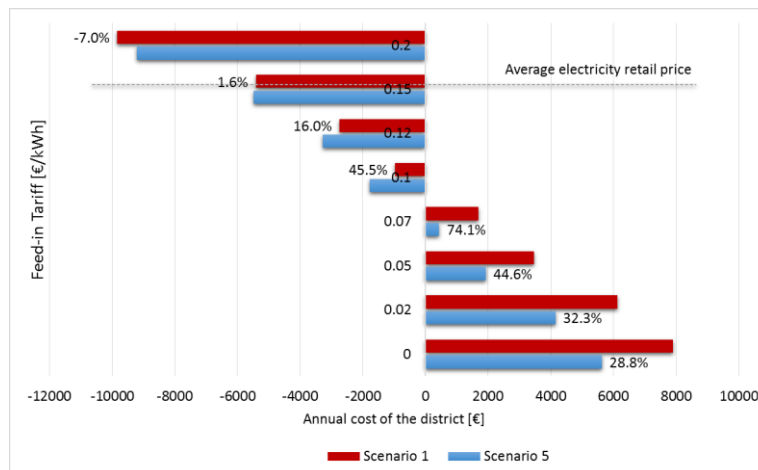


Figure 113: Sensitivity analysis of feed-in tariff rates for scenarios 1 and 5.

Hypothetically, if the exported electricity could not be sold to the grid (which might happen in some countries), the annual costs of the ESC scenario would be 28.8% less than those of the current self-consumption scenario (although in the reality, it must be said that if electricity could not be sold the PV systems would not be oversized or the electrical storage would be larger). If the feed-in tariff was increased up to 0.1 €/kWh, the district would be able to achieve annual economic profits, and the profits for the self-consumption scenario would still be 45.5% lower than those of the ESC concept. However, if the feed-in tariff kept increasing up to prices around 0.2 €/kWh, then the self-consumption scenario would be more profitable.

The reason for this is that the self-consumption scenario exports more electricity to the grid. Therefore, the higher the feed-in tariff, the lower the difference between scenarios 1 and 5.

The main conclusion of these observations is that the lower the feed-in tariff, the more profitable the proposed ESC concept is, since it encourages the use of electricity surplus within the district. In parallel, if the feed-in tariffs were very high (higher than the purchase price), the traditional self-consumption scenario could be more profitable, due to higher electricity exports.

## 6.5. Conclusions and future work

This study has considered the microgrid of a district in La Graciosa Island (Spain), evaluating different energy sharing scenarios that included PV generation, electrical storage through batteries, preconditioning strategies by using the structural thermal energy storage capacity of the buildings and a prosumer-to-prosumer concept in which electricity can be shared among prosumers through an energy sharing coordinator. In this way, the proposed strategies ensured the exploitation of the synergies between the buildings of the district, prioritizing the sharing of electricity and highlighting their benefits in comparison to traditional self-consumption approaches that are usually implemented in the built environment together with renewable generation. The proposed novel ESC concept has demonstrated that it is possible to raise the cost savings, self-consumption and self-sufficiency ratios of a district in a similar way as batteries, but at less capital costs.

Several scenarios have shown that by promoting energy trading in districts it is possible to achieve significant economic savings (around 45 %), although the results are very dependent on the considered feed-in tariff. In general, it can be said that the lower the feed-in tariff, the more profitable it is to promote energy trading, since more locally produced electricity is retained within the district. Apart from the economic savings, in the ESC concept the electricity exchanges with the grid are diminished compared to the traditional self-consumption scenario, the self-consumption ratio can be increased up to 42 % and the self-sufficiency ratio may reach 64 %. Last of all, several precooling strategies were also implemented within the simulation framework to detect the most optimal ones during each time horizon. The results showed that precooling strategies were chosen instead of the normal schedule on around 66 % of the summer days for all the considered time horizons, although the benign climatic conditions of the island where the district is located only allowed to obtain a 3.7 % reduction of the air-conditioning costs. However, this benefit is available at no additional capital costs, making the proposed strategies very attractive.

This work has demonstrated the possibilities offered by trading energy in districts through an ESC, but further improvements could still be made in the future. First, it would be essential to replicate this study considering different climates, due to the minor impact of air-conditioning in the case study presented in this work. More severe climates might produce more attractive results regarding the preconditioning strategies, including also preheating. Also, it would be very interesting to evaluate the influence of the construction characteristics of the buildings regarding the benefits obtained by the preconditioning strategies, since in this case only the real characteristics of the buildings of the district were considered. Another possibility would be to investigate the influence of the size of the district, since one might expect that the inclusion of more buildings could improve the flexibility of the system and increase the economic savings at district level. The influence of the sizes of the electric batteries is worth investigating too, due to their high impact on the self-consumption and self-sufficiency ratios.

Finally, it should be mentioned that some reforms are necessary on current energy systems and policies before promising approaches such as the ones proposed in this chapter can be more widely implemented. New mechanisms for small-scale energy trading are also needed. For instance, there is no regulation yet in Spain for demand response at a district level through aggregators. In some European countries such aggregators are entering the electricity markets, but there is a clear lack of regulatory frameworks. However, the outlook is more promising today, since new electricity market designs that will allow the emergence and widespread use of new energy models are being developed.

# 7. CONCLUSIONS AND FUTURE DEVELOPMENTS

---

## 7.1. Conclusions and summary of key findings

In view of the environmental sustainability issues that humanity is facing, mainly in cities, a thorough regeneration of the energy systems is required at all scales. The present Thesis aimed to justify the selection of the district scale as the optimal one to improve the energy performance of the built environment, increasing renewable energy integration and exploring new energy models such as demand side management on a district scale. The motivation was the fact that further research is necessary to understand the potential benefits of urban scale implementations, since most previous research has traditionally focused on individual buildings.

Supported by recently published studies, Chapter 1 of this Thesis established that the former approach, in which the Near Zero Energy concept mainly focused on the individual level performance, was not optimal. This was justified by the fact that looking beyond the individual level offers many advantages, such as the exploitation of the synergies between different buildings. In addition, most approaches on a large scale lack adequate representations of the buildings and make many simplifications in their calculations. Thus, further research was necessary to develop robust evidence on the behavior of innovative energy models at large scales.

### 7.1.1. Achieving accurate energy analyses on a district scale

In Chapter 2, the drawbacks of most current approaches for urban energy analyses (which make use of simplified methods) were highlighted. In addition, the chapter also made some progress to set up the means to achieve accurate evaluations of solar potentials, energy demands or demand side management opportunities on a district scale, which require dynamic interactions that are often disregarded in previous studies.

First, a study to determine what fraction of the electricity demand could be covered by using solar PV potentials at an urban and regional scale was presented. This was done by using CityGML 3D city models and real electricity consumption data of the municipalities involved. According to the results that were obtained, PV systems could generate 77% of the electricity consumption in the region by using all available roof space, or 56 % considering only roofs with a minimum surface area and insolation for an economically feasible PV installation. The main conclusion that was reached was that, when properly designed, PV systems could significantly decrease primary energy consumption and emissions at large scales, reaffirming their usefulness and their important role in future energy-efficient districts.

The next application that was included in Chapter 2 aimed to overcome the computational issues of evaluating mutual shading at urban level when using 3D models, since the number of surface interactions and radiation exchanges increase exponentially with the scale of a district. In addition, considering this matter is very important for any reliable energy analysis in an urban context. The previous approach on the evaluation of the PV potentials was very complete, but mutual shading was evaluated through reduction coefficients found in the literature due to the impossibility of evaluating all the interactions between such a huge amount of buildings. To overcome this issue, the new study introduced innovative tiling strategies that, when applied to 3D models, allowed to quantify the impacts of urban shading and multiple reflections

accurately. Two different case studies of different densities, Manhattan (New York) and Ludwigsburg (Germany) were chosen, quantifying the solar potentials, urban shading ratios and distinguishing between roofs and facades of different orientations. The results showed that for instance, high-density urban areas such as Manhattan might reduce their annual solar irradiance by up to 60% in facades and 25 % in roofs. In this case, using tiles of 500 meters and 200 meters overlap would be a minimum requirement to compute solar irradiance with an acceptable accuracy, whereas in medium density areas such as Ludwigsburg tiles of 300 meters width and 100 meters overlap would be sufficient.

Another of the possibilities offered by the use of 3D models is the evaluation of the thermal performance of all the buildings of a district or municipality, which is very important to improve energy efficiency at such scales. Urban 3D models enriched with semantic data on building's use, year of construction or thermal properties allow quantifying measures to improve energy efficiency or the integration of renewable energies, offering an excellent support for establishing climate protection concepts and policies on a municipal and regional level. Chapter 2 takes a step in this direction, including a study on urban energy demand evaluation through 3D city models. This study allowed us to conclude that, with reliable input data such as updated 3D models as well as buildings' construction and usage data, it is possible to quantify refurbishment scenarios or renewable integration for whole regions in an accurate way.

Even though tools such as SimStadt are able to calculate the energy demands of thousands of buildings in a region, as seen in the previous study, simplified calculations such as steady-state methods are frequently used. The interconnection between 3D models and tools that are able to assess the thermal performance of whole districts in an accurate and dynamic way is however necessary to assess time-dependent strategies such as demand side management on a large scale. To overcome these drawbacks of simplified energy performance simulations, a new open-source tool was developed in this Thesis, which allows performing dynamic simulations of whole districts in an accurate and user-friendly way. This was done by creating a plugin programmed in Python within the QGIS software, and an additional tool programmed in VBA that allows to simulate whole districts, considering any scenario that involves changing the characteristics of construction, ventilation or operating schedules. This tool is currently able to model any district of the world where open-source geometric data is available, but it could also be coupled with different 3D model formats, which would provide the necessary geometric information to be used as input for the HULC software.

As a last step, Chapter 2 mentioned clustering techniques which would allow to reduce the study domain and choose the representative (or archetype) buildings of a district. The reason for this is that dealing with models that contain even hundreds of buildings is quite complex if their thermal performance wants to be evaluated in a dynamic way. In addition, when a district needs to be characterized accurately, a monitoring campaign should be planned to evaluate their real performance and use. However, the budgetary and technical constraints might only allow to monitor a few buildings, which is why clustering techniques should be used beforehand. Once the sample of buildings is reduced, detailed monitoring and modeling of the buildings could be carried out.

### **7.1.2. Exploring demand side management opportunities**

Having already explored the advantages offered by urban scale analyses, the next issue addressed in this Thesis was the evaluation of the benefits that could be obtained from demand side management approaches, with an emphasis on the exploitation of the structural thermal energy storage capacity of buildings. To prove the benefits of DSM in buildings and districts, Chapter 3 presented two new applications.

The first application focused on the individual level performance of a dwelling located in a plus-energy district in Germany, evaluating the impacts of different dynamic pricing strategies by managing the activation of a heat pump in response to price changes. A validation of the model was carried out by using experimental data of the dwelling under study. In this study, evidence was obtained on the importance of choosing the correct price thresholds if dynamic pricing strategies are considered for DR purposes, concluding that dynamic thresholds that depend on the variations of electricity prices within the day are a



better alternative than fixed thresholds. Savings up to 25 % were achieved by using optimal strategies, also increasing the self-consumption ratio of the household and without sacrificing the thermal comfort of the occupants noticeably. In summary, the outcomes of the study showed the great benefits that can be derived from the use of heat pumps and the thermal energy storage capacity of buildings within a DR framework. However, the results also emphasized the importance of looking at all the implications of using a certain strategy, since the decisions to choose optimal strategies should not rely solely on one aspect such as cost savings.

As a follow up to the previous work, the second application increased the scale and evaluated the benefits of allowing direct control of the heat pumps in a district through a cluster manager, to provide flexibility and obtain benefits from the participation in secondary reserve markets. Again, this was done by taking advantage of the structural thermal energy storage capacity of the buildings of the district. By performing simulations with a time resolution of 30 minutes, the study concluded that the DR potential is significant, but for profits to be made some changes are necessary before these approaches can be put into practice, even if the prices paid for providing flexibility were higher. Particular attention should be given to the activation times, and most importantly their duration, due to the minimum running time of the heat pumps. Nevertheless, their benefits with regards to providing flexibility for reserve markets were demonstrated.

### **7.1.3. Development of energy baselines**

Once the benefits of widening the scale of energy analyses as well as the implementation of demand side management approaches were evidenced, Chapter 4 of this Thesis focused on defining a methodology for a proper characterization of districts through monitoring. From the point of view of the author, this is the best way in which a real district should be evaluated, reflecting the reality of the operation of the buildings with sufficient accuracy.

A novel proposal for obtaining energy baselines in residential buildings was developed and validated, both theoretically and experimentally. The proposed model, named QT, consists of a transfer function that is able to characterize any building based on measured data of its thermal performance. This model depends on the indoor air temperature, as a thermal response of the building, and the air-conditioning consumption, as response to the air-conditioning systems. Also, the model contemplates the dynamic effects due to the high thermal inertia of buildings, considering what is happening in the current time-step but also in the previous ones. The procedure is also sensitive to different operating conditions of the buildings, which may vary through time.

A dwelling monitored in a social housing district in southern Spain was used to validate the methodology, with very satisfactory results. Last of all, several possibilities for combining the QT model and DSM techniques were suggested for the application of the energy baselines.

### **7.1.4. Characterization of districts: application of the methodology**

The author of this Thesis believes that one of the most distinguished advantages provided by the application of the energy baselines presented in Chapter 4 is the characterization of districts. In Chapter 5, the methodology that was developed was first applied to characterize a district. In this case, temperature and total electricity consumption measurements were available through a monitoring campaign, but with no disaggregation of the air-conditioning consumptions. A methodology is presented for such cases, obtaining satisfactory results from the application of the baseline models.

Frequently, improving the thermal comfort of buildings involves the implementation of thermal mitigation strategies by retrofitting the building stock. By contrast, an innovative study was proposed in Chapter 5 of this Thesis, which introduced the possibility of using surplus electricity to power the heat pumps of a social housing district to improve the thermal comfort conditions of the occupants. In this way, the benefits of

exploiting the rooftop PV potential of the district was assessed to mitigate extreme high and low temperatures, reducing also the energy bills of the occupants. Once the optimal strategies from an electrical and economical point of view were selected, the surplus electricity was used to power the heat pumps of the 235 dwellings of the district, heating or cooling the dwellings depending on the season. The results showed that the thermal comfort could be improved in average by up to 11% in winter and 26% in summer, or 24% and 44% respectively if the electricity was not used also to reduce the energy bills. In all cases, the thermal comfort differences among the dwellings of the district, which presented large disparities in the initial situation, were significantly reduced.

### **7.1.5. Exploiting the synergies between buildings through DSM approaches**

Finally, Chapter 6 of the Thesis combined several of the elements, tools and strategies of the previous chapters. The purpose was to figure out whether further benefits could be obtained from the exploitation of the synergies between buildings, by implementing demand side management approaches on a district scale. Although in the literature it is frequent to find studies that focus on achieving cost savings by promoting energy sharing in districts, or others that use thermostatically controlled loads to perform demand side management at large scales, it is very unusual to find studies that combine both approaches, which motivated the study that was developed.

A case study was therefore proposed (a district in La Graciosa Island in Spain), in which a monitoring campaign allowed to know the real electricity consumptions of all the buildings in the district. The application included PV production, electrical storage, the use of the thermal energy storage capacity of the buildings as well as the possibility of sharing surplus electricity between different buildings. A novel rule-based algorithm, programmed in Fortran, was applied at 15 minutes intervals to encourage sharing surplus electricity between the prosumers of the district. The main purpose was to maximize the cost savings and the use of renewable energy. Different preconditioning strategies under 3 alternative time horizons were also evaluated.

Compared to the traditional situation in which each building self-manages its own importation and exportation of electricity, the proposed novel ESC concept demonstrated that it is possible to raise the cost savings, self-consumption and self-sufficiency ratios of a district in a similar way as batteries, but at less costs. Several scenarios showed that the new concept allowed to achieve significant savings, around 45%. However, a sensitivity analysis regarding the feed-in tariff showed that the results are very dependent on it. In general, the less the district is paid for selling the electricity, the more interesting it is to promote energy trading, since more locally produced electricity is retained within the district.

Apart from the economic benefits, the electricity exchanges with the power grid were also diminished, increasing the self-consumption ratio up to 42% and the self-sufficiency ratio up to 64%. Regarding the preconditioning strategies, the results showed that precooling was chosen instead of the normal schedule on around 66% of the summer days for all the considered time horizons, although the reductions of the air-conditioning costs were rather low. However, their use is justified by the fact that preconditioning measures are available at no additional costs.

## 7.2. A new methodology towards achieving comprehensive energy analyses at large scales

The present Thesis has justified the selection of the district scale as the optimal one to improve the energy performance of the built environment, increase renewable energy integration and carry out innovative approaches such as demand side management, which need to consider dynamic interactions. In addition, it also allowed to reach important conclusions with regards to solar potential estimations, accurate energy demand calculations and demand side management strategies. The drawbacks of most current approaches for urban analyses which make use of simplified methods were highlighted, and an alternative tool was developed to couple 3D models with detailed dynamic simulations of the thermal performance of buildings. Then, a methodology was proposed to develop energy baselines through monitoring, with which the real performance of districts can be characterized. Also, due to the complexity of dealing with models that may contain even hundreds of buildings, the importance of reducing the study domain was also brought forward, emphasizing the usefulness of clustering techniques for the purpose of choosing the most representative buildings of a district.

As a last contribution of this Thesis, this section aims to propose a new comprehensive methodology for the characterization of any existing district as well as mention the necessary tools and procedures so that traditional energy efficiency improvement strategies or demand side management approaches can be assessed precisely on a large scale. This would be done by creating 3D models that help in the process of choosing the representative buildings of a district, which should afterwards be monitored and modelled in detail for an accurate assessment.

### **First step: preliminary analysis of the district**

The first logical step when dealing with a district is to gather information about its location and all the resources at hand. The HULCGIS tool is capable of modelling any district in the world (as long as open-source geometric information is available), but other data such as the use of the buildings or the year of construction are also necessary. This information could be obtained from sources such as the cadaster of the municipality where the district is located.

### **Second step: creation of the 3D model of the district**

The geometry of the district needs to be generated so as to create the building representations. A 3D model of the whole area could be produced by using HULCGIS, including all the necessary information of each individual building. As mentioned in Chapter 2, this could be done by creating manually the polygons of each building of the district using open-source layers. Another possibility could be to use files that already include the geometry of all the buildings of the district, adapting their format through the QGIS platform. Eventually, even CityGML files could be used through data interoperability extensions.

### **Third step: characterization of the energy demands with a low LOD**

Once the 3D model of the district is available through HULCGIS, it can be coupled with the HULC simulation software. Iterating building by building and considering mutual shading, this software is able to perform an accurate dynamic simulation of every building of the district at hourly time-steps, considering standard uses and construction materials that depend on the year of construction. After every building has been simulated, the hourly heating and cooling demands are obtained.

### **Fourth step: application of clustering techniques**

Due to the large quantity of buildings that may be found in a district, clustering techniques are necessary. Once every building of a district has been simulated and their heating and cooling demands are known, it is possible to apply clustering techniques to choose the representative dwellings of the district through algorithms such as k-medoids. As an example, the methodology proposed in [184], which could be adapted to our purposes, is going to be shown. The mentioned study is based on clustering techniques to aggregate a large and diverse building stock of residential buildings to a smaller, representative ensemble of buildings.

Its main novelty is to apply an aggregation method called “Cluster-Centre Aggregation” to effectively characterize the electrical energy demand of air-conditioning systems in residential buildings under flexible operation. However, it could be applied for other purposes such as the ones proposed in this work.

The aim in that study is to reduce the overall building stock to a number of representative buildings so as to be able to assess, with sufficient accuracy, the total building electric energy demand dynamics to be used in integrated power system representations. The clustering algorithm is applied to electric power or air-conditioning data obtained by means of a simulation tool that reproduces in detail all the buildings contained in a considered building stock. The total electricity demand profile from the simulation tool is then compared with the prediction of the aggregated demand side model that scales up the electricity demand of the representative buildings.

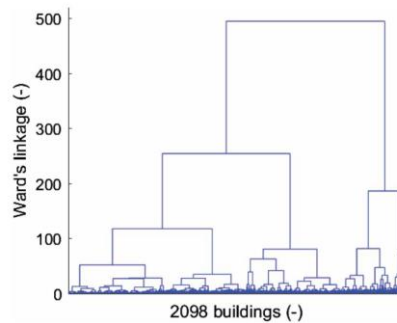


Figure 114: Example of dendrogram of hierarchical clustering on energy demand data as shown in [184].

The objective of this comparison is the determination of the proper number of representative buildings (i.e. number of clusters) in order to balance the opposing needs of reduced computational burden and loss of accuracy when assessing the demand flexibility of a building stock. Then, for every cluster, the building with the electric energy demand profile closest to the average electricity demand or air-conditioning modulation data profile of that cluster is selected as a representative building.

As mentioned before, this methodology could be applied after modeling and simulating a district by using HULCGIS, selecting the representative buildings of the district.

#### **Fifth step: detailed model and monitoring of building archetypes**

Having selected the representative buildings of the district, these should then be modeled in more detail. Although the building models obtained by HULCGIS are quite precise, a more detailed modelling of the archetypes allows for even more accurate simulations, considering for example the real position of the windows, shape of the roof, or real building schedules. These detailed multi-zone models should be developed in parallel to a building monitoring campaign of the archetype buildings of the district, which would allow model calibration and the development of the energy baselines introduced in Chapter 4.

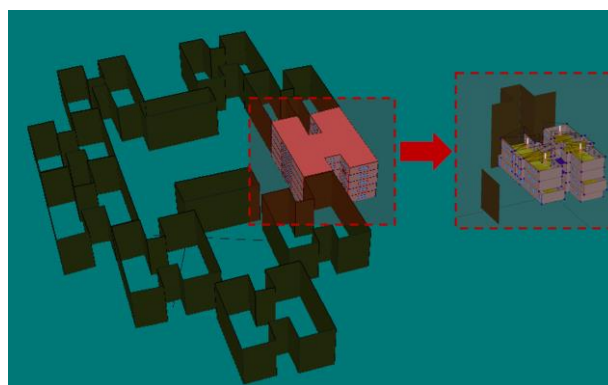


Figure 115: Depiction of the transition from the HULCGIS model of a representative building to a more detailed, multi-zone model.

### Final step: Identification of measures and optimization of the district's energy performance

Once all the previous steps have been fulfilled, the district's energy performance can be optimized, following for instance approaches related to demand side management like the ones proposed in Chapters 3, 5 or 6. As previously mentioned, the monitoring of the district together with a detailed model of each archetype building would allow to obtain energy baselines, in such a way that model calibration can be performed and the real performance and operation of the buildings of the district can be considered. Only in this way is it possible to guarantee a very realistic assessment of innovative approaches such as demand side management on a large-scale, since they require considering the dynamic interactions between the buildings of the district.

## 7.3. Future work

The research presented in this Thesis can be seen as a stepping-stone towards the achievement of energy-efficient districts, and has provided many interesting insights regarding demand side management approaches on a large-scale. However, the scope of the proposed measures is very wide, and there are several lines of research arising from this work that should be pursued in the future.

- An innovative tool for the dynamic simulation of whole districts was presented, and used to produce simplified models of whole districts for the application of demand side management approaches. However, the tool was not applied to analyze the thermal performance of a district under different retrofitting scenarios. Since a tool was also developed for that purpose, it would be very interesting to apply the methodology for implementing thermal mitigation strategies. These strategies could involve changing the characteristics of construction of the buildings of the district, internal gains, influence of shading devices, ventilation (both during the day or night ventilation in summer), or operating schedules of the air-conditioning systems. The energy demands under different scenarios could be compared, but it would also be possible to perform the assessment for districts with a null use of air-conditioning, comparing the comfort indices in that case. It would also be possible to change the climate zone where the district is located, as well use real weather files created by following the methodology proposed in Annex A.
- The synergies between the approaches shown in this Thesis and traditional approaches could be further analyzed. For instance, the combination of DSM and traditional energy efficiency strategies such as retrofitting has not been frequently evaluated in the literature, but the author of this Thesis believes that it would be very advantageous to consider their synergies. One of the reasons is that reducing the thermal losses of the buildings would allow to store the energy inside the buildings for longer periods when exploiting their structural thermal energy storage capacity.
- Regarding the strategies that promote energy sharing in districts, studying different climates and building types would be necessary to investigate the usefulness of preconditioning approaches depending on the location of the district.
- In Chapter 6 of this Thesis, a rule-based control algorithm was developed to prioritize sharing the electricity between the buildings of a district instead of interacting with the power grid. However, optimization through MPC strategies combined with the proposed baselines and preconditioning strategies could present many advantages to optimize the management of a district. Although MPC approaches are more complex to implement, they could analyze many different possibilities to minimize the costs of a district over a certain time horizon, instead of considering a fixed rule-based control. For instance, if there is an electricity surplus it could be used to charge the batteries, to share it with other households, or to export it to the grid, making a different decision in each time-step depending for example on the electricity prices, the SOC of the batteries, or the indoor temperatures.
- Alternatively, the influence of the size of the district should also be further investigated, since including more buildings in the assessment could improve flexibility, increase the economic savings and enhance the self-consumption and self-sufficiency of a district.



# ACKNOWLEDGMENTS OF FUNDING

---

I would like to take this opportunity to thank the University of Seville for its financial support through the US Research Plan V (VPPI-US), which funded my research during the past four years, including two research stays. Thank you for supporting young researchers on our first steps in scientific research. Special thanks to Esperanza Ramirez, who was my link with the university regarding administrative procedures and was always available to help with any issue that I encountered.

Also, I would like to thank:

- The Agency for Housing and Rehabilitation in Andalusia (AVRA) for our fruitful long-term cooperation in social housing districts.
- The Sim4Blocks project and the researchers from HFT Stuttgart, especially Ursula Eicker.
- The project G.R.A.C.I.O.S.A. for providing measurement data.
- The DACAR project “Zero-Energy Balance Districts Through Algorithms of Adaptive Comfort and Optimal Management of Energy Networks” funded by Ministry of Economy and Competitiveness (Government of Spain) for its partial support.





# ANNEX A. MATCHING CLIMATE

## A.1 Introduction

The energy performance of a building is highly influenced by the action of climate and solar radiation, which contribute to increasing or decreasing the energy demand of the building as well as its energy consumption and CO<sub>2</sub> emissions. When dealing with a detailed building analysis, for example through simulations, it is of paramount importance to have access to real climatic measurements with which more accurate results may be obtained. However, in most cases the availability of climatic data is limited, meaning that some variables such as the sky temperature or the decomposition of global radiation into its direct and diffuse components are not available. The present section describes a novel procedure to obtain a weather file at any location, modified through those real measurements that are typically obtained from weather stations and a model capable of estimating those which are not available.

## A.2 Reference weather file

The State Meteorology Agency in Spain (AEMET) provides typical hourly climatic values of every province in Spain. Among the available data, the values of direct and diffuse horizontal radiation are known, as well as the azimuth and solar height for every hour of the year determined as a function of the latitude and longitude of the location. Therefore, it is possible to know the solar position at any time.

MONTH	DAY	HOUR	T_OUT	T_SKY	DIRECT RAD	DIFFUSE RAD	ABS. HUM.	REL. HUM.	WIND VEL.	AZIMUTH	ZENITH
1	1	1	13.1	-2.04976	0	0	0.005936	63.505	3.28883	0	90
1	1	2	12.1	-3.00016	0	0	0.00593	67.7449	3.28912	0	90
1	1	3	11.5	-3.56065	0	0	0.005944	70.6483	3.28941	0	90
1	1	4	10.8	-4.20435	0	0	0.005979	74.4406	3.28971	0	90
1	1	5	10.5	-4.45849	0	0	0.006034	76.6359	3.29	0	90
1	1	6	10	-4.89386	0	0	0.006105	80.1648	3.29029	0	90
1	1	7	9.8	-5.03865	0	0	0.006189	82.354	3.29059	0	90
1	1	8	9.7	-5.08464	17	22	0.006282	84.142	3.29088	-57.3	86
1	1	9	10.8	-3.99182	57	89	0.006379	79.3702	3.29117	-48.4	77.4
1	1	10	12.1	-2.71077	256	78	0.006474	73.8955	3.29147	-36.8	69.3
1	1	11	13.7	-1.14904	354	85	0.006562	67.4409	3.29176	-23.2	63.2
1	1	12	15.5	1.8181	330	125	0.006638	60.725	3.29205	-8	60
1	1	13	17.2	2.23922	373	104	0.006699	54.9855	3.29235	8	60
1	1	14	17.9	4.15694	288	117	0.006742	52.9426	3.29264	23.2	63.2
1	1	15	17.8	5.48516	132	132	0.006765	53.457	3.29293	36.8	69.3
1	1	16	17.2	5.16712	63	87	0.006768	55.5458	3.29323	48.4	77.4
1	1	17	16.2	4.41568	17	22	0.006753	59.0607	3.29352	57.3	86
1	1	18	15.2	3.62758	0	0	0.006722	62.6813	3.29381	0	90
1	1	19	14.1	2.71721	0	0	0.006678	66.8603	3.29411	0	90
1	1	20	13.6	2.36638	0	0	0.006627	68.5466	3.2944	0	90
1	1	21	12.5	1.4285	0	0	0.006572	73.0545	3.29469	0	90
1	1	22	12.5	1.54467	0	0	0.00652	72.4825	3.29499	0	90
1	1	23	11.6	0.797359	0	0	0.006476	76.3989	3.29528	0	90
1	1	24	11.3	0.632851	0	0	0.006443	77.5392	3.29557	0	90
1	2	1	11.4	0.864161	0	0	0.006427	76.8376	3.29587	0	90
1	2	2	11.7	1.30115	0	0	0.006429	75.3502	3.29616	0	90

Table 20: Example of data in the reference weather files.

The availability of such climate data allows to have a reference of every Spanish province. The process which is going to be described below will be fed by the data of those standard files, so that the modified weather file will be done by comparing the real measurements with the data of the reference climate of the same province in which the building is located.

## A.3 Outdoor climatic conditions: real measurements

The parallel use of a building energy performance simulation tool and real measurements requires to have access to the data of the real weather conditions to which the building under study is subjected. Since it is not common to have an onsite weather station, it is necessary to make use of the data of weather stations that are close to the area in which the building is located.

The hourly data which are normally available in weather stations are:

- Outdoor temperature.
- Relative humidity.
- Wind velocity.
- Global horizontal radiation.

It should be mentioned that it would be interesting to take into account the measurements of wind velocity and direction, but these data are not very realistic since they depend on the urban pattern surrounding the building, which may significantly modify these values with respect to the ones registered in weather stations. For this reason, they have not been considered in this process.

Weather stations are capable of providing hourly values of the global horizontal radiation. However, it is necessary to determine the proportions of direct and diffuse radiation, which are very important due to their influence with respect to the solar gains of the buildings.

As an example of available climate data, the Ministry of Agriculture and Fisheries, Food and Environment has made available to the users all the information gathered through their weather stations network (SiAR). In the case of the province of Granada, the following weather stations are close to Almanjayar (which is an example of location where climate data are needed, shown with the orange mark): Loja (blue mark, 45 km away), Iznalloz (green mark, 30 km), IFAPA Centro Camino del Purchil (yellow mark, 5 km) and Padul (purple mark, 20 km).

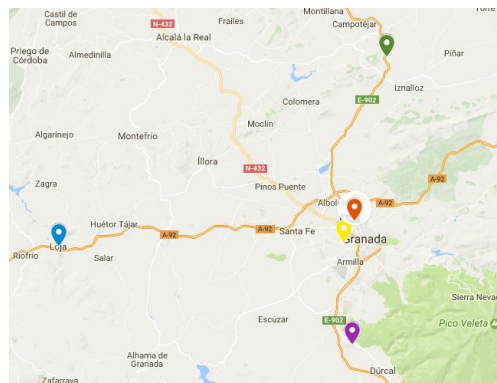


Figure 116: Location of the closest weather stations in the case of Almanjayar.

#### A.4 Procedure to obtain the matching climate

The procedure which is going to be explained in the following sections is summarized in the following figure.

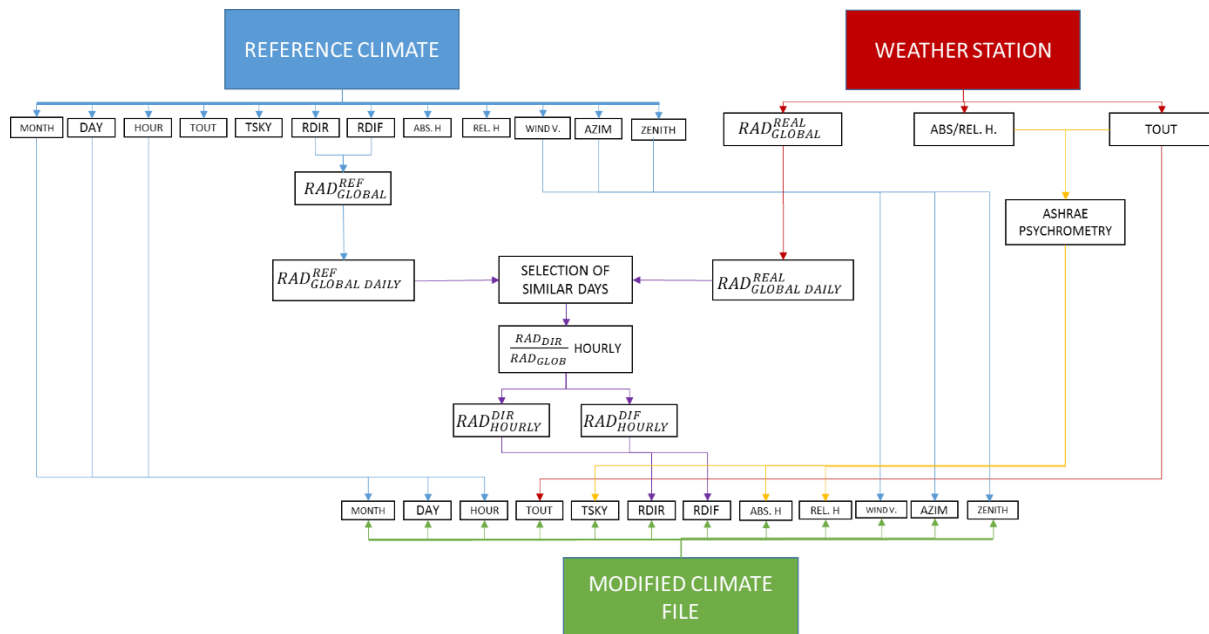


Figure 117: Procedure to obtain the modified weather file.

#### A.4.1. Outdoor temperature

In the case of the outdoor temperature, the modified weather file will directly include the measurements which are obtained from the weather station for every hour of the year.

#### A.4.2. Sky temperature

The calculation of the sky temperature depends on the measured outdoor temperature and humidity, so the values of the reference weather file should not be used. For this reason, a series of intermediate variables will be obtained with the purpose of estimating the sky temperature.

#### Saturation pressure

The calculation of the saturation pressure for liquid water has been obtained from the document "ASHRAE FUNDAMENTALS 2009". In the range from 0 to 200 °C the liquid water saturation pressure is calculated in the following way:

$$\ln p_{ws} = C_8/T + C_9 + C_{10}T + C_{11}T^2 + C_{12}T^3 + C_{13} \ln T$$

where

$$C_8 = -5.800\ 220\ 6\ E+03$$

$$C_9 = 1.391\ 499\ 3\ E+00$$

$$C_{10} = -4.864\ 023\ 9\ E-02$$

$$C_{11} = 4.176\ 476\ 8\ E-05$$

$$C_{12} = -1.445\ 209\ 3\ E-08$$

$$C_{13} = 6.545\ 967\ 3\ E+00$$

In both Equations (5) and (6),

$p_{ws}$  = saturation pressure, Pa

$T$  = absolute temperature, K = °C + 273.15

## Dew-point temperature

The dew-point temperature can be calculated directly by using the following equations, also included in the document "ASHRAE FUNDAMENTALS 2009":

Between dew points of 0 and 93°C,

$$t_d = C_{14} + C_{15}\alpha + C_{16}\alpha^2 + C_{17}\alpha^3 + C_{18}(p_w)^{0.1984}$$

Below 0°C,

$$t_d = 6.09 + 12.608\alpha + 0.4959\alpha^2$$

where

$t_d$  = dew-point temperature, °C

$\alpha$  =  $\ln p_w$

$p_w$  = water vapor partial pressure, kPa

$C_{14}$  = 6.54

$C_{15}$  = 14.526

$C_{16}$  = 0.7389

$C_{17}$  = 0.09486

$C_{18}$  = 0.4569

## Cloudiness

Identified as  $I_N$ . In summer it will have a value of 3. In winter the value will be 5.

### Cloudiness factor

$$F_{\text{CLOUDINESS}} = 1 + 0.024 \cdot I_N - 0.0035 \cdot (I_N^2) + 0.00028 \cdot (I_N^3)$$

### Sky emissivity

$$\varepsilon = F_{\text{CLOUDINESS}} \cdot (0.787 + 0.764 \cdot \ln [(T_{\text{DEW}} + 273.15) / 273.15])$$

$T_{\text{DEW}}$  is the dew-point temperature in °C.

### Sky temperature

Finally, the sky temperature will be obtained from:

$$T_{\text{SKY}} = T_{\text{SKY-DOE}} = (\varepsilon^{0.25}) \cdot (T_{\text{OUT}} + 273.15) - 273.15$$

### A.4.3. Relative and absolute humidity

For the calculation of the absolute and relative humidity, the values of humidity given by the weather station will be used (usually relative humidity), as well as the dry bulb temperature, which is also available. Through both of them, a tool capable of obtaining the rest of psychrometric variables is used, resulting in data of:

- Outdoor temperature.
- Relative humidity.
- Absolute humidity.
- Wet bulb temperature.
- Enthalpy.

### A.4.4. Decomposition of global radiation into its direct and diffuse components

Solar radiation is the energy flow that we receive from the sun in the form of electromagnetic waves of different frequencies. The following types of solar radiation may be distinguished:

- Direct or beam radiation: solar radiation received without modifying its direction when crossing the atmosphere.
- Diffuse radiation: solar radiation received after modifying its direction when crossing the atmosphere as a consequence of the atmospheric dispersion. In the isotropic models it is considered to be uniformly distributed in every direction.

- Global radiation: it is the sum of the direct and diffuse radiation.

On a clear day, the direct radiation is preponderant over the diffuse radiation. In addition, this type of radiation is characterized by its way of casting a shadow defined by the opaque obstacles that intercept it. On the contrary, during a cloudy day there is no direct radiation and all the incident radiation is diffuse.

Although weather stations are capable of providing hourly values of the global radiation on a horizontal surface, the proportions of direct and diffuse radiation, which are extremely important due to their influence regarding the solar gains of buildings, are unknown. Their values will be estimated in the following way.

First of all, a reference weather file with all the necessary hourly data is used, located in the same province as the building under study: outdoor temperature, direct and diffuse radiation, azimuth, zenith and so on are known. By using this reference weather file which contains all the necessary variables, the daily global radiation is calculated for every day of the year. The same is done for the measured global radiation, which is available from the weather station.

Then, a comparison is made between the measured daily global radiation with respect to the daily global radiation of the previous and the following 15 days of the reference weather file. Having a sample of 30 days, the two most similar days of the reference weather file are chosen. Then, the proportion of direct/global radiation of the two days is calculated for every hour. Finally, in the modified weather file the decomposition of direct and diffuse radiation is made by considering the average proportions of direct/diffuse radiations of those two days for every hour.

In short, the direct and diffuse hourly radiation of the modified weather file will be calculated by keeping the direct/global and diffuse/global average proportions of the two most similar days of the reference weather file, for every hour independently. Below, an example of this procedure on the 15<sup>th</sup> of March is shown.

DAY OF THE YEAR	DATE	REFERENCE GLOBAL RADIATION	MEASURED GLOBAL RADIATION		DAY	MONTH	MOST SIMILAR DAY	SECOND MOST SIMILAR DAY
60	1/3	3878.00	4853.74		1	3	65	58
61	2/3	3935.00	4818.02		2	3	76	65
62	3/3	1516.00	4695.77		3	3	76	65
63	4/3	2795.00	4055.23		4	3	69	61
64	5/3	4520.00	2953.34		5	3	50	71
65	6/3	4531.00	4260.08		6	3	69	64
66	7/3	3403.00	3316.50		7	3	72	66
67	8/3	2633.00	5012.63		8	3	75	77
68	9/3	1530.00	2376.37		9	3	81	73
69	10/3	4156.00	4698.57		10	3	76	65
70	11/3	1205.00	5401.77		11	3	80	77
71	12/3	3044.00	5357.48		12	3	77	80
72	13/3	3351.00	5497.54		13	3	87	80
73	14/3	2533.00	5453.96		14	3	87	80
74	15/3	3591.00	4750.36		15	3	76	88
75	16/3	5111.00	5481.51		16	3	87	80
76	17/3	4883.00	5043.47		17	3	75	77
77	18/3	5213.00	4007.47		18	3	85	82
78	19/3	5782.00	3253.37		19	3	72	66
79	20/3	5625.00	3185.43		20	3	71	72
80	21/3	5570.00	3490.64		21	3	66	74
81	22/3	2450.00	4085.61		22	3	89	69
82	23/3	3887.00	5832.88		23	3	92	91
83	24/3	2085.00	6045.01		24	3	84	92
84	25/3	5960.00	3311.60		25	3	72	98
85	26/3	2700.00	5265.15		26	3	77	97
86	27/3	3645.00	6183.76		27	3	96	84
87	28/3	5448.00	2611.23		28	3	73	85
88	29/3	4604.00	4844.37		29	3	76	101
89	30/3	4052.00	6026.00		30	3	84	92
90	31/3	3657.00	4547.67		31	3	88	76

Table 21: Example of the selection of the two most similar days. 15<sup>th</sup> of March.

## A.5 Solar radiation on inclined surfaces

We should take into account that the solar radiation received by a surface depends on its plane, since the direction of the direct solar radiation depends on the relative position between the sun and the receiving surface. The procedure which has been developed will allow the definition of a surface through its azimuth and tilt angle, after which the necessary geometrical conversions will be carried out so as to know the direct radiation that reaches the defined surface in every hour, since its position as well as that of the sun is known at any time by using the reference weather file.

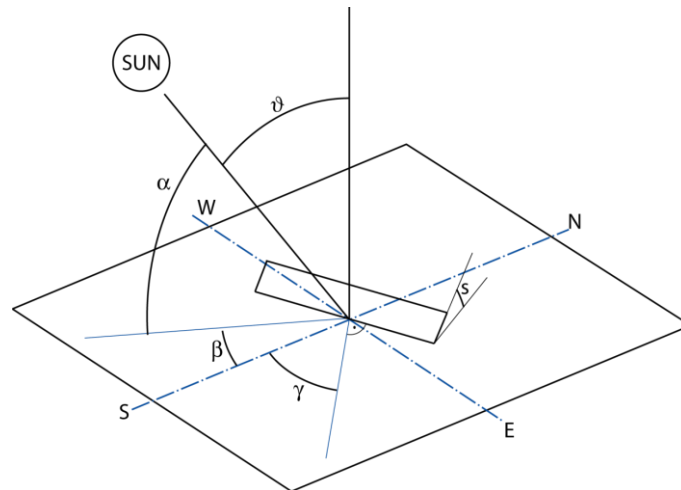


Figure 118: Direct solar radiation: angles between the sun and the receiving surface.

The solar radiation data of the reference weather file are referred to a horizontal surface, so the conversion of that radiation into that of the inclined surface is necessary. The direct radiation depends on the one hand on the azimuth and tilt angle of the receiving surface, and on the other hand on the position of the sun in that instant.

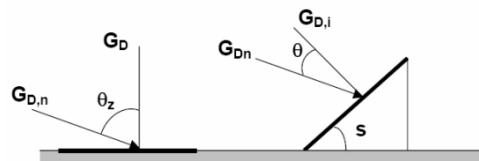


Figure 119: Direct radiation on a horizontal and inclined surface.

### Solar angles

- $\alpha$ : Solar height.
- $\vartheta Z$ : Zenith angle of the sun.
- $\beta$ : Solar azimuth.
- $s$ : Surface tilt angle.
- $\gamma$ : Surface azimuthal angle.

### Direction cosines of the sun ray

They are west, south and zenith respectively. We will name them  $W, S$  y  $Z$ .

The direction cosines of the sun ray obtained from the solar height and azimuth are:

$$\cos(Zs) = \text{sen}(\text{height}) \cdot \cos(Ws) = \text{sen}(\text{height}) \cdot \cos(\text{height})$$

$$\cos(Ss) = \sqrt{1 - (\cos(Zs))^2 + \cos(Ws)^2}$$

### Direction cosines of the defined surface

Direction cosines of the defined surface obtained from its azimuth and inclination:

$$\cos(Zp) = \cos(\text{inclination}) \cdot \cos(Wp) = \text{sen}(\text{azimuth}) \cdot \text{sen}(\text{inclination})$$

$$\cos(Sp) = \sqrt{1 - (\cos(Zp))^2 + \cos(Wp)^2}$$

### Direct normal irradiance

$$DNI = \frac{DHI}{\cos(Z_s)}$$

Incidence angle between the sun ray and the defined surface (inner product):

$$\cos(\vartheta) = \cos(Z_s) \cdot \cos(Z_p) + \cos(W_s) \cdot \cos(W_p) + \cos(S_s) \cdot \cos(S_p)$$

### Direct radiation on the inclined plane

Once the process has been done, the value of the  $\vartheta$  angle in the previous figure (between the direct radiation and the normal to the surface) is obtained for every hour of the year, as well as the results of the direct, diffuse and global radiation for the inclined surface.

$$DPI = DNI \cdot \cos(\vartheta)$$

#### A.5.1. Monthly solar radiation for different orientations

Another interesting result which may be obtained through the transformation of the solar horizontal radiation into that of an inclined surface are the monthly values of the solar radiation for different orientations. In particular, the radiation in the south orientation will be of great importance, since it plays a major role in the methods of Equivalent South Solar Area calculation in buildings. An example is shown in the following figure.

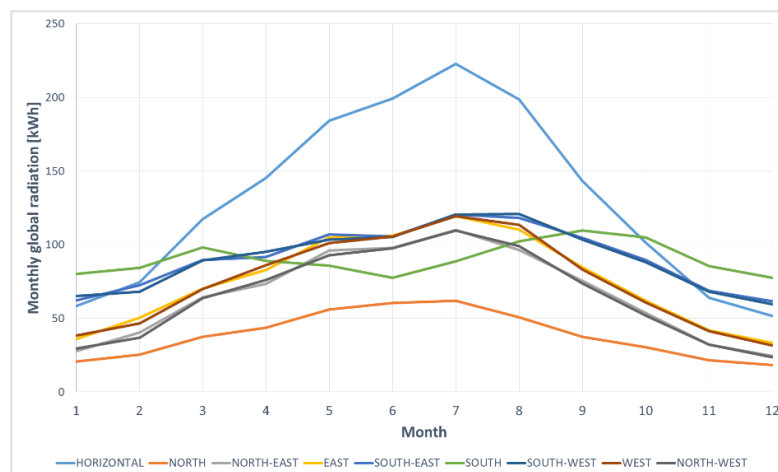


Figure 120: Monthly radiation for different orientations in a specific location.

#### A.5.2. Equivalent South Solar Area calculation

When dealing with the assessment of the energy behaviour of a building, solar gains are very important. Their influence may be observed in the following graph, which shows the average temperatures of a building in freefloating under different conditions.

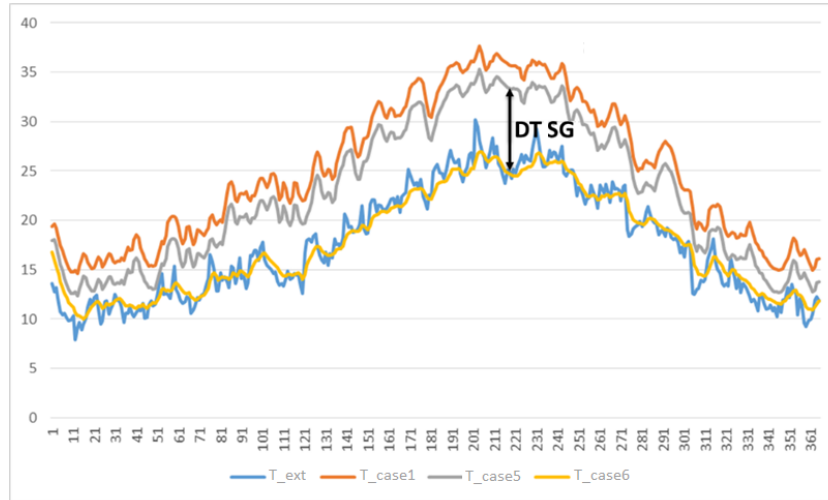


Figure 121: Influence of the solar and internal gains on the average daily temperature of a building.

It can be seen that the average daily temperatures of the building in the case 1 (free-floating with solar and internal gains) are slightly higher than those of case 5 (which has no internal gains). If the solar gains are also removed, the reached temperatures are those of case 6. Due to this, a temperature difference related to the solar gains is observed.

The quantification of the solar gains can be carried out through the calculation of the ESSA, which allows also the comparison of the obtained values with certain established ranges, determining if they are admissible or if an intervention is necessary so as to put them between the acceptable limits.

The establishment of the real solar gains of a building and the ESSA without using a robust simulation software would be very complex, since every hour of the year has different own and remote shadows and what is reflected out of the building is unknown. However, the simulation tools do take into account the solar gains which reached and stayed in the building, so they are an indispensable tool for their accounting.

In order to calculate the ESSA, we must first remember how the simplified calculation of the heating and cooling demand of a building is carried out. The following equations show the losses (up) and the net gains (down) in the case of heating.

$$Q = \left( \sum_{i=1}^n U_i \cdot A_i + \sum_{j=1}^m \phi_j \cdot I_j + \rho_a c_{pa} nV \right) GD \cdot 24$$

$$Q = \left( \sum_{i=1}^{no} I_i \sum_{j=1}^{ne_i} A_{s,j,i} + \bar{\phi}_a \cdot t \right) \cdot \eta$$

Also, in the cooling season, the following equations show the net losses (up) and the gains (down).

$$Q = (\rho_a c_{pa} n_{noche} V) GD_{noche} \cdot 24 \cdot \eta$$

$$Q = \left( \sum_{i=1}^{no} I_i \sum_{j=1}^{ne_i} A_{s,j,i} + \bar{\phi}_a \cdot t \right)$$

The building is then simulated under the following conditions:

- Indoor temperature=Outdoor temperature=Sky temperature = 0.
- Internal gains = 0.



Therefore:

$$\text{CoolingDemand} = \text{ESSA} \cdot I_{\text{south}}$$

Isolating for every month:

$$\text{ESSA} = \frac{\text{CoolingDemand}}{I_{\text{south}}}$$

Consequently, the ESSA of a building may be estimated through its simulation under the described conditions and the knowledge of the solar radiation in the south orientation, which was shown in the previous section. This may be carried out both at hourly or monthly levels. An example of the monthly ESSA calculation for a building located in Cordoba, Spain is shown.

	JAN	FEB	MAR	APR	MAY	JUN	JUL	AUG	SEPT	OCT	NOV	DEC
Solar gains	4263.88	4574.36	5565.40	5739.08	7037.81	7294.27	8018.05	7578.96	6445.17	5408.67	4624.26	3884.45
Isouth	111.38	103.86	104.66	86.95	86.96	77.91	86.25	103.87	112.70	113.42	117.58	104.05
ESSA	38.28	44.04	53.18	66.01	80.93	93.62	92.96	72.97	57.19	47.69	39.33	37.33

Table 22: Monthly values of the solar gains, radiation in the south orientation and obtained ESSA.

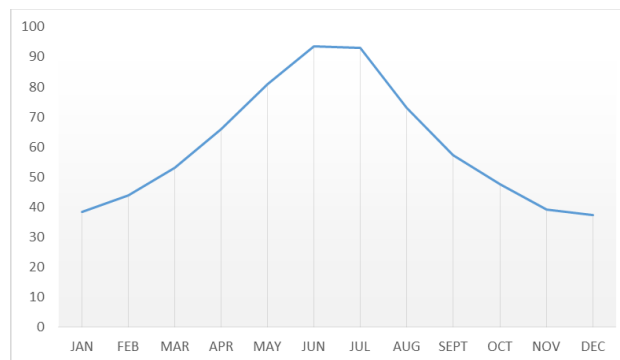


Figure 122: Evolution of the monthly ESSA.

The proportion of the solar gains at hourly, daily and monthly levels for the same building can be seen in the following graphs:

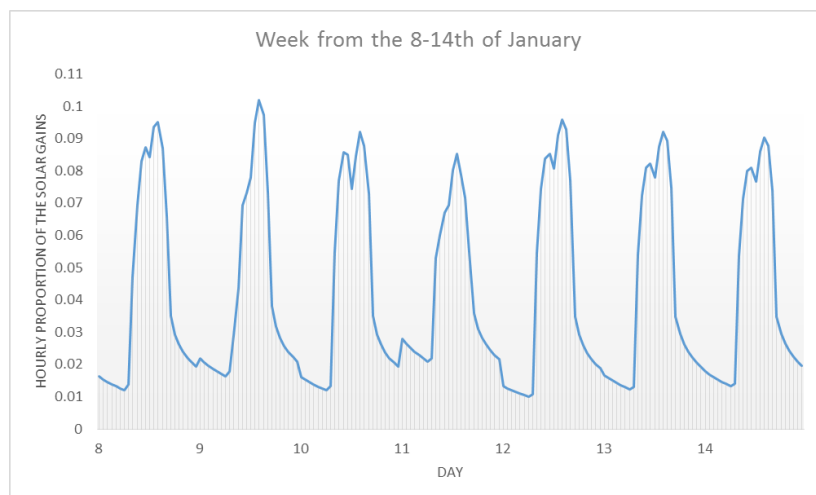


Figure 123: Hourly proportion of the solar gains during the second week of January.

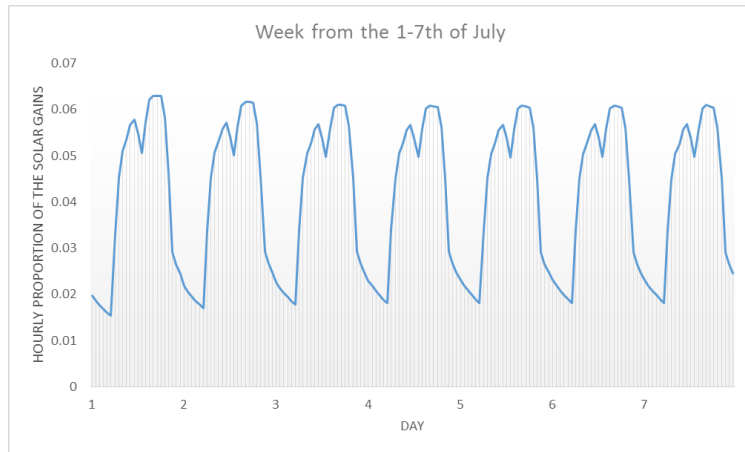


Figure 124: Hourly proportion of the solar gains during the first week of July.

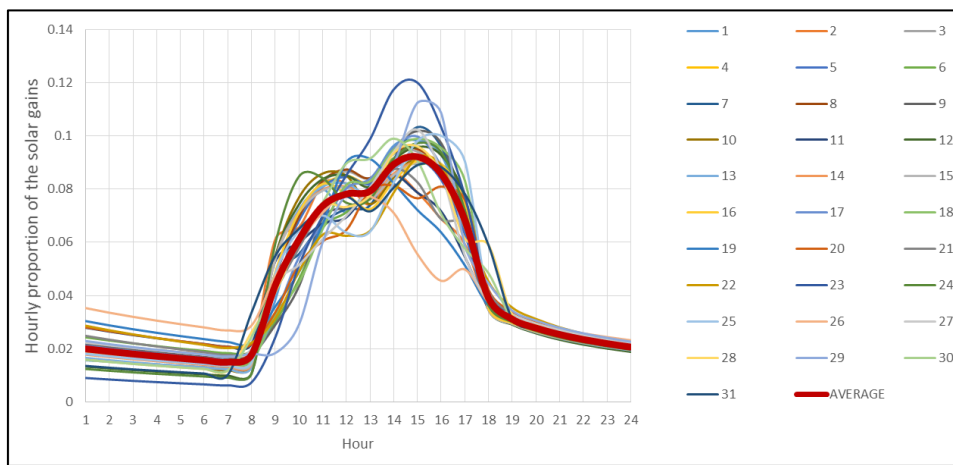


Figure 125: Comparison of hourly values of the solar gains for every day in January.

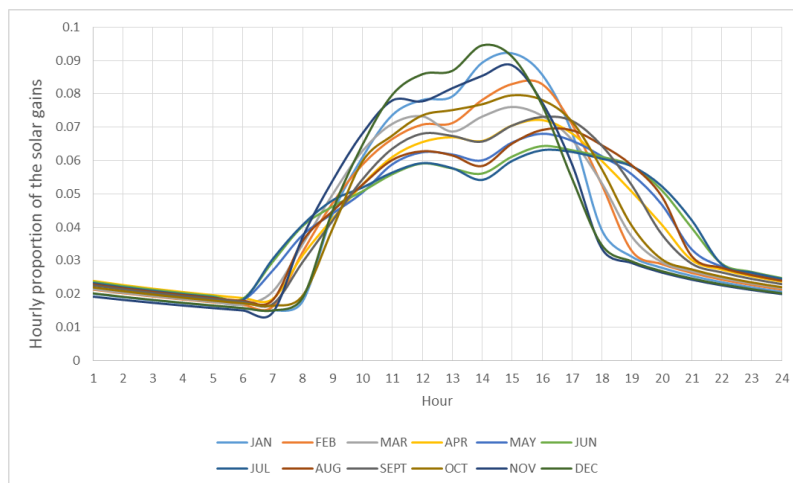


Figure 126: Monthly averages of the hourly solar gains.

### A.6 Modified weather file generation

The final result of the described procedure is a modified weather file with the “.met” extension, which contains the hourly real outdoor temperature, humidity and global radiation data measured by the weather station. In addition, the sky temperature is estimated through a psychrometry-based tool, and the

decomposition of the direct and diffuse radiation is done by comparing the measured global radiation with that of the reference weather file. The generated modified weather file has also the necessary format for its use in building energy performance simulation tools.

### A.7 Validation of the described procedure

Last of all, in order to check the accuracy of the described procedure, the results obtained of the direct and diffuse radiation decomposition have been validated. For that purpose, measured data from a weather station in Madrid have been used, which include measures of direct and diffuse horizontal radiation. Feeding the described procedure with just the measured hourly global radiation, the estimated direct and diffuse radiations have been compared to the reality. The following figure shows the result of that comparison for the direct radiation.

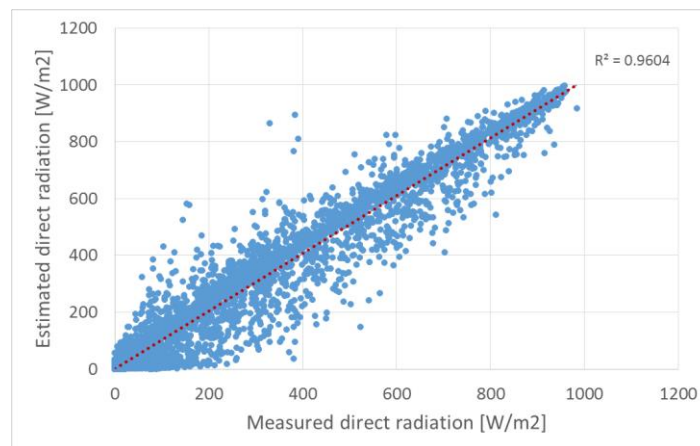


Figure 127: Validation of the hourly direct radiation.

As it can be observed, the adjustment for the direct radiation is fairly good, obtaining a coefficient  $R^2=0.96$ . The following figure shows the comparison of the hourly direct radiation for the months of January and June.

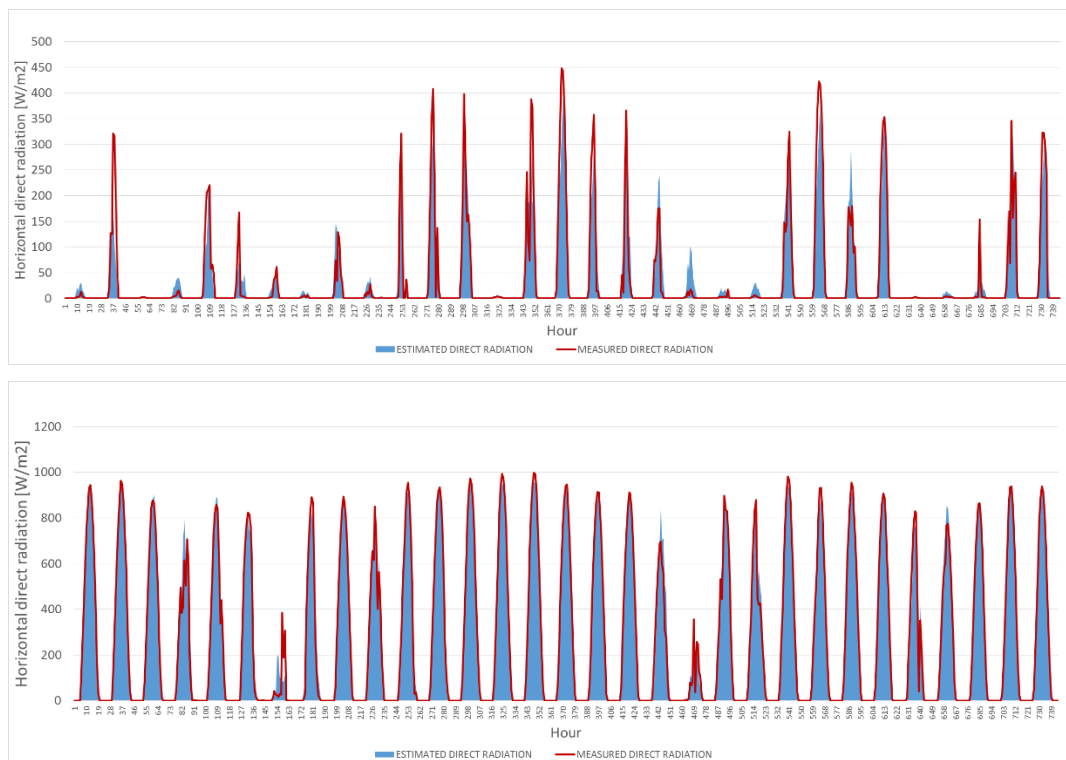


Figure 128: Comparison of the measured and estimated direct radiation. Months of January and July.

On the other hand, one of the restrictions imposed by the described procedure was to keep the value of the measured hourly global radiation. The figure below shows this fact in April.

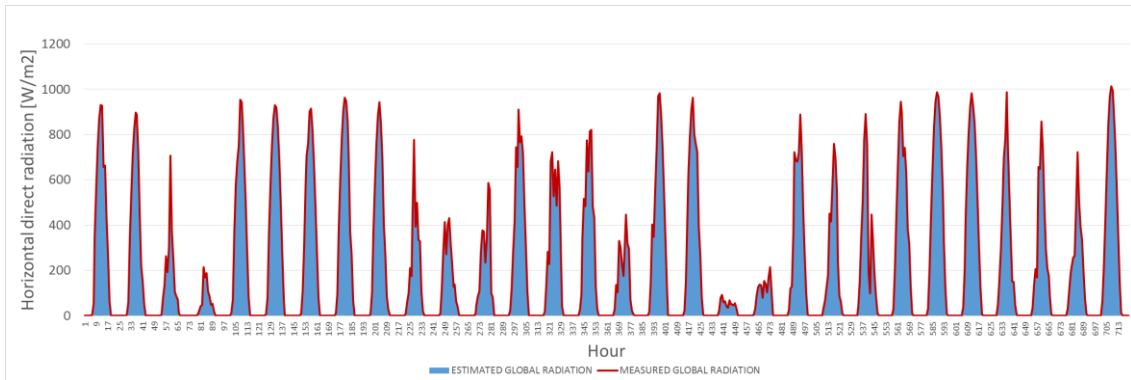


Figure 129: Comparison of the measured and estimated global radiation. Month of April.

Last of all, the comparison of the monthly values for direct, diffuse and global radiation is shown.

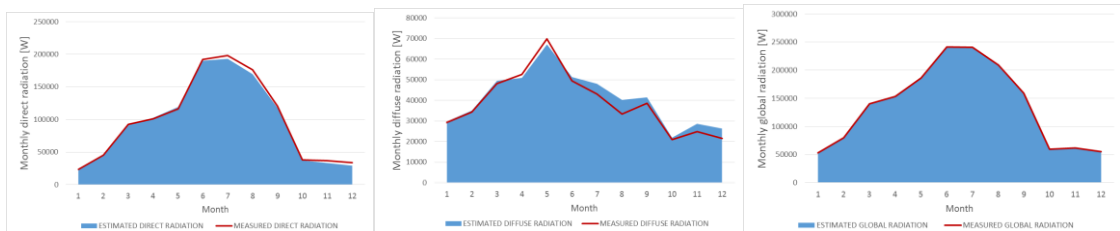


Figure 130: Monthly comparison between the estimated and measured direct, diffuse and global radiations.

# ANNEX B. PROCEDURE FOR THE DISAGGREGATION OF HOUSEHOLD ELECTRICITY CONSUMPTIONS

An accurate assessment of a district requires data of the electricity consumption of its buildings. In addition, being able to disaggregate the various consumptions is of vital importance when dealing with data of the total energy consumption of a specific dwelling. If this information were available, it would be possible to assess for example how much electricity is used for the appliances or the lighting inside the dwellings, separating them from the HVAC energy consumptions. However, estimating these electricity consumptions in residential buildings is an intricate task. The main reason is that the consumptions are very volatile, and dependent on the number of occupants, their behavior, income, size of the dwelling or climatic zone. The following sections propose several options to disaggregate the air-conditioning consumption from that of the rest of electricity uses in a household.

## B.1 Option 1: disaggregation through detailed monitoring

Ideally, if a district has to be evaluated in an accurate way, the real household electricity consumption profiles of its buildings should be obtained. This could be achieved by having access to the data of the hourly total electricity consumption of each dwelling, which is becoming easier in the past years due to the widespread implementation of smart meters. If smart meters are available, the utility companies usually provide hourly consumption data (see Figure 131). This allows to obtain typical consumption profiles for a household, and eventually for a district. Nevertheless, smart meter data do not show a disaggregation of the consumptions: they only show the total electricity consumption of a household during each hour.

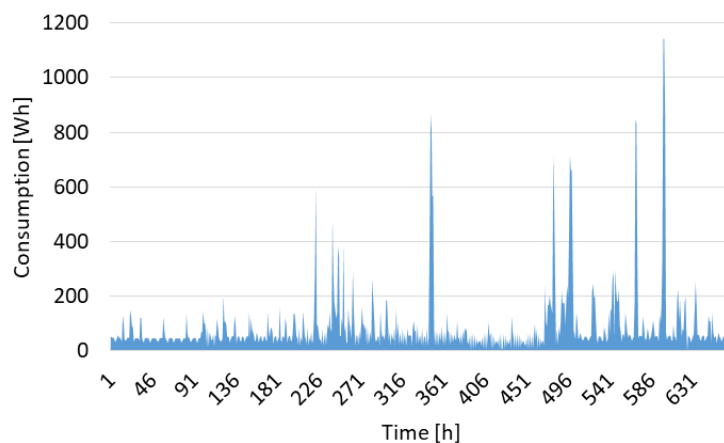


Figure 131: Example of data obtained from the Smart Meter of a dwelling in Seville, Spain.

In order to estimate the disaggregated consumptions, one option could be to monitor all the appliances of the dwellings. This would allow to obtain the consumption patterns of the different devices, and also their contribution to the total electricity consumption. A detailed monitoring campaign carried out in a dwelling in Seville, Spain allowed to visualize the consumption patterns of all of its appliances by using a Smart Plug (see Figure 132, Figure 133 and Figure 134 for some examples). As it can be seen, the consumption patterns of different elements are very different. When comparing old devices with new devices, significant differences can also be observed.

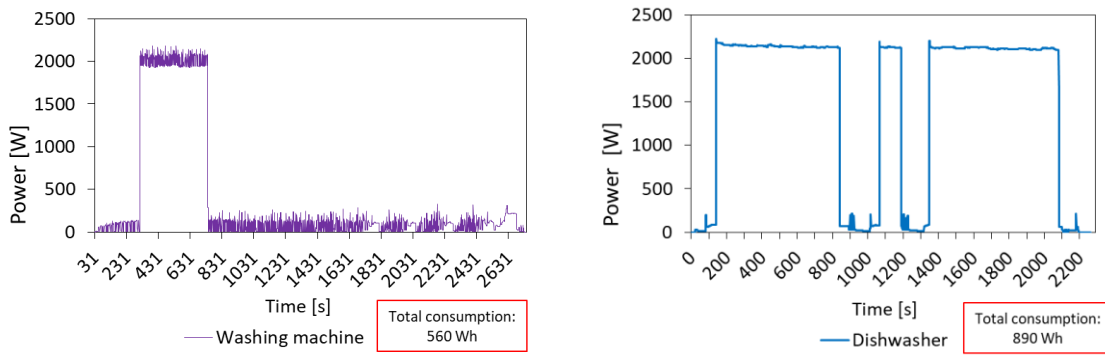


Figure 132: Consumption pattern of one use of a washing machine (left) and dishwasher (right).

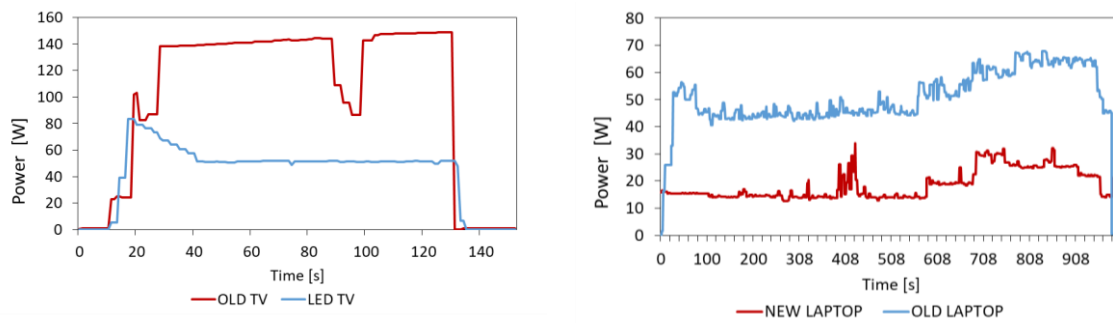


Figure 133: Consumption patterns of different TVs (left) and laptops (right).

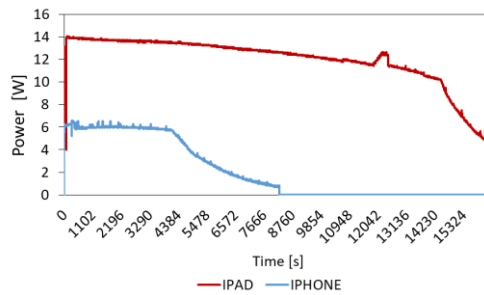


Figure 134: Consumption patterns of a Smartphone and a Tablet.

A detailed survey was then conducted on this dwelling, estimating the amount of time that each device was used during a whole month. This allowed obtaining an estimation of the contributions of the different elements of the household for a whole month (see Figure 135).

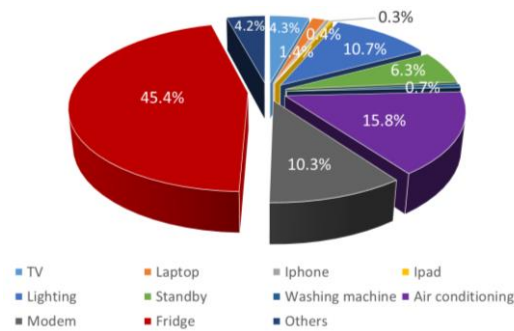


Figure 135: Disaggregated monthly energy consumption.

However, obtaining a disaggregation of the electricity consumption for each hour would require to use a smart plug or smart meter for each device of the dwelling simultaneously, which is unfeasible. Another option would be to consider the Non-Intrusive Load Monitoring (NILM) technique, which is a process for analyzing changes in the voltage and current of the total electricity consumption and deducing which appliances are used in the dwelling as well as their individual energy consumption. However, that is out of the scope of this work. Therefore, two proposals are going to be presented for cases where it is not possible to disaggregate the air-conditioning consumptions.

## B.2 Option 2: disaggregation through temperature and total consumption monitoring

The second option to discern air-conditioning consumption from that of the other devices in a dwelling is to observe the relationship between the indoor temperature and the total electricity consumption. In this way, deviations of indoor temperature from the full free-floating values may be identified. Days without these temperature deviations may be used to calculate the average household electricity consumptions, since when the indoor temperature is similar to the full free-floating temperature it means that there is no air-conditioning consumption.

The household electricity consumptions can be inferred by using graphs such as the one presented in Figure 136. In this case, the average daily electricity consumption in intermediate months without air-conditioning is around 4600 Wh. As may be observed, whenever the average daily temperature is below 20 °C, the total daily electricity consumption increases. In parallel, the same happens if the average indoor temperature goes above 25 °C during summer months. This can also be observed in Figure 137 for a dwelling in a different city during the heating season.

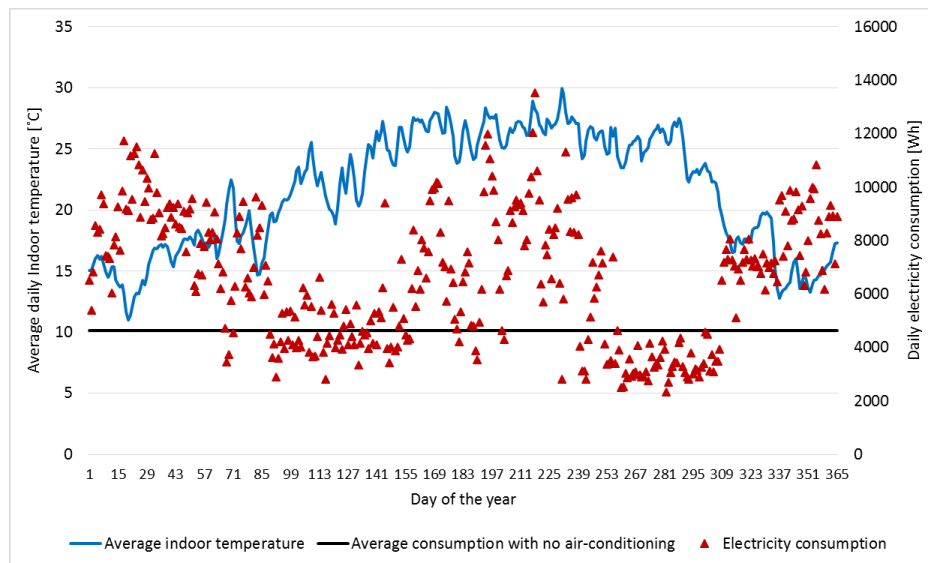


Figure 136: Example of average daily indoor temperature and total daily electricity consumption of a household in Seville, Spain.

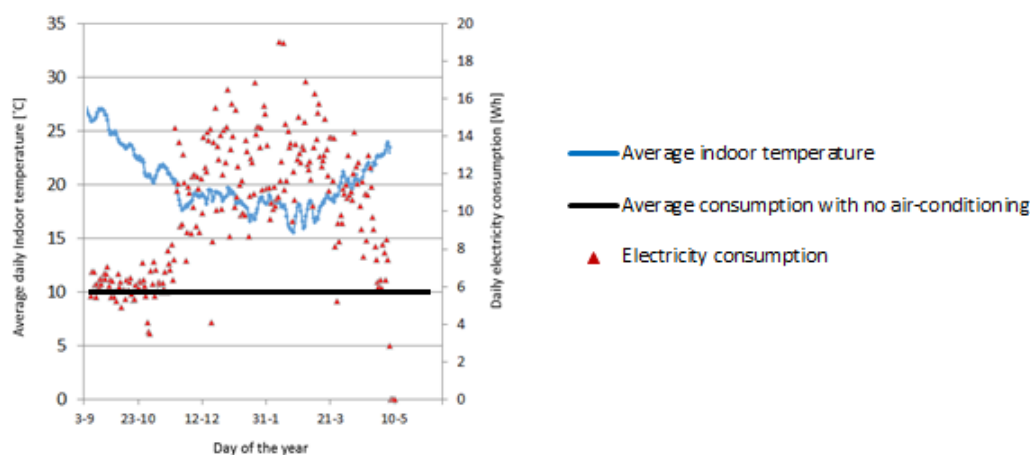


Figure 137: Example of average daily indoor temperature and total daily electricity consumption of a household in Granada, Spain.

### B.3 Option 3: estimated disaggregation through a tool for obtaining hourly profiles

In order to estimate the average hourly electricity consumption patterns in residential buildings, a tool has been developed. After studying the available information, annual data and daily profiles of certain appliances provided by the projects “EURECO”, “SPAHOUSEC” and “ENCERTICUS” are used. The “ENCERTICUS” project is also based on experimental measurements, and thus was used merely to verify the consistency of the obtained results.

The total annual consumptions for cooking, lighting and appliances were obtained from the SPAHOUSEC project, discerning between the climatic zones of Northern Atlantic, Continental, Mediterranean and all Spain. The types of dwellings could be either flats or detached, and the HVAC energy consumptions are not taken into account here. These data come from a large monitoring campaign that was carried out throughout Spain. Therefore, they are very representative of the Spanish building stock. In addition, to disaggregate the total energy consumptions, information from the EURECO project was used, obtaining average daily consumption profiles for each type of appliance. In the case of lighting, the monthly variations were taken from the ECODROME project. A summary of the sources of information is shown in Table 23.



Project	Aggregate Annual Output	Monthly Variations	Daily profiles	
EURECO	-	X	X	Lighting
				Clothes-dryer
				Freezer
				TV
				Computer
SPAHOUSEC	X	X	X	Cooking
				Clothes-washer
				Dishwasher
				Standby
				Refrigerator
				Oven
ENCERTICUS	X	-	-	-
ECODROME	-	X	-	Lighting

Table 23: Daily profiles, monthly variation and yearly output provided by several projects on consumption patterns in residential buildings.

A tool was developed for the purpose of automatizing this process. After choosing the type of dwelling, climatic zone, month (or annual) and type of cooking, this tool generates an average consumption profile with the disaggregation of all the different energy consumptions for each hour: lighting, appliances, standby and so on. An example is shown below in Figure 138.

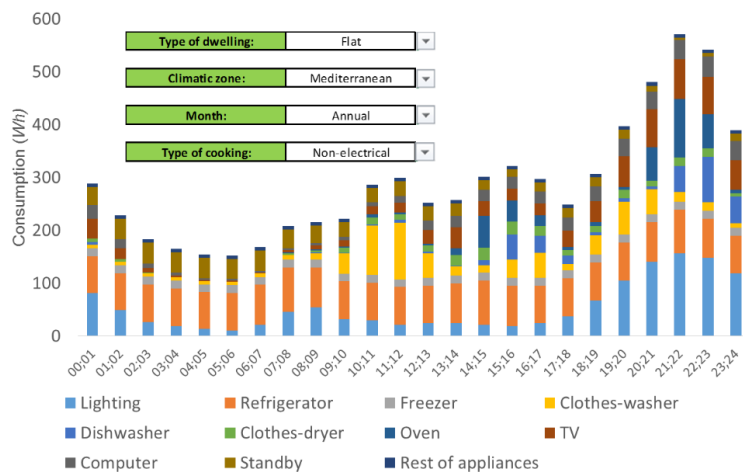


Figure 138: Example of average daily consumption profile.

With the purpose of validating the results produced by the tool, the annual average profile obtained in the case of a flat in the Mediterranean with non-electrical cooking has been compared to the measurements taken in a social housing district in southern Spain. Ten dwellings were monitored during 2017 with Smart Meters at 1 hour intervals, and the average daily consumption profiles for each month were obtained. As it can be seen in Figure 139, the annual average daily consumption profile generated by the estimation tool is not very different from that of the real hourly measurements in this district.

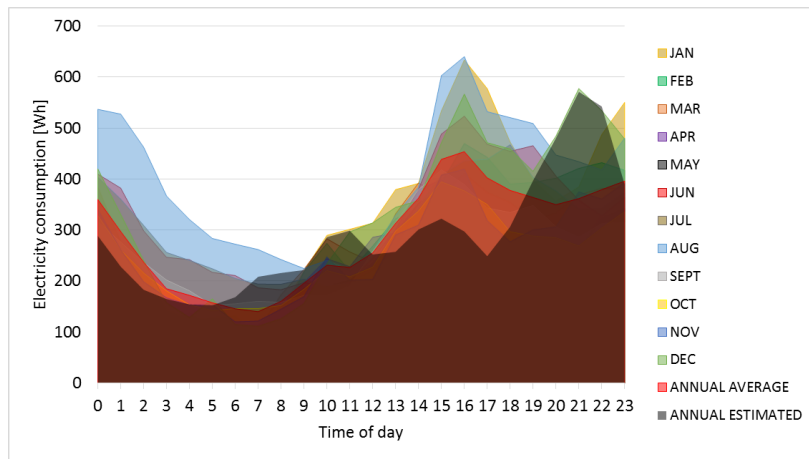


Figure 139: Comparison between measurements and the estimation made by the tool.

As can be seen in Figure 140, if we focus on the average daily consumption for each month, the differences are also rather small. However, it can be observed that the estimated consumption for the summer months and holidays, particularly in August, is much lower than the measurements. After conducting a survey, it was concluded that one of the reasons is that the occupants of the district under study stay at home very frequently during their holidays.

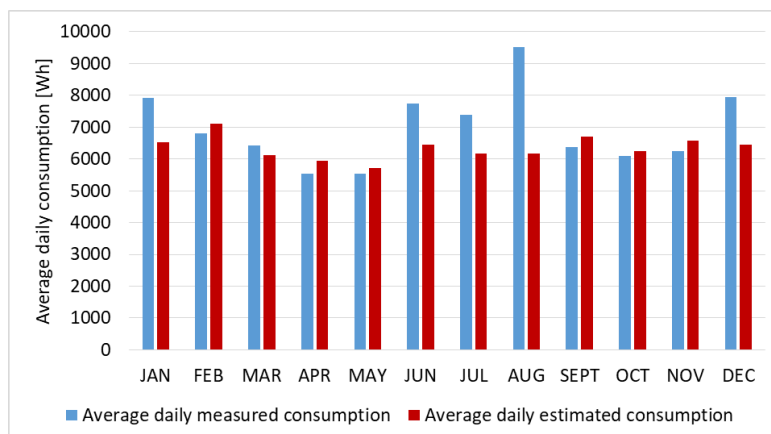


Figure 140: Comparison between the estimated and the real average daily consumptions of the dwellings in the district.

Although the results of the estimations made by the tool are (to a certain extent) quite accurate when comparing the average monthly or annual consumption profiles of a district composed of several buildings, this resemblance may not be fulfilled during a specific day, for a specific building. Figure 141 compares the profile estimated for the month of April with the electricity consumption measurements of 5 different dwellings of the district on the 3<sup>rd</sup> of April, 2017 (Monday). It can clearly be seen that dwelling 1 is not occupied. Also, peaks can be observed at lunch time in dwellings 3, 4 and 5, which have electrical cooking. The peak in dwelling 2 is not so pronounced, since they use bottled butane gas for cooking. As is apparent, focusing on a specific day shows that the differences between dwellings are significant, and also contrast with the profile estimated in the previous section.

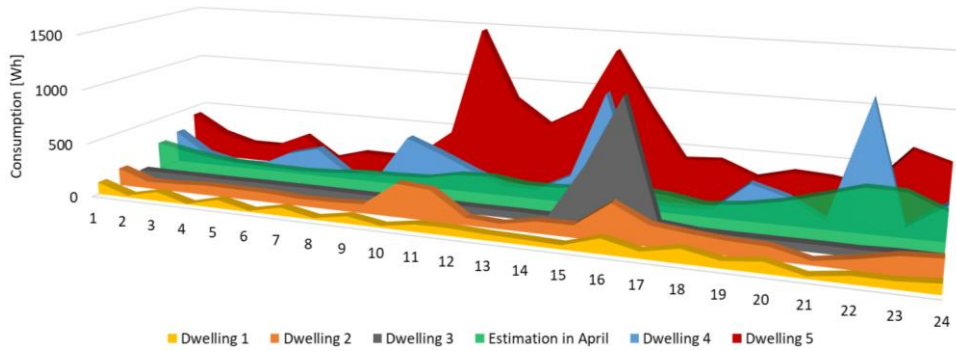


Figure 141: Measured hourly consumption of different dwellings on the 3<sup>rd</sup> of April 2017 and estimated profile for April.

If we look at the consumption of the same dwellings during a whole week (Figure 142), it can be seen that the pattern of each household is somewhat similar during the weekdays, and a bit different during the weekends. When we focus on the electricity consumption of dwelling 5 (Figure 143) during the weekdays (3<sup>rd</sup> to 7<sup>th</sup> of April 2017) and repeat the Monday pattern, we can see that the behavior is some days similar and some days different.

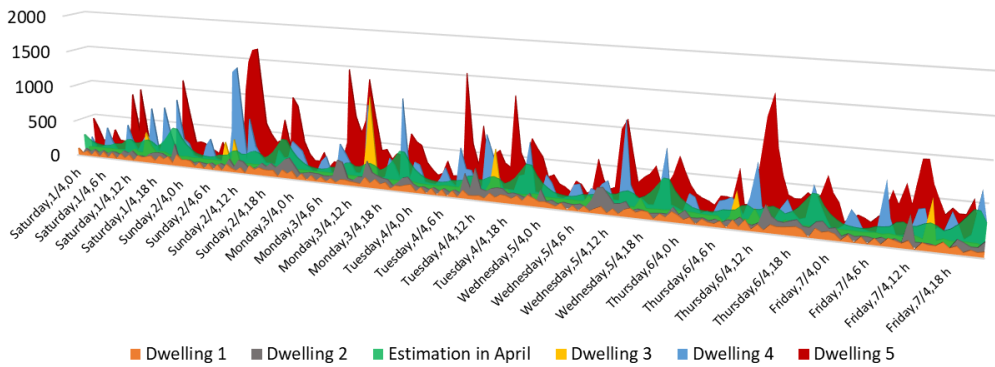


Figure 142: Hourly consumption of several dwellings during a whole week and comparison with the estimated profile for April.

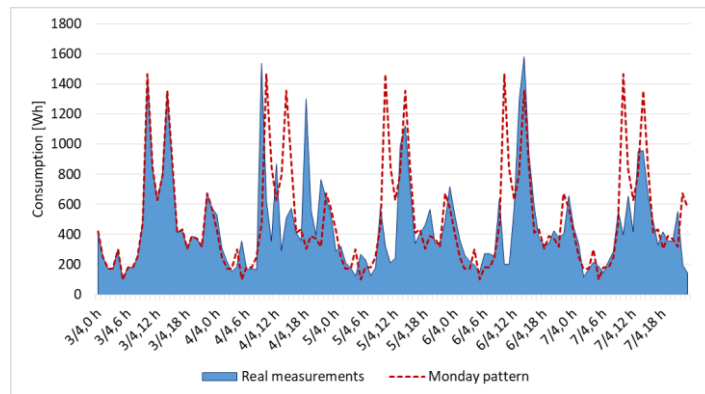


Figure 143: Comparison between the real measurements and the electricity consumption pattern of Monday.

All these results allow us to reach the following conclusion: at district level, the estimation of the average electricity consumption profile of its buildings is more accurate, due to the fact that the aggregation of the electricity consumptions of households with different patterns of behavior eliminates the differences that are observed when focusing on a specific dwelling at hourly intervals. However, it is almost impossible to predict the real hourly consumption patterns of a specific dwelling during a specific day.



# ANNEX C. GENERAL CONCEPTS OF DEMAND SIDE MANAGEMENT

In this annex, general concepts about Demand Side Management will be explained due to its importance in this Thesis. This includes the different techniques available, the distinction between DR and DSM, some notions about smart buildings, sensors and actuators, the role of the users or the importance of energy storage. This information is present in the literature, but in a very uncoordinated way. For that reason, this annex aims to summarize the available facts in an understandable manner.

## C.1 General framework

Since there are different points of view with regards to defining a framework for DSM, we will consider different alternatives. According to [66], DSM results in the implementation of four types of components:

- Energy efficient devices.
- Additional equipment, systems and controls enabling load shaping.
- Standard control systems to turn devices on/off.
- Communication systems between the end-user and an external party.

On the other hand, [185] depicts the overall system architecture of a DSM system dividing the different components in the following way:

- Smart Home Controller*: main component in charge of dynamically managing the loads inside the house, prices coming from high level actors and the information collected from the devices in the home domain. Its role is played by a home residential gateway.
- Smart appliances*: provide consumption forecasts for each requested program.
- Smart plugs*: power metering and on/off control.
- Smart meter*: collects and provides aggregated metering data.

Looking at a broader picture, [96] considers the basic components of a DSM framework as:

- Local generators*.
- Smart devices*: able to monitor themselves and remotely controlled.
- Sensors*: temperature, light or power meter sensors.
- Energy storage systems*.
- Energy management units*: exchange information and manage the electric resources.
- Smart grid domains*: distribution, operation, market and service provider.

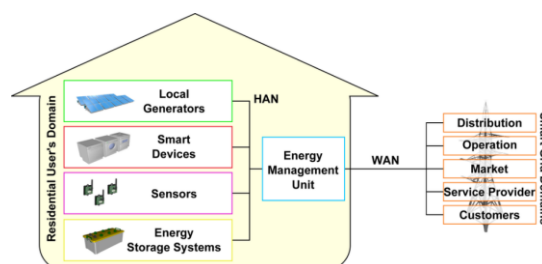


Figure 144: General architecture of DSM frameworks [186].

With regards to the different types of loads that can be found, the literature review which has been carried out revealed different approaches when dealing with the distinction of the various electrical loads present in a dwelling. Loads can be categorized in the following way according to [185]:

-*Plannable loads*: those for which consumption forecasts are available and it is possible to choose start times. Only plannable loads can directly participate to a planning problem.

-*Controllable loads*: connected to smart plugs and can be switched on/off.

-*Monitorable loads*: connected to smart plugs but cannot be switched on/off.

-*Detectable loads*: their consumption can be estimated by calculating the difference between the power measures provided by the smart meter and all the smart plugs and appliances. Therefore, they are not smart appliances and are not connected to smart plugs.

## C.2 DSM techniques

There are six categories in the context of DSM, which are considered basic load shaping techniques [65]:

1. *Peak clipping*: It is one of the most traditional alternatives and involves the reduction of the system peak loads in specific periods. When the utility is not capable of satisfying the demand during peak times, this strategy becomes particularly important. Lowering peak demands can help to lower service costs by reducing the operation of the most expensive units.
2. *Valley filling*: It encompasses building off-peak loads.
3. *Load shifting*: Shifting load from peak to off-peak periods without necessarily changing the energy consumption. Appropriate loads are moved in time for an economic or environmental benefit. It can be considered to have the same effect as the combination of valley filling and peak clipping.
4. *Flexible load curve*: Variations of interruptible loads. The users agree to the possibility of their energy supply being variably controlled by the utility, reducing or postponing their demand so as to achieve operating and fixed costs.
5. *Strategic conservation*: Involving a reduction in sales as well as a change in the pattern of use. It diminishes the overall demand by increasing the energy efficiency. It does not only reduce the demand during peak periods, but also in off-peak periods. Strategic means that these measures as intended on purpose, not happening in a natural manner.
6. *Strategic load growth*: Increased market share of loads. The utilities encourage users to replace inefficient fuel equipment or improve their quality of life and productivity, operating during periods of low demand so as to achieve an efficient plant operation. In this way, the average cost of service is reduced by dispersing fixed costs.

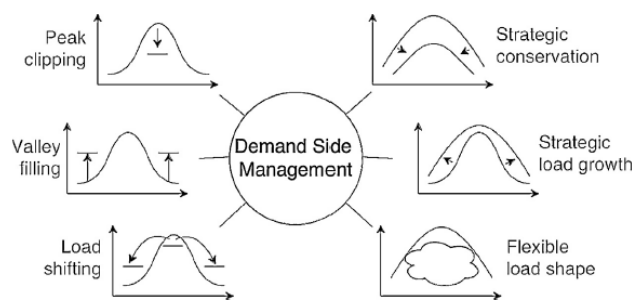


Figure 145: Basic load shaping techniques [87].

### C.3 Demand response vs. Demand Side Management

As a general rule, DSM measures can be divided into:

- Energy efficiency: using less power to perform the same tasks.
- Demand Response.
- Financial incentives.
- Behavioral change through education.

Demand Response, which is a form of Demand Side Management, is frequently used to name programs developed to encourage users to adjust their energy demand in response to price signals. DR can be performed by using different techniques such as heating/cooling storage, batteries, or switching on/off electrical loads automatically. DR programs can be categorized as incentive based, in which the users are offered payments when they reduce their loads on a given time period, or price based, in which they reduce the loads by responding to economic signals.

The distinction between DSM and DR is often confusing for many researchers. We should take into account that DR is normally measured in kW reduced (although that can lead to kWh reduced), and it enables to solve peak-load problems. On the other hand, DSM is measured in kWh (which in turn can also lead to kW reduced), encouraging the users to be more efficient enabling carbon mitigation goals or supplying capacity for example. Generally speaking, we can say that DR is generally more focused on the short term, and DSM in the long term. When certain conditions are met, a combination of DSM and DR actions could be very effective. The user would not be forced to choose one program or the other, benefitting from DR programs which could be then used to fund long-term DSM programs. Automatic control achieves higher participation in DR than manual control [15].

The study presented in [187] made a thorough review of existing DR programs around the world, demonstrating a highly asymmetrical development between regions and how the USA is leading the adoption of DR. Despite the lack of homogeneity, efforts to develop DR programs are pursued globally, indicating that utilities are starting to perceive DR as a useful resource instead of a complicating factor. Given the available infrastructure, the current barriers are mainly regulatory and economic.

Demand side economic incentives by using dynamic pricing are another promising way to reduce energy costs, but first it is important to understand how the electricity market works. Since electricity cannot be economically stored it is subject to short-term capacity constraints. However, demand is highly variable, which means that in some cases there will be plenty of capacity and in others the capacity constraint will be binding, increasing the incremental costs dramatically. As a result, the electricity price varies constantly. Thus, many programs have been implemented in order to give customers economic incentives depending on the time that the energy is used. Advanced telecommunication systems and smart meters particularly are essential elements of dynamic pricing, making them more feasible today than in the past. Different DSM approaches such as load shifting can benefit from dynamic pricing, since being able to move the time of use of reschedulable loads may reduce the energy costs. Time-of-use tariffs could also be considered.

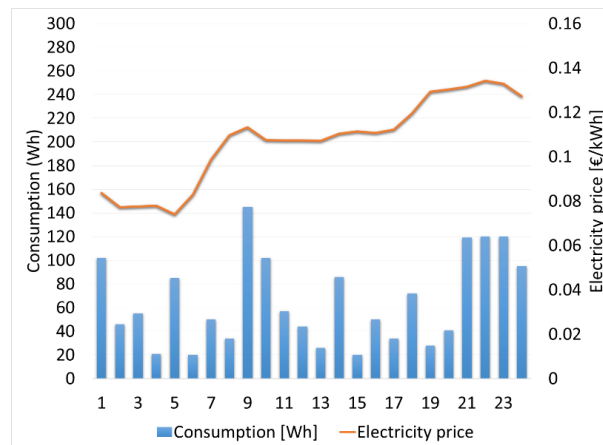


Figure 146: Example of hourly electricity demand and prices.

#### C.4 Smart buildings: current state of the technology

Buildings are an essential part of the energy system, and their smartness could help the integration of DSM approaches. According to [188], it is still unproven and unclear how much building automation could save in terms of energy and cost, and there have been no sufficient justifications for the investments. The demonstrated energy savings when using smart homes are relatively small, but the potential savings during peak times are higher.

One of the latest trends in our consumerist society is the introduction of domestic automation into our homes, also known as home energy management systems, which also play a crucial role in realizing residential DR programs in the smart environment [189]. While until recently its complete implementation was regarded as unaffordable and only available for high-income customers, it could set the path for the large scale deployment of smart devices directed at enabling DSM approaches, even for low-income users.

From the point of view of Energy Policy, Smart Homes are one of the EU's priority action areas in its *Strategic Energy Technology Plan: Create technologies and services for smart homes that provide smart solutions to energy consumers* [190]. Due to this, Smart Homes are seen as an integral part of a future energy system, since they help to reduce the overall demand as well as alleviate supply constraints during periods of peak load [190]. The Smart Home is seen as an important technological solution in delivering an affordable low-carbon energy transition, with associated benefits for households, utilities and policymakers [191]. The objectives of households which intend to save energy and money align with the efforts of the utilities to improve energy system management and those of policymakers which pursue emission reduction and a secure and reliable energy supply. The uptake of Smart Homes will lead to an increase in the amount of measured data available, providing unparalleled insights into how our homes perform [192].

Traditionally, smart home systems have been sold as a whole and the consumer has to rely on the same seller for the hardware, communications protocol, central hub and user interface. Each platform has essentially its own language, which is capable to interact with the connected devices and give them instructions. This situation is parallel to the one of the market of computation about thirty years ago. There were several important computer companies such as IBM, Digital Equipment Corporation, Hewlett Packard and so on. Each of these companies had its own operating system and its own communication protocol (Token-Ring, Decnet, etc.). In practice a company could only use computers of the same company (captive market), which made the communication between computers of different companies very arduous. This situation changed dramatically when the main computer companies decided to use open-source communication protocols (Ethernet and TCP-IP) and operating systems (UNIX and its many variants). These changes led to the current situation, which is very different from that of thirty years ago.



Currently, there are open-source software systems for Smart Home devices which can be used with proprietary hardware. This may be considered as a first step in the way to open the market of Smart Homes. These smart devices can be controlled remotely by using a computer, smartphone or tablet in such a way that:

1. The possibilities are endless: from turning a device on or off, to scheduling a washing machine or controlling the temperature at home.
2. The overall or disaggregated consumption could be knowable. This would facilitate the implementation of DSM approaches, since understanding the load profile together with being able to shift the loads, controlling shading (and therefore solar gains) or controlling the set-point temperatures make it possible.
3. Smart Home implementation can therefore optimize energy usage and save a significant amount of energy, guaranteeing the comfort of the occupants. However, it should be mentioned that the energy consumption of some appliances (such as laptops, fridges or irons) cannot be reduced by using smart systems, since they would consume the same energy with or without it.

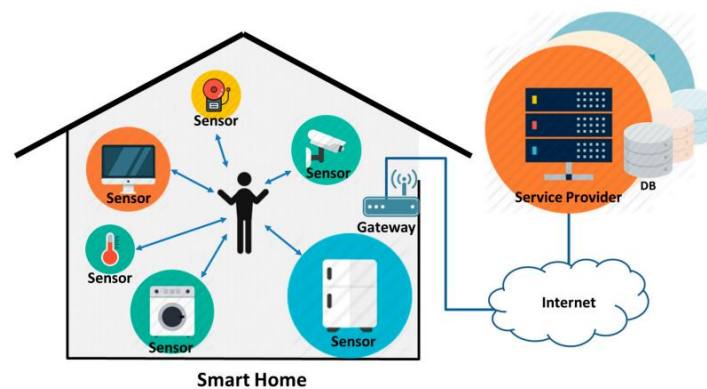


Figure 147: Example of a Smart Home and its sensors [193].

There are many different applications of smart devices for control and automation, some of them not quite useful for DSM implementation, but others of paramount importance. The ones which are going to be mentioned here can be equipped with Wi-Fi or Bluetooth connectivity, allowing their control through computers, tablets or mobile apps. They are commercially available, although their prices may be (still) significantly high. Individual splits are very frequent in households compared to centrally controlled systems, especially in Spain. They are starting to be sold with Wi-Fi by some manufacturers, but the prices are comparably high and therefore unaffordable for most users.

A Smart Home comprises a variety of systems and appliances with a main control, including sensors, appliances and smart devices:

1. *Central hub or gateway*: it allows the control of the whole system through a user interface.
2. *Shading controls*: blinds or shutters can be remotely controlled so as to harness the energy of the sun or prevent rooms from getting too hot.
3. *Lighting*: lights triggered by motion sensors, dimmed lighting, remote control.
4. *Air-conditioning*: smart thermostats are capable of controlling and maintaining room temperatures by turning on or off many types of air-conditioning systems.
5. *Ventilation control*.
6. *Smart appliances*: washing machines, fridges, freezers, dryers, dishwashers and so on.
7. *Smart meters*: they monitor the consumption and report that information remotely.
8. *Smart plugs*: able to monitor the consumption of the devices connected to them as well as turn them on or off remotely.

9. *Alarm systems*: home security systems which make it possible to check remotely when motion sensors are activated.
10. *Others*: locks, doors, humidifiers, smoke detectors, irrigation systems, multimedia, cameras, swimming pools control, bells, air purifiers, audio devices and so on.

Home automation has evolved into more than a connection between autonomous devices: it has evolved towards systems and processes that are becoming more intelligent and capable of communicating with people [194]. However, the impact of Smart Home systems depends on how developers, manufacturers and retailers design and market them (and also on how the users utilize them), but once they are adopted their impact is not easy to evaluate [190]. In addition, improving the performance of a building through building automation requires adequate measurements and justification of the economic gains that could be offered before its realization, which might differ depending on the user behavior. The study presented in [188] suggests that results from observations and product research for residential homes indicates that the investment cost of building automation ranges from 500 to 2000 Euros, depending on the building type.

### C.5 Smart meters

Smart meters are the new generation of gas and electricity meters. In the case of Spain, electricity meters started to be installed in 2010 and they are expected to be implemented in every household by 2019. They are devices that record the electricity consumption usually in intervals of one hour, and communicate the information to the utility. The implementation of smart meters means the replacement of traditional meters which still use technology created many years ago. This means that dwellings will no longer have to rely on reading the meters manually or paying estimated energy bills.



Figure 148: Smart meters implementation. Source: Endesa.

There are several benefits to smart meters:

- Hourly data: The energy consumption can be monitored online by the user, thus increasing the understanding of the household energy use and the direct impact of different habits and lifestyles.
- Faster to fix problems in case of failure.
- Estimated readings are no longer necessary.
- New energy tariffs: By being able to know the energy consumption each hour, it is possible to establish different tariffs depending on the time of day.
- Energy saving possibilities: Electricity suppliers may use the data collected to create cheaper prices for off-peak use and optimal time-of-use tariffs. The users can also know the energy prices beforehand and schedule their energy consumption in consequence. In the case of Spain, the hourly electricity prices are available at 20:15h the day before.

The new data streams coming from electricity and gas measurements made by smart meters will also lead to several innovations in the building retrofit process [192] such as:

- Improved identification of the households which would gain the most through retrofit measures.
- Improved predictions of the energy savings by using consumption data, to infer heating/cooling practices (a home constantly heated is likely to have greater savings than one which is rarely heated).
- Quality assurance checks of retrofit works through pre and post-installation comparisons of energy consumption data.

## C.6 Sensors and actuators

Smart gateways are often needed in smart buildings. Sensors can communicate directly with the gateway, measuring environmental parameters such as temperature, humidity, light or motion. These systems can incorporate algorithms controlled by the gateway which allows the control through on-site or remote interfaces (such as PCs, tablets or smartphones). They are usually wireless, using standardized communication protocols. Rules can be defined for automation (for example turning on a light when the main door opens or presence is detected). The data are measured by sensors at regular intervals or when an event occurs, and can be saved in cloud servers so as to provide historic data when needed. The individual appliance data streams coming from smart plugs can also be used to make better predictions of saving potentials, thanks to the understanding of detailed electricity consumption of each device, frequency of use, etc.

The most important sensors and actuators which can be implemented into a smart home are:

1. *Temperature and humidity sensors*: able to provide data at regular intervals.
2. *Motion sensors*: able to detect when a home/room is occupied and save the data when an event occurs.
3. *Door/window sensors*: able to detect when a door or window opens/closes.
4. *Smart plugs*: capable of measuring the consumption of the appliances connected to them as well as turning them on or off at any desired time. The data obtained can be then sent to the local controller or a cloud server.
5. *Smart thermostats*: set-point temperatures can be adjusted depending on the measurements of other sensors and the algorithms used by the smart gateway. They enable an automatic control for heating and cooling, and have increased noticeably their market share in recent years.
6. *Motorized blinds or shutters*: they can automatically open or close when certain conditions are met.



Figure 149: From left to right: temperature and humidity sensor, motion sensor, door/window sensor.

## C.7 Communication Networks

In the past, the infrastructure needed for distributed sensing and monitoring was significant. However, in the last few years the vast majority of buildings have been retrofitted with Wi-Fi capability, which permits the communication of the devices between themselves and also back to internet based servers [63]. Advancements in communication networks and sensors have consequently smoothed the path for researchers to use their capabilities in their fields of interest [195]. These low-cost wireless sensors could mean cost-effective mechanisms for energy management systems.

A Home-Area Network is operated within a small boundary such as a house, and enables the connection and sharing of resources of in-home digital devices such as smart appliances, mobile phones, tablets, computers, sensors, actuators, smart plugs, smart thermostats or security systems within a common network. The modem provides wired LAN ports or wireless connectivity to host users. This may extend the scope of the utilities beyond the smart meters, enabling demand response and energy efficiency programs. Smart devices can be connected in a HAN with either wired or wireless communication technologies such as Wi-Fi, ZigBee, Z-Wave, Ethernet, KNX, etc. [189]. Many applications of wireless communications have been developed and investigated on various studies such as electronics, buildings electrical safety and energy management and conservation [195].

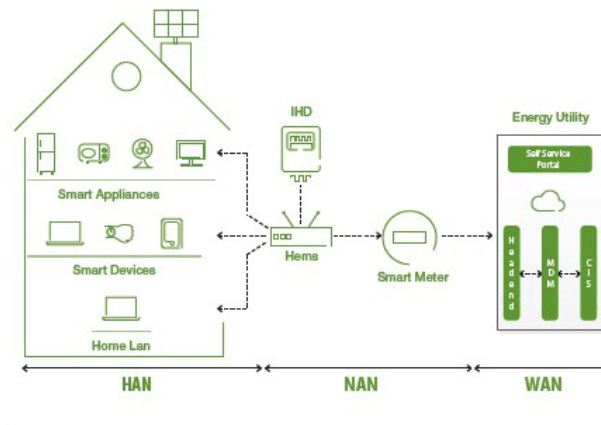


Figure 150: Example of Area Network boundaries. Source: Fusion Energy Consortium.

On the other hand, there have been significant advances in power management of the devices, and it is possible now to have a temperature sensor which reports to the internet every 2 minutes for two years just using AA batteries [63]. Such low energy devices make it possible to implement DSM approaches. Wireless sensors have the advantage of an easy implementation, since they do not need a wired installation and therefore can be installed without restrictions. With the market penetration of mobile communications, command and control of heating and cooling systems in commercial and domestic buildings is becoming a viable and cost-effective option, particularly in the existing building stock [63]. What is needed, is the system and processes to link mobile devices to a smart command and control system which can manage the appliances, thus achieving energy savings which are shown to the consumer. It must also be said that, as a by-product, the environment of home automation may generate an enormous amount of data, which contributes to relatively new research fields such as the Internet of Things (IoT), Big Data and others [194]. The consequences of this research are relatively unexplored, but it seems evident that it may help to obtain a detailed account on the global behavior of a population from the energy consumption point of view.

### C.8 Smart homes as a means to improve the assessment of energy saving measures

Demand reduction in buildings is one of the clearest paths towards achieving emission savings at a large scale, and it has traditionally been accomplished through the refurbishment of the thermal envelope of the buildings. This includes an increase on the insulation of roofs, walls and floors, changing the glazing or improving the efficiency of the air-conditioning equipment. Refurbishment can provide long-term savings, but it involves high investment costs. In addition, accurate estimates of the potential savings which can be expected are, more often than not, unavailable. Therefore, providing this information is a very promising challenge.

This has been considered by some studies such as [192], which explores the potential of smart home monitoring technologies (with room temperatures, occupancy and real consumption data) to estimate the energy savings available from retrofitting, since using Smart Home data streams can improve our understanding of the real building performance and help to identify more clearly the strategies so as to reduce the energy demand.

In addition, the temperature data streams can provide information of the heat loss of a building by observing the rate of decrease of room temperatures when the heating system is switched off. The authors of [192] suggest that this information should lead to greater uptake of retrofit alternatives, since by better understanding the fabric and ventilation characteristics of a building, improved predictions of the retrofit effects can be made. Moreover, [196] claims that observing the rapid rate at which a room heats may indicate that the heating system is functioning efficiently, and in contrast that the rate at which the heat is lost may indicate whether it is sufficiently insulated or not.

## C.9 The role of users

Substantial savings can be obtained by investing in equipment and infrastructure in the residential sector, but the behavior of the end-users is of paramount importance. This behavior can be influenced by smart metering, consumption feedback systems and awareness campaigns [197]. The energy used can represent a significant proportion of household budgets, but consumers are often lacking a clear understanding on how to reduce their energy demand [192]. The energy use in homes is complex, with a mixture of different fuels (electricity, Liquid Petroleum Gas or Natural gas for instance) which provide various services (air-conditioning, lighting, cooking, communications...). The current energy system in which energy is mostly centrally generated on the one hand, and is consumed by individual users on the other, offers a framework in which users can play a major role so as to produce considerable energy savings. In this context, we can safely say that the popular proverb “knowledge is power” is of particular significance. For this reason, personalized, tailored and real-time information and feedback on energy use and tariffs by using smart meters and In-Home Displays may help to “make energy visible” [191].

The study presented in [198] offers a very comprehensive analysis of information-based energy conservation experiments conducted until 2012, quantifying the energy savings from strategies such as energy saving tips or conducting home audits. Comparing individuals to the average energy used could be more effective than other strategies at reducing energy usage. On average, they claim that individuals in the experiments reduced their electricity consumption by 7.4 %. In [199] we can see a useful insight of the role that in-home feedback displays can play to help households understand patterns of behavior and the relative impacts of the different appliances and equipment. The common impact factors leading from occupant behavior to energy consumption have been identified by [200] as shown in Figure 151.

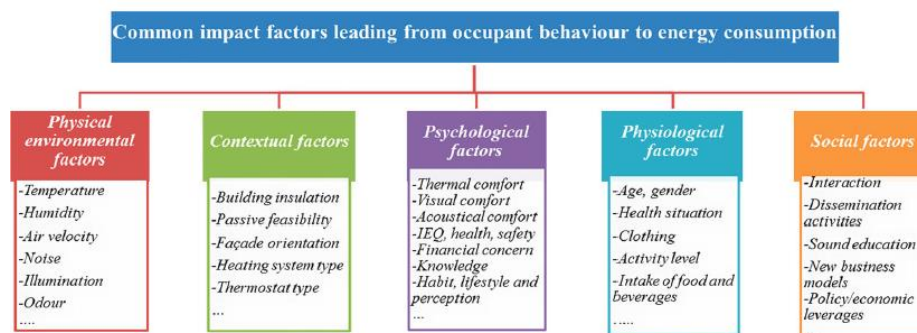


Figure 151: Common impact factors leading from occupant behavior to energy consumption [200].

The effects of various direct feedback systems on consumer behavior have been researched for some time, and they have consistently demonstrated that direct feedback motivates energy savings which range up to 20 % [201]. Policy makers should consider the high impact of information programs, which are relatively low-cost and can produce many savings. This feedback is proving to be a critical first step in engaging and empowering consumers to manage their energy resources. However, some types of feedback appear to be more effective than others [202], since past studies suggest that daily/weekly and real-time feedback generate the highest savings per household. Figure 152 shows the average savings of a household depending on the feedback type, obtained by the previously mentioned work based on 36 studies implemented between 1995 and 2010.

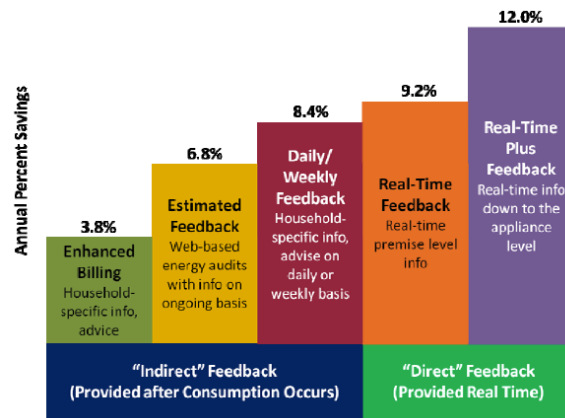


Figure 152: Average household electricity savings by feedback type [202].

Another type of feedback on energy savings are real-time appliance-level energy consumption data, which have the potential to empower consumers to effectively manage their household energy consumption and encourage conservation [203]. Many studies have investigated the influence of real-time information on the energy use of households, which is considered to be more effective than traditional monthly reports. Some of them investigate this by using in-home displays for example, which give information about the costs and electricity usage. However, none of them explain why real-time information affects the energy consumption. The causal mechanisms are therefore explored in [204]. In this study, the authors conclude after doing some experiments that those who receive real-time information reduce their energy consumption, but the effect diminishes over time. This conclusion is also reached by [191]. This fact suggests that energy conservation policies that target learning might be more cost-effective than installing in-home devices.

Additionally, the study presented by [201] establishes that consumers who actively use an in-home display can reduce their electricity consumption by at least 7% on average. The study presented by [200] demonstrates that in-home displays could lead to around 9.1% reduction in monthly electricity consumption and about 11% cut off in monthly electricity bills. The study shown in [197], which focuses on low-income households, shows electricity savings between 22% and 27% when individualized awareness campaigns and consumption feedback are introduced in the households. On the other hand, [205] suggests that despite all the efforts, the implementation of useful feedback is lagging way behind knowledge since it is usually not driven by scientific findings but by political interest or incentives.

### C.10 The role of energy storage and renewable energy on DSM approaches

By nature, renewable energy sources are intermittent, causing problems of grid stability. For this reason, there are some limitations on the amount of renewable energy which can be fed into the electricity grid. Generally, renewable energy production is governed by environmental conditions, not being able to respond to changes in demand. However, controlling reschedulable loads could be an effective strategy, mitigating the fluctuations introduced by renewable energy production. In this case, it is the demand which responds to changes in generation and not the other way around. That is the basis of demand response.

Thermal Energy Storage (TES) systems are usually used to integrate renewable energies, but they can also be used for load shifting, reducing the energy costs and becoming a powerful DSM tool, especially in presence of renewable energies [66]. DSM often works best when there is storage available for the user, either inside the building or storing the energy in tanks [63]. A TES system can store energy by heating, cooling, melting, solidifying or vaporizing a material, using different substances depending on the required storage capacity, temperatures or the economic feasibility. Energy storage is usually characterized through the power capacity (allowing to respond to mismatches of higher magnitudes) and the size of the energy storage (responding to shorter/longer mismatches). Storage can also help to flatten the customer's load profile. Therefore, effective TES can potentially impact several categories of DSM, including peak load shifting, valley filling and strategic conservation [88].

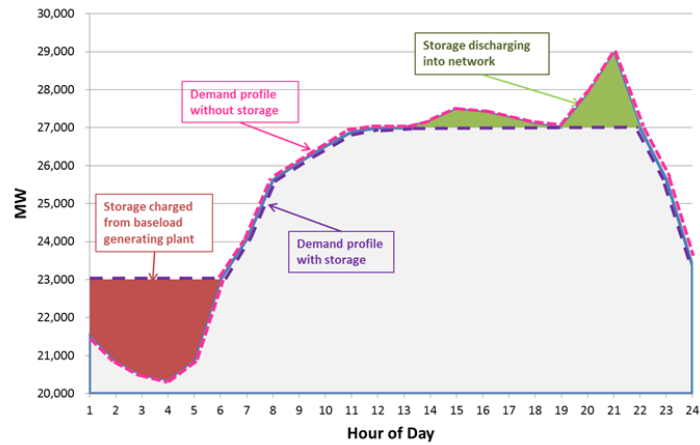


Figure 153: Integration of storage and Demand Side Management. Source: Energy Storage Association, 2012.

Another way in which DSM can be beneficial is by relying on the inherent properties of buildings, for example by changing the temperature thanks to their thermal mass or disengaging heating or cooling for short periods. Literature shows that the DSM potential is in this case a function of the available thermal mass and the geometry of the building [92]. However, the use of the thermal mass only enables short-term storage. The DSM potential is higher for massive buildings compared to lightweight buildings, and it could be expected that the efficiency of the structural energy storage is higher for well insulated buildings [92].





# ANNEX D. IMPROVEMENT MEASURES CONSIDERED IN THIS THESIS

The present annex focuses on justifying the consideration of some of the improvement measures that were examined in this Thesis, since improving the thermal performance of a district or diminishing the energy costs through automation requires a previous study of the feasibility of the systems that may be implemented. The reductions of the energy demands in buildings have been traditionally addressed in multiple ways. The author of this Thesis considers that some of the most interesting approaches are preconditioning, solar control and night ventilation, which is why they will be analyzed and explained in detail in this annex. In the past, solar control and ventilation approaches were only viewed as traditional energy efficiency strategies, but they will be considered here within a DSM framework since they are capable of indirectly changing load shapes by reducing the consumptions or altering the times of use. In this annex, basic concepts about these strategies will be explained, along with a review of some of the alternatives that are usually implemented. Then, a case study will be considered to evaluate their energy and economic feasibility.

## D.1 Structural thermal energy storage: preheating/precooling strategies

Buildings have a thermal mass that provides inertia, taking some time to heat up or cool down. Like other technologies to store energy, this inherent property can be used to store energy at peak periods and preheat or precool the building, but is available at no additional investment cost. Given the right control system, an electric heater or electric Heat Pump could be used flexibly depending on the grid conditions, without significantly compromising the thermal comfort of the occupants and contributing to the reduction of peak loads. Thanks to the thermal inertia, electricity and thermal demand can be partially decoupled through flexible HVAC operation while maintaining thermal comfort. During hours of no occupancy this strategy has an even higher impact, since it allows to relax the comfort constraints.

If the electricity market conditions are favorable, heat could be produced by the HVAC systems to preheat or even overheat the buildings, storing energy in the building thermal mass or in storage tanks. This of course depends on the availability of pricing programs which allow time-of-use tariffs. In these tariffs, the prices are set in advance and vary throughout the day. They are higher in peak periods and lower in off-peak periods. Conversely, in dynamic or Real-Time Pricing the prices are usually notified to the users on a day-ahead or hour-ahead basis. A dynamic electricity market is already available in many countries for large consumers, and it is being extended to residential customers, which increasingly generate their own renewable energy and become prosumers.

Activating the structural thermal energy storage demands for active control of the indoor temperature and increases the total energy used [92], since the utilization of structural storage might result in increased transmission and ventilation losses. The building could be preheated and its storage capacity activated by increasing the indoor temperature set-point when the price of the electricity is low. Alternatively, the set-point could be lowered with high electricity prices, releasing the stored energy and thus reducing the electricity demand. Building mass can be used for either an active (under floor heating) or a passive thermal storage system [66]. The study presented by [92] evaluated a floor heating system and low temperature radiators for their potential to activate the thermal mass of the building. It concluded that the floor heating system showed better peak shaving potential since it was able to activate the thermal mass directly, unlike the radiators which tended to heat mostly the indoor air.

Simulation and experimental results show that a Model Predictive Control strategy that considers both the structural storage capacity and the active thermal storage may result in considerable savings while maintaining comfort, mainly due to the free cooling potential (e.g., through night ventilation), a higher contribution of solar and internal gains for passive heating and the price differences between peak and off-

peak periods [92]. Nevertheless, it should be noted that thermal comfort plays an important role in pre-heating/pre-cooling strategies, since it limits the allowable temperature fluctuations. It can be introduced into cost functions in order to optimize the calculation of the temperature set-points, but specifying the cost of comfort violations has proven difficult due to its subjective nature. For this reason, thermal comfort standards are often considered.

A promising technology to activate the thermal storage mass in buildings is the Thermally Activated Building Systems (TABS), which includes pipes or ducts embedded in the building surfaces to work as heat exchangers, providing heating or cooling and storing heat in the thermal mass [206]. TABS help to activate the thermal mass of the building, allowing load shifting strategies. By making use of dynamic pricing strategies there might be significant cost savings, but overheating the building above its normal set-point temperature results in energy losses, therefore increasing the energy consumption.

Among the different technologies available to carry out DR strategies, heat pumps play a vital role. According to [207], there are three main categories of applications using heat pumps in a smart grid context: stable and economic operation of grids, integration of renewable energy systems and operation under variable electricity prices. Changing residential space heating from the use of gas boilers towards heat pumps is also recognized as a method to reduce emissions and increase the energy efficiency [110]. Heat pumps might be effective in balancing the electricity supply and demand when combined with the thermal inertia of buildings, contributing as well to the integration of renewable energies. They could therefore be employed to make use of dynamic pricing or the advantages offered by Frequency Restoration Reserve markets as a means to induce users to generate or absorb electricity depending on the grid imbalance, obtaining economic benefits in the process. Last of all, it should be mentioned that the main benefit of preconditioning approaches is that the capital costs needed for their implementation are minimum, and in some cases even non-existent.

## D.2 Solar shading control strategies

Solar-control systems are beneficial if the artificial lighting and cooling energy consumptions want to be reduced, but they have to be realistically assessed when they want to be implemented in buildings. Their main function is to intercept the sun's rays before reaching the building in cooling periods and permitting the wanted solar gains in heating periods. A very interesting review and state of the art of advanced solar control devices for buildings is presented in [208]. Figure 154 summarizes in a very clear way the different design parameters for solar-control systems, including the different technologies available.

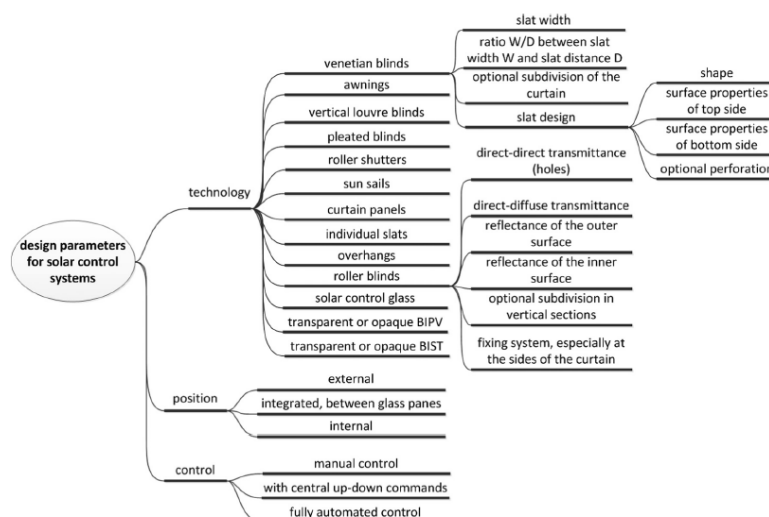


Figure 154: Design parameters for solar-control systems [208].

It has already been proven that controlled shading devices on windows have a major effect on the energy

consumption due to solar heat gains, heat transmission and infiltration [209]. The solar gains of a building mostly depend on the following aspects:

- Orientation of the glazed areas.
- Size of the glazed areas.
- Shading losses due to surrounding buildings, trees and shadows produced by the own building.
- Transmittance of the thermal envelope of the building.
- Solar heat gain coefficient (SHGC): fraction of the solar radiation which enters a building through a window compared to the total radiation that the window receives. Apart from SHGC, several names are used for it: solar factor, g-value, or Total Solar Energy Transmittance (TSET).
- Use of the solar control systems.

Solar gains are unwanted during the cooling season, and desired whenever the building is in heating mode. Therefore, the solar heat gain coefficient is of great importance to achieve energy savings in buildings. In fact, the study presented by [210] indicates that automatic control of shadings used in conjunction with controllable lighting systems can produce substantial reductions of energy demand for cooling and lighting. As a new tendency in the building sector, shading devices can potentially be replaced by building integrated solar thermal shading systems, which are small-sized solar thermal collectors for heat generation, solar gain reduction and glare protection [211].

The review of 109 papers on the use of shading devices in buildings included in [212] includes the following findings:

- The number of papers on shading devices has increased dramatically in the recent years. This reveals the importance of shading control systems on the energy consumption of a building.
- Using simulation programs to solve the complex relationships between climate, occupancy, energy-efficiency issues and design characteristics is a strong way of coping with these problems.
- Office buildings are the most selected case studies.
- Venetian blinds are the most commonly studied shading devices.

### **D.2.1. Dynamic shading**

Dynamic shading is commonly suggested as a means of reducing overheating while at the same time letting daylight and solar irradiation in when needed, without compromising thermal comfort [213]. The implementation of this measure is interesting in buildings with shading elements and a high percentage of glazing in east, west and south orientations. The goal during heating periods is to improve the solar gains through the glazed areas with an important solar radiation potential. On the other hand, during cooling periods the goal is to reduce the solar radiation penetrating on the building through the glazing, which may be the most important component of the cooling demand. In southern orientations using horizontal laths are more convenient, whereas in west and east orientations vertical laths are preferable. Shading elements also contribute to the reduction of the infiltrations since they act as an additional layer against wind.

Various shading control algorithms have been used in the existing literature: based on incident solar radiation, internal temperatures and others [214]. An experimental and analytic study was performed by [215] in order to compare different external solar screens, with a dynamic analysis of the energy performances. Also, [216] presents a field study to investigate occupant interactions with motorized shading systems. With regards to the role of the users in dynamic shading, it should be mentioned that manual control should be avoided because users of buildings tend to leave the blinds either open or closed regardless of what is optimal for the cooling or heating needs [217].

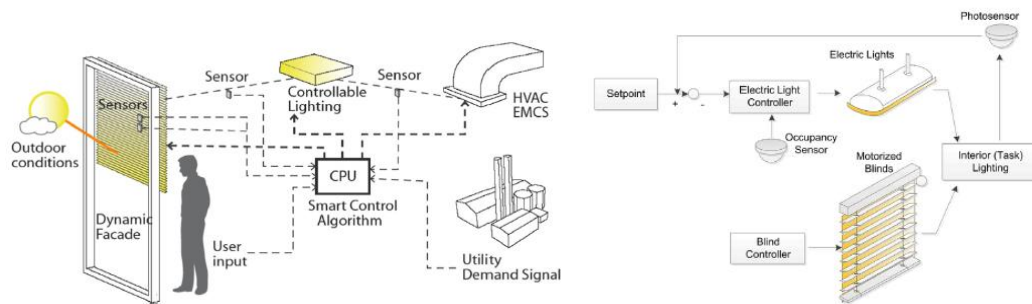


Figure 155: Example of control of automatic shading devices [218].

Globally, the results obtained in [219] show that movable solar shades used for south-facing windows reduced the energy demand by almost 31%, improving the thermal comfort. In that study, using motorized blinds with a smart controller produced energy savings reaching up to 20% for cooling and 50% for lighting in comparison to static systems. On the other hand, [209] show maximum energy savings of 14.9 % in June, and an average of 9.8% annually by using movable exterior window shading for a building in a tropical climate. [209] suggests that movable shadings do not have much impact on North, East and West orientation, so they should only be applied to southern windows.

Strategies for shading of an external mobile screen based on both internal temperature and solar irradiation thresholds are said to be more efficient than strategies based on solar irradiation or internal temperature alone [220]. However, a distinction should be made between external and internal shading. [219] claims that external shading has a better performance at reducing heat gains than internal windows coverings, since the solar radiation absorbed by internal ones will finally increase indoor heat gains. However, due to relatively high initial costs external solar shading receives less research focus, although this fact strongly depends on the country considered.

### D.3 Night ventilation strategies

The forecasted climate change will not only produce an increase on the cooling demand of buildings, but also indoor conditions that are less healthy for the occupants, particularly in urban areas. For this reason, ventilation strategies which focus for example on the exploitation of the free cooling potential are also of paramount importance.

If the outdoor air temperature at night is low enough, natural or mechanical ventilation can be used to cool the exposed thermal mass of a building. By doing this, a heat sink is provided for the following day, ensuring thermal comfort by limiting the overheating hours. This advantage has already been widely studied, and night ventilation appears to be one of the most promising passive cooling techniques [221]. For these reasons, free cooling by enhanced night-time ventilation could be an efficient technique so as to decrease the cooling demand of buildings.

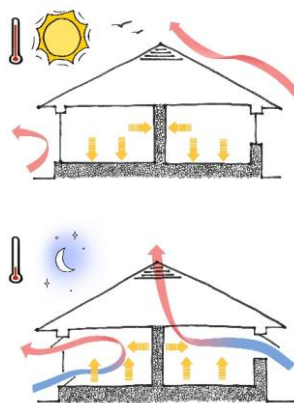


Figure 156: Night cooling technique. Source: Illinois Institute of Technology.

This measure can be applied when the following conditions are given:

- The zone has a cooling demand.
- The exterior air has certain temperature-humidity conditions which allow to satisfy totally or partially the cooling demand.
- Its application extends to constant or variable flow systems.

In order to use free-cooling with an existing air treatment unit, the following elements are required:

- The installation of an air return fan.
- The addition of an air damper.
- The automation of the outside, return and exhaust air dampers.
- A possible increment of the air intake section and its channeling from the Air Treatment Unit.

The efficiency of night ventilation is strongly related to the difference between the indoor and outdoor temperatures at night, the air flow rate and the thermal capacity of the building [222]. On the other hand, weather-predicted controlling seems to be most effective [223]. Despite the simplicity of the concept, the effectiveness of night-time cooling is affected by many parameters, which makes predictions uncertain [224]. Most studies conclude that night ventilation in free floating buildings may decrease the next day peak indoor temperature up to 3K [221]. In air-conditioned buildings, a considerable reduction of the cooling peaks may be expected.

#### D.4 Example of DSM implementation

In this section, we propose a DSM implementation with sensors and actuators, including dynamic shading and ventilation strategies. The proposal is to follow algorithms composed of a set of “IF-THEN” rules, which determine how to react if any change of the parameters that are measured by the sensors occur, such as inside or outside temperature, presence and so on. A set of rules will be therefore designed and embedded into an intelligent algorithm.

##### D.4.1. Description of the case study

A household located in a social housing district in Seville (Spain) built in 1983 will be used as a case study, following the procedure to obtain the energy baselines explained in Chapter 4. A monitoring campaign allowed to measure the indoor temperatures and the total electricity consumption of the household through temperature sensors and a smart meter during the whole year 2017. The measured temperatures motivated a study on the implementation of solar shading and night ventilation strategies, which might be able to improve the thermal comfort of the occupants who have to withstand temperatures up to 33 °C inside the dwelling.

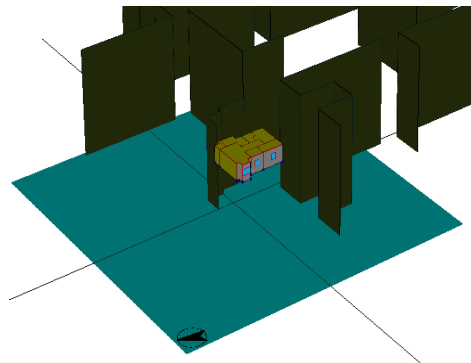


Figure 157: Model of the dwelling and surrounding buildings.

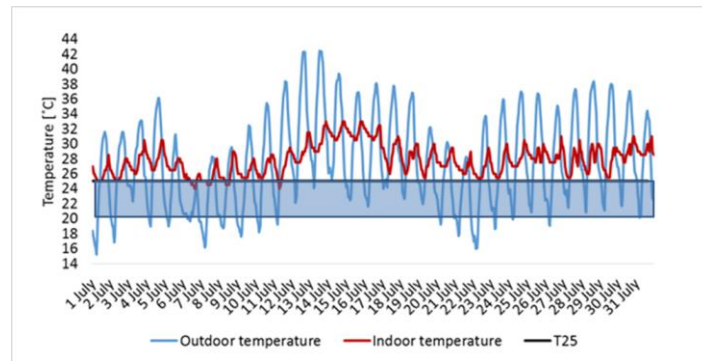


Figure 158: Measured temperature of the household, July 2017.

The following sections will synthesize the results of the measures that will be evaluated by applying the energy baselines.

#### D.4.2. Solar control strategies

Solar control systems reduce the cooling energy consumption of buildings by decreasing solar gains. Several strategies have been simulated to evaluate the potential comfort improvement (with no air-conditioning system) and energy savings (standard user) that may be achieved.

- Standard solar control (SC\_ST): no DSM. Blinds are lowered up to 30 % during summer.
- Presence solar control (SC\_PRES): blinds are lowered if there is no occupancy.
- Presence solar control with lighting consideration (SC\_PRES\_LIGHT): blinds are lowered if there is no occupancy, and if there is occupancy the blinds are lowered up to 10% (for natural lighting).

The last two strategies would require the installation of a gateway, a motion sensor, and an actuator in each blind of the household.

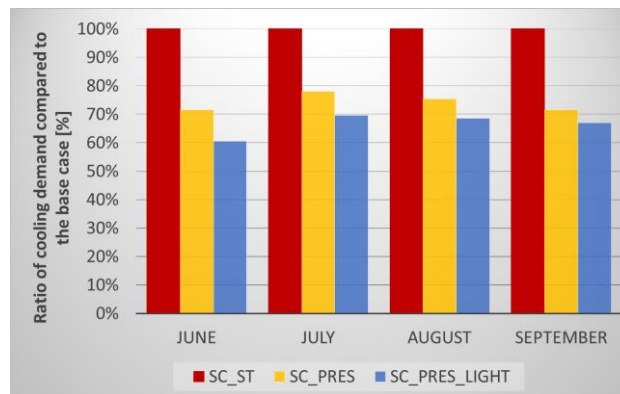


Figure 159: Results of cooling demand reduction for the analyzed solar control strategies.

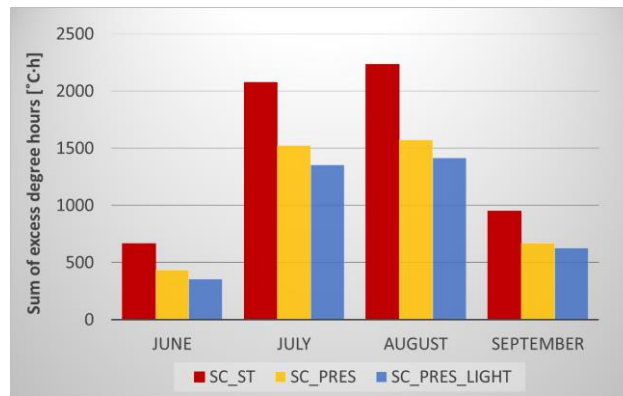


Figure 160: Results of excess degree-hours reduction for the analyzed solar control strategies

As it can be seen, the studied measures are able to achieve high cooling demand reductions up to 40 %, as well as an improvement of the thermal comfort of the occupants if no air-conditioning systems were used.

#### D.4.3. Night ventilation strategies

Free cooling by enhanced night-time ventilation is also an efficient technique to decrease cooling demands, especially when integrated with sensors. The air flow-rates during the night in summer could be modified depending on the outdoor air conditions, requiring the installation of temperature sensors which could add intelligence to the system so as to determine when to activate the systems.

The secondary baseline allows analyzing different night ventilation strategies, as mentioned in Chapter 4. The following figures show an example of its effect both in free-floating and when considering a standard user (with air-conditioning).

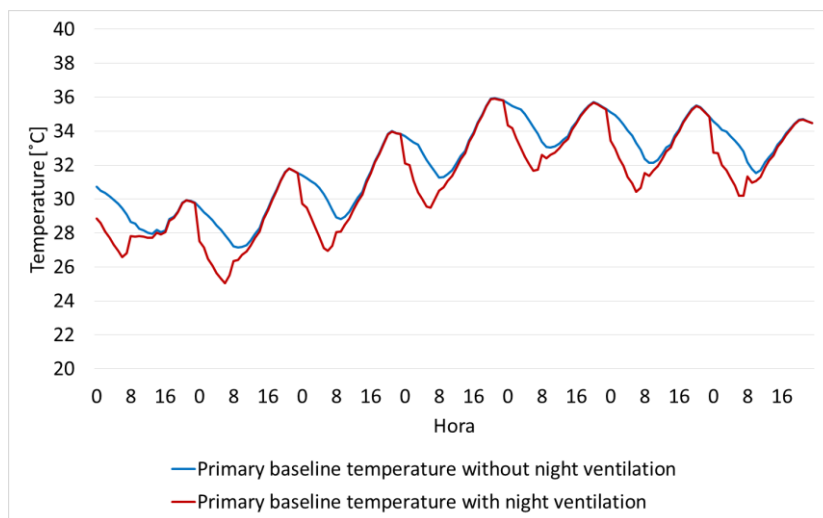


Figure 161: Example of baseline in summer with and without night ventilation. Free-floating mode.

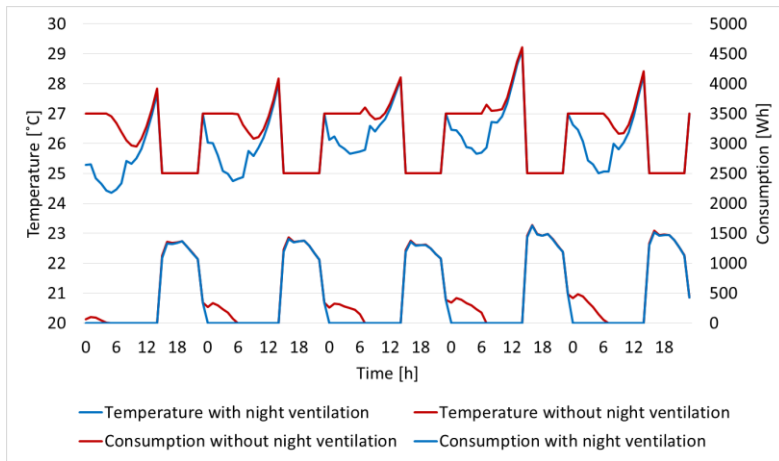


Figure 162: Example of the evolution of the indoor temperature and consumption with and without night ventilation. 6<sup>th</sup> to 10<sup>th</sup> of July. Standard climate and user.

The strategies that have been analyzed are:

- Night ventilation during 8 hours with 4 Air Changes per Hour (ACH).
- 8 ACH during the night only if the outdoor temperature is below 25°C.
- 12 ACH during the night only if the outdoor temperature is below 25°C.

These last two strategies would need the installation of a temperature sensor and a control system.

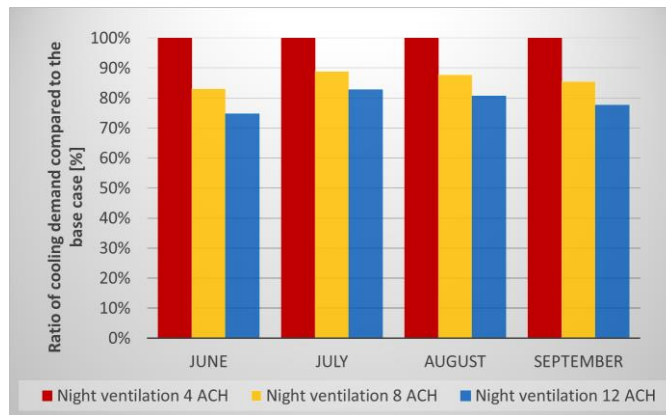


Figure 163: Results of cooling demand reduction for the analyzed solar control strategies.

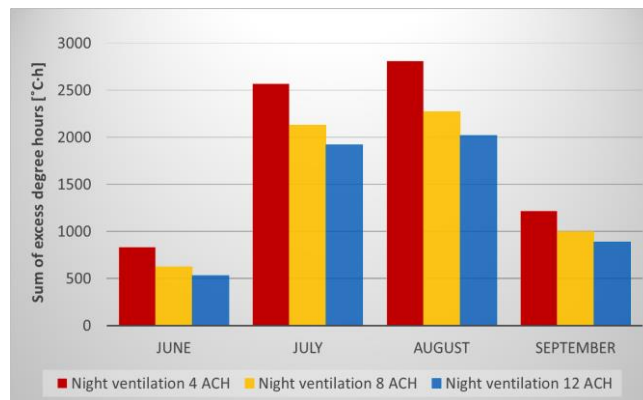


Figure 164: Results of excess degree-hours reduction for the analyzed solar control strategies.

The proposed night ventilation strategies are also able to reduce the cooling demands up to 25 %, as well as improve noticeably the indoor conditions if no air-conditioning systems were used.



#### D.4.4. Evaluating the economics

Once the results of energy demands were obtained for the evaluated solar control and night ventilation approaches, it is necessary to evaluate the investments needed for their implementation. Without this assessment, it would not be possible to quantify their feasibility in a proper way, since high investments could be done for systems with minimum savings. The following table shows the estimated investments that would be necessary for each of the analyzed strategies. These investments were estimated by searching information published by many manufacturers of the needed devices, including the gateway, temperature sensors, motion sensors and other devices that would be needed for the implementation of the strategies.

Strategy	Total investment [€]	Annual savings [€/year]
VENT_NOCT_DSM4	0 €	0.0
VENT_NOCT_DSM8	503 €	18.4
VENT_NOCT_DSM12	503 €	28.0
SC_ST	0 €	0.0
SC_PRES	1,860 €	30.1
SC_PRES_LIGHT	1,860 €	39.2

Table 24: Total costs and annual savings of the strategies that were evaluated.

As is apparent, the energy savings linked to the approaches that were evaluated are not enough to obtain acceptable repayment periods, since the necessary investments are quite high. In the case of the solar control strategies, this conclusion is even more evident. The reason is that the necessary actuators of the windows and the communication system with the gateway still have high costs. One possible and more affordable solution in the future will be the substitution of the windows for others which already have integrated temperature, motion and luminosity sensors.

#### D.4.5. Conclusions

The results have revealed the great potential of the proposed strategies in order to improve the thermal comfort of buildings, as well as the energy and economic savings that may be achieved. Solar control and night ventilation strategies are interesting solutions when cooling buildings (with savings around 30%), and this annex combined them with sensors and actuators which until recently were traditionally used only in smart homes. However, the high costs of the needed devices (especially for solar shading systems) do not allow yet to obtain high economic profits.



# ANNEX E. JOURNAL PUBLICATIONS

This annex includes a summary of the journal publications made by the author of this Thesis, as well as the front page of the published manuscripts.

Number	Title	Journal	Year	Citations (Updated 09/10/18)
1	Analysis of the economic feasibility and reduction of a building's energy consumption and emissions when integrating hybrid solar thermal/PV/ micro-CHP systems	Applied Energy	2016	50
2	Assessment of the photovoltaic potential at urban level based on 3D city models: A case study and new methodological approach	Solar Energy	2017	14
3	Setting intelligent city tiling strategies for urban shading simulations	Solar Energy	2017	4
4	New 3D model based urban energy simulation for climate protection concepts	Energy and Buildings	2018	3
5	Contributions of heat pumps to demand response: A case study of a plus-energy dwelling	Applied Energy	2018	4
6	Mitigating energy poverty: potential contributions of combining PV and building thermal mass storage	Energy conversion and management	2018	0
7	Heuristic Optimization of Clusters of Heat Pumps: A Simulation and Case Study of Residential Frequency Reserve	Applied Energy	2018 (In press)	0

## E.1 Analysis of the economic feasibility and reduction of a building's energy consumption and emissions when integrating hybrid solar thermal/PV/ micro-CHP systems

Applied Energy 165 (2016) 828–838

---



ELSEVIER

Contents lists available at ScienceDirect

# Applied Energy

journal homepage: [www.elsevier.com/locate/apenergy](http://www.elsevier.com/locate/apenergy)



---

## Analysis of the economic feasibility and reduction of a building's energy consumption and emissions when integrating hybrid solar thermal/PV/ micro-CHP systems

Laura Romero Rodríguez <sup>a,\*</sup>, José Manuel Salmerón Lissén <sup>a</sup>, José Sánchez Ramos <sup>b</sup>, Enrique Ángel Rodríguez Jara <sup>b</sup>, Servando Álvarez Domínguez <sup>a</sup>

<sup>a</sup> Grupo de Termotecnia, Escuela Superior de Ingenieros, Universidad de Sevilla, Camino de los Descubrimientos S/N, 41 092 Sevilla, Spain  
<sup>b</sup> Escuela Superior de Ingeniería, Departamento de Máquinas y Motores Térmicos, Universidad de Cádiz, C/Chile 1, 1 1002 Cádiz, Spain

 CrossMark

---

**HIGHLIGHTS**

- Several designs of hybrid systems are analysed in different locations of Spain.
- An innovative electricity consumption profile for dwellings is presented.
- The relevance of the cogeneration engine working hours is emphasised.
- Primary energy consumption, emissions and Life Cycle Costs are calculated.
- All the case studies are compared in order to determine the most optimal solutions.

---

**ARTICLE INFO**

*Article history:*  
 Received 20 July 2015  
 Received in revised form 15 December 2015  
 Accepted 17 December 2015  
 Available online 11 January 2016

*Keywords:*  
 Energy consumption in buildings  
 Distributed generation  
 Hybrid systems  
 Micro-CHP  
 Microcogeneration  
 TRNSYS

**ABSTRACT**

The aim of this paper is to assess the performance of several designs of hybrid systems composed of solar thermal collectors, photovoltaic panels and natural gas internal combustion engines. The software TRNSYS 17 has been used to perform all the calculations and data processing, as well as an optimisation of the tank volumes through an add-in coupled with the GENOPT® software. The study is carried out by analysing the behaviour of the designed systems and the conventional case in five different locations of Spain with diverse climatic characteristics, evaluating the same building in all cases. Regulators, manufacturers and energy service engineers are the most interested in these results.

Two major contributions in this paper are the calculations of primary energy consumption and emissions and the inclusion of a Life Cycle Cost analysis. A table which shows the order of preference regarding those criteria for each considered case study is also included. This was fulfilled in the interest of comparing between the different configurations and climatic zones so as to obtain conclusions on each of them. The study also illustrates a sensibility analysis regarding energy prices. Finally, the exhaustive literature review, the novel electricity consumption profile of the building and the illustration of the influence of the cogeneration engine working hours are also valuable outputs of this paper, developed in order to address the knowledge gap and the ongoing challenges in the field of distributed generation.

© 2015 Elsevier Ltd. All rights reserved.

---

**1. Introduction**

*1.1. Background and main achievements*

In the recent years, the concept of energy efficiency has been receiving widespread attention due to the realization that fossil fuel resources required for energy generation are finite and that

climate change is linked to carbon emissions. This has encouraged a tremendous amount of studies with different approaches related to the implementation of technologies capable of both producing energy in a more efficient way and diminishing its environmental impact.

These studies include the use of technologies such as Combined Heat and Power (CHP) production, also known as cogeneration systems, which are able to produce electricity and thermal energy from the same source. They are considered to be crucial to achieve such goals by many international organisms due to their many

---

\* Corresponding author. Tel.: +34 954 487 471.  
 E-mail address: [lrr@us.es](mailto:lrr@us.es) (L. Romero Rodríguez).

<http://dx.doi.org/10.1016/j.apenergy.2015.12.080>  
 0306-2619/© 2015 Elsevier Ltd. All rights reserved.



Applied Energy

## Awards of highly cited original papers (2016)

- The effect of renewable energy consumption on economic growth: Evidence from top 38 countries, *By Bhattacharya M., Paramati S.R., Ozturk I., Bhattacharya S.*
- The Calcium-Looping technology for CO<sub>2</sub> capture: On the important roles of energy integration and sorbent behavior, *By Perejon A., Romeo L.M., Lara Y., Lisbona P., Martinez A., Valverde J.M.*
- A systematic state-of-charge estimation framework for multi-cell battery pack in electric vehicles using bias correction technique, *By Sun F., Xiong R., He H.*
- Assessing the benefits of residential demand response in a real time distribution energy market, *By Siano P., Sarno D.*
- Consumption-based emission accounting for Chinese cities, *By Mi Z., Zhang Y., Guan D., Shan Y., Liu Z., Cong R., Yuan X.-C., Wei Y.-M.*
- Optimal allocation and sizing of PV/Wind/Split-diesel/Battery hybrid energy system for minimizing life cycle cost, carbon emission and dump energy of remote residential building, *By Ogunjuyigbe A.S.O., Ayodele T.R., Akinola O.A.*
- Parabolic trough receiver with corrugated tube for improving heat transfer and thermal deformation characteristics, *By Fuqiang W., Qingzhi L., Huaizhi H., Jianyu T.*
- Least-cost options for integrating intermittent renewables in low-carbon power systems, *By Brouwer A.S., van den Broek M., Zappa W., Turkenburg W.C., Faaij A.*
- Impact of energy conservation policies on the green productivity in China's manufacturing sector: Evidence from a three-stage DEA model, *By Li K., Lin B.*
- Analysis of the economic feasibility and reduction of a building's energy consumption and emissions when integrating hybrid solar thermal/PV/micro-CHP systems, *By Romero Rodriguez L., Salmeron Lissen J.M., Sanchez Ramos J., Rodriguez Jara E.A., Alvarez Dominguez S.*
- Energy performance of building envelopes integrated with phase change materials for cooling load reduction in tropical Singapore, *By Lei J., Yang J., Yang E.-H.*
- Driving-behavior-aware stochastic model predictive control for plug-in hybrid electric buses, *By Li L., You S., Yang C., Yan B., Song J., Chen Z.*
- Green growth: The economic impacts of large-scale renewable energy development in China, *By Dai H., Xie X., Xie Y., Liu J., Masui T.*
- Methanol synthesis using captured CO<sub>2</sub> as raw material: Techno-economic and environmental assessment, *By Perez-Fortes M., Schoneberger J.C., Boulamanti A., Tzimas E.*
- Hybrid PV and solar-thermal systems for domestic heat and power provision in the UK: Techno-economic considerations, *By Herrando M., Markides C.N.*

## E.2 Assessment of the photovoltaic potential at urban level based on 3D city models: A case study and new methodological approach

Solar Energy 146 (2017) 264–275



Contents lists available at ScienceDirect

# Solar Energy

journal homepage: [www.elsevier.com/locate/solener](http://www.elsevier.com/locate/solener)



---

## Assessment of the photovoltaic potential at urban level based on 3D city models: A case study and new methodological approach

Laura Romero Rodríguez<sup>a,\*</sup>, Eric Duminił<sup>b</sup>, José Sánchez Ramos<sup>a</sup>, Ursula Eicker<sup>b</sup>

<sup>a</sup> Grupo de Termotecnia, Escuela Superior de Ingenieros, Universidad de Sevilla, Camino de los Descubrimientos s/n, 41092 Sevilla, Spain

<sup>b</sup> Research Center for Sustainable Energy Technologies, Stuttgart University of Applied Sciences, Schellingstr. 24, 70174 Stuttgart, Germany



---

**ARTICLE INFO**

*Article history:*  
 Received 8 July 2016  
 Received in revised form 20 February 2017  
 Accepted 21 February 2017  
 Available online 6 March 2017

*Keywords:*  
 Urban energy consumption  
 PV potential  
 Urban solar potential  
 Roof-top photovoltaic systems  
 Distributed generation  
 3D city models

**ABSTRACT**

The use of 3D city models combined with simulation functionalities allows to quantify energy demand and renewable generation for a very large set of buildings. The scope of this paper is to determine the solar photovoltaic potential at an urban and regional scale using CityGML geometry descriptions of every building. An innovative urban simulation platform is used to calculate the PV potential of the Ludwigsburg County in south-west Germany, in which every building was simulated by using 3D city models.

Both technical and economic potential (considering roof area and insolation thresholds) are investigated, as well as two different PV efficiency scenarios. In this way, it was possible to determine the fraction of the electricity demand that can be covered in each municipality and the whole region, deciding the best strategy, the profitability of the investments and determining optimal locations. Additionally, another important contribution is a literature review regarding the different methods of PV potential estimation and the available roof area reduction coefficients. An economic analysis and emission assessment has also been developed.

The results of the study show that it is possible to achieve high annual rates of covered electricity demand in several municipalities for some of the considered scenarios, reaching even more than 100% in some cases. The use of all available roof space (technical potential) could cover 77% of the region's electricity consumption and 56% as an economic potential with only high irradiance roofs considered. The proposed methodological approach should contribute valuably in helping policy-making processes and communicating the advantages of distributed generation and PV systems in buildings to regulators, researchers and the general public.

© 2017 Elsevier Ltd. All rights reserved.

---

### 1. Introduction

It is an undeniable fact that our present living standard strongly depends on electricity and other forms of energy. Urbanization has led to a high increase in energy use, with buildings being one of its largest contributors and playing a significant role on climate change. As part of the sustainability strategy in Europe, the Energy Performance of Buildings Directive (EU, 2010) and others such as the Renewable Energy Directive (EU, 2009) have defined a package of measures that sets the path for notable and long term improvements in the energy performance of Europe's building stock. Some examples are the introduction of Nearly Zero Energy Buildings (NZEB) or the obligation to utilize on-site renewable energy. In addition, the tendency of new regulations is to extend the system boundaries from a single building to the urban area, allowing the interaction between different energy flows.

The new concept of distributed energy generation is becoming increasingly important, with the effect that the distribution network is evolving from a once passive power-consuming to an active power-generating part of the electric power system (Srećković et al., 2016). Among the different widespread distributed energy applications, there is a growing consensus that the deployment of photovoltaic (PV) systems in buildings is an attractive option. Analyses have shown that about 60% of the roof area in Europe is suitable for solar technologies (IEA, 2002; Weiss and Biermayr, 2010), which could be solar thermal ( $S_{TH}$ ) or photovoltaics. In this work the focus is on solar photovoltaics. However, in spite of the fact that the advantages for individual buildings have been studied, there is little understanding of the potential benefits of an urban scale implementation of such systems (Jo and Otanicar, 2011).

Electricity production by PV is growing world-wide and grid-parity is a reality in many places, even in low irradiance countries such as Sweden (Molin et al., 2016). Solar radiation is a clean and abundant source of energy and PV is expected to contribute even more significantly in the future, since rooftops provide large areas suitable for solar energy exploitation. However, unlike the

---

\* Corresponding author.  
 E-mail address: [lr@us.es](mailto:lr@us.es) (L. Romero Rodríguez).

<http://dx.doi.org/10.1016/j.solener.2017.02.043>  
 0038-092X/© 2017 Elsevier Ltd. All rights reserved.

## E.3 Setting intelligent city tiling strategies for urban shading simulations

Solar Energy 157 (2017) 880–894

Contents lists available at ScienceDirect

**Solar Energy**

journal homepage: [www.elsevier.com/locate/solener](http://www.elsevier.com/locate/solener)




## Setting intelligent city tiling strategies for urban shading simulations

Laura Romero Rodríguez<sup>a,\*</sup>, Romain Nouvel<sup>b</sup>, Eric Duminił<sup>b</sup>, Ursula Eicker<sup>b</sup>

<sup>a</sup> Grupo de Termotecnia, Escuela Técnica Superior de Ingeniería, Sevilla, Spain  
<sup>b</sup> Research Center for Sustainable Energy Technologies, Stuttgart University of Applied Sciences, 70174 Stuttgart, Germany

**ARTICLE INFO**

**Keywords:**  
 Radiation models  
 Tiling strategies  
 Solar potential  
 Urban shading ratio

**ABSTRACT**

Assessing accurately the solar potential of all building surfaces in cities, including shading and multiple reflections between buildings, is essential for urban energy modelling. However, since the number of surface interactions and radiation exchanges increase exponentially with the scale of the district, innovative computational strategies are needed, some of which will be introduced in the present work. They should hold the best compromise between result accuracy and computational efficiency, i.e. computational time and memory requirements.

In this study, different approaches that may be used for the computation of urban solar irradiance in large areas are presented. Two concrete urban case studies of different densities have been used to compare and evaluate three different methods: the Perez Sky model, the Simplified Radiosity Algorithm and a new scene tiling method implemented in our urban simulation platform SimStadt, used for feasible estimations on a large scale. To quantify the influence of shading, the new concept of Urban Shading Ratio has been introduced and used for this evaluation process. In high density urban areas, this index may reach 60% for facades and 25% for roofs. Tiles of 500 m width and 200 m overlap are a minimum requirement in this case to compute solar irradiance with an acceptable accuracy. In medium density areas, tiles of 300 m width and 100 m overlap meet perfectly the accuracy requirements. In addition, the solar potential for various solar energy thresholds as well as the monthly variation of the Urban Shading Ratio have been quantified for both case studies, distinguishing between roofs and facades of different orientations.

### 1. Introduction

Urban energy modelling and simulation has seen a substantial development during the last decade, boosted by two factors: the shift of the energy transition paradigm to a city scale level and the increasingly high computational performances reached by multi-core microprocessors and Graphic Processing Units. In order to provide new digital methods for energy planning and decision support, several international research centers and private sector actors have developed urban-specific algorithms and software tools, such as CitySim (Robinson et al., 2009), UMI (Reinhart et al., 2013), or SimStadt (Nouvel et al., 2015a). These software solutions allow accurate calculations of the solar radiation on each building surface of a city. However, the scale of the case study may present a significant impediment, due to the large number of surface interactions (i.e. occlusions and reflections) and radiation exchanges which take place.

The present study addresses the issue of calculating accurately and efficiently the solar potential in such cases by using 3D city models, which are increasingly being used for complex simulations. Studies

based on these models such as the one presented here are essential for energy planning, with the aim of helping to guide the process of developing future policies and being able to make informed decisions at large scales. This work has been possible through the use of innovative tiling strategies which were implemented in an urban simulation platform. In addition, the shading and reflection effects have been quantified and compared for two case studies with medium and high building densities, including analyses on roofs and facades with different orientations.

#### 1.1. The importance of assessing the solar potential at an urban level

An accurate assessment and understanding of the solar potential of cities is paramount in the context of the urban energy transition. In the conceptual phase of new urban environments, it enables urban planners to design sustainable urban layouts and forms with optimized passive (influencing the heating and cooling demand) or active (integration of photovoltaic or solar thermal systems) solar energy strategies and better quality of life (daylighting). In existing neighborhoods, a solar

\* Corresponding author.  
 E-mail address: [lrr@us.es](mailto:lrr@us.es) (L. Romero Rodríguez).

<http://dx.doi.org/10.1016/j.solener.2017.09.017>  
 Received 9 June 2017; Received in revised form 2 September 2017; Accepted 6 September 2017  
 Available online 14 September 2017  
 0038-092X/© 2017 Elsevier Ltd. All rights reserved.



## E.4 New 3D model based urban energy simulation for climate protection concepts


Energy and Buildings 163 (2018) 79–91

Contents lists available at ScienceDirect

**Energy and Buildings**

journal homepage: [www.elsevier.com/locate/enbuild](http://www.elsevier.com/locate/enbuild)



## New 3D model based urban energy simulation for climate protection concepts

Ursula Eicker<sup>a</sup>, Maryam Zirak<sup>a,\*</sup>, Nora Bartke<sup>a</sup>, Laura Romero Rodríguez<sup>c</sup>, Volker Coors<sup>b</sup>

<sup>a</sup> Research Center for Sustainable Energy Technologies (zafh.net), University of Applied Sciences HFT Stuttgart, Germany  
<sup>b</sup> Faculty of Geoinformatics, University of Applied Sciences HFT Stuttgart, Germany  
<sup>c</sup> Grupo de Termotecnia, Escuela Técnica Superior de Ingenieros, Seville, Spain

---

**ARTICLE INFO**

*Article history:*  
 Received 31 January 2017  
 Received in revised form 7 December 2017  
 Accepted 8 December 2017  
 Available online 3 January 2018

*Keywords:*  
 Climate protection concepts  
 Urban energy simulation  
 3D city model  
 CityGML  
 Photovoltaic analysis  
 Decision making

**ABSTRACT**

Climate protection concepts for cities and regions are designed to establish CO<sub>2</sub> emission baselines and develop measures for climate change mitigation. Up to now such concepts were based on aggregated consumption and emission data and only qualitative estimations of the effect of measures were possible. To better quantify the impact of mitigation measures, a large amount of data on the building stock is needed. Very powerful analysis possibilities for an energetic and economic evaluation of scenarios arise, if continuously growing data stock organized in geographical information systems are combined with simulation models of buildings and energy systems. In this work, 3D data models in CityGML format of the entire building stock of Ludwigsburg, a German county with 34 municipalities, were used and enriched with building's year of construction and its function to allow an automatized quantifying the climate protection indicators. In this regard, the heating demand of each individual building in the region in the current state and after two refurbishment scenarios are calculated. In addition, the local solar photovoltaic potential is determined, as the exact size and orientation of each building surface is in the 3D model available. Besides, some new methodologies are described to better quantify the costs and benefits of CO<sub>2</sub> mitigation strategies on a local or regional level and to support decision making.

© 2017 Published by Elsevier B.V.

---

### 1. Introduction

Many cities and regions are committed to develop climate protection concepts and have set ambitious CO<sub>2</sub> reduction targets. In many international urban networks information and best practice examples are exchanged, such as the Cities for Climate Protection Program (CCP) established in 1993 or the C40 network founded in 2005. Local authorities are crucial actors in climate change mitigation, as they can regulate, advise, and facilitate action by local communities and stakeholders, and have considerable experience in addressing environmental impacts within the fields of energy management, transport, and planning [1]. A precondition for action is a model for local energy use and greenhouse gases, because without detailed information on urban energy flows strategy development and management of measures is not possible [2].

The determination of the baseline energy consumption and CO<sub>2</sub> emissions in climate protection concepts is today mainly based on aggregated statistics or average values. Whereas, in a bottom up approach specific values related to the building space and the building footprint as a function of buildings' type and age are used to determine the status quo of consumption [3–5]. Such approaches have the advantage to include occupant behaviour and macro-economic and socioeconomic effects in the consumption, but its reliance on historical consumption information does not necessarily allow projections for the future.

It is a major challenge to quantify and predict the urban energy demand [6]. The two main modeling strategies for building energy consumption are top-down and bottom-up methods [7,8]. Depending on the input data and structure, bottom-up methods apply either statistical or physical models [9]. The former has some limitations, like the need of a large sample group, and not specifying the impact of the energy conservation measures, which is important for urban energy strategies. Modeling the thermal energy consumption with a physical approach is based on algorithms like quasi-steady state or dynamic hourly models using geometrical and semantic data [10].

Urban energy modeling is computationally intensive, due to the increasing level of detail and amount of building data, such as construction and usage data, attached. Either the processing power can

\* Corresponding author at: Hochschule für Technik Stuttgart, Schellingstrasse 24, 70174 Stuttgart, Germany.  
 E-mail address: [Maryam.Zirak@hft-stuttgart.de](mailto:Maryam.Zirak@hft-stuttgart.de) (M. Zirak).

<https://doi.org/10.1016/j.enbuild.2017.12.019>  
 0378-7788/© 2017 Published by Elsevier B.V.



## E.5 Contributions of heat pumps to demand response: A case study of a plus-energy dwelling

Applied Energy 214 (2018) 191–204



Contents lists available at ScienceDirect

## Applied Energy

journal homepage: [www.elsevier.com/locate/apenergy](http://www.elsevier.com/locate/apenergy)



---

### Contributions of heat pumps to demand response: A case study of a plus-energy dwelling

Laura Romero Rodríguez<sup>a,\*</sup>, José Sánchez Ramos<sup>a</sup>, Servando Álvarez Domínguez<sup>a</sup>, Ursula Eicker<sup>b</sup>

<sup>a</sup> Grupo de Termotecnia, Escuela Técnica Superior de Ingenieros, Sevilla, Spain

<sup>b</sup> Research Center for Sustainable Energy Technologies, Stuttgart University of Applied Sciences, 70174 Stuttgart, Germany



---

#### HIGHLIGHTS

- Assessment of several dynamic pricing strategies in a plus-energy dwelling.
- Evaluation of consumption, cost, heat pump use in peak hours and thermal comfort.
- Using heat pumps and the storage capacity of buildings for DR proved highly beneficial.
- Optimal strategies were found choosing different temperature and price thresholds.
- Cost savings up to 25% may be achieved without significant thermal comfort losses.

---

#### ARTICLE INFO

**Keywords:**  
Demand response  
Demand side management  
Dynamic pricing  
Setpoint temperature  
Plus energy dwellings

#### ABSTRACT

Demand Response programs are increasingly used in the electricity sector, since they allow consumers to play a significant role for balancing supply and demand by reducing or shifting their electricity consumption. For that purpose, incentives such as time-based rates have been proposed. The present study analyzes the potential benefits of operating the heat pump of a plus-energy dwelling which participates in a dynamic pricing market, benefitting from the thermal storage capacity of the building. The software TRNSYS 17 has been used to model the building and the supply system. A validation of the model was carried out by using available measurements of the dwelling.

Three setpoint temperature scenarios have been considered for sixteen different strategies which depend on temperature and electricity price thresholds, with the aim of determining which alternatives could lead to significant savings while maintaining an acceptable thermal comfort. Several factors such as cost savings, heat pump consumption, ratio of self-consumption of the dwelling and use of the heat pump during peak hours were also evaluated in every case.

The results show that dynamic price thresholds should be used instead of fixed price thresholds, which may cause low activations of the heat pump or overheat the building above the comfort limits. Cost savings up to 25% may be achieved by using optimal strategies, increasing the self-consumption ratio, having almost no influence on the thermal comfort and achieving significant peak reductions on the grid. The outcomes of this study show the importance of looking at the implications of such strategies on several criteria within a demand response framework.

---

#### 1. Introduction the need for demand response

Unlike other energy resources, electricity has to be used when it is generated, since its storage on a large scale is still an intricate task. Utility companies increasingly have to deal with peak demands in constrained networks, so regulating the electricity use is critical. The grid frequency is the indicator of the balance between supply and demand, dropping when the consumption exceeds the supply and

increasing when generation exceeds consumption. In addition, with the increasing penetration of intermittent renewable generation there is a growing need for ancillary services to absorb the related disruptions [1].

Blackouts happen if the supply is incapable of meeting the demand, which can be solved either by investing in new power plants and transmission lines, or by reducing the electricity demand. However, the first option might not be economically feasible, since critical periods

---

<sup>\*</sup> Corresponding author.  
E-mail address: [lrr@us.es](mailto:lrr@us.es) (L. Romero Rodríguez).

<https://doi.org/10.1016/j.apenergy.2018.01.086>

Received 6 November 2017; Received in revised form 25 January 2018; Accepted 28 January 2018

Available online 02 February 2018

0306-2619/ © 2018 Elsevier Ltd. All rights reserved.

## E.6 Mitigating energy poverty: potential contributions of combining PV and building thermal mass storage

Energy Conversion and Management 173 (2018) 65–80



Contents lists available at ScienceDirect

## Energy Conversion and Management

journal homepage: [www.elsevier.com/locate/enconman](http://www.elsevier.com/locate/enconman)



---

### Mitigating energy poverty: Potential contributions of combining PV and building thermal mass storage in low-income households

Laura Romero Rodríguez<sup>a,\*</sup>, José Sánchez Ramos<sup>b</sup>, MCamen Guerrero Delgado<sup>a</sup>,  
José Luis Molina Félix<sup>a</sup>, Servando Álvarez Domínguez<sup>a</sup>

<sup>a</sup> Grupo de Termotecnia, Escuela Técnica Superior de Ingenieros, University of Sevilla, Spain  
<sup>b</sup> Departamento de Máquinas y Motores Térmicos, University of Cadiz, Spain



---

**ARTICLE INFO**

**Keywords:**  
Energy poverty  
Fuel poverty  
PV potential  
Thermal comfort

**ABSTRACT**

The issue of energy poverty has devastating implications for the society, and it has been aggravated in the past years due to the economic crisis and the increase of energy prices. Among the most affected are those with low incomes and living in inefficient buildings. Unfortunately, the bitter reality is that sometimes this part of the population are facing the next question: Heating, or eating? The declining prices of distributed energy technologies such as photovoltaics provides an opportunity for positive social change. Although their use does not address energy poverty directly, substantial contributions may be made.

Measurements of indoor temperatures in a social housing district of southern Spain in 2017 have revealed the unbearable temperatures that the occupants have to endure, both in summer and winter. Using this district as a case study, the present work aims to evaluate the benefits of exploiting its rooftop PV potential to cover part of the electricity consumption of the district (reducing the energy bills), and use the surplus electricity to supply power for the heat pumps in the district. Optimal alternatives regarding maximum PV production, maximum self-sufficiency ratio and minimum investment costs have been found, considering as well different options when sharing the available electricity surplus to improve the thermal comfort of the occupants. As far as the authors know, no previous study has followed an approach aimed at energy poverty alleviation such as the one presented in this work. The results show that using the surplus electricity to heat or cool the whole dwellings would improve the thermal comfort of the occupants in average up to 11% in winter and 26% in summer. If all the PV generation was used or more buildings in the area were employed to install PV modules, improvements up to 33% in winter and 67% in summer could be obtained, reducing at the same time the thermal comfort differences among the dwellings of the district.

---

#### 1. Introduction

##### 1.1. Background

Cities have become one of the cornerstones in fighting climate change due to their increasing electricity demand. Although in the past this was mostly covered by using fossil fuels in large centralized power plants, the use of renewable energies is becoming widespread due to their proven contribution to mitigate global warming and the fact that they provide local, clean and abundant sources of energy. The transition to smart microgrids which make use of distributed renewable energy generation systems such as photovoltaic (PV) or wind energy is also being promoted, and there is a huge potential to utilize them not only to satisfy demand and provide decentralized generation, but also

to help tackling fuel poverty and achieving emission reductions [1]. Due to its decreasing prices and market availability, photovoltaic generation is frequently considered to be the best candidate on a large scale.

Despite the enormous benefits of renewable energy systems (RES), there is a drawback that should be considered: an extensive use inserts uncertainty into the grid due to their dependency on weather conditions. A large amount of intermittent renewable energy in the energy system is a major challenge, since supply and demand must match at any time [2]. For this reason there is a need for power reserve, and energy storage systems play a central role since they provide the means to balance energy generation and demand. Buildings can be part of the solution in future smart grids, offering different storage potentials in the structure itself (thermal storage) or in individual units such as water

---

\* Corresponding author.  
E-mail address: [lr@us.es](mailto:lr@us.es) (L. Romero Rodriguez).

<https://doi.org/10.1016/j.enconman.2018.07.058>  
Received 28 April 2018; Received in revised form 1 July 2018; Accepted 19 July 2018  
0196-8904/ © 2018 Elsevier Ltd. All rights reserved.



## E.7 Heuristic Optimization of Clusters of Heat Pumps: A Simulation and Case Study of Residential Frequency Reserve

Applied Energy xxx (2018) xxx–xxxx

Contents lists available at ScienceDirect

**Applied Energy**

journal homepage: [www.elsevier.com](http://www.elsevier.com)

---

### ARTICLE INFO

**Keywords:**  
 Frequency restoration reserve  
 Power flexibility  
 Demand response  
 Heat pumps  
 Plus-energy dwellings

### ABSTRACT

The technological challenges of adapting energy systems to the addition of more renewables are intricately interrelated with the ways in which markets incentivize their development and deployment. Households with own onsite distributed generation augmented by electrical and thermal storage capacities (prosumers), can adjust energy use based on the current needs of the electricity grid. Heat pumps, as an established technology for enhancing energy efficiency, are increasingly seen as having potential for shifting electricity use and contributing to Demand Response (DR).

Using a model developed and validated with monitoring data of a household in a plus-energy neighborhood in southern Germany, the technical and financial viability of utilizing household heat pumps to provide power in the market for Frequency Restoration Reserve (FRR) are studied. The research aims to evaluate the flexible electrical load offered by a cluster of buildings whose heat pumps are activated depending on selected rule-based participation strategies.

Given the prevailing prices for FRR in Germany, the modelled cluster was unable to reduce overall electricity costs and thus was unable to show that DR participation as a cluster with the heat pumps is financially viable. Five strategies that differed in the respective contractual requirements that would need to be agreed upon between the cluster manager and the aggregator were studied. The relatively high degree of flexibility necessary for the heat pumps to participate in FRR activations could be provided to varying extents in all strategies, but the minimum running time of the heat pumps turned out to be the primary limiting physical (and financial) factor. The frequency, price and duration of the activation calls from the FRR are also vital to compensate the increase of the heat pumps' energy use. With respect to thermal comfort and self-sufficiency constraints, the buildings were only able to accept up to 34% of the activation calls while remaining within set comfort parameters. This, however, also depends on the characteristics of the buildings. Finally, a sensitivity analysis showed that if the FRR market changed and the energy prices were more advantageous, the proposed approaches could become financially viable. This work suggests the need for further study of the role of heat pumps in flexibility markets and research questions concerning the aggregation of local clusters of such flexible technologies.

---

### 1. Introduction

As countries continue to implement support mechanisms for volatile renewable energy production, the systems and processes needed to maintain balance in power grids continue to increase in importance, and are consequential for the success of energy transitions. Methods for accommodating this volatile generation in the grid are being supported by new technologies (e.g., battery storage), regulatory measures such as strategic stability reserve plants, and innovation in the private sector

with tariffs incentivizing flexible demand for electricity users [1,2]. The demand side has been acknowledged as an important part of ensuring this future stability in power grids more dependent on the fluctuations of renewables [3]. Especially, heating applications coupled with heat storage have shown promise in providing a significant contribution to power grid stability. Heat pumps, especially when they are ground coupled, offer the potential to both increase efficiency in building heating applications while being able to use available excess power from distributed renewables [4].

---

Email address: [lr@us.es](mailto:lr@us.es) (L.R. Rodríguez)

<https://doi.org/10.1016/j.apenergy.2018.09.103>  
 Received 28 April 2018; Received in revised form 6 July 2018; Accepted 9 September 2018  
 Available online xxx  
 0306-2619/© 2018.



# REFERENCES

---

- [1] European Commission. 2050 low-carbon economy n.d. [https://ec.europa.eu/clima/policies/strategies/2050\\_en](https://ec.europa.eu/clima/policies/strategies/2050_en).
- [2] European Commission. 2030 Energy Strategy n.d. <https://ec.europa.eu/energy/en/topics/energy-strategy-and-energy-union/2030-energy-strategy>.
- [3] European Commission. 2020 climate & energy package n.d. [https://ec.europa.eu/clima/policies/strategies/2020\\_en](https://ec.europa.eu/clima/policies/strategies/2020_en).
- [4] Rueda S. Charter for the ecosystemic planning of cities: Charter for designing new urban developments and regenerating existing ones. 2018.
- [5] Mkrtychev O, Starchyk Y, Yusupova S, Zaytceva O. Analysis of various definitions for Smart City concept. IOP Conf Ser Mater Sci Eng 2018;365. doi:10.1088/1757-899X/365/2/022065.
- [6] Meeus L, Delarue E, Fernandes E de O, Leal V, Azevedo I, Glachant J-M, et al. Smart Cities Initiative: how to foster a quick transition towards local sustainable energy systems. 2010. doi:10.2870/34539.
- [7] Prajapati JK, Ghadiali S, Vora DR. Smart Grid – A Vision For The Future 2012:672–7.
- [8] Ancillotti E, Bruno R, Conti M. The role of communication systems in smart grids: Architectures, technical solutions and research challenges. Comput Commun 2013;36:1665–97. doi:10.1016/j.comcom.2013.09.004.
- [9] Gungor VC, Sahin D, Kocak T, Ergut S, Buccella C, Cecati C, et al. Smart Grid Technologies: Communication Technologies and Standards. IEEE Trans Ind Informatics 2011;7:529–39. doi:10.1109/TII.2011.2166794.
- [10] Ellis M. Smart grid: The components and integrating communication. 2012 IEEE Green Technol Conf 2012. doi:10.1109/GREEN.2012.6200970.
- [11] Thermal S, Storage E, To R, Flexibility P, Grid THEE. Heavy weight buildings – analysis and final report structural thermal energy storage in heavy weight buildings n.d.
- [12] Reynders G. Quantifying the impact of building design on the potential of structural storage for active demand response in residential buildings 2015:266. doi:10.13140/RG.2.1.3630.2805.
- [13] Carvalho AD, Moura P, Vaz GC, De Almeida AT. Ground source heat pumps as high efficient solutions for building space conditioning and for integration in smart grids. Energy Convers Manag 2015;103:991–1007. doi:10.1016/j.enconman.2015.07.032.
- [14] Arteconi A, Patteeuw D, Bruninx K, Delarue E, D’haeseleer W, Helsen L. Active demand response with electric heating systems: Impact of market penetration. Appl Energy 2016;177:636–48. doi:10.1016/j.apenergy.2016.05.146.
- [15] Patteeuw D, Henze GP, Helsen L. Comparison of load shifting incentives for low-energy buildings with heat pumps to attain grid flexibility benefits. Appl Energy 2016;167:80–92. doi:10.1016/j.apenergy.2016.01.036.
- [16] Aduda KO, Labeodan T, Zeiler W, Boxem G, Zhao Y. Demand side flexibility: Potentials and building performance implications. Sustain Cities Soc 2016;22:146–63. doi:10.1016/j.scs.2016.02.011.
- [17] Xu P. Evaluation of Demand Shifting Strategies With Thermal Mass in Two Large Commercial Buildings. Simbuild 2006 91AD:91–8.

- [18] Synnefa A, Laskari M, Gupta R, Pisello AL, Santamouris M. Development of Net Zero Energy Settlements Using Advanced Energy Technologies. *Procedia Eng* 2017;180:1388–401. doi:10.1016/j.proeng.2017.04.302.
- [19] Santamouris M. Innovating to zero the building sector in Europe: Minimising the energy consumption, eradication of the energy poverty and mitigating the local climate change. *Sol Energy* 2016;128:61–94. doi:10.1016/J.SOLENER.2016.01.021.
- [20] Nadav Malin. The Problem with Net-Zero Buildings n.d. <https://www.buildinggreen.com/feature/problem-net-zero-buildings-and-case-net-zero-neighborhoods>.
- [21] Koutra S, Becue V, Gallas MA, Ioakimidis CS. Towards the development of a net-zero energy district evaluation approach: A review of sustainable approaches and assessment tools. *Sustain Cities Soc* 2018;39:784–800. doi:10.1016/j.scs.2018.03.011.
- [22] Aghamolaei R, Shamsi MH, Tahsildoost M. A Review of District-scale Energy Performance Analysis: Outlooks towards Holistic Urban Frameworks. *Sustain Cities Soc* 2018;98:1–30. doi:10.1016/j.scs.2018.05.048.
- [23] European Commission. H2020 Topic: Smart Cities and Communities n.d. <http://ec.europa.eu/research/participants/portal/desktop/en/opportunities/h2020/topics/lc-sc3-scc-1-2018-2019-2020.html>.
- [24] Fonseca JA, Schlueter A. Integrated model for characterization of spatiotemporal building energy consumption patterns in neighborhoods and city districts. *Appl Energy* 2015;142:247–65. doi:10.1016/j.apenergy.2014.12.068.
- [25] International Energy Agency (IEA). *Energy Efficient Communities: Case Studies and Strategic Guidance for Urban Decision Makers (Annex 51)* 2014.
- [26] McKenna R, Merkel E, Fichtner W. Energy autonomy in residential buildings: A techno-economic model-based analysis of the scale effects. *Appl Energy* 2017;189:800–15. doi:10.1016/j.apenergy.2016.03.062.
- [27] Polly B, Kutscher C, Macumber D, Schott M, Pless S, Livingood B, et al. From Zero Energy Buildings to Zero Energy Districts. *ACEEE Summer Study Energy Effic. Build.*, 2017.
- [28] Sandvall AF, Ahlgren EO, Ekvall T. Cost-efficiency of urban heating strategies – Modelling scale effects of low-energy building heat supply. *Energy Strateg Rev* 2017;18:212–23. doi:10.1016/j.esr.2017.10.003.
- [29] Nutkiewicz A, Yang Z, Jain RK. Data-driven Urban Energy Simulation (DUE-S): A framework for integrating engineering simulation and machine learning methods in a multi-scale urban energy modeling workflow. *Appl Energy* 2018;225:1176–89. doi:10.1016/j.apenergy.2018.05.023.
- [30] Tardioli G, Kerrigan R, Oates M, O'Donnell J, Finn D. Data driven approaches for prediction of building energy consumption at urban level. *Energy Procedia* 2015;78:3378–83. doi:10.1016/j.egypro.2015.11.754.
- [31] Biljecki F, Ledoux H, Stoter J. An improved LOD specification for 3D building models. *Comput Environ Urban Syst* 2016;59:25–37. doi:10.1016/J.COMPENVURBSYS.2016.04.005.
- [32] Biljecki F, Stoter J, Ledoux H, Zlatanova S, Çöltekin A. Applications of 3D City Models: State of the Art Review. *ISPRS Int J Geo-Information* 2015;4:2842–89. doi:10.3390/ijgi4042842.
- [33] Monien D, Strzalka A, Koukofikis A, Coors V, Eicker U. Comparison of building modelling assumptions and methods for urban scale heat demand forecasting. *Futur Cities Environ* 2017;3:2. doi:10.1186/s40984-017-0025-7.

- [34] Ghiassi N, Mahdavi A. Reductive bottom-up urban energy computing supported by multivariate cluster analysis. *Energy Build* 2017;144:372–86.
- [35] Morille B, Lauzet N, Musy M. SOLENE-microclimate: A tool to evaluate envelopes efficiency on energy consumption at district scale. *Energy Procedia* 2015;78:1165–70. doi:10.1016/j.egypro.2015.11.088.
- [36] Li X, Yao R, Liu M, Costanzo V, Yu W, Wang W, et al. Developing urban residential reference buildings using clustering analysis of satellite images. *Energy Build* 2018;169:417–29. doi:10.1016/j.enbuild.2018.03.064.
- [37] Izquierdo S, Rodrigues M, Fueyo N. A method for estimating the geographical distribution of the available roof surface area for large-scale photovoltaic energy-potential evaluations. *Sol Energy* 2008;82:929–39. doi:10.1016/j.solener.2008.03.007.
- [38] IEA. Potential for building integrated photovoltaics. Rep IEA - PVPS T7-4 2002;2002.
- [39] CUNY. New York City Solar Map. <http://www.cuny.edu/about/resources/sustainability/solar-america/map.html> 2016.
- [40] LUBW. Roof surface potential analyse of the Landesanstalt für Umwelt, Messungen und Naturschutz Baden-Württemberg (LUBW). <http://www.energieatlas-bw.de/sonne/dachflächen> 2015.
- [41] Molin A, Schneider S, Rohdin P, Moshfegh B. Assessing a regional building applied PV potential – Spatial and dynamic analysis of supply and load matching. *Renew Energy* 2016;91:261–74. doi:10.1016/j.renene.2016.01.084.
- [42] Freitas S, Catita C, Redweik P, Brito MC. Modelling solar potential in the urban environment: State-of-the-art review. *Renew Sustain Energy Rev* 2015;41:915–31. doi:10.1016/j.rser.2014.08.060.
- [43] Horváth M, Kassai-Szoó D, Csoknyai T. Solar energy potential of roofs on urban level based on building typology. *Energy Build* 2016;111:278–89. doi:10.1016/j.enbuild.2015.11.031.
- [44] Shukla KN, Rangnekar S, Sudhakar K. Comparative study of isotropic and anisotropic sky models to estimate solar radiation incident on tilted surface: A case study for Bhopal, India. *Energy Reports* 2015;1:96–103. doi:10.1016/j.egypr.2015.03.003.
- [45] Romero Rodríguez L, Nouvel R, Duminil E, Eicker U. Setting intelligent city tiling strategies for urban shading simulations. *Sol Energy* 2017. doi:10.1016/j.solener.2017.09.017.
- [46] Jo JH, Otanicar TP. A hierarchical methodology for the mesoscale assessment of building integrated roof solar energy systems. *Renew Energy* 2011;36:2992–3000. doi:10.1016/j.renene.2011.03.038.
- [47] Schallenberg-Rodríguez J. Photovoltaic techno-economical potential on roofs in regions and islands: The case of the Canary Islands. Methodological review and methodology proposal. *Renew Sustain Energy Rev* 2013;20:219–39. doi:10.1016/j.rser.2012.11.078.
- [48] Li D, Liu G, Liao S. Solar potential in urban residential buildings. *Sol Energy* 2015;111:225–35. doi:10.1016/j.solener.2014.10.045.
- [49] Karteris M, Slini T, Papadopoulos AM. Urban solar energy potential in Greece: A statistical calculation model of suitable built roof areas for photovoltaics. *Energy Build* 2013;62:459–68. doi:10.1016/j.enbuild.2013.03.033.
- [50] Melius J, Margolis R, Ong S. Estimating Rooftop Suitability for PV : A Review of Methods , Patents , and Validation Techniques. Technical Report NREL/TP-6A20-60593. 2013.
- [51] Ramirez Camargo L, Zink R, Dorner W, Stoeglehner G. Spatio-temporal modeling of roof-top photovoltaic panels for improved technical potential assessment and electricity peak load offsetting at the municipal scale. *Comput Environ Urban Syst* 2015;52:58–69.

- doi:10.1016/j.compenvurbsys.2015.03.002.
- [52] SimStadt. <http://www.simstadt.eu/en/index.html> 2016.
- [53] INSEL. A Simulation System for Renewable Energy Supply Systems. Version 8.2. <<http://www.insel.eu>> 2014.
- [54] Romero Rodríguez L, Duminil E, Sánchez Ramos J, Eicker U. Assessment of the photovoltaic potential at urban level based on 3D city models: A case study and new methodological approach. *Sol Energy* 2017;146:264–75. doi:10.1016/j.solener.2017.02.043.
- [55] Compagnon R. Solar and daylight availability in the urban fabric. *Energy Build* 2004;36:321–8. doi:10.1016/j.enbuild.2004.01.009.
- [56] Brito MC, Freitas S, Guimaraes S, Catita C, Redweik P. The importance of facades for the solar PV potential of a Mediterranean city using LiDAR data. *Renew Energy* 2017;111:85–94. doi:10.1016/j.renene.2017.03.085.
- [57] Eicker U, Zirak M, Bartke N, Rodríguez LR, Coors V. New 3D model based urban energy simulation for climate protection concepts. *Energy Build* 2018. doi:10.1016/j.enbuild.2017.12.019.
- [58] Keirstead J, Jennings M, Sivakumar A. A review of urban energy system models: Approaches, challenges and opportunities. *Renew Sustain Energy Rev* 2012;16:3847–66. doi:10.1016/J.RSER.2012.02.047.
- [59] Nouvel R, Brassel K-H, Bruse M, Duminil E, Coors V, Eicker U, et al. SIMSTADT , a New Workflow-driven Urban Energy Simulation Platform for CityGML City Models. CISBAT 2015 - Lausanne, Switz 2015:889–94.
- [60] QGIS Development Team. QGIS Geographic Information System. Open Source Geospatial Found Proj 2015. doi:<http://www.qgis.org/>.
- [61] Tardioli G, Kerrigan R, Oates M, O'Donnell J, Finn DP. Identification of representative buildings and building groups in urban datasets using a novel pre-processing, classification, clustering and predictive modelling approach. *Build Environ* 2018;140:90–106. doi:10.1016/j.buildenv.2018.05.035.
- [62] Gaitani N, Lehmann C, Santamouris M, Mihalakakou G, Patargias P. Using principal component and cluster analysis in the heating evaluation of the school building sector. *Appl Energy* 2010;87:2079–86. doi:10.1016/j.apenergy.2009.12.007.
- [63] Robert D, Brian R. Innovative Solutions for Energy Conservation Through Commercial and Domestic Demand Side Management. vol. 79. Elsevier B.V.; 2015. doi:10.1016/j.egypro.2015.11.457.
- [64] Yin R, Kara EC, Li Y, DeForest N, Wang K, Yong T, et al. Quantifying flexibility of commercial and residential loads for demand response using setpoint changes. *Appl Energy* 2016;177:149–64. doi:10.1016/j.apenergy.2016.05.090.
- [65] Gellings CW. The concept of demand-side management for electric utilities. *Proc IEEE* 1985;73:1468–70. doi:10.1109/PROC.1985.13318.
- [66] Arteconi A, Hewitt NJ, Polonara F. State of the art of thermal storage for demand-side management. *Appl Energy* 2012;93:371–89. doi:10.1016/j.apenergy.2011.12.045.
- [67] Roldán Fernández JM, Burgos Payán M, Riquelme Santos JM, Trigo García ÁL. Renewable generation versus demand-side management. A comparison for the Spanish market. *Energy Policy* 2016;96:458–70. doi:10.1016/j.enpol.2016.06.014.
- [68] Hoogvliet TW, Litjens GBMA, van Sark WGJHM. Provision of regulating- and reserve power by electric vehicle owners in the Dutch market. *Appl Energy* 2017;190:1008–19. doi:10.1016/j.apenergy.2017.01.006.



- [69] Chassin DP, Stoustrup J, Agathoklis P, Djilali N. A new thermostat for real-time price demand response: Cost, comfort and energy impacts of discrete-time control without deadband. *Appl Energy* 2015;155:816–25. doi:10.1016/j.apenergy.2015.06.048.
- [70] Bertoldi P, Zancanella P, Boza-Kiss B. Demand Response status in EU Member States. 2016. doi:10.2790/962868.
- [71] SEDC. Mapping Demand Response in Europe Today. SEDC Smart Energy Demand Coalit 2014:92.
- [72] Hu Z, Kim JH, Wang J, Byrne J. Review of dynamic pricing programs in the U.S. And Europe: Status quo and policy recommendations. *Renew Sustain Energy Rev* 2015;42:743–51. doi:10.1016/j.rser.2014.10.078.
- [73] Ogunjuyigbe ASO, Monyei CG, Ayodele TR. Price based demand side management: A persuasive smart energy management system for low/medium income earners. *Sustain Cities Soc* 2015;17:80–94. doi:10.1016/j.scs.2015.04.004.
- [74] Gottwalt S, Ketter W, Block C, Collins J, Weinhardt C. Demand side management-A simulation of household behavior under variable prices. *Energy Policy* 2011;39:8163–74. doi:10.1016/j.enpol.2011.10.016.
- [75] Finn P, Fitzpatrick C. Demand side management of industrial electricity consumption: Promoting the use of renewable energy through real-time pricing. *Appl Energy* 2014;113:11–21. doi:10.1016/j.apenergy.2013.07.003.
- [76] Doostizadeh M, Ghasemi H. A day-ahead electricity pricing model based on smart metering and demand-side management. *Energy* 2012;46:221–30. doi:10.1016/j.energy.2012.08.029.
- [77] Campillo J, Dahlquist E, Wallin F, Vassileva I. Is real-time electricity pricing suitable for residential users without demand-side management? *Energy* 2016;109:310–25. doi:10.1016/j.energy.2016.04.105.
- [78] Barbato A, Capone A, Chen L, Martignon F, Paris S. A distributed demand-side management framework for the smart grid. *Comput Commun* 2015;57:13–24. doi:10.1016/j.comcom.2014.11.001.
- [79] Blasques LCM, Pinho JT. Metering systems and demand-side management models applied to hybrid renewable energy systems in micro-grid configuration. *Energy Policy* 2012;45:721–9. doi:10.1016/j.enpol.2012.03.028.
- [80] Kyriakarakos G, Piromalis DD, Dounis AI, Arvanitis KG, Papadakis G. Intelligent demand side energy management system for autonomous polygeneration microgrids. *Appl Energy* 2013;103:39–51. doi:10.1016/j.apenergy.2012.10.011.
- [81] Ghasemi A, Shayeghi H, Moradzadeh M, Nooshyar M. A novel hybrid algorithm for electricity price and load forecasting in smart grids with demand-side management Sub-Business Entities Commercial users. *Appl Energy* 2016;177:40–59. doi:10.1016/j.apenergy.2016.05.083.
- [82] Jalali MM, Kazemi A. Demand side management in a smart grid with multiple electricity suppliers. *Energy* 2015;81:766–76. doi:10.1016/j.energy.2015.01.027.
- [83] Stimoniari D, Kollatou T, Tsiमितros D, Zehir MA, Batman A, Bagriyanik M, et al. Demand-side management by integrating bus communication technologies into smart grids. *Electr Power Syst Res* 2016;136:251–61. doi:10.1016/j.epsr.2016.02.026.
- [84] Muralitharan K, Sakthivel R, Shi Y. Multiobjective optimization technique for demand side management with load balancing approach in smart grid. *Neurocomputing* 2016;177:110–9. doi:10.1016/j.neucom.2015.11.015.
- [85] Macedo MNQ, Galo JJM, De Almeida LAL, De C. Lima AC. Demand side management using artificial neural networks in a smart grid environment. *Renew Sustain Energy Rev* 2015;41:128–33. doi:10.1016/j.rser.2014.08.035.

- [86] Mahmood A, Ullah MN, Razzaq S, Basit A, Mustafa U, Naeem M, et al. A new scheme for demand side management in future smart grid networks. *Procedia Comput Sci* 2014;32:477–84. doi:10.1016/j.procs.2014.05.450.
- [87] Gelazanskas L, Gamage KAA. Demand side management in smart grid: A review and proposals for future direction. *Sustain Cities Soc* 2014;11:22–30. doi:10.1016/j.scs.2013.11.001.
- [88] Qureshi W a., Nair N-KC, Farid MM. Impact of energy storage in buildings on electricity demand side management. *Energy Convers Manag* 2011;52:2110–20. doi:10.1016/j.enconman.2010.12.008.
- [89] Wolisz H, Punkenburg C, Streblow R, Müller D. Feasibility and potential of thermal demand side management in residential buildings considering different developments in the German energy market. *Energy Convers Manag* 2016;107:86–95. doi:10.1016/j.enconman.2015.06.059.
- [90] Arteconi A, Xu J, Ciarrocchi E, Paciello L, Comodi G, Polonara F, et al. Demand Side Management of a Building Summer Cooling Load by Means of a Thermal Energy Storage. *Energy Procedia* 2015;75:3277–83. doi:10.1016/j.egypro.2015.07.705.
- [91] Laicane I, Blumberga D, Blumberga A, Rosa M. Reducing household electricity consumption through demand side management : the role of home appliance scheduling and peak load reduction. *Energy Procedia* 2015;72:222–9. doi:10.1016/j.egypro.2015.06.032.
- [92] Reynders G, Nuytten T, Saelens D. Potential of structural thermal mass for demand-side management in dwellings. *Build Environ* 2013;64:187–99. doi:10.1016/j.buildenv.2013.03.010.
- [93] Setlhaolo D, Xia X. Combined residential demand side management strategies with coordination and economic analysis. *Int J Electr Power Energy Syst* 2016;79:150–60. doi:10.1016/j.ijepes.2016.01.016.
- [94] Castillo-Cagigal M, Gutierrez A, Monasterio-Huelin F, Caamaño-Martin E, Masa D, Jimenez-Leube J. A semi-distributed electric demand-side management system with PV generation for self-consumption enhancement. *Energy Convers Manag* 2011;52:2659–66. doi:10.1016/j.enconman.2011.01.017.
- [95] Khoury J, Mbayed R, Salloum G, Monmasson E. Predictive demand side management of a residential house under intermittent primary energy source conditions. *Energy Build* 2016;112:110–20. doi:10.1016/j.enbuild.2015.12.011.
- [96] Esther BP, Kumar KS. A survey on residential Demand Side Management architecture, approaches, optimization models and methods. *Renew Sustain Energy Rev* 2016;59:342–51. doi:10.1016/j.rser.2015.12.282.
- [97] Mesaric P, Krajcar S. Home demand side management integrated with electric vehicles and renewable energy sources. *Energy Build* 2015;108:1–9. doi:10.1016/j.enbuild.2015.09.001.
- [98] Xia L, de Hoog J, Alpcan T, Brazil M, Thomas DA, Mareels I. Local measurements and virtual pricing signals for residential demand side management. *Sustain Energy, Grids Networks* 2015;4:62–71. doi:10.1016/j.segan.2015.10.002.
- [99] Beil I, Hiskens IA, Backhaus S. Round-trip efficiency of fast demand response in a large commercial air conditioner. *Energy Build* 2015;97:47–55. doi:10.1016/j.enbuild.2015.03.028.
- [100] Shen L, Li Z, Sun Y. Performance evaluation of conventional demand response at building-group-level under different electricity pricings. *Energy Build* 2016;128:143–54. doi:10.1016/j.enbuild.2016.06.082.
- [101] Yau YH, Lee SK. Feasibility study of an ice slurry-cooling coil for HVAC and R systems in a tropical building. *Appl Energy* 2010;87:2699–711. doi:10.1016/j.apenergy.2010.02.025.
- [102] Avci M, Erkoc M, Rahmani A, Asfour S. Model predictive HVAC load control in buildings using real-time electricity pricing. *Energy Build* 2013;60:199–209. doi:10.1016/j.enbuild.2013.01.008.

- [103] Alibabaei N, Fung AS, Raahemifar K, Moghimi A. Effects of intelligent strategy planning models on residential HVAC system energy demand and cost during the heating and cooling seasons. *Appl Energy* 2017;185:29–43. doi:10.1016/j.apenergy.2016.10.062.
- [104] Yoon JH, Bladick R, Novoselac A. Demand response for residential buildings based on dynamic price of electricity. *Energy Build* 2014;80:531–41. doi:10.1016/j.enbuild.2014.05.002.
- [105] Perez KX, Baldea M, Edgar TF. Integrated HVAC management and optimal scheduling of smart appliances for community peak load reduction. *Energy Build* 2016;123:34–40. doi:10.1016/j.enbuild.2016.04.003.
- [106] Escrivá-Escrivá G, Segura-Heras I, Alcázar-Ortega M. Application of an energy management and control system to assess the potential of different control strategies in HVAC systems. *Energy Build* 2010;42:2258–67. doi:10.1016/j.enbuild.2010.07.023.
- [107] Korkas CD, Baldi S, Michailidis I, Kosmatopoulos EB. Occupancy-based demand response and thermal comfort optimization in microgrids with renewable energy sources and energy storage. *Appl Energy* 2016;163:93–104. doi:10.1016/j.apenergy.2015.10.140.
- [108] Ghahramani A, Zhang K, Dutta K, Yang Z, Becerik-Gerber B. Energy savings from temperature setpoints and deadband: Quantifying the influence of building and system properties on savings. *Appl Energy* 2016;165:930–42. doi:10.1016/j.apenergy.2015.12.115.
- [109] Alimohammadisagvand B, Alam S, Mubbashir Ali, Merkebu Degefa JJ, Siren K. Influence of energy demand response actions on thermal comfort and energy cost in electrically heated residential houses. *Indoor Built Environ* 2015;0:1–19. doi:10.1177/1420326X15608514.
- [110] Baeten B, Rogiers F, Helsen L. Reduction of heat pump induced peak electricity use and required generation capacity through thermal energy storage and demand response. *Appl Energy* 2017;195:184–95. doi:10.1016/j.apenergy.2017.03.055.
- [111] Yoon JH, Baldick R, Novoselac A. Demand response control of residential HVAC loads based on dynamic electricity prices and economic analysis. *Sci Technol Built Environ* 2016;4731:1–15. doi:10.1080/23744731.2016.1195659.
- [112] Smart Energy Demand Coalition. *Explicit Demand Response in Europe*. Brussels 2017.
- [113] Klobasa M. *Dynamische Simulation eines Lastmanagements und Integration von Windenergie in ein Elektrizitätsnetz auf Landesebene unter regelungstechnischen und Kostengesichtspunkten*. 2007. doi:10.3929/ethz-a-005484330.
- [114] Dena. *Integration erneuerbarer Energien in die deutsche Stromversorgung im*. Berlin: 2010.
- [115] European Commission. *Commission Regulation (EU) 2017/2195: Establishing a guideline on electricity balancing*. Official Journal of the European Union. 2017.
- [116] Pavlak GS, Henze GP, Cushing VJ. Optimizing commercial building participation in energy and ancillary service markets. *Energy Build* 2014;81:115–26. doi:10.1016/j.enbuild.2014.05.048.
- [117] Gorecki TT, Fabiatti L, Qureshi FA, Jones CN. Experimental demonstration of buildings providing frequency regulation services in the Swiss market. *Energy Build* 2017;144:229–40. doi:10.1016/j.enbuild.2017.02.050.
- [118] Martin Almenta M, Morrow DJ, Best RJ, Fox B, Foley AM. Domestic fridge-freezer load aggregation to support ancillary services. *Renew Energy* 2016;87:954–64. doi:10.1016/j.renene.2015.08.033.
- [119] Kremers E, González de Durana JM a., Barambones O. Emergent synchronisation properties of a refrigerator demand side management system. *Appl Energy* 2013;101:709–17. doi:10.1016/j.apenergy.2012.07.021.
- [120] Fleer J, Stenzel P. Impact analysis of different operation strategies for battery energy storage systems

- providing primary control reserve. *J Energy Storage* 2016;8:320–38. doi:10.1016/j.est.2016.02.003.
- [121] Majzooobi A, Khodaei A. Application of microgrids in providing ancillary services to the utility grid. *Energy* 2017;123:555–63. doi:10.1016/j.energy.2017.01.113.
- [122] Tulabing R, Yin R, DeForest N, Li Y, Wang K, Yong T, et al. Modeling study on flexible load's demand response potentials for providing ancillary services at the substation level. *Electr Power Syst Res* 2016;140:240–52. doi:10.1016/j.epsr.2016.06.018.
- [123] Ali M, Alahaivala A, Malik F, Humayun M, Safdarian A, Lehtonen M. A market-oriented hierarchical framework for residential demand response. *Int J Electr Power Energy Syst* 2015;69:257–63. doi:10.1016/j.ijepes.2015.01.020.
- [124] Biegel B, Andersen P, Stoustrup J, Madsen MB, Hansen LH, Rasmussen LH. Aggregation and control of flexible consumers - A real life demonstration. *IFAC Proc Vol* 2014;19:9950–5. doi:10.3182/20140824-6-ZA-1003.00718.
- [125] Thien T, Schweer D, Stein D vom, Moser A, Sauer DU. Real-world operating strategy and sensitivity analysis of frequency containment reserve provision with battery energy storage systems in the german market. *J Energy Storage* 2017;13:143–63. doi:10.1016/j.est.2017.06.012.
- [126] Litjens GBMA, Worrell E, van Sark WGJHM. Economic benefits of combining self-consumption enhancement with frequency restoration reserves provision by photovoltaic-battery systems. *Appl Energy* 2018;223:172–87. doi:10.1016/j.apenergy.2018.04.018.
- [127] Kilkki O, Seilonen I, Zenger K, Vyatkin V. Optimizing residential heating and energy storage flexibility for frequency reserves. *Int J Electr Power Energy Syst* 2018;100:540–9. doi:10.1016/j.ijepes.2018.02.047.
- [128] Aliasghari P, Mohammadi-Ivatloo B, Alipour M, Abapour M, Zare K. Optimal scheduling of plug-in electric vehicles and renewable micro-grid in energy and reserve markets considering demand response program. *J Clean Prod* 2018;186:293–303. doi:10.1016/j.jclepro.2018.03.058.
- [129] Meesenburg W, Ommen T, Elmegaard B. Dynamic exergoeconomic analysis of a heat pump system used for ancillary services in an integrated energy system. *Energy* 2018;152:154–65. doi:10.1016/j.energy.2018.03.093.
- [130] Mathieu JL, Dyson MEH, Callaway DS. Resource and revenue potential of California residential load participation in ancillary services. *Energy Policy* 2015;80:76–87. doi:10.1016/j.enpol.2015.01.033.
- [131] De Coninck R, Helsen L. Quantification of flexibility in buildings by cost curves - Methodology and application. *Appl Energy* 2016;162:653–65. doi:10.1016/j.apenergy.2015.10.114.
- [132] Georges E, Cornelusse B, Ernst D, Lemort V, Mathieu S. Residential heat pump as flexible load for direct control service with parametrized duration and rebound effect. *Appl Energy* 2017;187:140–53. doi:10.1016/j.apenergy.2016.11.012.
- [133] Safdarian A, Ali M, Fotuhi-Firuzabad M, Lehtonen M. Domestic EWH and HVAC management in smart grids: Potential benefits and realization. *Electr Power Syst Res* 2016;134:38–46. doi:10.1016/j.epsr.2015.12.021.
- [134] Romero Rodríguez L, Sánchez Ramos J, Álvarez Domínguez S, Eicker U. Contributions of heat pumps to demand response: A case study of a plus-energy dwelling. *Appl Energy* 2018;214:191–204. doi:10.1016/j.apenergy.2018.01.086.
- [135] Klein SA. TRNSYS 17: A Transient System Simulation Program. Sol Energy Lab Univ Wisconsin, Madison, USA 2010;1:1–5.
- [136] Vesterberg M, Krishnamurthy CKB. Residential end-use electricity demand: Implications for real time pricing in Sweden. *Energy J*, vol. 37, 2016, p. 141–64. doi:10.5547/01956574.37.4.mves.

- [137] Eid C, Koliou E, Valles M, Reneses J, Hakvoort R. Time-based pricing and electricity demand response: Existing barriers and next steps. *Util Policy* 2016;40:15–25. doi:10.1016/j.jup.2016.04.001.
- [138] Schill W-P, Zerrahn A, Kunz F. Prosumage of Solar Electricity: Pros, Cons, and the System Perspective 2017;36. doi:10.5547/2160-5890.6.1.wsch.
- [139] Energy U. D of. M&V Guidelines: Measurement and Verification for Performance-Based Contracts n.d.
- [140] Ko J-H, Kong D-S, Huh J-H. Baseline building energy modeling of cluster inverse model by using daily energy consumption in office buildings. *Energy Build* 2017;140:317–23. doi:10.1016/j.enbuild.2017.01.086.
- [141] Zhao H, Magoulès F. A review on the prediction of building energy consumption. *Renew Sustain Energy Rev* 2012;16:3586–92. doi:10.1016/j.rser.2012.02.049.
- [142] ISO 52016-1:2017 - Energy performance of buildings -- Energy needs for heating and cooling, internal temperatures and sensible and latent heat loads -- Part 1: Calculation procedures. n.d.
- [143] Söderström T. System identification. UK: Prentice Hall International; 1989.
- [144] Sánchez Ramos J. Metodología aplicada de caracterización térmica inversa para edificios 2015.
- [145] Terés-Zubiaga J, Martín K, Erkoreka A, Sala JM. Field assessment of thermal behaviour of social housing apartments in Bilbao, Northern Spain. *Energy Build* 2013;67:118–35. doi:10.1016/j.enbuild.2013.07.061.
- [146] Tirado Herrero S, Jiménez Meneses L, López Fernández JL, Perero Van Hove E, Irigoyen Hidalgo VM, Savary P. Pobreza, vulnerabilidad y desigualdad energética. Nuevos enfoques de análisis. 2016.
- [147] Folsom Labs. Helioscope 2018. <https://www.helioscope.com/>.
- [148] Hafez AZ, Soliman A, El-Metwally KA, Ismail IM. Tilt and azimuth angles in solar energy applications – A review. *Renew Sustain Energy Rev* 2017;77:147–68. doi:10.1016/J.RSER.2017.03.131.
- [149] Mehleri ED, Zervas PL, Sarimveis H, Palyvos JA, Markatos NC. Determination of the optimal tilt angle and orientation for solar photovoltaic arrays. *Renew Energy* 2010;35:2468–75. doi:10.1016/J.RENENE.2010.03.006.
- [150] Gharakhani Siraki A, Pillay P. Study of optimum tilt angles for solar panels in different latitudes for urban applications. *Sol Energy* 2012;86:1920–8. doi:10.1016/J.SOLENER.2012.02.030.
- [151] Bakirci K. General models for optimum tilt angles of solar panels: Turkey case study. *Renew Sustain Energy Rev* 2012;16:6149–59. doi:10.1016/J.RSER.2012.07.009.
- [152] Romero Rodríguez L, Ramos JS, Delgado G, Luis J, Félix M, Álvarez Domínguez S. Mitigating energy poverty: Potential contributions of combining PV and building thermal mass storage in low-income households 2018. doi:10.1016/j.enconman.2018.07.058.
- [153] Koirala BP, Koliou E, Friege J, Hakvoort RA, Herder PM. Energetic communities for community energy: A review of key issues and trends shaping integrated community energy systems. *Renew Sustain Energy Rev* 2016;56:722–44. doi:10.1016/j.rser.2015.11.080.
- [154] Zafar R, Mahmood A, Razzaq S, Ali W, Naeem U, Shehzad K. Prosumer based energy management and sharing in smart grid. *Renew Sustain Energy Rev* 2018;82:1675–84. doi:10.1016/j.rser.2017.07.018.
- [155] Qi W, Shen B, Zhang H, Shen ZJM. Sharing demand-side energy resources - A conceptual design. *Energy* 2017;135:455–65. doi:10.1016/j.energy.2017.06.144.
- [156] Zhou Y, Wu J, Long C. Evaluation of peer-to-peer energy sharing mechanisms based on a multiagent simulation framework. *Appl Energy* 2018;222:993–1022. doi:10.1016/j.apenergy.2018.02.089.
- [157] Zhang C, Wu J, Long C, Cheng M. Review of Existing Peer-to-Peer Energy Trading Projects. *Energy*

- Procedia 2017;105:2563–8. doi:10.1016/j.egypro.2017.03.737.
- [158] Luo Y, Itaya S, Nakamura S, Davis P. Autonomous cooperative energy trading between prosumers for microgrid systems. *Proc - Conf Local Comput Networks, LCN 2014;2014–Novem:693–6*. doi:10.1109/LCNW.2014.6927722.
- [159] Zhou Y, Wang C, Wu J, Wang J, Cheng M, Li G. Optimal scheduling of aggregated thermostatically controlled loads with renewable generation in the intraday electricity market. *Appl Energy* 2017;188:456–65. doi:10.1016/j.apenergy.2016.12.008.
- [160] Long C, Wu J, Zhou Y, Jenkins N. Peer-to-peer energy sharing through a two-stage aggregated battery control in a community Microgrid. *Appl Energy* 2018;226:261–76. doi:10.1016/j.apenergy.2018.05.097.
- [161] Zhou Y, Wu J, Long C, Cheng M, Zhang C. Performance Evaluation of Peer-to-Peer Energy Sharing Models. *Energy Procedia* 2017;143:817–22. doi:10.1016/j.egypro.2017.12.768.
- [162] Long C, Wu J, Zhang C, Cheng M, Al-Wakeel A. Feasibility of Peer-to-Peer Energy Trading in Low Voltage Electrical Distribution Networks. *Energy Procedia* 2017;105:2227–32. doi:10.1016/j.egypro.2017.03.632.
- [163] Zhang C, Wu J, Cheng M, Zhou Y, Long C. A Bidding System for Peer-to-Peer Energy Trading in a Grid-connected Microgrid. *Energy Procedia* 2016;103:147–52. doi:10.1016/j.egypro.2016.11.264.
- [164] Liu N, Yu X, Wang C, Li C, Ma L, Lei J. Energy-Sharing Model with Price-Based Demand Response for Microgrids of Peer-to-Peer Prosumers. *IEEE Trans Power Syst* 2017;32:3569–83. doi:10.1109/TPWRS.2017.2649558.
- [165] Calvillo CF, Sánchez-Miralles A, Villar J, Martín F. Optimal planning and operation of aggregated distributed energy resources with market participation. *Appl Energy* 2016;182:340–57. doi:10.1016/j.apenergy.2016.08.117.
- [166] Kanchev H, Colas F, Lazarov V, Francois B. Emission reduction and economical optimization of an urban microgrid operation including dispatched PV-based active generators. *IEEE Trans Sustain Energy* 2014;5:1397–405. doi:10.1109/TSTE.2014.2331712.
- [167] Taşçıkaraoğlu A. Economic and operational benefits of energy storage sharing for a neighborhood of prosumers in a dynamic pricing environment. *Sustain Cities Soc* 2018;38:219–29. doi:10.1016/j.scs.2018.01.002.
- [168] Alam MR, St-Hilaire M, Kunz T. An optimal P2P energy trading model for smart homes in the smart grid. *Energy Effic* 2017;10:1475–93. doi:10.1007/s12053-017-9532-5.
- [169] Le Dréau J, Heiselberg P. Energy flexibility of residential buildings using short term heat storage in the thermal mass. *Energy* 2016;111:991–1002. doi:10.1016/j.energy.2016.05.076.
- [170] Robillart M, Schalbart P, Chaplais F, Peuportier B. Model reduction and model predictive control of energy-efficient buildings for electrical heating load shifting. *J Process Control* 2018. doi:10.1016/j.jprocont.2018.03.007.
- [171] Perfumo C, Kofman E, Braslavsky JH, Ward JK. Load management: Model-based control of aggregate power for populations of thermostatically controlled loads. *Energy Convers Manag* 2012;55:36–48. doi:10.1016/j.enconman.2011.10.019.
- [172] Behboodi S, Chassin DP, Djilali N, Crawford C. Transactive control of fast-acting demand response based on thermostatic loads in real-time retail electricity markets. *Appl Energy* 2018;210:1310–20. doi:10.1016/j.apenergy.2017.07.058.
- [173] Alahäivälä A, Corbishley J, Ekström J, Jokisalo J, Lehtonen M. A control framework for the utilization of heating load flexibility in a day-ahead market. *Electr Power Syst Res* 2017;145:44–54.

doi:10.1016/j.epsr.2016.12.019.

- [174] Lakshmanan V, Marinelli M, Kosek AM, Nørgård PB, Bindner HW. Impact of thermostatically controlled loads' demand response activation on aggregated power: A field experiment. *Energy* 2016;94:705–14. doi:10.1016/j.energy.2015.11.050.
- [175] Sossan F. Equivalent electricity storage capacity of domestic thermostatically controlled loads. *Energy* 2017;122:767–78. doi:10.1016/j.energy.2016.12.096.
- [176] Péan TQ, Salom J, Costa-Castelló R. Review of control strategies for improving the energy flexibility provided by heat pump systems in buildings. *J Process Control* 2018. doi:10.1016/j.jprocont.2018.03.006.
- [177] Kakran S, Chanana S. Smart operations of smart grids integrated with distributed generation: A review. *Renew Sustain Energy Rev* 2018;81:524–35. doi:10.1016/j.rser.2017.07.045.
- [178] Sichilalu S, Tazvinga H, Xia X. Optimal control of a fuel cell/wind/PV/grid hybrid system with thermal heat pump load. *Sol Energy* 2016;135:59–69. doi:10.1016/j.solener.2016.05.028.
- [179] Sani Hassan A, Cipcigan L, Jenkins N. Optimal battery storage operation for PV systems with tariff incentives. *Appl Energy* 2017;203:422–41. doi:10.1016/j.apenergy.2017.06.043.
- [180] Wang Y, Huang Y, Wang Y, Zeng M, Li F, Wang Y, et al. Energy management of smart micro-grid with response loads and distributed generation considering demand response. *J Clean Prod* 2018;197:1069–83. doi:10.1016/j.jclepro.2018.06.271.
- [181] O'Shaughnessy E, Cutler D, Ardani K, Margolis R. Solar plus: Optimization of distributed solar PV through battery storage and dispatchable load in residential buildings. *Appl Energy* 2018;213:11–21. doi:10.1016/j.apenergy.2017.12.118.
- [182] Salpakari J, Lund P. Optimal and rule-based control strategies for energy flexibility in buildings with PV. *Appl Energy* 2016;161:425–36. doi:10.1016/j.apenergy.2015.10.036.
- [183] Timothée C, Perera ATD, Scartezzini JL, Mauree D. Optimum dispatch of a multi-storage and multi-energy hub with demand response and restricted grid interactions. *Energy Procedia* 2017;142:2864–9. doi:10.1016/j.egypro.2017.12.434.
- [184] Patteeuw D, Henze GP, Arteconi A, Corbin CD, Helsén L. Clustering a building stock towards representative buildings in the context of air-conditioning electricity demand flexibility. *J Build Perform Simul* 2018;0:1–12. doi:10.1080/19401493.2018.1470202.
- [185] Di Giorgio A, Pimpinella L. An event driven Smart Home Controller enabling consumer economic saving and automated Demand Side Management. *Appl Energy* 2012;96:92–103. doi:10.1016/j.apenergy.2012.02.024.
- [186] Barbato A, Capone A. Optimization models and methods for demand-side management of residential users: A survey. *Energies* 2014;7:5787–824. doi:10.3390/en7095787.
- [187] Paterakis NG, Erdinç O, Catalão JPS. An overview of Demand Response: Key-elements and international experience. *Renew Sustain Energy Rev* 2017;69:871–91. doi:10.1016/j.rser.2016.11.167.
- [188] Sangogboye FC, Droegehorn O, Porras J. Analyzing the payback time of investments in Building Automation n.d.
- [189] Amer M, El-zonkoly AM, Naamane A, Sirdi NKM. Smart Home Energy Management System for Peak Average Ratio Reduction 2014.
- [190] Wilson C, Hargreaves T, Hauxwell-Baldwin R. Benefits and risks of smart home technologies. *Energy Policy* 2017;103:72–83. doi:10.1016/j.enpol.2016.12.047.
- [191] Wilson C, Hargreaves T, Hauxwell-Baldwin R. Smart homes and their users: a systematic analysis

- and key challenges. *Pers Ubiquitous Comput* 2015;19:463–76. doi:10.1007/s00779-014-0813-0.
- [192] Firth SK, Fouchal F, Kane T, Dimitriou V, Hassan TM. Decision support systems for domestic retrofit provision using smart home data streams. *CIB W78 2013 30th Int Conf Appl IT AEC Ind Move Toward Smart Build Infrastructures Cities* 2013.
- [193] Kang J, Kim M, Park JH. A reliable TTP-based infrastructure with low sensor resource consumption for the smart home multi-platform. *Sensors (Switzerland)* 2016;16:1–15. doi:10.3390/s16071036.
- [194] Toschi GM, Campos LB, Cugnasca CE. Home automation networks: A survey. *Comput Stand Interfaces* 2017;50:42–54. doi:10.1016/j.csi.2016.08.008.
- [195] Keshtkar A, Arzanpour S, Keshtkar F. Adaptive residential demand-side management using rule-based techniques in smart grid environments. *Energy Build* 2016;133:281–94. doi:10.1016/j.enbuild.2016.09.070.
- [196] Coleman M, Kane T, Dimitriou V, Firth SK, Hassan T, Hauxwell-Baldwin R, et al. Utilizing smart home data to support the reduction of energy demand from space heating—insights from a UK field study. *8th Int Conf Energy Effic Domest Appliances Light* 2015:1–14.
- [197] Podgornik A, Sucic B, Blazic B. Effects of customized consumption feedback on energy efficient behaviour in low-income households. *J Clean Prod* 2015;130:25–34. doi:10.1016/j.jclepro.2016.02.009.
- [198] Delmas MA, Fischlein M, Asensio OI. Information strategies and energy conservation behavior: A meta-analysis of experimental studies from 1975 to 2012. *Energy Policy* 2013;61:729–39. doi:10.1016/j.enpol.2013.05.109.
- [199] Berry S, Whaley D, Saman W, Davidson K. Finding faults and influencing consumption: the role of in-home energy feedback displays in managing high-tech homes. *Energy Effic* 2016:1–21. doi:10.1007/s12053-016-9489-9.
- [200] Zhang X, Shen J, Yang T, Tang L, Wang L, Liu Y, et al. Smart meter and in-home display for energy savings in residential buildings: a pilot investigation in Shanghai, China. *Intell Build Int* 2016;0:1–23. doi:10.1080/17508975.2016.1213694.
- [201] Faruqui A, Sergici S, Sharif A. The impact of informational feedback on energy consumption—A survey of the experimental evidence. *Energy* 2010;35:1598–608. doi:10.1016/j.energy.2009.07.042.
- [202] Ehrhardt-Martinez AK, Donnelly K a. Advanced Metering Initiatives and Residential Feedback Programs : A Meta-Review for Household Electricity-Saving Opportunities. *Energy* 2010;123:128.
- [203] Chen VL, Delmas MA, Kaiser WJ, Locke SL. What can we learn from high-frequency appliance-level energy metering? Results from a field experiment. *Energy Policy* 2015;77:164–75. doi:10.1016/j.enpol.2014.11.021.
- [204] Lynham J, Nitta K, Saijo T, Tarui N. Why does real-time information reduce energy consumption? *Energy Econ* 2016;54:173–81. doi:10.1016/j.eneco.2015.11.007.
- [205] Fischer C. Feedback on household electricity consumption: A tool for saving energy? *Energy Effic* 2008;1:79–104. doi:10.1007/s12053-008-9009-7.
- [206] Romani J, Perez G, de Gracia A. Experimental evaluation of a heating radiant wall coupled to a ground source heat pump. *Renew Energy* 2017;105:520–9. doi:/10.1016/j.renene.2016.12.087.
- [207] Fischer D, Madani H. On heat pumps in smart grids: A review. *Renew Sustain Energy Rev* 2017;70:342–57. doi:10.1016/j.rser.2016.11.182.
- [208] Kuhn TE. State of the art of advanced solar control devices for buildings. *Sol Energy* 2017. doi:10.1016/j.solener.2016.12.044.
- [209] Dutta A, Samanta A, Neogi S. Influence of orientation and the impact of external window shading



- on building thermal performance in tropical climate. *Energy Build* 2017;139:680–9. doi:10.1016/j.enbuild.2017.01.018.
- [210] Tzempelikos A, Athienitis AK. The impact of shading design and control on building cooling and lighting demand. *Sol Energy* 2007;81:369–82. doi:10.1016/j.solener.2006.06.015.
- [211] Li L, Qu M, Peng S. Performance evaluation of building integrated solar thermal shading system: Building energy consumption and daylight provision. *Energy Build* 2016;113:189–201. doi:10.1016/j.enbuild.2015.12.040.
- [212] Kiritat A, Koyunbaba BK, Chatzikonstantinou I, Sariyildiz S. Review of simulation modeling for shading devices in buildings. *Renew Sustain Energy Rev* 2016;53:23–49. doi:10.1016/j.rser.2015.08.020.
- [213] Skarning GCJ, Hviid CA, Svendsen S. The effect of dynamic solar shading on energy, daylighting and thermal comfort in a nearly zero-energy loft room in Rome and Copenhagen. *Energy Build* 2017;135:302–11. doi:10.1016/j.enbuild.2016.11.053.
- [214] Tzempelikos A, Shen H. Comparative control strategies for roller shades with respect to daylighting and energy performance. *Build Environ* 2013;67:179–92. doi:10.1016/j.buildenv.2013.05.016.
- [215] Stazi F, Marinelli S, Di Perna C, Munafò P. Comparison on solar shadings: Monitoring of the thermo-physical behaviour, assessment of the energy saving, thermal comfort, natural lighting and environmental impact. *Sol Energy* 2014;105:512–28. doi:10.1016/j.solener.2014.04.005.
- [216] Sadeghi SA, Karava P, Konstantzos I, Tzempelikos A. Occupant interactions with shading and lighting systems using different control interfaces: A pilot field study. *Build Environ* 2016;97:177–95. doi:10.1016/j.buildenv.2015.12.008.
- [217] Grynning S, Time B, Matusiak B. Solar shading control strategies in cold climates - Heating, cooling demand and daylight availability in office spaces. *Sol Energy* 2014;107:182–94. doi:10.1016/j.solener.2014.06.007.
- [218] Konstantoglou M, Tsangrassoulis A. Dynamic operation of daylighting and shading systems: A literature review. *Renew Sustain Energy Rev* 2016;60:268–83. doi:10.1016/j.rser.2015.12.246.
- [219] Yao J. An investigation into the impact of movable solar shades on energy, indoor thermal and visual comfort improvements. *Build Environ* 2014;71:24–32. doi:10.1016/j.buildenv.2013.09.011.
- [220] van Moeseke G, Bruyère I, De Herde A. Impact of control rules on the efficiency of shading devices and free cooling for office buildings. *Build Environ* 2007;42:784–93. doi:10.1016/j.buildenv.2005.09.015.
- [221] Santamouris M, Sfakianaki A, Pavlou K. On the efficiency of night ventilation techniques applied to residential buildings. *Energy Build* 2010;42:1309–13. doi:10.1016/j.enbuild.2010.02.024.
- [222] Wang Z, Yi L, Gao F. Night ventilation control strategies in office buildings. *Sol Energy* 2009;83:1902–13. doi:10.1016/j.solener.2009.07.003.
- [223] Vidrih B, Arkar C, Medved S. Generalized model-based predictive weather control for the control of free cooling by enhanced night-time ventilation. *Appl Energy* 2016;168:482–92. doi:10.1016/j.apenergy.2016.01.109.
- [224] Artmann N, Manz H, Heiselberg P. Parameter study on performance of building cooling by night-time ventilation. *Renew Energy* 2008;33:2589–98. doi:10.1016/j.renene.2008.02.025.

